Temperature-dependent regulation in the *Bacillus cereus*-*Bacillus anthracis* crossover strain, *Bacillus cereus* G9241

Thomas Adam Brooker

Thesis submitted for the degree of Doctor of Philosophy in Medical Sciences

University of Warwick, Warwick Medical School

September, 2019

Table of Contents

List of Figures

List of Tables

Acknowledgements

I have to start by saying an incredulous thank you to my supervisor Dr. Nick Waterfield. Thank you to a man who looks like Father Ted, but behaves like Father Jack, for being the most outrageously raucous yet informative and supportive supervisor. Thanks for giving me the opportunity to learn so much and making it such a fun venture along the way. You have been brilliant and I really can't thank you enough for being the Lister to my Rimmer. Thank you to Professor Petra Oyston and Dr. Ken Kinnear for being supportive to the project, the collaboration and me personally over the last five years. Also, I'm sorry to all of the above for the rigmarole of the last year, teaching is more work than I thought. Thank you to Emma, Chrystala, Meera and Andy for all the help and support too.

This gratitude extends to the most fantastic colleagues and friends an initially clueless PhD student could ask for. Alexia is an absolute lab God who provided an endless amount of advice and help throughout my PhD – thank you so much! In addition to our lab God, I have to thank Gemma, Holly and (lab) Emily. Without them all I don't think the foundations of the lab would have even existed. You guys provided so much advice, wisdom and hilarity; the PhD would have been boring and bloody difficult without you. Thank you to Josie and Ross for being two of the loveliest people I've ever met but also making me laugh at things I definitely shouldn't have. Thanks to Joe, Branko and Nabil for providing genuinely interesting arguments whilst also having some "grumpy-old man views". I learned a lot and laughed a lot with you three, often begrudgingly at my own expense. Thank you to Slaw for being a gaming bud, thanks to Maciej for teaching me Polish phrases and thanks to Blessing for supporting my cake baking ventures. Thanks to Arnaud for unapologetically being you at all times, thanks to Sandra for being one of the loveliest human beings ever, thanks to Seb for the cookies and boardgames, thanks to Leo and Nina for the laughs and thanks to Kathryn for the cakes, boardgames and being an all-round delightful person. Lastly I offer a big thank you to Grace. You may not have learned anything from me, but getting to teach you for a few months cemented the idea that I wanted to teach for a career… those poor kids. Thanks everyone, you all made it a wonderful four years!

Thank you to my amazing Mum and of course Dave for letting me lodge with them for four years. I know it's not ideal to have your smart-arse son back in the house after four years away, but I actually really enjoyed being home. It has set me up for life and I'm not sure I'll ever be able to repay you.

Lastly I want to thank Emily for being the most supportive and wonderful human being I have ever had the pleasure of meeting. You suffered through your PhD whilst I enjoyed mine and yet you never begrudged me for it. Instead you encouraged me when times got tough and helped me persevere to the end. I will be forever grateful for your friendship, whatever the future may hold.

Author's Declaration

This thesis is submitted to the University of Warwick in support of my application for the degree of Doctor of Philosophy. The work carried out is my own work and has not been submitted in any previous application for any degree in this or any other university.

The work presented was carried out solely by the author except for those listed below:

- Chapter 1: The process of mass spectrometry was conducted by Dr Cleidiane Zampronio and Dr Juan Hernandez Fernaud (Proteomics Research Technology Platform, University of Warwick)
- Chapter 3: Electron microscopes were operated and images captured by Dr Saskia Bakker (Advanced Bioimaging Research Technology Platform Manager, university of Warwick)

Some strains used in this study were made prior to this project as listed below:

- *B. cereus* G9241 *ΔpBCX01* was constructed by Dr Sara Hernández-Rodriguez

Abstract

Bacillus cereus G9241 was originally isolated from a Louisiana welder suffering from an anthrax-like infection. A member of the *Bacillus cereus* sensu lato complex, strain G9241 is closely related to the mammalian pathogen *Bacillus anthracis*. It contains two plasmids pBCX01 and pBC218, which are homologous and analogous to pX01 and pX02 respectively, from *Bacillus anthracis*. In addition, it contains a phagemid, pBFH_1 encoding a putative prophage. The gene for PlcR, which is the pleiotropic quorum sensing regulator of secreted proteins, is truncated in all *B. anthracis* isolates. The current dogma suggests this truncation evolved to accommodate the acquisition of the anthrax toxin regulator, AtxA encoded on the pX01 plasmid. *B. cereus* G9241 appears to break this dogma as it encodes intact copies of both *plcR* and *atxA*.

Work prior to this study showed when cultured at 25 °C, cell free *B. cereus* G9241 culture supernatant is cytotoxic to human macrophages, PMNs and T2 lymphocytes in addition to insect haemocytes from *Manduca sexta*. However, the cytotoxic activity of the culture supernatant is lost at 37 °C. *B. cereus* G9241 is also motile at 25 °C but immotile at 37 °C.

This study proposes that *Bc*G9241 is able to switch between *B. cereus* and *B. anthracis* –like phenotypes in a temperature-dependent manner. A combination of RNAseq, whole cell and secretome proteomics suggests that differential regulation of PlcR at a post transcriptional level is responsible for the temperature-dependent cytotoxic activity of the culture supernatant and temperature-dependent motility. Furthermore, expression from the extrachromosomal elements increases at 37 °C, particularly from the phagemid pBFH_1. This study shows that pBFH_1 encoded phage particles are expressed at 37 °C and this may be a link to a rapid sporulation phenotype also seen at this temperature.

Abbreviations

ABC – Ammonium bicarbonate

AFLP – Amplified Fragment Length Polymorphism

bp – base pairs

BPS – Bacillus PolySaccharide capsule

BSAC – British Society of Antimicrobial Chemotherapy

bv – Biovar

ddH_2O – Double distilled water

DFA – Direct Fluorescence Assay

DS – Downstream

DTT – Dithiothreitol

ESI – Electrospray Ionisation

HA – Hyaluronic acid

HTH – Helix-turn-helix

IAA – Iodoacetamide

ISA – Iso-sensitest agar

Kbp – Kilo base pairs

LB – Lysogeny Broth

LFQ – Label-free quantification

MCP – Methyl-accepting chemotaxis protein

MLST – Multilocus Sequence Typing

MS – Mass spectrometry

nanoLC – Nano liquid chromatography

NEB – New England BioLabs

PA – Protective antigen

PCI – Phenol-chloroform-isoamyl alcohol

PRD – Phosphophenolpyruvate:sugar phospholtransferase system regulatory domains

PVOGs – Prokaryotic Virus Orthologous Groups

RBCs – Red Blood Cells

SNPs – Single Nucleotide Polymorphisms

sRNAs – Small RNAs

SOC – Super optimal broth with catabolite repression

TAE – Tris-acetate-EDTA

TFA – Trifluoroacetic acid

US – Upstream

WT – Wild type

1. Introduction

1.1. The *Bacillus cereus* sensu lato

1.1.1. The *Bacillus cereus* sensu lato

The *Bacillus cereus* sensu lato is a group of genetically similar but phenotypically diverse bacteria (Okinaka and Keim, 2016). Like all *Bacilli*, members of the sensu lato are Gram-positive, soil-borne, rod-shaped bacteria (Vilain et al., 2006) The sensu lato contains eight species, including the well-studied trio of *Bacillus anthracis*, *Bacillus cereus* and *Bacillus thuringiensis*. These species are widely studied due to their clinical importance (Carlson et al., 2018b; Dierick et al., 2005; Glasset et al., 2018) or use in biotechnology (Bishop, 2002). There are also less researched species within the group; *Bacillus mycoides*, *Bacillus pseudomycoides, Bacillus weihenstephanensis, Bacillus cytotoxicus* and *Bacillus toyonensis*.

The different species within this group display a great variation, both phenotypically and in the ecological niche they inhabit. *B. anthracis* is the etiological agent of anthrax (Carter, 1985), *B. thuringiensis* produces crystal toxins and is used as a pesticide (Dulmage, 1981) and *B. cereus* is commonly isolated from soils, but certain strains can be pathogenic (Dierick et al., 2005; Vilain et al., 2006). Despite these obvious phenotypic disparities, classical genetic sequencing methods do not differentiate them as species. Multilocus sequence typing (MLST) groups strains of *B. cereus* sensu lato into 5 distinct clades with similar phenotypes (Raymond and Federici, 2017). However, other studies postulate that *B. cereus* sensu lato species are often only differentiated by the presence of extrachromosomal DNA (Helgason et al., 2000).

1.1.2. *B. cereus* sensu stricto

The first *Bacillus cereus* strain described was isolated from the air inside a cow shed (Frankland and Frankland, 1887). The colonies were described as milky white and formed “wax-like” expansions on agar. Within this study, both spore

formation and arthromitic filamentous growth was described. The initial characterisation also described how *B. cereus* colonies were rounded but with "whip-like" protrusions. These observations represent classical phenotypes of the *B. cereus* sensu lato including biofilm formation, sporulation and motility. Since the initial identification, *B. cereus* strains have been isolated from soil samples world-wide (Garbeva, 2003; Von Stetten et al., 1999).

B. cereus sensu stricto is the most phenotypically diverse species of the sensu lato. *B. cereus* strains have been seen to form symbiotic relationships with *Flavobacterium* in plant root nodules (Pandey and Palni, 1997; Peterson et al., 2006) and form part of the commensal microflora of the gut of certain insects (Swiecicka and Mahillon, 2006). *B. cereus* sensu stricto strains have also been isolated from higher organisms, including various Chordata (Margulis et al., 1998) and are reported to be the most common contaminants in pharmaceutical laboratories (Sandle, 2014). Other strains of *B. cereus* sensu stricto are clinically important, causing the food-borne emetic and diarrhoeal infections (Mahler et al., 1997; Stenfors Arnesen et al., 2007).

Despite the huge diversity in ecological niche, all of these strains are classified as a single species. This classification is based on the presence of the gene encoding the pleiotropic regulator of virulence PlcR and the absence of extra-chromosomal DNA containing anthrax toxins or crystal toxins (Dai et al., 1995; Höfte and Whiteley, 1989). Genetic sequencing has revealed *B. cereus* sensu stricto strains are all highly similar at a chromosomal level (Helgason et al., 2000). Phenotypically, *B. cereus* strains are motile and have the potential to produce a wide range of cytolytic and haemolytic toxins, mediated by PlcR - the pleiotropic regulator of virulence (Granum, 2005; Guinebretiere et al., 2002; Hardy et al., 2001; Lund and Granum, 1996).

1.1.3. *B. anthracis*

1.1.3.1. *B. anthracis* sensu stricto

B. anthracis is the etiological agent of the disease anthrax (Koch, 1876). *B. anthracis* strains are described as monomorphic, meaning they have a relatively low level of genetic diversity (Keim et al., 2009). In addition to the chromosomal DNA, the majority of *B. anthracis* strains contain two virulence plasmids, pX01 and pX02. pX01 contains genes encoding the tripartite anthrax toxin whereas pX02 contains genes for capsule biosynthesis (Okinaka et al., 1999a; Okinaka et al., 1999b). Despite the prevalence of these plasmids, their presence is no longer thought to be a genetic marker of the *B. anthracis* species. This is due to the identification of other *B. cereus* sensu lato species containing one, or both of the plasmids (Hoffmaster et al., 2006; Hu et al., 2009). Arguably characterisation of *B. anthracis* species at a genetic level relies upon the presence of both the *atxA* gene and a nonsense mutation in the *plcR* gene (Slamti et al., 2004). However *B. anthracis* species are more likely to be characterised by a combination of genetic and phenotypic analysis (Marston et al., 2006). *B. anthracis* strains are differentiated from other *Bacillus* species, by their lack of motility, non-haemolytic activity on blood agar, gamma phage susceptibility and the ability to cause the disease anthrax (Leise et al., 1959).

1.1.3.2. The disease state anthrax

Anthrax is a zoonotic disease that primarily infects herbivorous grazing animals. Animals become infected upon the ingestion or inhalation of *B. anthracis* spores (Koch, 1876). Scholars believe occurrences of the disease anthrax in cattle have been recorded as early as 700 BC in Homer's the Iliad. However, until the 1700s, only literary accounts of anthrax existed. "Malignant pustules" were consistently identified in infected humans and cattle, but a link between the symptoms of the disease and a bacterium was not elucidated until the mid-1800s (CDC, 2016). In 1876 Robert Koch published one of microbiology's most influential papers proving that the bacterium *B. anthracis* is the aetiological agent of the disease

anthrax (Carter, 1985). He also showed that *Bacilli* or viable spores were necessary to cause the disease state anthrax (Koch, 1876).

Since the establishment of the disease state anthrax, *B. anthracis* has been shown to infect via four distinct routes: cutaneous, inhalational, gastrointestinal and injectional. Cutaneous anthrax infections occur when *B. anthracis* infects a host via wounds or micro-abrasions in the skin. Spores germinate locally and result in oedema and necrosis at the site of infection. Cutaneous infection is the most commonly occurring form of the disease making up for 95% of anthrax cases and without treatment 20% of cutaneous anthrax cases are lethal (CDC, 2014a).

Inhalational and gastrointestinal anthrax infections result from the inhalation or ingestion of *B. anthracis* spores respectively. These modes of infection are far more lethal with 45% of cases resulting in death despite antibiotic treatment. Both modes of infection are rare and are thought to occur in livestock grazing on ground with persisting *B. anthracis* spores. Cases in humans are thought to arise from the ingestion and inhalation of spores when handling infected meats (CDC, 2014b, c).

Since 2009, 70 cases of injectional anthrax have been confirmed across Europe with a mortality rate of 37% despite medical intervention. Injectional anthrax presents similarly to cutaneous anthrax with initial infection occurring at the site of injection. This infection leads to local necrosis and oedema before progressing to systemic infection and eventually multi-organ failure. All cases of injectional anthrax were confirmed to have arisen in heroin users and molecular evidence suggests that all 70 cases resulted from the same batch of heroin infected with *B. anthracis* (Price et al., 2012).

1.1.3.3. Inhalation anthrax mode of infection

Because of its potential use as a bioterror agent, *B. anthracis* is widely and well-studied. It has been postulated that the most likely route of infection to be

utilised by terrorist organisations would be inhalational anthrax due to easy transmission and high mortality rate.

Upon inhalation, spores are endocytosed by lung macrophages (Dixon et al., 2000). However there is some evidence to suggest that *B. anthracis* spores can also be endocytosed by dendritic cells (Brittingham et al., 2005). The CD14 receptor on the surface of mammalian macrophages binds various ligands on the *B. anthracis* exosporium and internalises the spore (Oliva et al., 2009). The spores germinate inside of the phagosome (Guidi-Rontani et al., 1999) and vegetative cells begin expressing the anthrax tripartite toxin as well as other proteases (Tonello and Zornetta, 2012). The combination of toxins and proteases allows *B. anthracis* to escape the maturing phagolysosome. InhA1 has also been shown to be essential for macrophage escape by *B. cereus* (Ramarao and Lereclus, 2005). After escaping the phagolysosome, the anthrax toxins aid lysis and apoptosis of the macrophages (Park et al., 2002). Vegetative cells are assumed to spread to neighbouring tissues eventually becoming systemic, infecting mainly the liver and the cardiovascular system before killing the host (Firoved et al., 2005; Remy et al., 2013).

1.1.3.4. *B. anthracis* in agriculture

As well as being medically important, *B. anthracis* has a big impact on agriculture. *B. anthracis* has the ability to persist as a spore in the environment and does so in soils globally (Carlson et al., 2018b). Spores are inhaled or ingested by the cattle when grazing and germinate inside the host. The host is killed by the systemic infection and it is thought that whilst the carcass rots, *B. anthracis* sporulates to survive an environment with limited nutrients. The cycle can propagate upon the arrival of a new host.

1.1.3.5. *B. anthracis* in bioterrorism

The earliest known instances of *B. anthracis* being used a biological weapon come from World War I (Wheelis, 1998). Post-war evidence suggests that the Germans injected *B. anthracis* into cattle set to be sent to the Allied Forces from

neutral partners. Other attempts to use *B. anthracis* as a biological weapon during the war included releasing spores in equine and cattle breeding centres throughout Allied Forces countries. Perhaps the most unusual attempt to utilise *B. anthracis* as a weapon was the attempt to infect Reindeer in Norway to prevent provisions being sent to the Russian front line (CDC, 2016).

The first widely known use of *B. anthracis* as a bioterror weapon against human life was by the Japanese against the Chinese. Great Britain and the US have also experimented with anthrax as a weapon. During World War II the US tested anthrax bombs in Utah and Mississippi, whilst the UK released *B. anthracis* on Gruinard Island in Scotland which killed all 80 sheep grazing on the island. These experiments highlighted the longevity of anthrax spores in the environment. Gruinard Island was deemed uninhabitable until 1986 after extensive formaldehyde treatment (CDC, 2016).

After decades developing and stockpiling biological weapons, "The 1972 Convention on the Prohibition of the Development, Production, and Stockpiling of Biological and Toxin Weapons" was created. This led to destruction of various stockpiles of anthrax worldwide. However in 1979 there was an outbreak of inhalational anthrax in the city of Sverdlovsk. Sverdlovsk is located downwind of a Soviet military microbiology facility and the outbreak resulted in 96 cases of anthrax, 64 of which were fatal. In 1992 it was confirmed that this outbreak was due to a leak in the facility which led to the dispersal of *B. anthracis* spores into the city. The most recent use of anthrax as a bioterror weapon occurred in the USA when a scientist attempted to poison members of the US senate by posting *B. anthracis* spores through the mail. Unfortunately due to the porous nature of the envelopes, mail handlers were exposed to airborne spores and subsequently 5 people died of inhalational anthrax. The impact of *B. anthracis* both on agriculture and in bioweapons has culminated in *B. anthracis* research garnering a lot of funding world-wide, especially in the US due to concerns over the need for biodefence.

1.1.4. Other species of the *B. cereus* sensu lato

1.1.4.1. *B. thuringiensis*

B. thuringiensis was first isolated by Ishiwatari Shigetane and Ernst Berliner whilst they were independently studying flacherie disease in silkworms (Berliner, 1915). The entemopathogen *B. thuringiensis* is perhaps the most well-studied species in the sensu lato due to its use as a pesticide (Roh et al., 2007). The insecticidal phenotype of the bacteria is due to the secretion of insecticidal crystal (Cry) toxins and cytolytic (Cyt) toxins (Bravo et al., 2007). The presence of extrachromosomal genes encoding the Cry toxins is what defines the species within the sensu lato (Berry et al., 2002). Without the extrachromosomal elements, *B. thuringiensis* strains are indistinguishable from *B. cereus* strains (Helgason et al., 2000).

1.1.4.2. *B. weihenstephanensis*

B. weihenstephanensis is a psychrophilic species able to grow at temperatures as low as 4 °C (Lechner et al., 1998). However a psychrophilic nature is not sufficient to define a strain as *B. weihenstephanensis*. Many strains of *B. cereus* are able to grow at psychrophilic temperatures (Stenfors and Granum, 2001). Rather, *B. weihenstephanensis* strains are characterised by being psychrophilic, but not mesophilic and must test positive for a psychrophilic variant of the major cold shock protein encoding gene (*cspA*). Since its initial isolation from cow's milk *B. weihenstephanensis* strains have been implicated in various forms of food-borne illnesses (Stenfors Arnesen et al., 2007; Thorsen et al., 2006).

1.1.4.3. *B. mycoides* and *B. pseudomycoides*

First described in 1886, *B. mycoides* is named after its hyphae-like growth pattern (Flugge, 1886). The species is ubiquitous in environments across the world. Strains have been isolated from the rhizosphere of tea bushes in Asia, peat bogs in Germany and marine environments worldwide (Ivanova et al., 1992; Pandey and Palni, 1997; Wintzingerode et al., 1997). *B. mycoides* displays an

elasticotactic phenotype meaning it can respond to elastic forces in the growth substrate. This is thought to aid its growth and dispersal in a rapidly changing environment (Stratford et al., 2013).

B. pseudomycoides is almost phenotypically identical to *B. mycoides* and 16S rRNA analysis reveals a 98% sequence similarity. Despite this the two species only have 30% DNA relatedness and clearly distinct fatty acid compositions (Nakamura, 1998). *B. pseudomycoides* produces the lantibiotic pseudomycoicidin (Basi-Chipalu et al., 2015).

1.1.4.4. *B. cytotoxicus* and *B. toyonensis*

Originally isolated during an outbreak of food poisoning in France that resulted in the deaths of 3 people, *B. cytotoxicus* is a newly identified species of the *B. cereus* sensu lato (Guinebretiere et al., 2013). 16S rRNA analysis reveals 97-98% similarity with the *B. cereus* sensu lato. *B. cytotoxicus* represents a thermotolerant cluster within the *B. cereus* sensu lato, with strains growing between temperatures of 20-50 °C.

Used in animal feed as a probiotic for over 30 years, *B. toyonensis* is being proposed as a novel species of the *B. cereus* sensu lato (Jiménez et al., 2013). This cluster of species is distinguished from other species in the *B. cereus* sensu lato at a genetic level as opposed to by a specific phenotype.

1.2. Regulation of pathogenicity in the *B. cereus* sensu lato

1.2.1 The PlcR-PapR regulon

PlcR is a 34 kDa protein first identified as a transcriptional regulator of phospholipase C, *plcB* at the onset of stationary phase in *B. thuringiensis* (Lereclus et al., 1996). PlcR contains a helix-turn-helix (HTH) domain for binding DNA and positively auto-regulates its own transcription. Since its identification in *B. thuringiensis*, *plcR* has been found to be well conserved in all species of the *B. cereus* sensu lato, with one major caveat. In *B. anthracis plcR* contains a nonsense mutation that results in an early transcription stop codon. The

truncated PlcR protein does not show transcriptional activity (Agaisse et al., 1999). PlcR has been shown to be a pleiotropic regulator in the *B. cereus* sensu lato with a regulon containing at least 45 genes in *B. cereus* ATCC14579 (Gohar et al., 2008). The vast majority of these genes encode secreted proteins that are virulence factors and expression of PlcR contributes heavily to virulence in mice and insects (Clair et al., 2010; Salamitou et al., 2000). Genes under transcriptional control of PlcR are identified by a conserved sequence upstream of the transcription start site, referred to as the *plcR* box (Økstad et al., 1999). The conserved *plcR* box sequence is TATGNAN$_4$TNCATA. However a variety of proteins that do not have *plcR* boxes upstream of the corresponding gene have also seen to be differentially regulated in comparative studies using *B. cereus ΔplcR* strains (Gohar et al., 2002; Ivanova et al., 2003).

PlcR alone is not sufficient to efficiently activate the transcription of genes with upstream *plcR* boxes. For full transcriptional activity, PlcR requires the co-activator PapR (Slamti and Lereclus, 2002). *papR* is located downstream of *plcR* and encodes a 48-amino acid peptide. PapR is secreted from the cell via the SecA-dependent system and processed to a heptapeptide by the neutral protease, NprB (Pomerantsev et al., 2009). *nprB* is often located within the *plcR* operon on the same strand as *plcR* but in the opposite orientation. The heptapeptide form of PapR is reimported into the bacterium by the oligopeptide permease, Opp import protein (Gominet et al., 2001). The heptapeptide form of PapR promotes the highest PlcR activity, but pentapeptide forms are sufficient to activate PlcR (Pomerantsev et al., 2009; Slamti and Lereclus, 2002). The active form of PlcR is constituted of a PlcR dimer and two PapR peptides (Declerck et al., 2007). PlcR dimers are locked into an inactive conformation by amino acid interactions between Ile68 and Tyr64. However upon PapR binding, the dimer changes conformation. This allows the HTH, DNA binding domains of PlcR to bind dsDNA and activate transcription (Grenha et al., 2013).

As PapR requires secretion and reimporting, it functions as a quorum sensing molecule. The PlcR-PapR transcriptional activator can “sense” the cell density of the bacterial population. This ensures cell numbers are sufficient before

becoming fully pathogenic. Perhaps because of this role, the PlcR-PapR quorum sensing system has evolved a polymorphism to make quorum sensing more specific (Slamti and Lereclus, 2005). Four distinct classes of PlcR-PapR systems have evolved differentiated by the sequence of the last 5 amino acids of the peptide they bind. These classes are named PlcR groups I-IV. PapR peptides from one group are unable to activate the transcriptional activity of PlcR from another. This allows a more specific quorum sensing system in a group of bacteria with such a high genomic sequence similarity (Helgason et al., 2000).

Environmental conditions that regulate PlcR expression include cell density, oxygen availability and temperature. In the laboratory, *plcR* transcription reaches a maximum level towards the end of exponential phase growth (Lereclus et al., 1996). This is consistent with PlcR being activated by the quorum sensing peptide PapR and PlcR-PapR being a positive autoregulator. Genes under PlcR transcriptional control are more highly transcribed during aerobic growth compared to anaerobic growth (Passalacqua et al., 2009). PlcR transcriptional regulation is higher at low temperatures, 15 °C than at high temperatures, 30 °C in *B. weihenstephanensis* KBAB4 strain (Rejasse et al., 2012).

PlcR Group	**PapR C-terminal amino acids**	***B. cereus* sensu lato species/strains**
I	L-P-F-E-(F/Y)	*B. weihenstephanensis* type strain, *B. cereus* strains ATCC14579
II	M-P-F-E-F	*B. cereus, B. thuringiensis*
III	V-P-(F/Y)-E-(E/Y)	*B. mycoides*, *B. thuringiensis, B. cereus, B. anthracis*
IV	L-P-F-E-H	*B. thuringiensis*, *B. cereus* G9241

Table.1.1. PlcR-PapR groups are based on the last 5 C-terminal amino acids. Amino acids are denoted by the single letter amino acid code. (F/Y) - indicates alternate amino acids. Where no strain is specified in a group, this indicates that many different strains of this species are present.

1.2.2. The Role of CodY in regulation of PlcR

Whilst PlcR is the main global regulator of virulence in *B. cereus* sensu lato, it is not the only one. CodY is a global regulator that senses the availability of branched chain amino acids (BCAAs) in the cell and is involved in the stringent response (Belitsky, 2015). However CodY is more recently reported as the link between the metabolism and virulence of a bacterium (Slamti et al., 2015). In *Bacilli* CodY senses the nutrient availability and redox state of the bacterium by binding GTP and BCAAs (Sonenshein, 2007). Throughout exponential growth when nutrients are plentiful, genes of the CodY regulon are repressed. In particular CodY represses competence and sporulation genes during exponential growth (Molle et al., 2003b).

In *B. cereus*, deletion of CodY results in a loss of non-haemolytic enterotoxin and phospholipase activity in the supernatant (Frenzel et al., 2012). This loss of PlcR-mediated toxicity is due to a failure to efficiently reimport PapR peptide (Slamti et al., 2015). However PapR is also differentially processed in a *B. thuringiensis ΔcodY* strain due to the loss of NprB expression. CodY is essential for the efficient reimport of PapR and therefore is essential for PlcR activity and toxicity of *B. cereus*. Interestingly, CodY is essential for AtxA-mediated virulence in *B. anthracis* where it aids AtxA accumulation (van Schaik et al., 2009). AtxA is the transcriptional activator of the genes encoding the anthrax tripartite toxin components (Fouet, 2010). Together this suggests that regulation by CodY in *Bacilli* has evolved to ensure bacterial populations do not commit to sporulation or competence until nutrient availability deems it necessary for survival.

1.3. Toxicity of *B. cereus* sensu lato

1.3.1. Toxins of *B. cereus* sensu stricto

The toxins of the *B. cereus* sensu stricto are divided into three main categories: emetic toxins, diarrhoeal toxins and the anthrax toxin. Foodborne emetic strains

of *B. cereus* named for the production of the cereulide emetic toxin, cause severe vomiting, muscle paralysis and death (Dierick et al., 2005). Diarrhoeal strains of *B. cereus* favour the production of enterotoxins in the small intestine and are responsible for the majority of food poisoning cases in Europe (Lund and Granum, 1996). Other *B. cereus* strains such as the *B. cereus*/*B. anthracis*-crossover strain G9241 cause a pneumonia-like inhalational disease by the production of anthrax tripartite toxin (Hoffmaster et al., 2004). Emetic, diarrhoeal and anthrax toxins are regulated by AbrB, PlcR and AtxA respectively (Dai et al., 1995; Gohar et al., 2008; Luecking et al., 2009).

1.3.1.1. PlcR-mediated toxins

PlcR is named for its positive transcriptional regulation of phospholipase C (Agaisse et al., 1999). Phospholipase C (PlcB) is a lecithinase enzyme that can hydrolyse cell membranes and cause the degranulation of human neutrophils (Kotiranta et al., 2000; McGregor et al., 1991). Tests for PlcB lecithinase activity are often used for determining the presence of a *B. cereus* sensu lato organism, with the exception of *B. anthracis* (Kim and Goepfert, 1971).

PlcR regulates more than just the transcription of *plcB*. The PlcR regulon contains many genes directly and indirectly upregulated by the protein (Clair et al., 2010; Gohar et al., 2008; Gohar et al., 2002). Toxins identified include, but are not limited to Hbl enterotoxin, Nhe enterotoxin and CytK cytotoxin. These three toxins are all classified as enterotoxins and have been isolated from patients suffering from food-borne, diarrhoeal infections.

Non-haemolytic enterotoxin is a tripartite toxin encoded on the *nheABC* operon (Lindback et al., 2004). The enterotoxin components were first isolated from a *B. cereus* strain that caused an outbreak of food poisoning in Norway (Lund and Granum, 1996). Nhe induces colloid osmotic lysis of cells resulting in cell death (Fagerlund et al., 2008) Haemolysin BL is similar to NheABC in that is a three-component toxin (Heinrichs et al., 1993). The three components are encoded on the operon *hblCDAB. hblA* encodes the toxin binding component (B), *hblD* encodes lytic component 1 (L_1), and *hblC* encodes lytic component 2 (L_2)

(Guinebretiere et al., 2002). Until recently, *hblB* was thought to encode a pseudogene resulting from an incomplete duplication of *hblA* (Stenfors Arnesen et al., 2008). However evidence suggests that *hblB* may be a monocystronic element, not regulated by PlcR. The gene product is secreted during early exponential growth and the high similarity to HblA suggests that it may reinforce the role of the Hbl binding component (Clair et al., 2010). Hbl and Nhe are both pore forming, α-helix toxins (Fagerlund et al., 2008). All three components of both Hbl and Nhe contain Sec-type signal peptides and subsequently are exported via the Sec secretion system (Fagerlund et al., 2010). After secretion, the components sequentially build upon the surface membrane of target cells (Sastalla et al., 2013). Hbl B component or NheC bind first, followed by Hbl L_1 component or NheB and finally Hbl L_2 or NheA. Sequencing of 125 strains of *B. cereus* suggests that the HblCDAB and NheABC operons have been horizontally exchanged constantly over the evolution of the *B. cereus* sensu lato helping to shape the group's evolution (Böhm et al., 2015). Cytotoxin K is a 34 kDa protein isolated from a strain of *B. cereus* responsible for a lethal food poisoning outbreak (Lund et al., 2000). CytK forms β-barrel pores in target cells leading to necrotic enteritis (Hardy et al., 2001). CytK has a small pore and it is unclear how exactly the pore formation leads to cell death.

1.3.1.2. Non-PlcR mediated toxins

As well as diarrhoeal infections, *B. cereus* strains have been isolated from emetic infections. The emetic toxin, named cereulide, was first identified in a *B. cereus* strain isolated from a lethal, food-borne infection (Mahler et al., 1997). The cereulide toxin causes vacuole formation in liver cells, but its mechanism of action is not yet elucidated (Agata et al., 1994; Marxen et al., 2015). Cereulide has been identified in *B. cereus* and *B. weihenstephanensis* and has been seen to be expressed more at lower temperatures (Thorsen et al., 2006). There are two classes of cereulide toxin-producing bacteria. In class 1 the cereulide encoding gene, *ces* is located on a pX01-like plasmid, whereas in class 2 *ces* is encoded on the chromosome or a plasmid unrelated to pX01 (Hoton et al., 2009) Interestingly the emetic virulence lifestyle characterised by emetic toxin

production is not regulated by PlcR. Ces synthesis is repressed by the transition state regulator AbrB and requires Spo0A for expression (Luecking et al., 2009).

1.3.1.3. Secretion of toxins in *B. cereus* sensu stricto

Due to their importance in food-borne pathogenesis, *B. cereus* toxin profiles have been widely studied. PlcB, Nhe, Hbl and CytK are all secreted during early stationary phase in *B. cereus* ATCC14579 (Gohar et al., 2002). Flagellin proteins, a component of the Opp permease import protein OppA and metalloproteases InhA1, InhA2 and InhA3 are also highly secreted during early stationary phase growth (Gohar et al., 2005). A highly similar secretion profile was seen in a *B. thuringiensis* strain cured of the crystal toxin plasmids. Across the growth course of *B. cereus*, transcription of PlcR-regulated genes increases with the level of PlcR regulator (Gilois et al., 2007). However levels of PlcR-regulated proteins peak at different times across the growth curve of *B. cereus*.

1.3.2. Toxins of *B. anthracis*

In *B. anthracis* a truncated PlcR protein means that PlcR-regulated genes are not efficiently promoted and gene products not expressed (Mignot et al., 2001). Instead *B. anthracis* toxicity relies on the expression of the tripartite anthrax toxin encoded on the pX01 plasmid (Firoved et al., 2005; Lehmann et al., 2009). The anthrax toxin is a tripartite toxin composed of a receptor-binding component named protective antigen (PA) and two catalytic components, the lethal factor (LF) and the oedema factor (ED) (Moayeri et al., 2015). The toxin components are positively promoted by the transcriptional regulator AtxA (Bourgogne et al., 2003; Uchida et al., 1993). AtxA is encoded on the pBCX01 plasmid and regulates genes on the chromosome and both virulence plasmids (Guignot et al., 1997; Uchida et al., 1997). It is widely reported that genes under transcriptional control by AtxA are more highly transcribed under high CO_2/bicarbonate conditions (Fouet, 2010). However there is evidence to suggest that growth at a higher temperature, i.e. 37 °C leads to higher levels of AtxA activity (Dai and Koehler, 1997).

Full length 83 kDa PA binds specific cell surface receptors of target cells. The only known receptors of PA are tumour endothelial marker 8 and capillary morphogenesis gene-2 (Bradley et al., 2001; Escuyer and Collier, 1991). Upon binding the cell receptor, PA cleaves itself to an active 63 kDa form (Beauregard et al., 2000). PA heptamers self-assemble on the cell surface to form a pre-pore and bind to either the LF of the EF (Elliott et al., 2000). When the pH falls, i.e. in the endosome of a phagocyte, the pre-pore converts to an active pore and translocates the EF or LF into the host cell (Miller et al., 1999). The LF is a metalloprotease which cleaves the N-terminus of various mitogen activated protein kinases (Klimpel et al., 1994). EF is a calmodulin-dependent adenylate cyclase that forces the host cell to over-produce cAMP (Leppla, 1982). The catalytic effects of both toxins result in the disruption of multiple cellular processes and ultimately host cell death.

In nutrient rich conditions, the secretome of the *B. anthracis* contains approximately 500 proteins (Chitlaru et al., 2007). This includes very low levels of PA and EF toxin components. When growing in a minimal media with high levels of oxygen, only two major proteins are secreted, the metalloprotease InhA1 and the neutral protease NprB. This finding was replicated in a *B. anthracis* strain cured of both virulence plasmids suggesting that in high-O_2 conditions the virulence plasmid-encoded proteins are not expressed (Gohar et al., 2005). As expected, when *B. anthracis* is grown in minimal media with high levels of CO_2, the most abundant protein in the secretome is the AtxA-regulated PA. EF and LF are both present but secreted at lower levels (Chitlaru et al., 2007). Fewer proteases are found in the *B. anthracis* secretome under high CO_2 conditions and NprB secretion is lost completely. This may be to prevent the cleavage of anthrax toxins needed for virulence.

1.3.3. Incompatibility of PlcR and AtxA

The nonsense frameshift mutation found in the *plcR* gene of all *B. anthracis* strains has led to the formation of the dogma that functional PlcR and AtxA regulators are incompatible within the same bacterium. It is suggested that the

horizontal acquisition of pX01 selected for the mutation in *plcR* (Mignot et al., 2001). Expression of WT levels of PlcR in *B. anthracis* led to a strain that sporulated poorly and overexpression of PlcR abolished sporulation completely. Despite this, over the last 15 years, strains of *B. cereus* able to express PlcR and AtxA have been discovered, suggesting the incompatibility dogma is not as straightforward as first described.

1.4. *B. cereus*/*B. anthracis* crossover strains

1.4.1. *B. cereus* G9241 – Louisiana isolate

1.4.1.1. Discovery and clinical appearance

In 1994 an otherwise healthy welder was hospitalised with a respiratory infection resulting in a case of pneumonia. The causative agent of the infection was isolated and retrospectively analysed ten years later. The bacterial strain named *B. cereus* G9241 caused an illness that presented with symptoms identical to that of victims of the postal anthrax attacks in America in 2001 (Hoffmaster et al., 2004). However, unlike any of the ten patients of the postal anthrax attacks, the patient infected with *B. cereus* G9241 also suffered with hemoptysis, the lysis of red blood cells.

1.4.1.2. Chromosomally encoded genes

Phenotypically, *B. cereus* G9241 is haemolytic, motile and resistant to γ-phage like other *B. cereus strains*. Direct fluorescence assays (DFA) reveal a cell wall but no capsule. However a capsule was expressed that is not a poly-γ-D-glutamic acid capsule. A proteome BLAST analysis shows that 60% of the proteome is more similar to a *B. cereus* proteome than a *B. anthracis* proteome (Hoffmaster et al., 2004). Proteomic and phenotypic analysis confirms that *B. cereus* G9241 is indeed a *B. cereus* sensu stricto species. *B. cereus* G9241 does not contain a nonsense frameshift mutation in the *plcR* gene synonymous with the *B. anthracis* species (Mignot et al., 2001). The chromosome of *B. cereus* G9241 contains a complete flagella biosynthetic cluster including 5 flagellin subunits.

The chromosome of *B. cereus* G9241 encodes a large range of toxins. Haemolysin A, BL, II and III are encoded on the chromosome (Hoffmaster et al., 2004). Haemolysin BL, *hblCDAB* is likely regulated by PlcR, determined by the PlcR box upstream of the gene in other *B. cereus* strains (Ivanova et al., 2003). The phospholipase C gene, *plcB* is present and under the control of PlcR. *B. cereus* G9241 also encodes the tripartite non-haemolytic enterotoxin *nheABC* within the chromosome, though the sequence contains a 96bp deletion at the beginning of the *nheA* gene (Swiecicka et al., 2006). The enterotoxin cytolysin K, *cytK* is also encoded on the chromosome. There is no evidence to suggest that *B. cereus* G9241 contains the emetic cereulide toxin. The range of diarrhoeal toxins is indicative of many *B. cereus* strains.

1.4.1.3. pBCX01

More interestingly, *B. cereus* G9241 contains 3 extrachromosomal elements (Hoffmaster et al., 2006; Hoffmaster et al., 2004). The 191,110 bp circular plasmid pBCX01 shares 99.6% sequence identity with the anthrax toxin plasmid, pX01 from *B. anthracis* strains. pBCX01 encodes the protective antigen (Pag), lethal factor (Lef), oedema factor (Cya) and AtxA regulator with 99.7%, 99%, 96% and 100% sequence identity to pX01 respectively. The identification of this plasmid has been controversial to the field of *B. cereus* sensu lato biology. As discussed previously, there exists a dogma that the regulators AtxA and PlcR are incompatible within a single organism (Mignot et al., 2001). However *B. cereus* G9241 contains fully intact DNA sequences that encode the PlcR and AtxA transcriptional regulators.

Haemolytic activity and PagA production have both been observed in *B. cereus* G9241 suggesting both regulators are functional and active. The pBCX01 plasmid also harbours a *hasACB* operon which encodes a hyaluronic acid (HA) capsule. AtxA is essential for the production of this capsule in *B. cereus* G9241. In a *B. cereus* G9241 *ΔatxA* strain there is a 150-fold reduction in hyaluronic capsule production (Scarff et al., 2016). The pBCX01 plasmid is essential for establishing a lethal infection in mice (Oh et al., 2011).

1.4.1.4. pBC210

pBC210 (previously referred to as pBC218) is analogous to, but shares little sequence identity with pX02 *of B. anthracis* (Hoffmaster et al., 2004). pBC210 encodes the *B. cereus* exo-polysaccharide (BPS) capsule biosynthesis genes, bpsXABCDEFGH. This capsule is also referred to as the tetrasaccharide capsule. *B. cereus* has been shown to produce both capsules forming an inner and an outer layer using BPS and HA respectively. Production of at least one of the capsules is essential for establishing a lethal infection in mice, albeit at a reduced mortality rate. BPS production occurs during infection of mice (Oh et al., 2011).

A novel toxin named certhrax is also encoded within the pBC210 plasmid (Fieldhouse et al., 2010). This toxin has 31% amino acid sequence identity with the lethal factor, Lef from *B. anthracis* and both are made of a PA-binding domain and a toxin domain. Lef binds to the protective antigen, PA to form the lethal toxin. Lethal toxin is an endopeptidase that triggers apoptosis in macrophages (Lehmann et al., 2009). Cytotoxic assays against mammalian cells reveal the certhrax toxin is 60-fold more toxic than Lef (Visschedyk et al., 2012). The certhrax toxin ADP-ribosylates vinculin. Vinculin is a protein that links the cytoskeleton and the extra cellular matrix. It is proposed that certhrax breaks the focal adhesion complexes between cells in tissues and leads to cell detachment. This may aid the mode of action of the anthrax tripartite toxin (Simon and Barbieri, 2014). However deleting the certhrax gene (*cer*) actually increases the virulence of *B. cereus* G9241 in mice. Only the enzymatic activity of the toxin domain decreases the virulence of *B. cereus* G9241 (Seldina et al., 2018).

Interestingly pBC210 also encodes gene products with amino acid sequences bearing partial sequence indentity to AtxA, and PagA of *B. anthracis* (Hoffmaster et al., 2004). Subsequently these genes have been named *atxA2* and *pagA2*. The amino acid sequence of AtxA2 is 79% identical to AtxA from *B. anthracis*. Despite the potential for redundancy, *atxA2* and *pagA2* play a unique role in the virulence of *B. cereus* G9241. Either AtxA or AtxA2 can positively regulate the production of BPS capsule. AtxA2 in the absence of AtxA is sufficient for

transcription of the anthrax toxin tripartite toxin genes, but the absence of AtxA2 does not significantly affect the level of toxin gene transcription (Scarff et al., 2016).

1.4.1.5. pBFH_1

pBFH_1 (previously referred to as pBClin29) is a 52,166 bp, linear phagemid (Hoffmaster et al., 2004; Oh et al., 2011). There is evidence to suggest that bacteriophages may play a role in the environmental survival of *B. anthracis* (Schuch and Fischetti, 2009). Though a sequence exists for the pBFH_1 phagemid, very little else is understood about if it contributes to the lifestyle of *B. cereus* G9241.

1.4.1.6. Regulation and compatibility of PlcR, AtxA and AtxA2

AtxA positively regulates anthrax toxin gene transcription on the pBCX01 plasmid but can also regulate the BPS capsule encoded by genes on pBC210 (Scarff et al., 2016). Dimerization of AtxA is required for it to function as a transcriptional regulator (Hammerstrom et al., 2011). AtxA2 is able to form homodimers as well as heterodimers with AtxA. AtxA homodimers have the most transcriptional activity and are stable structures, whereas AtxA2 homodimers have the lowest transcriptional activity and are relatively weak in structure (Scarff et al., 2016). AtxA/AtxA2 heterodimers are proposed to have an intermediate transcriptional activation activity. Subcutaneous and intranasal infection of mouse models with *B. cereus* G9241 spores shows that either AtxA or AtxA2 is sufficient for virulence (Scarff et al., 2016).

1.4.1.7. Differential transcription of genes in oxygenic and anaerobic environments in *B. cereus* G9241

Only one known transcriptional study has been conducted with *B. cereus* G9241 (Passalacqua et al., 2009). Within this study the transcriptional profile of *B. cereus* 10987, *B. cereus* G9241 and *B. anthracis* Sterne $34f_2$ strain were compared in O_2 and CO_2 conditions. Strain 10987 is a type strain of *B. cereus* and

Sterne $34f_2$ is an attenuated strain of *B. anthracis* that has been cured of the pX02 plasmid.

Of the three strains, *B. cereus* G9241 has the most genes differentially transcribed between the two growth conditions. Twenty-four genes from pBCX01 and 88 genes from pBC210 are more highly transcribed under CO_2 conditions compared to O_2 conditions. The *bps* operon, *atxA*, *lef* and *pagA* are all more highly transcribed by *B. cereus* G9241 in CO_2 compared to O_2 conditions. Genes more highly transcribed in O_2 conditions compared to CO_2 conditions include flagellin operons, *plcB*, *nhe* components and *hblCDA*.

B. cereus strain	Motile	Haemolytic	Gamma Phage Resistant	pX01 or pBCX01	pX02	pBC210	pBFH_1	*plcR*	*atxA*	*hasACB*	*bpsXABCDEFGH*	Reference
ATCC14579	Y	Y	Y	N	N	N	N	Y	N	N	N	(Hoffmaster et al., 2004)
G9241	Y	Y	Y	Y	N	Y	Y	Y	Y	Y	Y	
03BB87	Y	Y	Y	Y	N	Y	Y	Y	Y	Y[e]	Y	(Hoffmaster et al., 2006)
03BB102	Y	Y	Y	Y[a]	N	N	-	Y	Y	-	N	
03BB108	Y	Y	Y	Y[b]	N	N	-	Y	N	-	N	
FL2013	-	Y	Y	Y[c]	N	Y[f]	Y[d]	Y	Y	Y	N	(Marston et al., 2016)
Elc2	Y	Y	-	Y	N	N	-	Y	Y	Y[e]	N	(Wright, 2011)
LA2007	Y	Y	Y	Y	N	Y	Y	Y	Y	Y	Y	(Pena-Gonzalez et al., 2017)
Biovar Strains	Y	Y	Y	Y	Y	N	-	N	Y	Y	N	(Antonation et al., 2016; Klee et al., 2006)
B. anthracis	N	N	N	Y	Y	N	N	N	Y	N	N	(Oncu et al., 2003)

Table.1.2. Summary of phenotypic and genotypic analysis of known *B. cereus*/*B. anthracis* strains. Data on all known *B. cereus*/*B. anthracis* strains was collated. *B. cereus* and *B. anthracis* were included for direct comparison. The monomorphic nature of *B. anthracis* allows us to summarise the phenotypic and genotypic traits of the organism without focusing on a specific strain. Green/Y indicates if the phenotype is observed or if the gene/s are present with a complete sequence. Red/N indicates the phenotype was not observed or the gene is absent. Grey/- indicates the phenotype was never tested for, the genes were not screened for or commented on.

[a] – Not all pX01 ORFs amplified, only partial sequence identity to pX01; [b] – Not all pX01 ORFs amplified, only partial sequence identity to pX01, no anthrax tripartite toxin genes; [c] – 2.5 kbp deletion; [d] – Only 48 kbp contig identified with 98.74% sequence identity to pBFH_1 of *B. cereus* G9241; [e] – Presumed to be present as pBCX01 is complete sequence and a capsule has been observed by India ink staining; [f] – Only partial sequence, 108,352 bp of pBFC210 present.

1.4.2. Other *B. cereus*/*B. anthracis* crossover strains

1.4.2.1. *B. cereus* 03BB87, 03BB102 and 03BB108 – Texas isolates

In 2003 two otherwise healthy metalworkers died in Texas of a "fulminant *B. cereus* infection" (Avashia et al., 2007). Both presented with pneumonia and died from the progression of septicaemia and multiple organ failure. Two strains of *B. cereus* have been isolated from the two fatalities and one strain from the environment the two patients worked in (Hoffmaster et al., 2006). *B. cereus* 03BB102 and *B. cereus* 03BB87 are clinical isolates from the two fatalities and *B. cereus* 03BB108 was isolated from the environment.

All three strains were haemolytic, motile and resistant to gamma phage like *B. cereus* type strains. DFA reveals that none of the strains produce a *B. anthracis* capsule, but all have a *B. anthracis* cell wall. The two clinical isolates were seen to produce a non-poly-γ-D-glutamic acid capsule upon staining but the environmental isolate 03BB108 did not. Both clinical isolates contain a *pagA* sequence, but the environmental isolate does not. All three strains were screened for the presence of the anthrax plasmids pX01 and pX02, pBC210 and *B. anthracis*-specific chromosomal DNA.

The environmental strain *B. cereus* 03BB108 contains a partial sequence of pX01 but is missing the genes encoding the anthrax tripartite toxin, *lef*, *pagA* and *cya*. The pX02 and pBC210 plasmids are not present, but capsule genes homologous to those from pX02 are present. *B. cereus* 03BB102 contains genes with partial sequence identity to the pX01 plasmid. This includes the anthrax tripartite toxin genes, as well capsule genes encoded on pX02 in *B. anthracis. B. cereus* 03BB87 contains a full length pBCX01 and pBC210 plasmid, but no genes of pX02 were detected. 03BB87 also contains pBFH_1, called pBCN (Johnson et al., 2015b) None of the isolates contain signature DNA from the *B. anthracis* chromosome. Similar to the *B. cereus* biovar *anthracis* strains, the collection of strains isolated in Texas are *B. cereus* strains that have acquired *B. anthracis* extrachromosomal DNA.

Multilocus sequence typing (MLST) and amplified fragment length polymorphism (AFLP) show that *B. cereus* 03BB108 and *B. cereus* 03BB102 cluster together (fig 1.1). However *B. cereus* 03BB87 clusters together with *B. cereus* G9241.

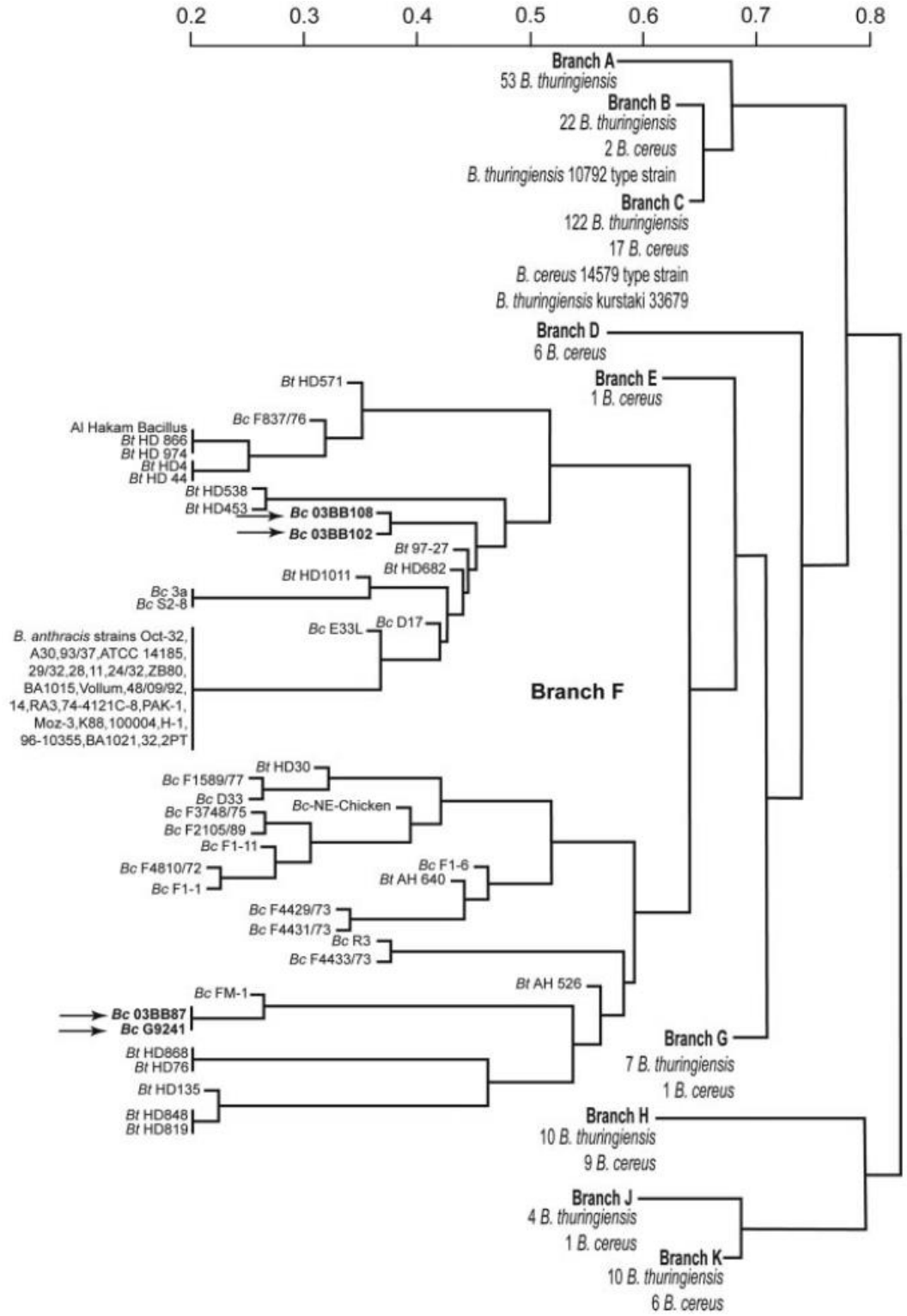

Fig.1.1. AFLP-based phylogeny tree for *B. anthracis*, *B. thuringiensis* and *B. cereus* isolates. Adapted from (Hoffmaster et al., 2006). *B. cereus* G9241, 03BB87, 03BB102 and 03BB108 are highlighted with arrows for clarity. All four strains cluster within the F branch with all known *B. anthracis* strains. *B. cereus* G9241 and 03BB87 cluster very closely together and may be classed as one strain. *B. cereus* 03BB102 and 03BB108 cluster together but are genetically distinct.

1.4.2.2. *B. cereus* FL2013 – Florida isolate

In 2013 a 70-year old male presented with an anthrax-like eschar on his cheek. The patient was hospitalised, treated and made a full recovery. The eschar was swabbed and bacteria isolated from it. The causative agent was a strain of *B. cereus* named *B. cereus* FL2013 (Marston et al., 2016). *B. cereus* FL2013 is haemolytic and resistant to γ-phage, indicative of a *B. cereus* strain, but motility has not been tested.

B. cereus FL2013 has an identical MLST sequence type as *B. cereus* G9241. Like *B. cereus* G9241, *B. cereus* FL2013 contains pBCX01 but with a 2.5 kbp deletion. Importantly the pBCX01 homologue in *B. cereus* FL2013 contains the anthrax tripartite toxin genes *pagA*, *lef* and *cya*, as well as the capsule operon *hasACB* with 100% sequence identity to the homologues of pBCX01 in *B. cereus* G9241. *B. cereus* FL2013 does not contain a pX02 homologue, but does contain a partial pBC210 sequence. 108,352 bp of pBC210 is present in *B. cereus* FL2013, but does not encode the *bpsXABCDEFGH* operon (Marston et al., 2016). A 48 kbp contig with 98.74% sequence identity to pBFH_1 is also present within *B. cereus* FL2013. *B. cereus* FL2013 is the only *B. cereus*/*B. anthracis* crossover strain to be known to have caused a cutaneous anthrax infection. Contrary to previous findings, the absence of the *bps* operon in *B. cereus* FL2013 suggests Bps capsule is not essential for infection (Hoffmaster et al., 2006).

1.4.2.3. *B. cereus* Elc2 – 2nd Texas Isolate

Following the infections seen in Texas in 2003, an otherwise healthy male welder also from Texas presented at a hospital with hemoptysis and shortness of breath. Despite antibiotic treatment and surgery, the man died 4 days later. Cultures were obtained from various organs of the body and a *B. cereus* strain was isolated from each one (Wright et al., 2011).

The *B. cereus* strain, named *B. cereus* Elc2 is haemolytic, motile and encapsulated. Full genome sequencing shows that *B. cereus* Elc2 contains a WT *plcR* gene and lacks three out of four of the *B. anthracis* prophage sequences. *B.*

cereus Elc2 contains a pBCX01 plasmid with a copy number of 4, but does not contain a pBC210 or pX02 homologue. MLST cluster analysis of 7 housekeeping genes shows that *B. cereus* Elc2 clusters closely with *B. cereus* 03BB102, and 033BB108, as well as *B. thuringiensis* Al Hakam (Wright et al., 2011).

1.4.2.4. *B. cereus* LA2007 – 2nd Louisiana isolate

In Louisiana in 1994, *B. cereus* G9241 was isolated from a welder as the etiological agent of an anthrax-like pneumonia (Hoffmaster et al., 2004). Thirteen years later another *B. cereus* strain, named *B. cereus* LA2007 was isolated from a female welder with a fatal case of pneumonia (Pena-Gonzalez et al., 2017).

The average nucleotide identity of *B. cereus* LA2007 is 99.99% similar to *B. cereus* G9241*, B. cereus* 03BB87 and *B. cereus* BcFL2013. *B. cereus* LA2007 also contains pBCX01 and pBC210 plasmids with 99.99% and 99.98% similarity to the equivalent plasmids of *B. cereus* G9241. Subsequently, all three genes encoding the anthrax tripartite toxins as well as both the *hasACB* and *bpsXABCDEFGH* capsule operons are present and intact (Pena-Gonzalez et al., 2017).

1.4.3. *B. cereus* biovar *anthracis*

An ongoing debate in the biology of the *B. cereus* sensu lato is that *B. cereus*, *B. thuringiensis* and *B. anthracis* are not separate species at a genetic level (Helgason et al., 2000). The classification of them as distinct species relies on phenotypic differences and the acquisition of extrachromosomal DNA. This lack of clarity on what defines each species is further compounded by the discovery and classification of the *B. cereus* biovar (bv) *anthracis* cluster of bacteria.

Five *B. cereus* bv *anthracis* strains have been isolated from West and central Africa (Antonation et al., 2016; Klee et al., 2006). The strains were isolated from chimpanzees, gorillas, elephants and goats. All five strains contain plasmids that are almost identical in sequence to pX01 and pX02 of *B. anthracis,* named pBCX01 and pBCX02 respectively. All five strains contain a frameshift mutation in the *plcR* gene and it is assumed this mutation creates a functional PlcR knockout. Subsequently all strains show no phospholipase C activity, indicative of a *plcR*

knockout, nor do the strains display any haemolytic activity. These genotypic and phenotypic traits are characteristic of the *B.* anthracis species. However, all strains are motile and resistant to Gamma phage, phenotypes characteristic of the *B. cereus* species (Marston et al., 2006).

Phylogenomic analysis using single nucleotide polymorphisms (SNPs) from both the chromosomal DNA and the plasmid DNA has revealed that *B. cereus* biovar *anthracis* forms a unique clade within the *B. cereus* sensu lato (fig 1.2). When the SNPs from the chromosome are analysed, the bv clade is most closely related to *B. cereus* ISP3191. However when plasmid SNPs are analysed the bv clade is most closely related to *B. anthracis*. Interestingly *B. cereus* ISP3191 also contains a frameshift mutation in the *plcR* gene. It has been proposed that these *B. cereus* strains have horizontally acquired the anthracis-like plasmids (Böhm et al., 2015). Whether or not the frameshift mutation in *plcR* is a cause or an effect of this acquisition has not been investigated.

Arguably the strains of the *B. cereus* biovar *anthracis* clade are more similar to *B. anthracis* species than *B. cereus* species. Bv strains don't translate a functional PlcR transcriptional regulator, but do contain genes encoding the AtxA regulator and cause an acute death in various animals (Leendertz et al., 2004; Zimmermann et al., 2017).

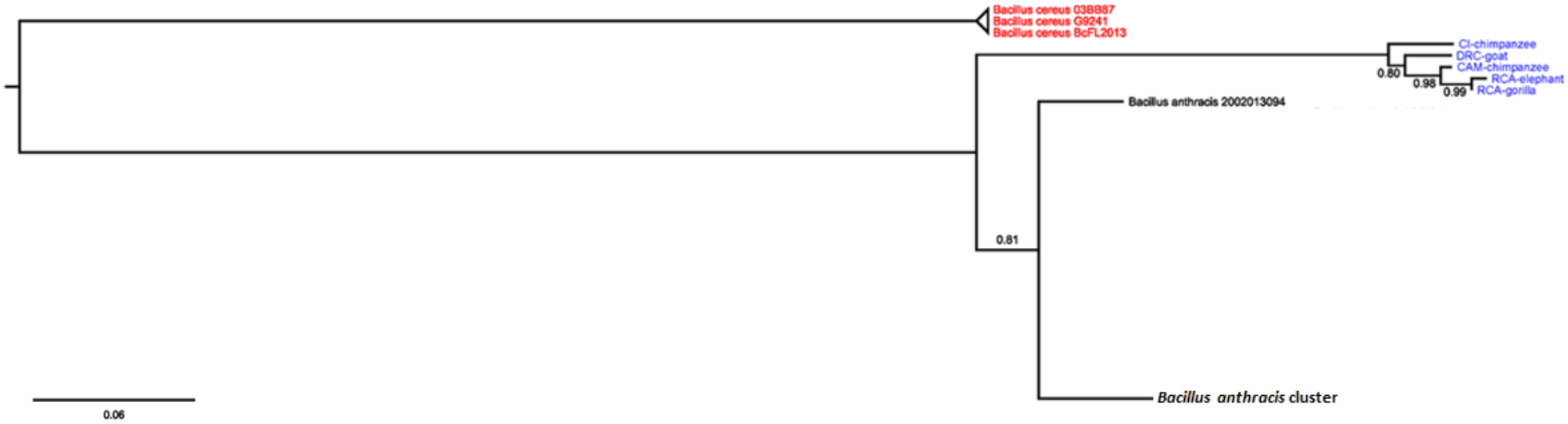

Fig.1.2. Maximum likelihood tree based on core pX01/pBCX01 SNP data. Adapted from (Antonation et al., 2016). Black denotes *B. anthracis* species. Blue denotes *B. cereus* biovar *anthracis* strains. Red denotes true *B. cereus*/*B. anthracis* crossover strains that contain the pBCX01 plasmid. It is clear that the biovar strains and *B. cereus*/*B. anthracis* strains are genetically distinct based on the sequence of the anthrax toxin plasmid they contain. Branch support values were estimated by approximate likelihood ratio tests and are only reported for internal branches not supported by maximal values. Tree was rooted with TempEst v1.5.

1.5. Sporulation in the *B. cereus* sensu lato

1.5.1. Sporulation in the lifestyle and virulence of *B. cereus* sensu lato

1.5.1.1. Sporulation of *B. cereus* sensu stricto

Spores of *B. cereus* sensu stricto are consistent in composition with other *Bacilli* spores. The core is encased by the inner membrane, the spore cortex, the inner coat and the outer coat in that order (Kotiranta et al., 2000). Spore formation allows *B. cereus* to survive in the low nutrient soil environment (Carlson et al., 2018a). Spores of *B. cereus* have also been isolated from high and low temperature environments throughout the dairy farming pasteurisation process (Scheldeman et al., 2005). Spores are able to survive ingestion by cows and have been found in their faeces and raw milk (Magnusson et al., 2007). The spores of *B. cereus* are extremely hydrophobic, especially compared to other *Bacillus* spores (Peng et al., 2001). This hydrophobicity is advantageous as a virulence factor as it allows stronger binding to surfaces. Spores of *B. cereus* strains that cause food poisoning can bind human epithelial cells to cause gastrointestinal disease (Andersson et al., 1998). Spore formation in *B. cereus* G9241, similar to *B. anthracis* may also allow for macrophage escape and immune evasion leading to a lethal systemic infection (Oh et al., 2011). In summary, sporulation of *B. cereus* is advantageous to its survival in a variety of environments, but also to its virulence.

1.5.1.2. Sporulation of *B. anthracis*

Sporulation in *B. anthracis* is widely and well-studied. This is due to the fact that in *B. anthracis* sporulation is not just advantageous to survival but essential for its ecological niche (Carlson et al., 2018a). In the environment, *B. anthracis* survives in warm, slightly alkaline soils (Van Ness, 1971). It is a matter of discussion whether *B. anthracis* populations in the soil survive in a vegetative cell cycle or as dormant spores. *B. anthracis* have been shown to germinate and form

stable populations of vegetative cells in sterile soils and rhizospheres (Minett and Dhanda, 1941; Saile and Koehler, 2006). However germinating spores in more natural soil environments leads to the death of vegetative cells (Bowen and Turnbull, 1992). Because of these findings, it is reported that sporulation is essential for *B. anthracis* survival in the environment, i.e. outside of a host.

Vegetative cells of *B. anthracis* can cause a host infection in laboratory conditions (van Sorge et al., 2008). However natural incidents of *B. anthracis* infection only occur when the infective particle is a spore. The spore morphology plays an essential role in virulence of *B. anthracis*. Upon ingestion of spores, various components of the spore coat and exosporium interact with immune cells to trigger engulfment for systemic infection (Basu et al., 2007).

1.5.2. Mechanism of sporulation in *Bacillus* genus

1.5.2.1. Overview of sporulation

A defining feature of the *Bacillus* genus is the ability to form endospores as part of their life cycle when facing environmental stressors. Stresses include limited nutrient availability, high and low temperatures, chemical stress amongst others. The mechanism of sporulation is a well conserved regulatory pathway amongst *Bacilli* (de Vries et al., 2004; Piggot and Hilbert, 2004). Due to the highly conserved nature of the regulatory pathway for sporulation, the vast majority of the research has been conducted in *B. subtilis* but is largely analogous to regulation of sporulation in *B. cereus* species. In brief, the spore cycle proceeds in eight distinct stages, named 0-VII (Ryter, 1965). At stage 0 and stage I the cell is preparing for sporulation by sensing the environment and replicating the genome. Stage II concerns the septation of the cell into the mother cell and the forespore and stage III sees the engulfment of the forespore. Coat and cortex assembly occur during stage IV and V. The spore matures and the mother cell lyses during stage VI and stage VII respectively.

In this study we will focus on the biochemical processes of the cell during stage 0. Stage 0 concerns the commitment to sporulation. By focusing on this early

stage of sporulation, we lessen the need to work with mature spores, known to be the infective form of *B. anthracis* (Ross, 1957).

1.5.2.2. Stage 0 phosphorelay

Sporulation in *Bacillus* is an irreversible process that is an energy intensive commitment for the cell. Because of this, initiation of sporulation is a tightly controlled process. Before a bacterial population commits to sporulation there will be several survival tactics to avoid the process. These include increasing motility to find other food sources, increasing competence to acquire advantageous genetic information and even cannibalism of bacteria within the population (Höfler et al., 2016; Msadek et al., 1998; Schultz et al., 2009). Concurrent to regulating alternative survival mechanisms, initiation of sporulation is regulated by many environmental and cell stressors (fig 1.3).

These include but are not limited to, cell density, DNA damage, redox state and nutrient availability (Grossman and LoSICK, 1988; Ochi et al., 1981; Okegbe et al., 2014; Oppenheimer-Shaanan et al., 2011). Environmental stressors are integrated into the initiation of sporulation via a multicomponent phosphorelay. In *Bacillus* species the phosphorelay is composed of five two-component sensor kinases (KinA-E), two phosphotransferases (Spo0B and spo0F) and the regulator of initiation of sporulation (Spo0A). The five histidine kinases KinA-E are thought to be the environmental sensors. KinA-E bind different ligands allowing *Bacilli* to sense various environmental stresses (Jiang et al., 2000). Upon ligand binding, the kinases auto-phosphorylate. The phosphoryl group is transferred down the phosphorelay to Spo0A via phosphotransferases Spo0F and spo0B.

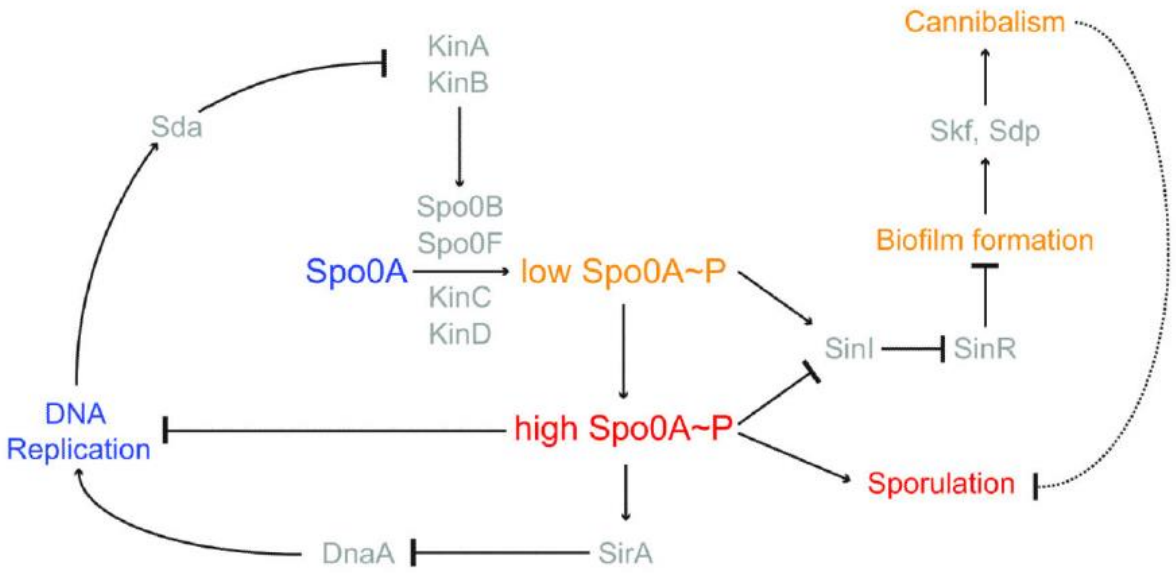

Fig.1.3. Regulation of sporulation initiation depends on high threshold levels of Spo0A-P. Adapted from (Tan and Ramamurthi, 2014). Arrow heads represent positive regulation of a pathway, gene or protein. Bars represent repression of a pathway, gene or protein. *Sda is only positively regulated upon DNA replication errors.

1.5.2.3. Spo0A transcriptional activator

Spo0A is a transcriptional activator and is itself activated upon phosphorylation (Baldus et al., 1994). The Spo0A operon contains approximately 121 genes in *B. subtilis* (Fujita et al., 2005). Spo0A is in constant flux between phosphorylated (Spo0A-P) and dephosphorylated forms (Fujita and Losick, 2005; Molle et al., 2003a). When sufficient environmental stimuli are present, the phosphorelay equilibrium shifts towards the phosphorylation of Spo0A. This operon contains four different regulatory mechanisms: genes activated at high levels of Spo0A-P, genes activated at low levels of Spo0A-P, genes repressed at high levels of Spo0A-P and genes repressed at low levels of Spo0A-P (fig 1.4). It should be noted that some evidence exists that disputes this model (Levine et al., 2012). The differential regulation by low and high levels of Spo0A-P is made possible by different binding affinities to sequences upstream of genes in the regulon. Survival genes such as spore killing factor, *skf* are in the regulon activated at low levels of Spo0A-P (Fujita et al., 2005). Skf is a protein that kills non-sporulating sister cells to provide a food source for the subpopulation of sporulating cells (González-Pastor et al., 2003). This allows the cell to respond to low levels of environmental stress with alternative survival tactics. The accumulation of environmental signals eventually leads to a high level of Spo0A-P and the transcriptional activation of genes with a low binding affinity for Spo0A-P. Genes identified in this regulon include *racA*, *spoIIG*, *spoIIE* and *spoIIA* (Fujita et al., 2005). RacA helps anchor chromosomal proteins during stage I of the sporulation cycle, whereas SpoIIG, SpoIIE and SpoIIA are positive regulators of the transition into stage II of the sporulation pathway (Piggot and Hilbert, 2004; Wu and Errington, 2003).

Category and gene	Function
High-threshold activated	
spoIIG	pro-σ^E processing protease/σ^E factor
spoIIE	Ser phosphatase (σ^F activation)/asymmetric septum formation
racA	Remodeling and anchoring of the chromosome
spoIIA	Anti-anti-σ^F/anti/σ^F/σ^F
yneE	Unknown
yttP	Similar to transcriptional regulator (TetR/AcrR family)
sinI	Antagonist of SinR (transcriptional regulator)
High-threshold repressed	
rapA	Asp phosphatase (dephosphorylation of Spo0F-P)
flgB	*fla/che* operon: motility and chemotaxis
ftsE	Cell division protein (ATP binding)
lytE	Cell wall hydrolase
divIVA	Cell division protein
yfmI	Similar to macrolide efflux transporter
yxbC	Unknown
sdp	Sporulation delaying protein
dltA	D-Alanyl-D-alanine carrier protein ligase
rocD	Ornithine aminotransferase
Low-threshold activated	
yxbC	Unknown
sdp	Sporulation delaying protein
yfmI	Similar to macrolide efflux transporter
yqcG	Unknown
yybN	Unknown
skf	Sporulation killing factor
yjcM	Unknown
rapA	Asp phosphatase (dephosphorylation of Spo0F-P)
spo0A	Transcriptional master regulator for sporulation
yqxI	Unknown
kinA	Sensor histidine kinase (initiation of sporulation)
ykzF	Unknown
spo0F	Response regulator (multicomponent P-relay)
Low-threshold repressed	
abrB	Transcriptional pleiotropic regulator of transition stage genes
fruR	Transcriptional repressor of the fructose operon
yqzD	Unknown
ykaA	Unknown
purT	Phosphoribosylglycinamide formyltransferase 2
med	Positive regulator of *comK*

Table.1.3. Gene regulation by Spo0A-P in *Bacillus subtilis.* Adapted from (Fujita et al., 2005). The regulon of Spo0A-P depends on the level of the phosphorylated protein. Genes involved in cell survival strategies, such as cannibalism (*skf*) and antimicrobial resistance (*yfmI*) are activated at low-threshold levels of Spo0A-P. Genes involved in propagating sporulation (*spoIIG*, *spoIIE*, *spoIIA*) are activated at high-threshold levels of Spo0A-P.

1.5.2.4. Integrating environmental signals into the phosphorelay

Various environmental signals feed into the phosphorelay during stage 0 of sporulation. Whilst there are many stresses are known to trigger sporulation in *Bacilli*, the mechanisms through which these stresses act have not yet been fully elucidated. The five histidine kinases act as the primary environmental sensors (fig 1.4).

KinA contains a PAS domain which binds ATP (Stephenson and Hoch, 2001). The presence of the PAS domain suggests that KinA is involved in sensing the redox state of the cell. Autophosphorylation of KinA is inhibited by the protein Sda (Rowland et al., 2004). Sda is a checkpoint protein upregulated upon DNA damage or replication stress (Burkholder et al., 2001). This prevents the production of spores with DNA damage.

When nutrient availability is high, the stringent response transcriptional regulator CodY is bound to GTP. CodY-GTP represses the transcription of *kinB* (Tojo et al., 2013). Via this mechanism *kinB* and its gene product KinB senses nutrient availability and regulates sporulation accordingly. When nutrient availability is high, CodY-GTP represses the transcription of *kinB*, which subsequently lowers the amount of Spo0A being phosphorylated. However when nutrient availability decreases CodY-GTP levels drop dramatically. This leads to the derepression of *kinB* and subsequently increases the levels of Spo0A-P leading to sporulation.

KinC is thought to be activated as a result of treating cells with surfactin (López et al., 2009). Surfactin is a strong surfactant that causes membrane permeabilization and is commonly used as an antimicrobial (Carrillo et al., 2003). KinC has been proposed to activate the phosphorelay in response to cell membrane stress caused by potassium leakage (López et al., 2009; Yepes et al., 2012). However some evidence exists in contrary to this (Devi et al., 2015). The KinD protein has recently been co-crystalized with its ligand pyruvate. Pyruvate binds two PAS domains located on a membrane distal loop (Wu et al., 2013). Because pyruvate has been identified as a ligand for KinD, it is believed that KinD

senses nutrient availability in the environment (Piggot and Hilbert, 2004). No known mechanism of action has been elucidated for how KinE activates the phosphorelay.

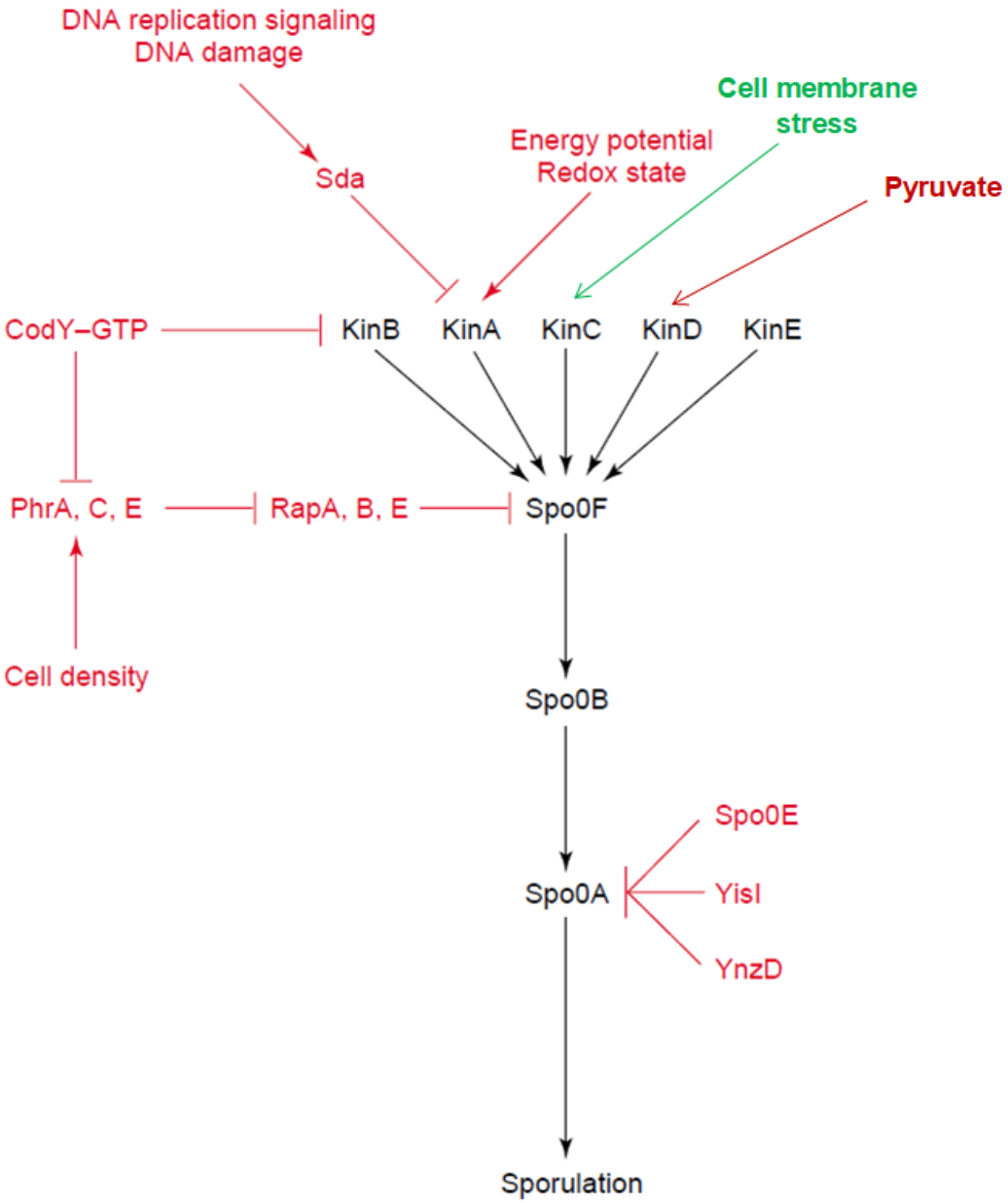

Fig.1.4. Sporulation stage 0. The Spo0A phosphorelay dictates the initiation of sporulation in *Bacilli* (Piggot and Hilbert, 2004). The phosphorelay is highlighted black. Red indicates the input from other regulatory pathways and stresses. Green indicates regulation mechanisms disputed in the literature.

Autophosphorylation of the histidine kinases is not the only point of control for the Spo0A phosphorelay. During vegetative growth, Spo0F is dephosphorylated by the three phosphatases RapA, RapB and RapE (Diaz et al., 2012). This prevents the phosphorylation of Spo0A and the initiation of sporulation. However, Rap proteins are inhibited by phosphatase repressor proteins PhrA, PhrC and PhrE (Gallego del Sol and Marina, 2013). When Phr proteins are abundant in the cell the Rap proteins phosphatase activity is repressed and thus Spo0A can be phosphorylated by the relay.

Like the PapR protein from *B. cereus*, Phr proteins are exported from cells, processed and reimported as pentapeptides (Grenha et al., 2013; Stephenson et al., 2003). These pentapeptides are the active form of the Phr proteins and function as inhibitors of the phosphatase Rap proteins. In this sense the Phr proteins are quorum sensing molecules that allow *Bacilli* to sense the cell density of the population (Bischofs et al., 2009). Therefore at high cell densities, sporulation can be activated. Phr proteins also integrate the signal for nutrient availability. CodY-GTP represses the transcription of *phrA* and *phrE* (Molle et al., 2003b). Therefore when nutrients are readily available and cell density is low, there is a low abundance of Phr proteins. This leads to a high phosphatase activity by Rap proteins and subsequently the prevention of the initiation of sporulation.

Spo0E and its homologues YisI and YnzD are Spo0A-P phosphatases. *spo0E* is under transcriptional repression by the transition state regulator AbrB (Kobir et al., 2014). As the cell density increases in a population, more Spo0A-P accumulates. Spo0A-P represses the transcription of *abrB*. Subsequently high Spo0A-P levels leads to the derepression of spo0E, which in turn dephosphorylates Spo0A-P (Perego et al., 1988; Shafikhani and Leighton, 2004). This auto-feedback loop is believed to be a final checkpoint to allow the cell to explore alternative survival mechanisms before committing irreversibly to sporulation.

1.5.3. The role of PlcR in sporulation of *B. cereus* sensu lato

PlcR is a pleiotropic regulator of virulence in *B. cereus* sensu lato (Salamitou et al., 2000). As discussed previously, *plcR* transcription is highest during late exponential phase. Spo0A-P has been shown to repress the transcription of *plcR* in *B. thuringiensis* (Lereclus et al., 2000). Spo0A-P levels increase during transition phase due to decreased nutrient availability and increased cell density. Thus *plcR* transcription is repressed during the onset of transition phase by the activity of Spo0A-P. Upstream of the *plcR* gene is the PlcR box needed for positive autoregulation. Spo0A-P binds to two 0A boxes situated either side of the PlcR box upstream of *plcR* (Lereclus et al., 2000). It is proposed that Spo0A-P represses the transcription of *plcR* by physically blocking PlcR binding to the PlcR box. Interestingly, when a functional *plcR* operon is forcibly expressed in *B. anthracis*, sporulation efficiency is reduced to 20% (Mignot et al., 2001). However in a pX01-cured background, forced expression of PlcR does not result in a reduction of sporulation in *B. anthracis*. In combination these observations suggest a role for both PlcR and AtxA in sporulation.

1.5.4. The roles of AtxA in sporulation

B. anthracis and the emerging *B. cereus/B. anthracis* crossover strains are defined by the extrachromosomal DNA they have acquired. Given that sporulation is essential for virulence of these strains it is not unfeasible to suggest that acquired genetic information may have altered the regulation of sporulation in these strains.

pX01 encodes the global virulence regulator AtxA (Okinaka et al., 1999b). AtxA regulates the transcription of genes in the chromosome and on both *B. anthracis* virulence plasmids (Fouet, 2010; Uchida et al., 1997). AtxA positively regulates two signal sensor domains located on pX01 and pX02 (White et al., 2006). These signal sensor domains are homologous to the signal sensor domain of a chromosomally encoded histidine kinase BA2291, *B. anthracis* Ames strain designation. These domains propagate the Spo0A phosphorylation cascade when

expressed in *B. subtilis*. However when expressed in *B. anthracis* they inhibit the sporulation phosphorelay via phosphatase action (Stranzl et al., 2011). Subsequently, AtxA expression has an inverse relationship with sporulation in a pX02-dependent manner (Dale et al., 2018).

Five histidine kinases initiate the Spo0A phosphorelay in *B. subtilis*. The sensor domains of the five kinases are very poorly conserved between *B. subtilis* and *B. anthracis* (Brunsing et al., 2005). Potential Spo0A kinases have been identified in *B. anthracis*, but two contain frameshift mutations in all *B. anthracis* strains. One of these frameshift mutations also exists in *B. cereus* G9241. It has been proposed that acquisition of pX01 or its homologue pBCX01 has potentially led to a reduction in activation of the Spo0A phosphorelay to aid pathogenesis.

As pX01 and pBCX01 share such a high sequence identity, it is assumed that proteins encoded by pX01 can in theory also be expressed in pBCX01-containing strains. However due to differences in chromosomal and plasmodial DNA of different strains, patterns of regulation cannot be assumed to be identical between pX01- and pBCX01- containing strains.

1.6. Phage in *B. cereus* sensu lato

Phage that infect the *B. cereus* sensu lato have been known of since the 1960s (Stiube and Dimitriu, 1969). However the understanding of the role of these phage in the lifestyles of the *B. cereus* sensu lato is not well understood. All *B. cereus* sensu lato phage identified are dsDNA viruses and belong to the order *Caudovirales* or the family *Tectiviridae*. Phage of the order *Caudovirales* are tailed phages belonging to one of three families: *Myoviridae*, *Siphoviridae* or *Podoviridae*. These families are defined by long contractile tails, long non-contractile tails and short non-contractile tails respectively (Gillis and Mahillon, 2014). Tectiviridae are icosahedral phage with an internal lipid vesicle (Ackermann, 2006). Phages of the *B. cereus* sensu lato have a range of diverse lifestyles including virulent phages, chromosome-integrated, plasmid-integrated or replicating as an independent genetic element. We should consider why phage has propagated and what evolutionary advantage they confer to *B. cereus*.

Transducing phages have been shown to aid horizontal gene transfer amongst *B. cereus* species, including antibiotic resistance cassettes (Ruhfel et al., 1984). Phage CP-51 was able to transfer the pX02 plasmid from *B. anthracis* into a *B. cereus* strain and induce capsule production (Green et al., 1985). CP-51 is also able to infect spores of *B. cereus* (Thorne, 1968). As well as transduction of advantageous genetic material, phages have been shown to be able to regulate sporulation. Phage phiCM3 from *B. thuringiensis* YM-03 encodes a SpoIIIE protein which may allow some regulation of sporulation in a host cell (Yuan et al., 2014). A virulent phage called Fah isolated from *B. anthracis* also encodes a SpoIIIE protein as well as the sigma factor σ^{Fah} (Minakhin et al., 2005). σ^{Fah} has homology to σ^{F} of *B. cereus* and may play a role in regulating sporulation. A 1967 study suggests that lysogeny by phage is essential for efficient sporulation of *B. anthracis*, though it isn't essential for virulence (Vera et al., 1968).

A genotyping method for differentiating *B. anthracis* from other species of the *B. cereus* sensu lato is detecting the presence of four putative prophages, lambdaBa01-04 (Read et al., 2003). These prophage regions have been identified as conserved in over 300 geographically divergent strains, but do not produce a viable phage particle under any condition (Sozhamannan et al., 2006). These prophage regions encode antibiotic resistance factors, regulatory proteins, membrane proteins and secreted proteins thought to be involved in interactions with the mammalian immune response (Read et al., 2003).

A range of lysogenic *B. anthracis* phages isolated from earthworm guts, soil and fern roots are able to specifically regulate several phenotypes of *B. anthracis* Sterne strains (Schuch and Fischetti, 2009). Lysogeny by phage alters cell morphology, sporulation and spore morphology. Phages were either able to block sporulation completely, or to rapidly increase the rate of sporulation. The ability to regulate sporulation may be due to proteins encoded by the phage DNA. Several genes encode proteins with partial similarity to σ^{F} and σ^{G}; both of which are transcriptional activators during spore formation (Piggot and Hilbert, 2004). It is clear that phages of the *B. cereus* sensu lato can alter various

phenotypes of the host bacterium. However, any mechanisms of regulation have not been elucidated.

1.7. Background to this project

Prior to this work, supernatants of *B. cereus* G9241 cultures growing exponentially (OD_{600} = 0.5) at 25 °C and 37 °C were extracted. Comparable supernatants were extracted from cultures of *B. cereus* ATCC14579, *B. thuringiensis ΔplcR*, *B. cereus* G9241 pBCX01$^-$ and *B. anthracis* Sterne. *B. cereus* ATCC14579 is a control *B. cereus* type strain. *B. thuringiensis ΔplcR* is widely accepted as analogous to a *B. cereus ΔplcR* strain. *B. cereus* G9241 pBCX01$^-$ is missing the regulator and components of the anthrax tripartite toxin: *atxA*, *lef*, *pagA* and *cya*. *B. anthracis* Sterne strain contains a functional anthrax tripartite toxin but is missing pX02.

Cytotoxicity of the collected supernatants was assayed against *Manduca sexta* haemocytes and human T2 lymphocytes. The supernatants showed the same pattern of toxicity against both the *M. sexta* haemocytes and the human T2 lymphocyte cells (fig 1.5). *B. cereus* ATCC14579 supernatant taken at 25 °C was highly toxic to haemocytes and lymphocytes, as was supernatant taken at 37 °C. Comparatively *B. anthracis* supernatant at either temperature showed little to no toxicity. This is consistent with the highly toxic secretion profile of *B. cereus* strains and the quiescence of *B. anthracis* cells. Similar to *B. anthracis* supernatant, *B. thuringiensis ΔplcR* supernatant was not toxic at either temperature to either cell line.

This suggests that the toxicity seen with the *B. cereus* ATCC14579 supernatant is mediated by PlcR. Supernatants taken at 25 °C from *B. cereus* G9241 and *B. cereus* G9241 pBCX01$^-$ were both toxic to haemocytes and lymphocytes. However, when supernatants were taken from 37 °C grown cultures, no toxicity was observed from either strain against any of the cell lines. Curing pBCX01 does not affect the toxicity of the supernatant and therefore the toxicity is likely not mediated by AtxA. *B. cereus* G9241 was also seen to be motile at 25 °C but lost motility at 37 °C.

In summary, at 25 °C *B. cereus* G9241 produces cytotoxic supernatants (likely mediated by PlcR) and is motile. However, at 37 °C *B. cereus* G9241 does not produce cytotoxic supernatants and is immotile. This switch in phenotypes is comparable to a switch between *B. cereus* and *B. anthracis* phenotypic traits.

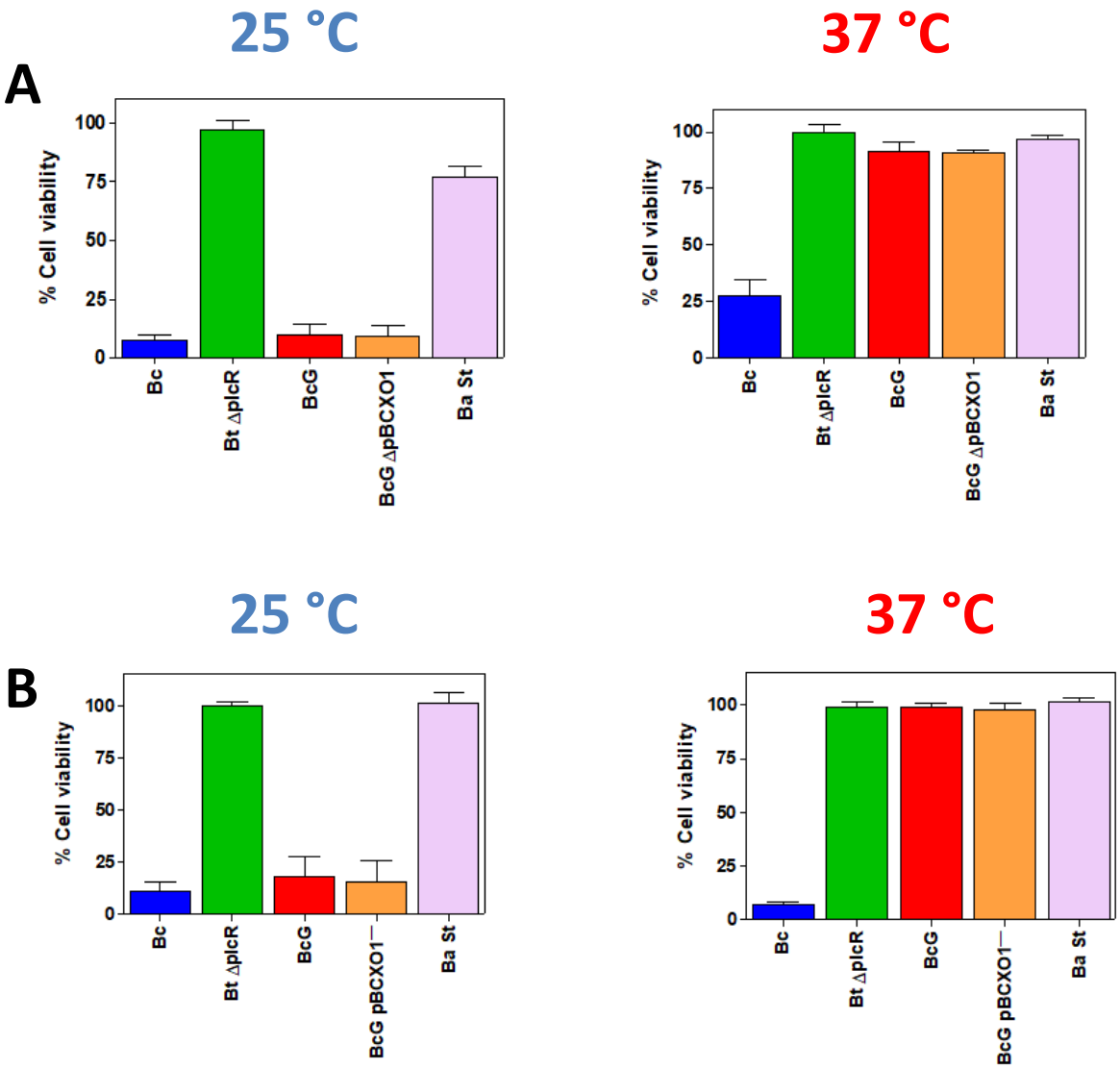

Fig.1.5. Cytotoxicity of supernatants extracted from *B. cereus* sensu lato strains against *Manduca sexta* haemocytes (A) and human T2 lymphocytes (B) is affected by growth temperature. Bc – *Bacillus cereus* ATCC14579, Bt – *Bacillus thuringiensis*, BcG – *Bacillus cereus* G9241, Ba – *Bacillus anthracis. B. cereus* supernatants are highly cytotoxic regardless of growth temperature, contrastingly *B. anthracis* and Bt *ΔplcR* supernatants show no cytotoxicity at all. BcG supernatant is cytotoxic at 25 °C but not at 37 °C. This cytotoxicity is independent of pBCX01.

1.8. Aims and Objectives

Overall, this study was designed to investigate the temperature-dependent haemolytic and cytotoxic phenotypes of *B. cereus* G9241. Investigating this and other temperature-dependent phenotypes may provide us with a better view of the ecological niche that *B. cereus* G9241 occupies. We may also gain a greater understanding of how this strain and other *cereus-anthracis* crossover strains accommodate functional copies of *plcR* and *atxA* in their genomes.

This study had the following specific aims:

1. To understand and characterise the temperature-dependent haemolytic phenotype observed in *B. cereus* G9241.

2. To investigate the transcriptional landscape of *B. cereus* G9241 to understand the role of PlcR and AtxA in global gene regulation.

3. To analyse the transcriptome and proteome of *B. cereus* G9241 to determine what causes the temperature-dependent haemolytic phenotype of the supernatant.

4. To discover phenotypes that may propose an ecological niche for *B. cereus* G9241 and other *cereus-anthracis* crossover strains.

5. To elucidate the role of pBFH_1 phagemid in *B. cereus* G9241 and to determine if the acquisition of this phagemid has contributed to its unique lifestyle.

2. Materials and Methods

2.1 Bacterial strains, media, plasmids and primers

2.1.1 Bacterial strains used in this study

Strain	Genotype	Source
Bacillus cereus ATCC14579	Wild Type	Ivanova et al., 2003
Bacillus cereus G9241	Wild Type	Hoffmaster et al., 2004
Bacillus cereus G9241	ΔpBCX01	This study
Escherichia coli ET12567/pUZ8002 (referred to as *E.coli* ET12567 herein)	F- *dam*-13::Tn9 *dcm*-6 *hsdM hsdR zjj*-202::Tn10 *recF143 galK2 galT22 ara-14 lacY*1 *xyl*-5 *leuB*6 *thi*-1 *tonA*31 *rpsL*136 *hisG*4 *tsx*-78 *mtl*-1 *glnV*44, pUZ8002 (Kan^R)	Macneil et al., 1992
Escherichia coli DH5α		NEB
Bacillus thuringiensis kurstaki	*plcR*$^-$	(Hernández-Rodriguez et al., 2013)

Table 2.1. Bacterial strains used in this study and their sources.

2.1.2 Plasmids used in this study

Plasmid	Description	Source
pBFH_1	Phagemid, isolated from *B. cereus* G9241	This study
pRN5101	Suicide vector used to create knock-out mutants in *B. cereus sensu lato*	Derived from pE194 (Villafane et al., 1987)
pHT304	Low-copy shuttle vector for *B. cereus sensu lato*	(Arantes and Lereclus, 1991)
pHT315	Low-copy shuttle vector for *B. cereus*	(Arantes and

	sensu lato	Lereclus, 1991)

Table 2.2. Plasmids used in this study and their sources.

2.1.3 Media and reagents used in this study

Name	Formula	Source
SOC Outgrowth Medium	2% Vegetable Peptone 0.5% Yeast Extract 10 mM NaCl 2.5 mM KCl 10 mM $MgCl_2$ 10 mM $MgSO_4$ 20 mM Glucose	New England BioLabs (NEB)
Laemlli Buffer (2x)	65.8 mM Tris-HCl, pH 6.8 26.3% (w/v) glycerol 2.1% SDS 0.01% bromophenol blue	Bio-Rad
Brain-Heart Infusion Broth	Beef heart, 5 g L^{-1} Calf brains 12.5 g L^{-1} Disodium hydrogen phosphate 2.5 g L^{-1} $D(^{+})$-glucose 2 g L^{-1} Peptone 10 g L^{-1} NaCl 5 g L^{-1}	Sigma-Aldrich®
Lysogeny Broth (LB)	Tryptone 10 g L^{-1} Yeast Extract 5 g L^{-1} NaCl 10 g L^{-1}	
E.coli transformation Solution I	10 nM Sodium acetate 50 mM $MnCl_2$ 5 mM NaCl pH 5.6 - 6	
E.coli	10 mM Sodium acetate	

transformation Solution II	5% Glycerol 70 mM $CaCl_2$ 5 mM $MnCl_2$ pH 5.6 - 6	
TM Buffer	20 mM Tris-HCl 20 mM $MgCl_2$ pH 7.4	
TAE Buffer (50x)	Tris Base 242 g L^{-1} 0.0571% (v/v) Acetic acid 10% 500 mM EDTA (pH 8) pH 8.3	

Table 2.3. Media and reagents used in this study and their sources, if applicable.

2.1.4. Primers used in this study

Primer No.	Primer Name	Primer Sequence 5' to 3'
Reverse Transcription PCR		
1	gatB_For	AGCTGGTCGTGAAGACCTTG
2	gatB_Rev	CGGCATAACAGCAGTCATCA
3	BcA_plcR_For	CCTGAATTCCAGCAATTTCTTCAATG
4	BcA_plcR_Rev	CCATCGTACTCCAACTTCCC
5	BcA_papR_For	ATGAAGAAATTACTTATTGGTAGTTTATTAAC
6	BcA_papR_Rev	TAATATTCAAAAGGTAAATCTTTAGCTAATTG
7	BcA_cytK_For	ACGACTGTAACATCTAGCGTATC
8	BcA_cytK_Rev	CCAACCCAGTTTGCAGTTCC
9	BcG_plcR_For	AAATTGTCCACCAATCATACGGAG
10	BcG_plcR_Rev	ATACTCTAATTTCTCCAGGCACTC
11	BcG_papR_For	ATGAAAAAATTACTTATTGGTAGTCTATTAAC
12	BcG_papR_Rev	AATGTTCAAATGGTAAATCTGAAGCTAATTG
13	BcG_cytK_For	ACAAATGCTGTAGAAGAAACGACTG
14	BcG_cytK_Rev	CCAACCCAGTTTGCAGTTCC
15	nheABC_For	ATGGCGAAGGACACAAATAG
16	nheABC_Rev	TACATCTTTCCAGCTATCTTTCG

17	plcB_For	CAAGAATATCCAAATCAAACAGCG
18	plcB_Rev	GCCATGATGTAACAGTCCAC
19	sfp_For	GTATTGATGTGTACGGATGGG
20	sfp_Rev	TTATGTAGCATTCCTTTCACTGG
21	clo_For	GAAAGTACCTTTACGGCTGTC
22	clo_Rev	TTGGTGGAAGAGGGATAACTG
23	nprP2_For	TAGCTGGGCATGAATTTACAC
24	nprP2_Rev	TTGTACCGCTTGAACTTCAG
25	hbl_For	ATGATAGGTGATGCAAGAGG
26	hbl_Rev	ACATATTCTTTACCATCCACTACTG
27	colA_For	AAATGGGAGTTTGGTGATGG
28	colA_Rev	TCTACCGTATAATTCCCTGTTCC
29	colC_For	CAGCATACTTCGTCAATTACCG
30	colC_Rev	TATGATTTCCATTTGCTTGACC
31	mpbE_For	ATTAGACAGCGAGCAAACAG
32	mpbE_Rev	ACTTGTTCTAAGCCATTCGG
33	atxA_For	TTCACAATGTATATGCGAGAAG
34	atxA_Rev	TCTGTTCAATTACCACTTTGC
35	atxA2_For	TAGCGTCTATAACCTCAGAGC
36	atxA2_Rev	ATGTCTTGGAGTGATTCGTTAG
Gibson Assembly, Toxin Knock-outs		
37	hblUS_For	TCATGGCGACCACACCCGTCCTGTGAAGATAGAAGGCTGCAAAG
38	hblUS_Rev	ATCACCTCAAATGAAGGAGAAATCTTTCAGATAC
39	hbl_KmR_For	AAGATTTCTCCTTCATTTGAGGTGATAGGTAAG
40	hbl_KmR_Rev	CAGTTTCCACTTTGTCGATACAAATTCCTCG
41	hblDS_For	AATTTGTATCGACAAAGTGGAAACTGTTACTC
42	hblDS_Rev	CCAGCAAGACGTAGCCCAGCGCGTCGTCTCTTTATGACTTCCAAATG
43	nheUS_For	TCATGGCGACCACACCCGTCCTGTGCATCTGTGAGTAAGTAGAG
44	nheUS_Rev	ATCACCTCAAATGCTCCATACTCTCTTGGATG
45	nhe_KmR_For	AGAGAGTATGGAGCATTTGAGGTGATAGGTAAG
46	nhe_KmR_Rev	TTTCCTTATAAGGGTCGATACAAATTCCTCG
47	nheDS_For	AATTTGTATCGACCCTTATAAGGAAAAAAGGTGAAAAG
48	nheDS_Rev	CCAGCAAGACGTAGCCCAGCGCGTCGGACTAATTCCTTTTACGTTTTG
49	cloUS_For	TCATGGCGACCACACCCGTCCTGTGGTTTCTGTTATTGGAATCGC
50	cloUS_Rev	ATCACCTCAAATGGCCATTGCGATTTCCATATTAC
51	clo_KmR_For	AAATCGCAATGGCCATTTGAGGTGATAGGTAAG
52	clo_KmR_Rev	AGGTGGAGCTGAAGTCGATACAAATTCCTCG

53	cloDS_For	AATTTGTATCGACTTCAGCTCCACCTGTCATG
54	cloDS_Rev	CCAGCAAGACGTAGCCCAGCGCGTCAACCCTTGGTACCAATTTG
Screening pBFH_1		
55	pBFH1_5877_For	ATGATAACTCTCGCTGAACGGAACGG
56	pBFH1_5877_Rev	CATCTGAATCAATCTTTCTATTAATCTGTCTTGCTTGTCC
57	pBFH1_5899_For	GTGTGTTAAACGCTTTGAAATGCGTTATACGG
58	pBFH1_5899_Rev	ATGGTTGTATTTATCGATTGGCGTACCG

Table 2.4. Primers used in this study. Primers were ordered from IDT. For denotes the forward primer, Rev denotes the reverse primer.

2.1.5. *Bacillus and E. coli* species culture conditions

Overnight cultures were grown in 5 ml of LB and with antibiotics as specified. They were incubated for 16 hours at 25 °C or 37 °C.

Larger cultures of *Bacillus* and *E. coli* strains were cultured in 50 ml of LB broth unless otherwise specified. Before cultures were seeded for RNA or protein extraction, pre-cultures of *B. cereus* G9241 were used to synchronise bacterial cell growth. Pre-cultures were inoculated into 50 ml of LB broth at OD_{600} = 0.05, whilst cultures for RNA or protein extraction were seeded at OD_{600} = 0.005

2.1.6. Growth curves for *B. cereus* G9241 strains

Overnight cultures of *B. cereus* G9241 strains were diluted to OD_{600} = 0.05 in 50 ml of LB broth to form pre-cultures. Mid-exponential, OD_{600} = 0.5 pre-cultures were diluted to OD_{600} = 0.005 in 50 ml of LB broth. 1 ml of culture was extracted every hour and OD_{600} measured. Where OD_{600} was higher than 1.0, cultures were diluted 1:10 or 1:20 as appropriate.

2.2. Molecular techniques

2.2.1. Isolation of gDNA from *Bacillus* species

2 ml of overnight culture of *B. cereus* was centrifuged at 14,000 rpm for 2 minutes. The supernatant was removed and the cell pellet was resuspended in 500 µl of Qiagen resuspension buffer (Qiagen) with 5 $mgml^{-1}$ lysozyme. The suspension was incubated for 10 minutes 37 °C. RNAse and proteinase K were

added at 20 $mgml^{-1}$, as well as 25 µl of 10% SDS. The suspension was further incubated at 37 °C for 10 minutes and then at 60 °C for 45 minutes.

565 µl (1 volume) of phenol-chloroform-isoamyl alcohol (PCI) was added and the solution was vortexed. This was centrifuged for 10 minutes at 14,000 rpm. The upper phase was then taken and the PCI addition and upper phase extraction was repeated two more times.

0.1 volumes of 3 M NaAc pH 5.2 and 1 volume of 96 % ethanol (pre-cooled to -20 °C) were added and the solution was inverted until DNA condensed. This was seen as white threads in solution. DNA was pelleted by centrifugation at 14,000 rpm for 5 minutes. The supernatant was discarded and the pellet washed in 200 µl 70 % ethanol. The DNA was pelleted by centrifugation at 14,000 rpm for 2 minutes. Ethanol was then removed and the pellet dried at 37 °C. The DNA was then resuspended in a final volume of 500 µl ddH_2O.

2.2.2. Creation of heat-shock competent *E. coli* DH5α

An overnight culture of *E. coli* DH5α was diluted 1:100 into 100 ml of LB. Cultures were incubated at 37 °C until they had grown to OD_{600}=0.5. After ample growth, cultures were incubated on ice for 15 minutes. Cells were harvested by centrifugation at 4 °C, for 10 minutes at 5200 rpm. Cell pellets were resuspended in 20 ml of 4 °C solution II.

Cultures were incubated on ice for a further 10 minutes before being centrifuged as before. Pellets were resuspended in 4 ml of solution II and 100 µl aliquots stored at -80 °C.

2.2.3. Transformation of heat-shock competent *E. coli* DH5α

Frozen cells were thawed on ice and 0.2-1.0 µg of plasmid was added. Transformations were incubated on ice for 20 minutes before heat shocking at 42 °C for 1 minute. Cells were returned to ice for 2 minutes and 1 ml of LB added to rescue the cells. Cells were incubated for 1 hour at 37 °C, shaking at 200 rpm.

Successful transformants were selected for on LB agar containing the appropriate antibiotic.

2.2.4. Creation of electro-competent *E.coli* ET12567

500 ml of *E. coli* were grown to OD_{600}=0.5 and cells were harvested by centrifugation at 5000 rpm for 15 minutes at 4 °C. Cells were washed first with 300 ml of 4 °C sterile H_2O, then with 50 ml 10% (v/v) glycerol at 4 °C and finally resuspended in 1ml 10% (v/v) glycerol. 50 µl aliquots were stored at -80 °C.

2.2.5. Electroporation of *E.coli* ET12567

80 µl of electrocompetent *E. coli* ET12567 cells were combined with 2 µl of plasmid in a pre-chilled Gene Pulser®/Micropulser™ electroporation cuvette, 2 mm (Bio-Rad). Cells were pulsed 2.5 kV, 25 µF and 200 Ω. 1 ml ice cold LB broth was added to cells after electroporation and bacteria were incubated at 37 °C for 1 hour to recover. Cells were plated onto selective media and successful transformants isolated.

2.2.6. Transformation of *Bacillus cereus* species

Overnight cultures were diluted 1:100 in 50 ml of LB medium. Cells were cultured at 37 °C and harvested at OD_{600} of 0.5 by centrifugation at 5000 g for 10 minutes. Cell pellets were resuspended in 1 ml of 10% glycerol in ddH_2O. The wash was repeated two more times. Washed cell pellets were resuspended in 100 µl of ddH_2O to create ~220 µl of competent cells.

Plasmids were first passaged through *E. coli* ET12567 in order to prevent methylation of DNA. 2 µg of plasmid DNA was added to the cells and 50 µl of this cell-plasmid mix was aliquoted into a pre-chilled 2 mm cuvette. Cells were electroporated at 2.5 kV, 25 µF and 200 Ω. 1 ml of SOC media (NEB) was immediately added to aid cell recovery. Cells were transferred to a 15 ml falcon tube and incubated at 37 °C for 3 hours at 30 °C. Transformants were selected on LB agar with the appropriate antibiotic.

2.2.7. Plasmid midi prep for isolation of pBFH_1 and pBFH_1<KmTn^5>

Plasmid midi preps were conducted in line with QIAGEN® protocol (Qiagen). 100 ml of bacterial culture was grown overnight and cells were harvested by centrifugation at 6000 g for 15 minutes at 4 °C. The cell pellet was resuspended in 4 ml of buffer P1. 4 ml of buffer P2 was added and cells were incubated at room temperature for 5 minutes. 4 ml of buffer P3 was added and cells were incubated on ice for 15 minutes. Lysates were centrifuged at 20,000 g for 30 minutes at 4 °C, supernatants were extracted and centrifuged again for a further 15 minutes under the same conditions.

The QIAGEN-tip 100 was equilibrated with 4 ml of buffer QBT and emptied under gravity. The cell supernatant was applied to the tip and it entered the resin under gravity. The column was washed twice with 10 ml of Buffer QC. DNA was eluted with 5 ml of buffer QF, which was pre-warmed to 65 °C.

DNA was precipitated by addition of 3.5 ml isopropanol. The solution was centrifuged at 15,000 g for 30 minutes at 4 °C and the supernatant discarded. The DNA pellet was washed with 2 ml ethanol 70% at room temperature, centrifuging at 15,000 g for 10 minutes. Supernatant was discarded and the DNA pellet was air dried for 10 minutes before being re-dissolved in 100 µl of H_2O.

2.2.8. BSAC Standardised disc antibiotic susceptibility Test (Wootton, 2015)

Bacillus cereus G9241, *Bacillus cereus* ATCC14579, *Staphylococcus aureus* Newman, *Staphylococcus* MRSA US300 and *Pseudomonas putida* UWC1 were streaked onto iso-sensitest agar (ISA) plates and incubated at 37 °C overnight. Five colonies of each bacterium were picked and resuspended in 3 ml ddH_2O. OD_{500} was measured against a ddH_2O blank. A volume of each suspension was added to 5 ml of ddH_2O depending on the OD_{500} (table 2.5).

Sterile cotton swabs were dipped in these new suspensions and spread across the plate in 3 directions to ensure an even lawn on each plate. Plates were allowed to dry and antibiotic discs were applied. The inoculated plates were incubated for 20 hours at 37 °C. BSAC guidelines do not include *Bacillus* species

per se, thus they were treated as Staphylococcus species, phylogenetically the closest organism listed in the BSAC guidelines (Andrews, 2009).

Organism	Absorbance reading at OD_{500}	Volume to transfer to 5 ml ddH_2O (µl)
Staphylococcus	>0.3 – 0.6	20
	>0.6 – 1.0	10
Bacillus	>0.3 – 0.6	20
	>0.6 – 1.0	10
Pseudomonas	>0.1 – 0.3	40

Table 2.5. BSAC antibiotic susceptibility test dilution guide.

2.3. Transcriptomics

2.3.1. RNA extraction for RNAseq and RT-PCR

Overnight cultures of *B. cereus* G9241 WT were grown at 25 °C or 37 °C. Cultures were diluted to OD_{600} = 0.05 and incubated at the corresponding temperature until they had grown to OD_{600} = 0.5. This pre-culture was diluted to OD_{600} = 0.005. Cells were cultured to mid exponential or stationary phase as determined by growth curves conducted in fig 3.4.

Cells were collected at the appropriate time point by centrifugation at 10,000g for 1 minute and pellets were resuspended in 5x volume of RNAprotect, as per the Qiagen specifications (Qiagen). Resuspended pellets were stored at -20 °C or used immediately. 1 ml of QIAzol (Qiagen) was added to each pellet suspension before being transferred to Lysing Matrix B tubes (MP Biomedicals).

Cells were lysed using the FastPrep®-24 Classic instrument (MP Biomedicals) with a COOLPREP™ adapter (MP Biomedicals). Bead beating was conducted at 6 ms^{-1} for 40 s for 2 cycles, with a 300 s pause between cycles. Lysates were centrifuged for 1 minute at 10,000 g and supernatant extracted.

The following steps were conducted in line with the RNeasy Micro Kit (Qiagen). The lysates were incubated at 20 °C for 5 minutes. 140 µl of 100% chloroform was added to each sample, before being homogenised and incubated at room temperature for 3 minutes. Samples were then centrifuged at 12,000 g for 15 minutes at 4 °C. The aqueous phase was extracted and mixed with an equal volume of 100% ethanol. 700 µl of each sample was applied to individual RNeasy columns before being centrifuged at 8000 g for 15 s at room temperature. The flow-through was discarded and 500 µl of Buffer RPE was applied to the column and centrifuged as before. The application of RPE buffer was repeated, but centrifuged for 2 minutes. Flow-through was discarded again and the membrane dried by centrifugation for 1 minute. RNA was eluted in 50 µl of Molecular-grade H_2O by centrifugation for 1 minute. The eluate was run through the column again for maximum RNA recovery.

The following steps were adapted from Ambion™ DNase I protocol (ThermoFisher Scientific). 50 µl of the extracted RNA was combined with 1 µl SUPERase-In™ (Invitrogen), 5 µl of Ambion™ DNase I buffer and 2 µl of Ambion™ DNase I. The reactions were incubated at 37 °C for 60 minutes with the addition of 2 µl Ambion™ DNase I half way through the incubation time. At the end of the incubation time, 3 µl of Dnase Inactivation Reagent was added to each sample. Mixtures were then centrifuged for 1.5 minutes at 10,000 g. 50 µl of supernatant was then extracted and split into 10 µl and 40 µl aliquots. The larger aliquot for each sample was stored at -80 °C.

RNA concentration was determined using Qubit 2.0 fluorometer (Life Technologies). DNA contamination was determined using Qubit 2.0 fluorometer and PCR against *plcR* and *gatB* genes using primers 9 and 10, and 1 and 2 respectively.

2.3.2. 2100 Agilent bioanalyzer (Agilent)

The Agilent 2100 Bioanalyzer was used to determine the quality of RNA extracted from *B. cereus* G9241, as well as cDNA library insert lengths. The Agilent Bioanalyzer was also used to prove rRNA had been depleted.

2.3.3. RNA quantification and quality analysis – Agilent RNA 6000 pico kit (Agilent)

The Chip Priming Station (Agilent) base plate was set to position C and the syringe clip set to the highest position. All reagents of the RNA 6000 Pico Kit were equilibrated to room temperature. RNA ladder was prepared by spinning down briefly and denaturing at 70 °C for 2 minutes. RNA ladder was incubated on ice and 90 µl RNase-free H_2O added. 1 µl aliquots of ladder were stored at -80 °C. RNA samples were diluted to 200 – 5000 $pg\mu l^{-1}$ and heat denatured at 70 °C for 2 minutes. Denatured samples and ladder aliquots were kept on ice until being loaded.

550 µl of RNA gel matrix was centrifuged through a spin filter at 1500 g for 10 minutes at room temperature. 65 µl aliquots were stored at 4 °C. RNA dye was equilibrated to room temperature and 1 µl of dye was combined with 65 µl of gel matrix. Gel dye matrix was vortexed and centrifuged at 13,000 g for 10 minutes at room temperature.

RNA 6000 Pico chip was placed into the priming station and 9 µl of gel-dye mix was loaded into the well labelled ‘G’. The priming station was closed and the syringe pressed from 1 ml until it was held by the clip. After 30 s the syringe was released and left for a further 5 s. The plunger was returned to the 1 ml position and the priming station opened. 9 µl of gel-dye mix was added to the other 2 wells labelled as ‘G’’. 9 µl of RNA conditioning solution was added to the well labelled ‘CS’ and 5 µl of RNA marker added into all sample wells and the ladder well.

1 µl of ladder was added into the appropriate well and 1 µl of sample loaded into the sample wells. The chip was vortexed for 1 minute at 2400 rpm before being run in the Agilent 2100 Bioanalyzer instrument.

2.3.4. cDNA quantification and fragment length determination – Agilent high sensitivity DNA kit (Agilent)

The Chip Priming Station (Agilent) base plate was set to position C and the syringe clip set to the lowest position. All reagents and samples were equilibrated to room temperature for 30 minutes before being loaded onto the High Sensitivity DNA Chip. cDNA library samples were diluted to between 0.1 – 10 ngµl^{-1} before being loaded.

15 µl of High Sensitivity DNA dye was added to a vial of DNA gel matrix. The solution mixed thoroughly and centrifuged through a spin filter at 2240 g for 10 minutes at room temperature.

A High Sensitivity DNA Chip was inserted into the priming station and 9 µl of gel-dye mix was loaded into the well labelled 'G'. The priming station was closed and the plunger pressed from the 1 ml mark until it was held by the clip. After 60 s incubation the clip was released. After a further 5 s the plunger was pulled upward to the 1 ml mark. 9 µl of gel-dye mix was loaded into the remaining wells marked 'G'.

5 µl of marker was loaded into every sample well and the well labelled with the ladder. 1 µl of High Sensitivity DNA ladder was loaded into the well labelled with a ladder. 1 µl of sample was loaded into the appropriate sample wells. The chip was vortexed at 2400 rpm for 1 minute and ran on the Agilent Bioanalyzer Instrument within 5 minutes.

2.3.5. Qubit® 2.0 fluorometer (Life Technologies)

Qubit™ dsDNA BR, Qubit™ dsDNA HS, Qubit™ RNA BR and Qubit™ Protein assay kits were used as appropriate. All assay kits followed the same protocol using the provided dyes (referred to as "reagent" within the assay kits) and buffers.

Qubit® Reagent was added to Qubit® Buffer in a ratio of 1:199. 10 µl of Qubit® Standard #1 and 10 µl of Qubit® Standard #2 were each separately combined with 190 µl of reagent-buffer in Qubit™ Assay tubes. 199 µl of reagent-buffer mix

was combined with 1 µl of DNA, RNA or protein sample. Qubit® 2.0 fluorometer plotted a standard curve using diluted standards and sample concentrations were calculated by comparison to the standard curve produced.

2.3.6. rRNA removal – Illumina Ribo-Zero® (illumina®)

After ensuring RNA has been successfully extracted using the Agilent RNA 600 Pico Kit, rRNA needed to be depleted. rRNA was depleted using the Ribo-Zero® rRNA removal kit and samples were cleaned up via ethanol precipitation.

225 µl of magnetic beads per RNA sample were left to stand on a magnetic stand until the suspension was clear. Supernatant was discarded a beads were washed twice with 225 µl RNase-free H_2O. The washed beads were returned to the magnetic stand and the water discarded. Magnetic beads were resuspended in 65 µl of Magnetic Bead Resuspension Solution and 1 µl of RiboGuard RNase Inhibitor added.

RNA samples were diluted to 2 µg in 28 µl and combined with 8 µl of removal solution buffer and 4 µl Ribo-Zero reaction buffer. Samples were incubated at 68 °C for 10 minutes and then incubated at room temperature for 5 minutes. Each RNA sample was added to a 65 µl aliquot of washed magnetic beads, vortexed for 10 seconds and incubated at room temperature for 5 minutes. Samples were then incubated at 50 °C for 5 minutes. Beads were then placed on a magnetic stand until the liquid was clear. 90 µl of each sample was then extracted.

To clean up RNA, ethanol precipitation was used. 90 µl of RNase-free H_2O, 18 µl of 3M sodium acetate and 2 µl of glycogen (10 $mgml^{-1}$) were added to each sample. Samples were vortexed, 600 µl 100% ethanol was added to each sample, before vortexing again. Samples were incubated at -20 °C for 1 hour before being centrifuged at 10,000 g for 30 minutes at 4 °C. Supernatant was discarded and samples were washed twice with 200 µl of 70% ethanol, with centrifugation at 10,000 g for 5 minutes at 4 °C. Supernatant was discarded and precipitate was air dried for 5 minutes. Pellets were then dissolved in 8.5 µ H_2O for TruSeq library prep.

2.3.7. Illumina™ MiSeq, RNA-Seq TruSeq library prep

TruSeq library prep was conducted in line with Illumina™ Low Sample (LS) Protocol (illumina, 2013). 5 µl of rRNA depleted RNA was combined with 13 µl of Fragment, Prime Finish Mix and samples were incubated for 8 minutes at 94 °C.

SuperScript II (Invitrogen™) was added to First Strand Synthesis Act D Mix in a 1:10 ratio. 8 µl of the mix was added to each RNA sample. The first cDNA strand was synthesised by incubating samples in a thermocycler:

1. 25 °C for 10 minutes
2. 42 °C for 15 minutes
3. 70 °C for 15 minutes
4. Hold at 4 °C

End Repair Control was diluted 1:50 in Resuspension Buffer and 5 µl of this mix was added to each sample. 20 µl of Second Strand Marking Master Mix was subsequently added and samples were incubated for 1 hour at 16 °C.

90 µl of AMPure XP beads were combined with 50 µl of each cDNA sample and were incubated at room temperature for 15 minutes. Samples were put on a magnetic stand for 5 minutes until the supernatant was clear. 135 µl of supernatant was removed and beads were washed twice with 200 µl of 80% ethanol without disturbing them. Beads were allowed to dry for 15 minutes at room temperature and then removed from the magnetic stand. 17.5 µl of Resuspension Buffer was added to the beads and samples were incubated at room temperature for 2 minutes. cDNA samples were returned to the magnetic stand for 5 minutes and 15 µl of supernatant was extracted.

To adenylate 3’ ends of the cDNA, A-Tailing Control was diluted 1:100 in Resuspension Buffer. 2.5 µl of diluted A-Tailing Control was added to each cDNA sample, followed by 12.5 µl of A-Tailing Mix. cDNA sampled were incubated in a thermocycler:

1. 37 °C for 30 minutes
2. 70 °C for 5 minutes
3. Hold at 4 °C

To ligate adapters, Ligation Control was diluted 1:100 in Resuspension Buffer and 2.5 µl of this dilution was added to each cDNA sample. 2.5 µl of the appropriate RNA Adapter Index was added to each sample (table 2.6). Adapters were ligated by incubation at 30 °C for 10 minutes. 5 µl of Stop Ligation Buffer was added to each sample to stop ligation.

42 µl of AMPure XP Beads were added to each library and incubated for 15 minutes. Samples were placed on a magnetic stand and incubated for 5 minutes. 79.5 µl of supernatant was discarded and beads were washed twice as before with 80% ethanol. Beads were air dried for 15 minutes at room temperature and removed from the magnetic stand. Beads were resuspended in 52.5 µl of Resuspension Buffer, returned to the magnetic stand and incubated for 5 minutes at room temperature. 50 µl of supernatant was extracted. This process was repeated using 50 µl of AMPure XP Beads, resuspending beads in 22.5 µl of Resuspension Buffer and extracting 20 µl of supernatant.

To amplify cDNA libraries, 5 µl of PCR Primer Cocktail and 25 µl of PCR Master Mix were added to each sample. Samples were incubated in a thermocycler:

1. 98 °C for 30 s
2. 98 °C for 10 s
3. 60 °C for 30 s
4. 72 °C for 30 s
5. Steps 2 - 4 repeated a further 14 times
6. 72 °C for 5 minutes
7. Hold at 4 °C

50 µl of AMPure XP Beads were added to each library and libraries were incubated for 15 minutes at room temperature. Samples were placed on a magnetic stand for 5 minutes and 95 µl of supernatant were discarded. Beads

were washed twice with 80% ethanol as before. Beads were removed from the stand, resuspended in 32.5 µl of Resuspension Buffer and incubated for 2 minutes. Libraries were returned to the stand, incubated at room temperature for 5 minutes and 30 µl of complete cDNA library extracted.

cDNA libraries were validated and insert lengths calculated using the Agilent Bioanalyser with Agilent High Sensitivity DNA kit (Agilent). Library concentrations were measured using Qubit 2.0 broad range DNA kit (Agilent)

Sample	RNA Adapter Index	Run No. and Cartridge Used
BcGWTExponential25.1	AD002	Run 1, Cartridge 150V3
BcGWTExponential25.2	AD007	Run 1, Cartridge 150V3
BcGWTExponential25.3	AD019	Run 1, Cartridge 150V3
BcGWTExponential37.1	AD002	Run 2, Cartridge 150V3
BcGWTExponential37.2	AD007	Run 2, Cartridge 150V3
BcGWTExponential37.3	AD019	Run 2, Cartridge 150V3
BcGWTStationary25.1	AD005	Run 3, Cartridge 150V3
BcGWTStationary25.2	AD006	Run 3, Cartridge 150V3
BcGWTStationary25.3	AD015	Run 3, Cartridge 150V3
BcGWTStationary37.1	AD005	Run 4, Cartridge 500V2
BcGWTStationary37.2	AD006	Run 4, Cartridge 500V2
BcGWTStationary37.3	AD015	Run 4, Cartridge 500V2

Table 2.6. Index of Illumina MiSeq RNAseq cDNA libraries used in this study.

2.3.8. Normalisation and Pooling of cDNA Libraries

The following equation was used to calculate the molarity of each cDNA library:

$$\frac{\text{concentration of library (ng}\mu\text{l}^{-1})}{660\ (\text{g mol}^{-1}\text{bp}^{-1}) \times \text{average insert size (bp)}} \times 10^6 = \text{Concentration (nM)}$$

Individual libraries were diluted to 4 nM in elution buffer and 5 µl of each library was combined to form a 4 nM library pool. 5 µl of this pool was combined with 5 µl of 0.2 M NaOH. Diluted pool was vortexed and centrifuged at 280 g for 1 minute at room temperature. The 2 nM pool was incubated at room temperature for 5 minutes before 990 µl of HTI buffer (pre-chilled to 4 °C) was

added to form a 20 pM pool. This pool was diluted further to 10 pM by combining 300 µl of pool with 300 µl of HTI buffer.

2.3.9. Loading the Illumina™ MiSeq RNAseq

The Illumina™ Flow Cell was cleaned with 80% ethanol in ddH_2O until the glass was completely transparent. 600 µl of 10 pM pool was loaded into each MiSeq cartridge and ran on the Illumina™ Miseq. The output of this process was paired-end sequencing reads.

2.3.10. RNAseq output analysis

The first read of the paired-end sequencing reads was reversed using the tool seqtk (GitHub). The reference genome of *B. cereus* G9241 WT (Johnson et al., 2015a) was indexed using bowtie2-build (Johns Hopkins University). This allowed the reads to be mapped to the reference genome using bowtie-2. The aligned reads were converted from SAM files into BAM files using samtools (GitHub). BAM files were sorted an indexed using samtools.

2.3.11. Normalisation of RNAseq analysis output

CoverageBed (bedtools) converted the sorted BAM files and a GFF file into txt files containing counts of the number of reads mapping to each gene feature annotated. A txt file was produced for each biological replicate sequenced and these were inputted into the R studio package DESeq2. The package was used to analyse differential gene expression using a negative binomial distribution model.

2.3.12. RT-PCR of *B. cereus* G9241 toxin genes, High-capacity RNA-to-cDNA™ kit (Applied Biosystems™)

RNA samples were reverse transcribed using a High-Capacity RNA-to-cDNA Kit as follows:

10 µl	2x RT Buffer Mix
1 µl	20x RT Enzyme Mix

9 µl RNA sample

The cDNA concentration was quantified using Qubit™ dsDNA HS assay kit. cDNA was amplified by PCR with *Taq* polymerase for 35 cycles. 6 ng and 4 ng of cDNA were loaded into each PCR reaction, for exponential phase and stationary phase RNA samples respectively. PCR products were run on a 0.8% agarose gel for imaging.

2.4. Proteomics

2.4.1. Protein extraction for secretome proteomics

Cultures for protein extraction were seeded using a pre-culture step. Secreted proteins were collected from mid exponential phase or late stationary phase at both 25 °C and 37 °C.

Once *B. cereus* G9241 had grown to the appropriate time point, 6.75 OD units of cells were centrifuged for 5 minutes at 8,000 rpm at 4 °C. One OD unit is equal to 1 ml of bacterial culture grown to a cell density of OD_{600} = 1.0. Supernatant was extracted and all samples were equilibrated to 15 ml using ddH_2O. Supernatants were acidified to pH 5 using 10% trifluoric acid (TFA). 50 µl of StrataClean resin (Agilent) was added to each sample before vortexing for 1 minute. All samples were incubated overnight on a rotor wheel mixer at 4 °C for efficient protein extraction.

StrataClean resin was collected by centrifugation at 870 g for 1 minute. Cell supernatant was removed and the beads resuspended in 100 µl of Laemlli buffer. The suspension was boiled at 95 °C for 5 minutes, to unbind the protein from the resin. Beads were pelleted at 870 g for 1 minute and protein-Laemlli buffer suspension collected.

2.4.2. In-gel protein digestion

25 µl of the secreted proteins were run on a Mini-PROTEAN® TGX™ precast gel (Bio-Rad). The whole lane of the gel for each sample was sliced into 4 mm sections and washed with 1 ml of 50% ethanol in 50 mM ammonium bicarbonate

–pH not altered (ABC). This wash was incubated for 20 minutes at 55 °C, shaking at 650 rpm. The wash solution was removed and this step was repeated twice more. The gel was dehydrated in 400 µl of 100% ethanol by incubation at 55 °C for 5 minutes, with 650 rpm shaking.

Once the gel was dehydrated, i.e. shrunken and white, remaining ethanol was removed. Disulphide bonds were reduced by addition of 300 µl of 10 mM dithiothreitol (DTT) in 50 mM ABC. This was incubated for 45 minutes at 56 °C with 650 rpm shaking. DTT was removed and samples were cooled to room temperature. Cysteine residues were alkylated by adding 300 µl of 55 mM iodoacetamide (IAA) in 50 mM ABC with incubation at room temperature, in the dark for 30 minutes.

IAA was removed and gel was washed as before by adding 1 ml of 50% ethanol in 50 mM and incubated at 55 °C for 20 minutes with shaking at 650 rpm. The ethanol was removed and this wash was repeated twice. Gel pieces were again dehydrated with 400 µl of 100% ethanol and incubated for 5 minutes at 55 °C. 200 µl of trypsin at 2.5 ngµl^{-1} was added to the dehydrated gel and ABC added to ensure the rehydrated gel was fully submerged. The trypsin digest was incubated for 16 hours at 37 °C with 650 rpm shaking.

The digest was stopped by addition of 200 µl 5% formic acid in 25% acetonitrile. The solution was sonicated for 10 minutes at 35 kHz and the supernatant extracted. This step was repeated three more times.

A C18 stage-tip (Thermo Scientific™) was made and conditioned by centrifuging 50 µl 100% methanol through the tip for 2 minutes at 2000 rpm. 100% acetonitrile was washed through the tip in the same manner to equilibrate it. The tip was further equilibrated with 2% acetonitrile with 1% TFA washed through the tip as before but for 4 minutes.

Samples were then diluted to a concentration of 10 µg of protein in 150 µl final volume of 2% acetonitrile/0.1% TFA. Samples were collected on the stage tip by centrifugation through the stage tip for 10 minutes under previous spin

conditions. The membrane was washed with 50 µl 2% acetonitrile/0.1% TFA by centrifugation at 2000 rpm for 4 minutes. Peptides were eluted in 20 µl 80% acetonitrile.

Samples were dried to a total volume of 40 µl at 40 °C in a speed-vac. Samples were rediluted in 55 µl of 2.5% acetonitrile containing 0.05% TFA and sonicated for 30 minutes at 35 kHz. Samples were dried to a total volume of 40 µl at 40 °C in a speed-vac again ready for mass spectroscopy.

2.4.3. Protein extraction for intracellular proteomics

B. cereus G9241 WT cells were grown to mid exponential phase in conditions matching RNAseq and secretome proteomic. 6.75 OD units of cells were collected by centrifugation as before. Cell supernatant was removed and cell pellets were suspended in 100 µl of 8M urea.

Suspensions were transferred to Lysing Matrix B tubes (MP Biomedicals) and cells were lysed using the FastPrep®-24 Classic instrument with a COOLPREP™ adapter (MP Biomedicals). Bead beating was conducted at 6 ms^{-1} for 40 s for 2 cycles, with a 300 s pause between cycles. Samples were filtered through nitrocellulose membranes to remove the beads and protein was quantified using a Qubit 2.0 fluorometer and a Qubit™ protein assay kit (Life Technologies).

2.4.4. In-urea protein digests

50 µg of protein sample was suspended in 50 µl of 8 M urea buffer. 5.5 µl of 10 mM DTT was added and the samples were incubated for 1 hour at room temperature. 6.2 µl of 55 mM IAA was added to samples before 45 minutes incubation at room temperature in the dark. Samples were then diluted to 100 µL total volume by addition of 50 mM ABC.

1 µg of trypsin was added to each sample per 50 µg protein and incubated for 16 hours at room temperature. Samples were filtered through a C-18 stage tip as described previously and concentrated to 40 µl in a speed-vac, ready for mass spectroscopy.

2.4.5. Nano liquid chromatography-electrospray ionisation-mass spectrometry (nanoLC-ESI-MS)/ mass spectrometry (MS) Analysis

Reversed phase chromatography was used to separate tryptic peptides prior to mass spectrometric analysis. Two columns were utilised, an Acclaim PepMap µ-precolumn cartridge 300 µm i.d. x 5 mm 5 µm 100 Å and an Acclaim PepMap RSLC 75 µm x 25 cm 2 µm 100 Å (Thermo Scientific). The columns were installed on an Ultimate 3000 RSLCnano system (Dionex). Mobile phase buffer A was composed of 0.1% formic acid in water and mobile phase B 0.1 % formic acid in acetonitrile. Samples were loaded onto the µ-precolumn equilibrated in 2% aqueous acetonitrile containing 0.1% TFA acid for 8 min at 10 µL min^{-1} after which peptides were eluted onto the analytical column at 300 nL min^{-1} by increasing the mobile phase B concentration from 4% B to 25% over 90 min, 35% over 10 min, then to 80% B over 5 min, followed by a 15 min re-equilibration at 4% B.

Peptides were eluted directly (300 nL min^{-1}) via a Triversa Nanomate nanospray source (Advion Biosciences, NY) into a Thermo Orbitrap Fusion (Q-OT-qIT, Thermo Scientific) mass spectrometer. Survey scans of peptide precursors from 375 to 1500 *m*/*z* were performed at 120K resolution (at 200 *m*/*z*) with automatic gain control (AGC) 4×10^5. Precursor ions with charge state 2-6 were isolated (isolation at 1.2 Th in the quadrupole) and subjected to HCD fragmentation with normalized collision energy of 33. It was used rapid scan MS analysis in the ion trap, the AGC was set to 1×10^4 and the max injection time was 200 ms. Dynamic exclusion duration was set to 45 s with a 10 ppm tolerance around the selected precursor and its isotopes. Monoisotopic precursor selection was turned on. The instrument was run in top speed mode with 2 s cycles.

2.4.6. Perseus analysis of proteomics data

The Perseus software platform (Max Planck Institute of Biochemistry) was used to analyse the highly multivariate proteomics data. Peptides only identified by site, reversed peptide sequences and potential contaminants were filtered out. Secretome data was normalised by the mean label-free quantification (LFQ)

intensity value. Whole cell proteomics data was normalised by median as the data was normally distributed. Protein hits were filtered out if they didn't have three values in at least one condition measured. Volcano plots were plotted using a p value = 0.05 and a log2-fold change = 1.

2.5. Phage techniques

2.5.1. Extraction of pBFH_1 phage particles

Phage extractions were conducted using *B. cereus* G9241 WT cultures grown to mid-exponential phase OD_{600}=0.5 or grown for 48 hours in LB broth. 5 x 50 ml cultures were inoculated at OD_{600}=0.005 using pre-culture and overnight culture steps.

When cultures had grown to either mid-exponential or for 48 hours, cultures were combined and bacteria pelleted at 8000 g for 30 minutes at 4 °C. A Beckman Avanti J-25 (Beckman) high speed centrifuge and a JLA16.250 rotor were used for centrifugation. Supernatant was extracted and DNAseI was added at a concentration of 0.25 units ml^{-1}. Supernatants were incubated at room temperature for 40 minutes at 200 rpm. NaCl and PEG6000 were added at concentrations of 0.5 M and 80 gL^{-1} respectively. Supernatants were incubated overnight at 4 °C at 200 rpm.

PEG6000 was pelleted by centrifugation at 8000 g for 30 minutes at 4 °C. Pellets were resuspended in 5 ml of TM buffer and incubated for 2 hours at 200 rpm at room temperature. Suspensions were centrifuged at 13,000 g for 10 minutes at 4 °C and supernatants extracted.

CsCl gradients were set up in 14 ml transparent ultracentrifugation tubes using 2 ml of 1.7, 3 ml of 1.5 and 3 ml of 1.45 density CsCl. CsCl solutions were diluted in TM buffer. 5 ml of phage extracts were pipetted above the CsCl gradients. After samples were loaded, tubes were balanced within 0.01 g of each other. CsCl gradients were centrifuged in a high speed centrifuge using a SW40Ti rotor (Beckman Coulter) at 35,000 rpm for 2 hours at 4 °C. Fractions of CsCl gradient were collected and stored at 4 °C.

2.5.2. Electron microscopy

Phage samples were negatively stained using 2% uranyl acetate for 4 minutes. Micrographs were collected on the JEOL2011 electron microscope (JEOL) using a US1000 CCD camera (Gatan Inc) at various levels of magnification.

2.5.3. Light microscopy of *Bacillus* species

DAPI (ThermoFisher) was diluted to 300 nM and FM 4-64 FX (ThermoFisher) diluted to working concentration. 1% agarose pads were made using 1.0 x 1.0 cm Gene Frames (ThermoFisher) on microscope slides. Approximately 65 µl of a 1% agarose in H_2O was loaded into each frame and pads were flattened using acetate cover slips.

25 µl of *B. cereus* cultures species were combined with 0.5 µl DAPI stain and 1 µl FM™ 4-64 FX membrane stain. Culture-stain mixes were incubated for 7 minutes in the dark at 37 °C. 1 µl of sample was applied to a prepared agarose pad and a cover slip placed over them. Images were captured on a Leica DMi8 premium-class modular research microscope with a Leica EL6000 external light source (Leica Microsystems), using an ORCA-Flash4.0 V2 Digital CMOS Camera (Hamamatsu) at 100x magnification.

2.5.4. Creation of pBFH_1 transposon library

The successful midi-prep of pBFH_1 was confirmed using both a diagnostic restriction digest with BamH1 and a PCR using primers 55 – 58. pBFH_1 concentration was measured using Qubit 2.0 with the Qubit™ dsDNA BR Assay kit.

The EZ-Tn5™ <KAN-2> transposon (Lucigen) was inserted into pBFH_1 as follows:

1 µl	EZ-Tn5 10x Reaction Buffer
5.26 µl	pBFH_1 (0.2 µg)
0.58 µl	EZ-Tn5 <KAN-2> Transposon
2.16 µl	H_2O

1 µl EZ-Tn5 Transposase

The reaction was incubated for 2 hours at 37 °C and stopped by addition of 1 µl of EZ-Tn55 10x Stop Solution. The reaction was then incubated for 10 minutes at 70 °C.

50 µl of TransforMax™ EC100D™ pir+ electrocompetent *E. coli* cells (Lucigen) were thawed on ice. 1 µl of transposon library reaction was added to the thawed cells and the cells were transferred to a pre-cooled Gene Pulser®/MicroPulser™ 2 mm electroporation cuvette (Bio-Rad). Cells were electroporated at 2.5 kV, 25 µF and 200 Ω.

2.6. Molecular genetic techniques

2.6.1. *Taq* PCR

Taq DNA Polymerase, recombinant (Invitrogen) was used for low-fidelity amplification of DNA. This was used in RT-PCR amplification and ensuring successful sub-cloning of DNA. Reactions were combined as follows:

2.5 µl 10x PCR Buffer Mg^-

0.75 µl 50 mM $MgCl_2$

0.5 µl 10 mM dNTP mix

1.25 µl 10 µM forward primer

1.25 µl 10 µM reverse primer

X µl 1 – 500 ng of Template DNA

0.3 µl *Taq* DNA Polymerase (5 Units μl^{-1})

Y µl Nuclease-free H_2O to 25 µl

The time course for Taq DNA Polymerase was as follows:

1. 94 °C for 3 minutes.
2. 94 °C for 45 s.

3. X °C for 30 s (X = annealing temperature of primer pair.
4. 72 °C 90 s kbp^{-1}.
5. Steps 2 – 4 repeated a further 29 times.
6. 72 °C 10 minutes.

2.6.2. Q5 PCR

Q5 High-Fidelity DNA Polymerase (NEB) was used for amplification of DNA with minimal errors. Reactions were combined as follows:

10 µl	5x Q5 Reaction Buffer
1 µl	10 nM dNTPs
2.5 µl	10 µM forward primer
2.5 µl	10 µM reverse primer
X µl	20-100 ng of template DNA
0.5 µl	Q5 High-Fidelity DNA Polymerase
Y µl	Nuclease-free H_2O to 50 µl

The time course for Q5 High Fidelity Polymerase was as follows:

1. 98 °C for 30 s.
2. 98 °C for 10 s.
3. X °C for 10 s (X = annealing temperature of primer pair.
4. 72 °C for 30 s Kbp^{-1} DNA.
5. Steps 2 – 4 repeated a further 29 times.
6. 72 °C for 2 minutes.

2.6.3 Gel electrophoresis conditions

Agarose gels were made at 0.8% w/v in tris-acetate-EDTA (TAE) buffer. SYBR Safe gel stain (Thermofisher Scientific) was added at 1:10,000 to melted agarose. Samples were combined 5:1 with 6x Gel Loading Dye (NEB) before being loaded.

2-log DNA Ladder (0.1 – 10.0 kb) or 100 bp DNA Ladder (NEB) were used for molecular weight standards. Gels were run at 100 V in TAE buffer.

2.6.4 Gel extraction, Illustra™ GFX™ PCR DNA and gel band purification kit (GE Healthcare)

Bands from agarose gels were excised and weighed. Agarose gel was combined with Capture buffer type 3 in a 1 mg:1 µratio and the mixture was incubated at 60 °C until the gel had melted fully. Up to 600 µl of melted gel was added to a GFX MicroSpin™ column and incubated at room temperature for 60 s. The column was centrifuged for 30 s at 16,000 g and this step was repeated until all the sample was bound to the column. 500 µlf Wash buffer type 1 was centrifuged through the column for 30 s at 16,000 g. The column was centrifuged again to remove residual wash buffer under the same conditions as before. 30 – 50 µl ddH_2O was added to the column and incubated at room temperature for 60 s. Purified DNA was eluted by centrifugation for 60 s at 16,000 g.

2.6.5 Restriction digests

Restriction enzymes from the NEB catalogue were used (NEB) for sub cloning DNA and confirming the midi-prep of pBFH_1. Restriction digests were conducted as follows:

5 µl	CutSmart® Buffer
1 µl	Restriction Enzyme 1
1 µl	Restriction Enzyme 2 (if used)
X µl	1 µg of DNA
Y µl	Nuclease-free H2O up to 50 µl

Digests were incubated for 2 hours at 37 °C.

2.6.6. Ligation of DNA fragments

T4 DNA ligase (NEB) was used to ligate DNA fragments cut in restriction digests. Reactions were set up as follows:

2 µl	T4 DNA Ligase Buffer (10x)
X µl	DNA fragment 1
Y µl	DNA fragment 2
1 µl	T4 DNA Ligase
Z µl	Nuclease-free H_2O up to a total reaction volume of 20 µl

DNA fragments were combined in an equimolar ratio. Vector and DNA fragments were combined in a 3:1 ratio. Reactions were ligated overnight (16 hours) at room temperature.

2.6.7. DNA purification from enzymatic reactions, illustra™ GFX™ PCR DNA and gel band purification kit (GE Healthcare)

500 µl of Capture buffer type 3 was combined with 50 µl of restriction digest reaction. This mix was applied to a GFX MicroSpin™ column and centrifuged for 30 s at 16,000 g. Flow-through was discarded and 500 µl of Wash buffer type 1 was applied to the column and centrifuged as before. Flow-through was discarded and the column was centrifuged as before to remove remaining wash buffer. 30 – 50 µl ddH_2O was added to the column and incubated at room temperature for 60 s. Purified DNA was eluted by centrifugation for 60 s at 16,000 g.

2.6.8. Gibson assembly, HiFi DNA assembly (NEB)

Gibson primers were designed manually with 40 bp overlaps or using the NEBuilder® Assembly Tool v1.12.17. Gibson assembly fragments were amplified using Q5 High-Fidelity Polymerase. Fragments were combined as follows:

25 µl	pRN5101

1.1 µl *hbl*US fragment

2.0 µl *hbl*DS fragment

2.4 µl Km^R fragment

30.5 µl NEBuilder HiFi DNA Assembly Master Mix

Reactions were incubated at 50 °C for 1 hour then incubated on ice until transformation.

Chemically competent NEB 5-alpha *E. coli* cells were thawed on ice. 2 µl of assembly mix was combined with 50 µl of competent cells and incubated on ice for 30 minutes. Cells were heat shocked at 42 °C for 30 s, the incubated on ice for 2 minutes. 950 µl of room temperature SOC media was added to cells and cultures were incubated at 37 °C for 60 minutes, shaking at 250 rpm. After incubation 100 µl of cells were plated onto LB agar with 50 µg $µl^{-1}$ kanamycin, pre-warmed to 37 °C.

2.6.9. Plasmid mini-prep (Qiagen)

4 ml of overnight culture of bacteria was centrifuged for 3 minutes at 8000 rpm at room temperature. Bacterial pellets were suspended in 250 µl Buffer P1. 250 µl Buffer P2 was added and samples were inverted 6 times. Samples were incubated for 3 minutes at room temperature before 350 µl Buffer N3 was added. Samples were inverted 6 times to mix and then centrifuged for 10 minutes at 13,000 rpm. The supernatant was applied to a QIAprep spin column and centrifuged at 13,000 rpm for 60 s. All steps were centrifuged under the same conditions. The supernatant was discarded and column washed by centrifuging 500 µl Buffer PB through the column. 750 µl Buffer PE was washed through the column in the same manner. Residual wash buffer was removed by another centrifugation step. 30 – 50 µl of ddH_2O was applied to the column and incubated for 60 s at room temperature. Purified DNA was eluted by centrifugation as before.

2.7. Haemolysis assays with *B. cereus* G9241 supernatant

B. cereus G9241 was grown at 25 °C and 37 °C to mid-exponential and stationary phase. Culture OD_{600} was measured and cells were pelleted by centrifugation at 8000 rpm for 10 minutes at 4 °C. Supernatants were extracted and residual cells removed using 0.22 µm syringe filters. Supernatant concentrations were normalised to the lowest culture OD_{600} by dilution in LB media. Sheep red blood cells (RBCs) were diluted to 4% in RPMI-1640 media. A 96-well microplate was set up with the following samples:

Sample Type	Reagents
Blank	50 µl 4% RBCs + 50 µl LB
+ve	50 µl 4% RBCs + 50 µl 2% Triton
-ve	100 µl LB
-ve	100 µl RPMI-1640
Supernatants	50 µl filtered supernatant + 50 µl 4% RBCs

Table 2.7. Haemolysis assay sample guide. +ve denotes the positive control; -ve denotes the negative control.

Plates were incubated at 37 °C for 1 hour with 250 rpm shaking. OD_{540} was measured and lysis calculated as a proportion of the expected lysis of 1% Triton; 70% RBC lysis.

3. Using mass spectroscopy to determine the temperature-dependent toxin profile of *B. cereus* G9241.

3.1. Introduction

In 1994 a welder was hospitalised with a severe, acute pneumonia-like infection (Hoffmaster et al., 2004). Symptoms presented were very similar to those suffered by the victims of the 2001 anthrax terror attacks but with the addition of haemoptysis – lysis of RBCs. One of the defining phenotypes of *B. anthracis* is that it is non-haemolytic (Marston et al., 2006) raising interest in the etiological agent that could cause both an anthrax-like disease and lyse RBCs. The infection was attributed to *B. cereus* G9241, isolated from the sputum and the blood of the welder (Hoffmaster et al., 2004). The bacterium was defined as a *B. cereus* species by classical phenotyping methods, despite causing an anthrax-like disease and possessing genes on the pBCX01 plasmid that encode the anthrax toxin components and the regulator AtxA. Characteristic of *B. cereus* type strains, *B. cereus* G9241 is haemolytic, motile and resistant to γ-phage and penicillin. 16S rRNA analysis and MLST confirm *B. cereus* G9241 is of the *B. cereus* sensu stricto (Sacchi et al., 2002). Haemolytic and motility phenotypes in the *B. cereus* sensu stricto are regulated by PlcR, a pleiotropic regulator of virulence (Agaisse et al., 1999). The characterisation of *B. cereus* G9241 has been controversial to the field of *B. cereus* sensu lato biology. It has been proposed that the regulators AtxA and PlcR are incompatible within a single organism and that the horizontal acquisition of AtxA by *B. anthracis* led to a point mutation in PlcR that created a nonsense frameshift in the gene (Mignot et al., 2001). The breaking of this paradigm has led to the question of how *B. cereus* G9241 seemingly incorporates the two regulators into a mammalian virulent lifestyle.

During work prior to this study *B. cereus* G9241 was shown to be able to cause a lethal infection in the insect infection models of *Manduca sexta* and *Galleria mellonella* when incubated at 25 °C (Hernández-Rodriguez et al., 2013). The model is commonly used to evaluate the pathogenesis of strains of the *B. cereus*

sensu lato. Other *B. cereus* sensu stricto and *B. thuringiensis* strains cause lethal infection in this model too, but *B. anthracis* is unable to kill *G. mellonella* when injected as either a spore or a vegetative cell (Fedhila et al., 2010). Further to these findings, Hernández-Rodriguez showed that *B. cereus* G9241 supernatant lysed *M. sexta* insect haemocytes in a temperature dependent manner (fig 1.5). Supernatant extracted from *B. cereus* G9241 growing at 25 °C lysed *M sexta* haemocytes, likely mediated by the PlcR regulon, while supernatant extracted from cultures growing at 37 °C did not result in haemocyte lysis. An identical pattern of cytolytic activity was seen against human immune cell lines (PMNs, Macrophages and T2 lymphocytes).

PlcR is the master regulator of many secreted toxins in the *B. cereus* sensu lato (Agaisse et al., 1999; Gohar et al., 2008; Gohar et al., 2002). The toxicity data suggested that the activity of the regulator PlcR, or cytotoxic members of its regulon, may be silenced during growth at 37 °C. That is, the lack of cytolytic activity of the supernatant is due to an absence of toxins at 37 °C. Mass spectrometry was used in this study to characterise the proteins secreted at both 25 °C and 37 °C to determine which toxins are responsible for the temperature-dependent haemolytic phenotype observed in the supernatant of *B. cereus* G9241. Mass spectrometry of the cell proteome was also conducted to elucidate the pattern of toxin expression in the cell and the possible role PlcR may have in the temperature-dependent toxicity phenotype.

Aims for this chapter were:

1. To confirm the temperature-dependent haemolytic phenotype of *B. cereus* G9241 supernatant at mid-exponential phase.
2. To use mass spectroscopy to propose which toxins are responsible for the cytolytic/haemolytic phenotype.
3. To create knock-out mutants using the suicide vector pRN5101 to confirm which toxins are responsible for the phenotype.

4. To analyse the proteomic data to propose other important temperature dependent phenotypes in *B. cereus* G9241 relating to its mimicry of anthrax.

3.2. Results

3.2.1. Haemolysis assays confirm *B. cereus* G9241 produces a haemolytic supernatant at 25 °C but not at 37 °C.

Data reported previously showed *B. cereus* G9241 produced a cytolytic supernatant at 25 °C but not at 37°C (fig 1.5). This phenotype was replicated to ensure the laboratory strain of *B. cereus* G9241 was still behaving like the original clinical isolate. Supernatants taken from *B. cereus* G9241 grown to mid-exponential phase at 25 °C and 37 °C were used to treat sheep erythrocytes (RBCs). The haemolysis assay (Fig 3.1) confirmed this temperature-dependent haemolytic phenotype. At 25 °C *B. cereus* G9241 supernatant lyses nearly 100% of RBCs whereas at 37 °C it lyses only 6.5%.

3.2.2. The temperature dependent secretome of *B. cereus* G9241 during exponential growth

3.2.2.1. Mass spectroscopy of secreted proteins of *B. cereus* G9241

The haemolysis assay identified the strong haemolytic activity of the *B. cereus* G9241 supernatant at 25 °C. To determine which toxins are responsible for this phenotype, the proteins of the supernatant were analysed by mass spectroscopy. Supernatant was extracted under growth conditions identical to the haemolysis assay. Proteins were run through nanoLC-ESI-MS and proteins detected in the supernatant at 25 °C were compared to those detected at 37 °C (fig 3.2).

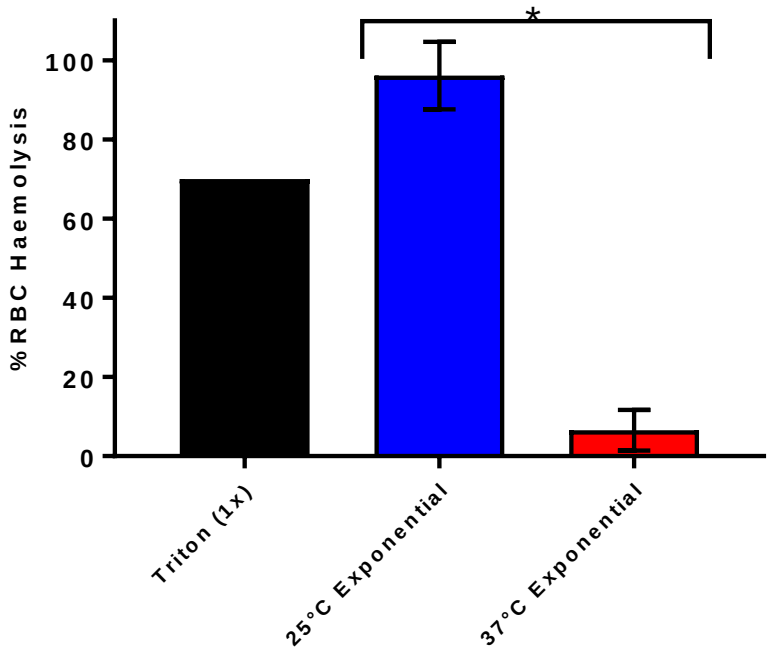

Fig 3.1: Fig. *B. cereus* G9241 supernatant is significantly more toxic to sheep red blood cells, when extracted from 25 °C grown culture compared to 37 °C grown. Supernatant was extracted from mid-exponential phase growing *B. cereus* G9241. Supernatant was filter-sterilised and incubated with 4% RBCs for 1 hour. OD_{540} was measured and % RBC lysis was calculated by comparison to the expected 70% lysis caused by 1x Triton. * denotes an unpaired t-test with a p-value of 0.0232. Error bars denote one standard deviation and all samples were to an n=3.

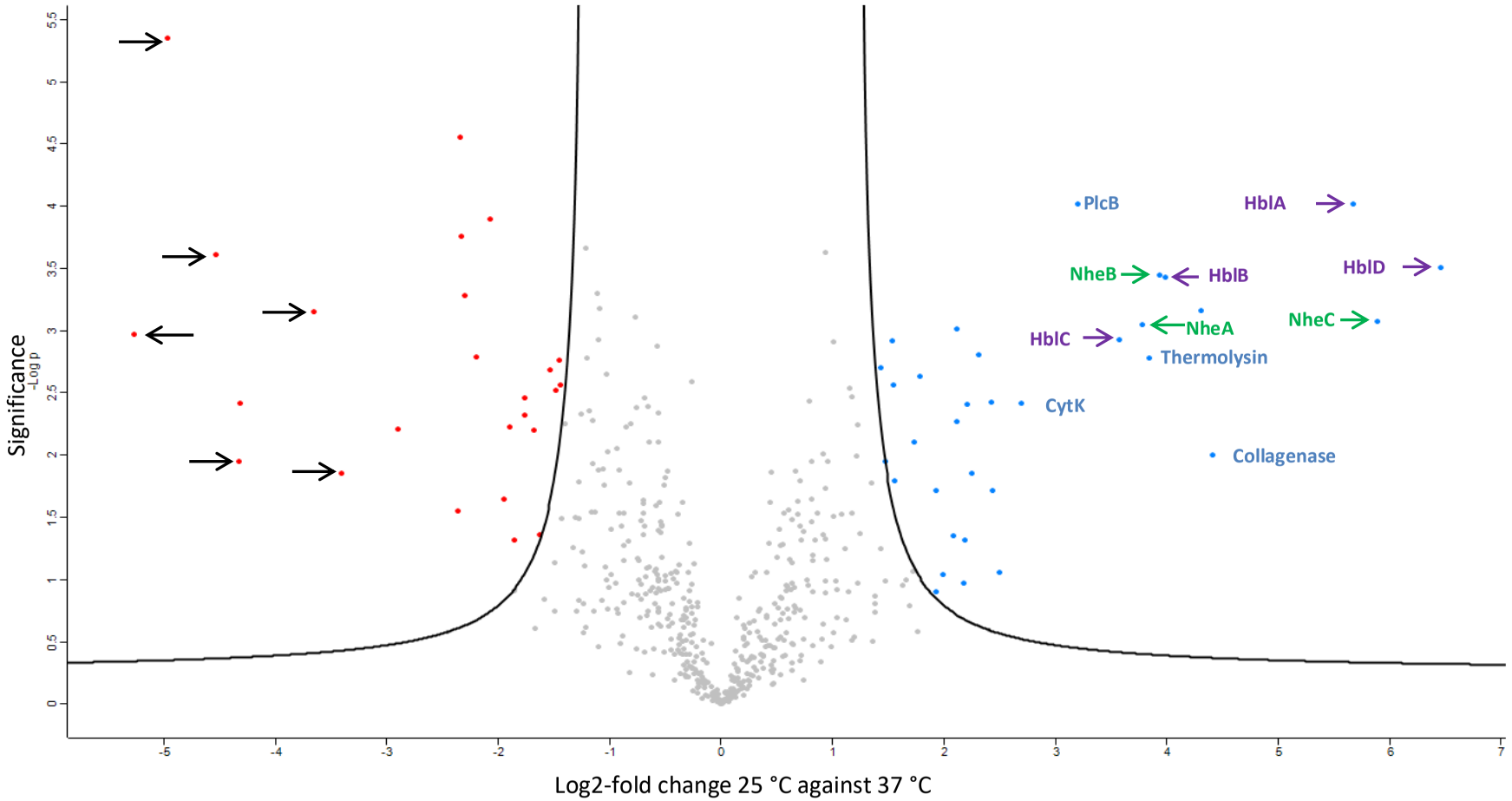

Fig.3.2 *B. cereus* G9241 secretes a large profile of toxins at 25 °C compared to 37 °C when growing exponentially. Mass spectroscopy was used to analyse the proteins in the culture supernatant of *B. cereus* G9241 WT, growing exponentially (OD_{600} = 0.5) at both 25 °C and 37 °C in LB broth, 200 rpm. Peptide reads were counted using MaxQuant (Max Planck Institute) and comparisons were made with Perseus software and plotted as the difference in proteins expressed at 25 °C against 37 °C. At 25 °C the *B. cereus* G9241 secretome contains various toxins including all components of the Hbl toxin (purple arrows), all components of the Nhe toxin (green arrows) and various other toxins. However at 37 °C, the secretome contains phage capsid proteins encoded on the pBFH_1 phagemid (black arrows). All samples were collected at n=3. Points above solid black lines are both statistically significant and have a significant fold change.

3.2.2.2. *B. cereus* G9241 secretes a large toxin profile during exponential growth at 25 °C

Using a p-value of 0.05 and a cut-off of a 2-fold change in protein level, 33 proteins were identified as being significantly higher at 25 °C compared to 37 °C in the *B. cereus* G9241 WT supernatant. Of these proteins, 11 of the 12 highest at 25 °C compared to 37 °C are known toxin homologs (Table 3.1). See table 8.1 in the appendices for a full list of proteins significantly higher at 25 °C compared to 37 °C.

Log2-Fold Change	Protein	Gene Loci (AQ16_)
6.46	Haemolysin BL lytic component L2	4931
5.89	(NheC) Non-haemolytic enterotoxin binding component	658
5.67	(HblA) Hemolysin BL-binding component	4932
4.42	Collagenase family protein	1941
3.99	(HblA) Hemolysin BL-binding component	4933
3.94	(NheA) Non-hemolytic enterotoxin lytic component L2	660
3.84	Thermolysin metallopeptidase, catalytic domain protein	5317
3.78	(NheB) Non-hemolytic enterotoxin lytic component L1	659
3.57	Haemolysin BL lytic component L1	4930
3.20	(Plc) Phospholipase C	1823
2.70	(CytK) Leukotoxin	1392

Table.3.1 Toxins higher at 25 °C compared to 37 °C in the secretome of *B. cereus* G9241 WT during exponential growth.

All proteins encoded by the *hbl* operon (AQ16_4930 – 4933) were seen as higher in the supernatant at 25 °C. The haemolytic Hbl toxin was the most likely

candidate for the temperature-dependent haemolytic phenotype observed. Cytolytic toxins were also abundant in the supernatant at 25 °C compared to 37 °C, with all proteins encoded by the *nhe* operon found to be present (AQ16_658 – 660). Other toxins with cytolytic activity were found too; including a collagenase (AQ16_1941), a neutral protease (AQ16_5317), Phospholipase C (AQ16_1823) and a leukotoxin (AQ16_1392).

3.2.2.3. *B. cereus* G9241 releases phage proteins at 37 °C

Twenty-five proteins were found to be more abundant in the secretome at 37 °C compared to 25 °C using the same significance criteria as used previously. The 8 highest proteins and 40% of the total proteins higher at 37 °C compared to 25 °C were encoded on the pBFH_1 phagemid (Table 3.2). See table 8.2 in the appendices for a full list of proteins significantly higher at 37 °C compared to 25 °C.

Log2-Fold Change	Protein	Gene Loci (AQ16_)
5.27	(Gp49) Phage family protein	5822
4.97	(Gp34) Putative phage major capsid protein	5824
4.53	Prophage minor structural protein	5836
4.32	(Gp14) Putative gp14-like protein	5832
4.32	N-acetylmuramoyl-L-alanine amidase family protein	5839
3.66	Phage tail family protein	5835
3.41	(GpP) Putative major capsid protein	5831
2.90	Uncharacterized protein	5823
2.33	Phage antirepressor KilAC domain protein	5855
1.53	Uncharacterized protein	5849

Table.3.2 Proteins highest at 37 °C compared to 25 °C in the secretome of *B. cereus* G9241 WT during exponential growth.

Several phage capsid head proteins were identified in the supernatant at 37 °C. A tail protein and a phage anti-repressor were also seen to increase in the supernatant at 37 °C. Together this may indicate the increased expression of whole phage particles at 37 °C.

3.2.3. PlcR binding motifs are present in toxins more highly represented at 25 °C

Examining the DNA regions upstream of the 11 toxin genes identified (section 3.2.2.1) revealed that they all contain a PlcR box motif, TATGNAN$_4$TNCATA (Table 3.3). For the *hbl* and *nhe* operons, PlcR binding motifs were only identified upstream of the first gene. The PlcR box upstream of the collagenase gene contains a point mutation A→T in the last base. PlcR boxes vary in how far upstream of the corresponding toxin they are.

Gene	Upstream of Loci	Sequence
nhe	AQ16_660 – 658	$_{550}$TTTGTATACACTATGCATAATTGCATATGAGTCCAAAA$_{509}$
hbl	AQ16_4930 – 4933	$_{907}$TATCTACATTTTATGCAATTATACATAACTAAATAAAG$_{866}$
Collagenase	AQ16_1941	$_{95}$AGAAGAAATAATATGAAATATTGCATTTTATATTGTTG$_{56}$
Thermolysin	AQ16_5317	$_{123}$CGTCCTTATATTATGTAATTTTGCATAATGTTACATAA$_{86}$
plc	AQ16_1823	$_{150}$AGTTATAATGATATGAACATTTGCATATTTTAATTTAG$_{113}$
cytK	AQ16_1392	$_{112}$CAAAACTCACCTATGCAATTATGCATAACTATCCCTTC$_{75}$

Table.3.3 Toxins more abundant at 25 °C compared to 37 °C all contain a PlcR-box motif (highlighted grey). Subscript numbers denote the distance in bp upstream of gene

3.2.4. The temperature dependent cellular proteome of *B. cereus* G9241

3.2.4.1. Mass spectroscopy of cellular proteins

To deduce whether PlcR has a role in the temperature-dependent regulation of toxins, mass spectroscopy was used to analyse the whole cell proteome. *B. cereus* G9241 was grown under the same conditions as used for the haemolysis and the secreted proteome studies. Cells were harvested and washed to prevent contamination with the secreted proteins. Proteins were run through nanoLC-ESI-MS and proteins detected at 25 °C were compared to those detected at 37 °C (fig 3.3).

3.2.4.2. Cell proteome: more abundant proteins at 25 °C

67 proteins were found to be significantly higher at 25 °C compared to 37 °C, i.e. are at least 2-fold higher. The proteins highest at 25 °C compared to 37 °C included cold shock proteins CspA and YdoJ family proteins (Table 3.4). A flagellin operon was also significantly higher at 25 °C (AQ16_827 – 830). Only two of the toxin proteins seen as higher at 25 °C in the secretome were also significantly higher in the cell proteome, NheA and NheB (AQ16_659 and 660).

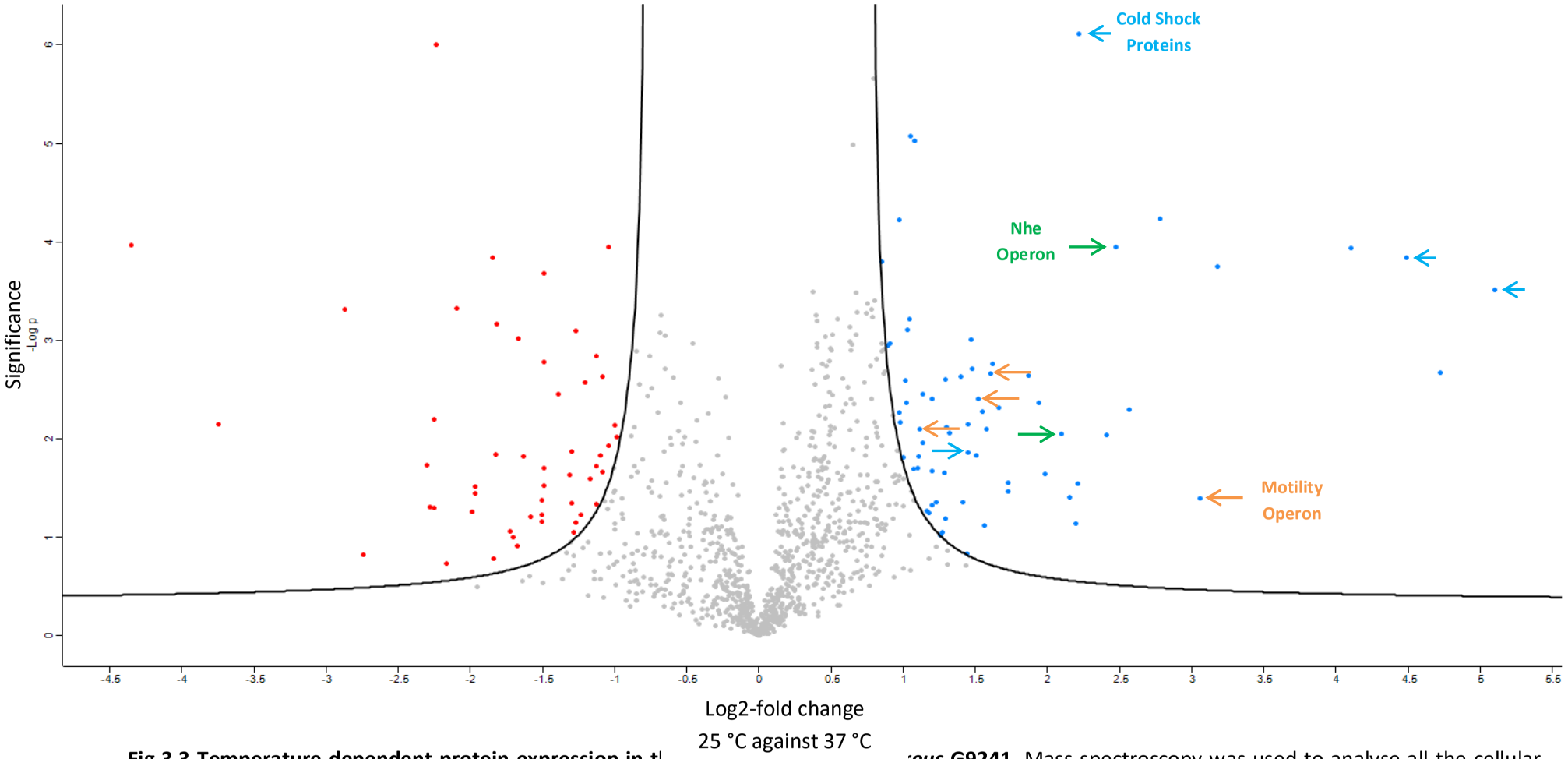

Fig.3.3 Temperature-dependent protein expression in the cell proteome of *B. cereus* G9241. Mass spectroscopy was used to analyse all the cellular proteins of *B. cereus* G9241 WT, growing exponentially (OD_{600} = 0.5) at both 25 °C and 37 °C in LB broth, 200 rpm. Peptide reads were counted using MaxQuant (Max Planck Institute) and comparisons were made with Perseus software and plotted as the difference in proteins expressed at 25 °C against 37 °C. Cold shock proteins (light blue arrows), a flagellin motility operon (orange arrows) and 2 genes of the *nhe* operon (green arrows) are higher at 25 °C compared to 37 °C. All samples were collected at n=3. Points above solid black lines are both statistically significant and have a significant fold change.

Log2-Fold Change	Protein	Gene Loci (AQ16_)
5.10	(CspA) Major cold shock protein	1368
4.72	Uncharacterized protein	4251
4.49	Cold-inducible YdjO family protein	175
4.10	Uncharacterized protein	4821
3.18	Transglutaminase-like superfamily protein	1487
3.06	Flagellar motor switch FliM family protein	858
2.78	(AzoR4) FMN-dependent NADH-azoreductase	2611
2.57	Uncharacterized protein	1372
2.47	Hemolytic enterotoxin family protein	659
2.41	Uncharacterized protein	1559
2.22	(CspA) Major cold shock protein	174
2.21	SET domain protein	2908
2.20	Transposase family protein	1725 / 4355
2.15	Rhodanese-like domain protein	1704
2.10	Hemolytic enterotoxin family protein	660

Table.3.4. Top 15 proteins higher at 25 °C compared to 37 °C in the cell proteome of *B. cereus* G9241 growing exponentially**.**

3.2.4.3. Cell proteome: more abundant proteins at 37 °C

Fifty-one proteins were identified as being higher in the cell proteome at 37 °C compared to 25 °C (Table 3.5). An operon of WxL domain surface cell wall-binding family proteins was seen to be higher at 37 °C (AQ16_3217 – 3219). Various heat stress response proteins were identified as higher at 37 °C too. These include: AQ16_3857, a DNA repair protein; AQ16_512, a DNA protection protein and a thermosensor operon, AQ16_3712 – 3714, involved in protein refolding. Only 2 proteins encoded on the pBFH_1 phagemid were identified in the cell proteome and both are uncharacterised, (AQ16_5849 and _5858).

Log2-Fold Change	Protein	Gene Loci (AQ16_)
4.35	WxL domain surface cell wall-binding family protein	3218
3.75	Uncharacterized protein	3219
2.87	(PflB) Formate acetyltransferase	2025
2.74	Uncharacterized protein	1429
2.30	(RecN) DNA repair protein	3857
2.28	(Dps1) DNA protection during starvation protein 1	512
2.25	Uncharacterized protein	5765
2.25	(PflA) Pyruvate formate-lyase-activating enzyme	2024
2.24	(Ldh) L-lactate dehydrogenase	3111
2.17	CamS sex pheromone cAM373 family protein	2171
2.09	L-asparaginase, type I family protein	4939
1.99	(HrcA) Heat-inducible transcription repressor	3712
1.97	Uncharacterized protein	5849
1.97	Membrane MotB of proton-channel complex MotA/MotB family protein	3490
1.84	Periplasmic binding family protein	1888

Table.3.5. Top 15 proteins higher at 37 °C compared to 25 °C in the cell proteome of *B. cereus* G9241 growing exponentially.

3.2.4.4. Cell proteome: PlcR and secretome toxins

Given the fall in the levels of various PlcR-regulon toxins, we might have expected to see less of the autoregulated PlcR protein in the cell at 37 °C compared to 25 °C. Unexpectedly however, the levels of PlcR did not show any significant temperature dependence (Table 3.6). PlcR levels were in fact 1.05 fold higher at 37 °C, although we speculate that this negligible difference is not likely to be biologically relevant. PlcR was not detected in the secretome as expected. Only four of the toxin proteins more abundant in the 25 °C secretome were also

identified in the cell proteome and only the two Nhe components showed significant temperature dependent changes.

Log2-Fold Change Secretome	Log2-Fold Change Cell Proteome	Protein	Gene Loci (AQ16_)
5.89	-	(NheC) Non-haemolytic enterotoxin binding component	658
3.78	2.47	(NheB) Non-hemolytic enterotoxin lytic component L1	659
3.94	2.10	(NheA) Non-hemolytic enterotoxin lytic component L2	660
2.70	-	(CytK) Leukotoxin	1392
3.20	-	(Plc) Phospholipase C	1823
4.42	-	Collagenase family protein	1941
-	-0.07	(PlcR) Helix-turn-helix family protein	2669
3.57	0.08	Haemolysin BL lytic component L1	4930
6.46	-	Haemolysin BL lytic component L2	4931
5.67	-	(HblA) Hemolysin BL-binding component	4932
3.99	-	(HblA) Hemolysin BL-binding component	4933
3.84	0.44	Thermolysin metallopeptidase, catalytic domain protein	5317

Table.3.6. Regulation of PlcR and toxins containing a PlcR-binding motif, in the secretome and the cell proteome. Values are denoted as comparison of protein levels at 25 °C compared to 37 °C. Negative numbers represent proteins detected as higher at 37 °C. '-' denotes that no peptides were detected for the protein.

3.2.5. Growth curves of *B. cereus* G9241 reveal the onset of stationary phase

In other members of the *B. cereus sensu lato* PlcR is more highly expressed in stationary phase (Agaisse et al., 1999). If toxins containing a PlcR motif upstream are regulated by PlcR, we may see an interesting pattern of toxin expression during stationary phase. To determine the onset of stationary phase, *B. cereus* G9241 WT was cultured in LB broth at 200 rpm at 25 °C and 37 °C. The ΔpBCX01 strain was also grown under the same conditions to determine the effects of pBCX01 on the growth kinetics of *B. cereus* G9241. Cells were sampled every hour for 10 hours. Mid exponential phase was defined in previous work (section 1.7) as OD_{600} = 0.5 (hashed line Fig.3.4). Both strains reached mid exponential phase after 1.9 hours and 3.75 hours at 37 °C and 25 °C respectively. Whilst both *B. cereus* G9241 strains grew more slowly at 25 °C, after 8 hours growth they reached the same OD_{600} as the WT when grown at 37 °C. Both *B. cereus* G9241 strains grown at 25 °C eventually plateau at the same OD_{600} as the WT when grown at 37 °C.

At 25 °C *B. cereus* G9241 WT and the ΔpBCX01 mutant grew exponentially for up to 5 hours. They transitioned into stationary phase growth at the 6 hour mark and stationary phase culture samples were taken after 10 hours growth.

At 37 °C *B. cereus* G9241 WT grew exponentially up to the 2 hour mark. From this it was estimated that the WT transitioned from exponential to stationary phase growth after 3 hours growth. Stationary phase culture samples were taken after 7 hours growth at 37 °C.

Interestingly there was a disparity in the growth kinetics of *B. cereus* G9241 WT and the ΔpBCX01 mutant when grown at 37 °C. The ΔpBCX01 grew marginally more quickly (purple line) and plateaued at a higher OD_{600} than the WT (red line).

3.2.6. The secretome of *B. cereus* G9241 at stationary phase

3.2.6.1. Mass spectroscopy of the secreted proteins during stationary phase

Supernatant was collected from *B. cereus* G9241 cultures grown to stationary phase as determined in the previous section. Supernatant was extracted after 10 hrs growth at 25 °C and after 7 hrs growth at 37 °C. Proteins were run through nanoLC-ESI-MS and proteins detected in the supernatant at 25 °C were compared to those detected at 37 °C.

Between the two temperatures, only 51 proteins were seen to be significantly more abundant at one temperature compared to the other (fig 3.6). Twenty-two proteins were more abundant at 25 °C and 29 proteins at 37 °C. The biggest log2-fold change seen when comparing the secretomes during exponential phase was Haemolysin BL lytic component L2 (AQ16_4931), 6.5 log2-fold higher at 25 °C. When comparing the stationary phase secretomes, the highest change seen was a chitinase A1 (AQ16_2089), 9.2 log2-fold more abundant at 37 °C compared to at 25 °C. A PCA plot was produced using both exponential and stationary phase secretome data sets (Fig 3.5).

The PCA plot revealed that protein extracts from the supernatant during exponential phase were highly reproducible (fig 3.6 red and blue dots). The plot also showed that growth temperature affected the protein profile more significantly at stationary phase compared to exponential phase. Proteins extracted from stationary phase growth at 37 °C were less reproducible than other conditions, showing a higher diversity on the plot (fig 3.6 orange circles).

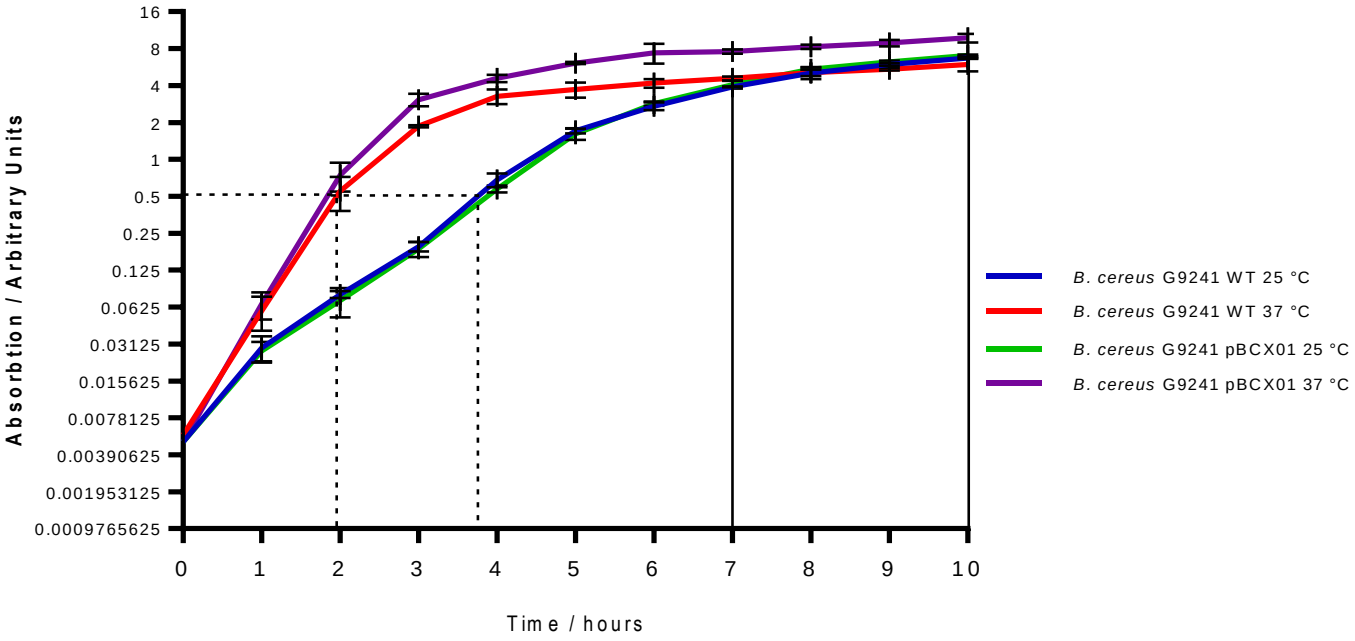

Fig.3.4. *B. cereus* G9241 WT and ΔpBCX01 grow faster at 37 °C compared to 25 °C. Strains were grown in LB broth for 10 hours, shaking at 200 rpm. A pre-culture step was used to remove a lag phase. *B. cereus* G9241 WT and ΔpBCX01 grow almost identically at 25 °C (blue and green lines respectively). However, at 37 °C the WT (red line) grows slower than the ΔpBCX01 strain (purple line). Dashed lines indicate time points for mid-exponential phase (OD_{600} = 0.5). Solid black lines indicate stationary phase time points, estimated to be 4 hours after transition phase (not annotated). All points plotted are averages of at least 3 measurements (n=3).

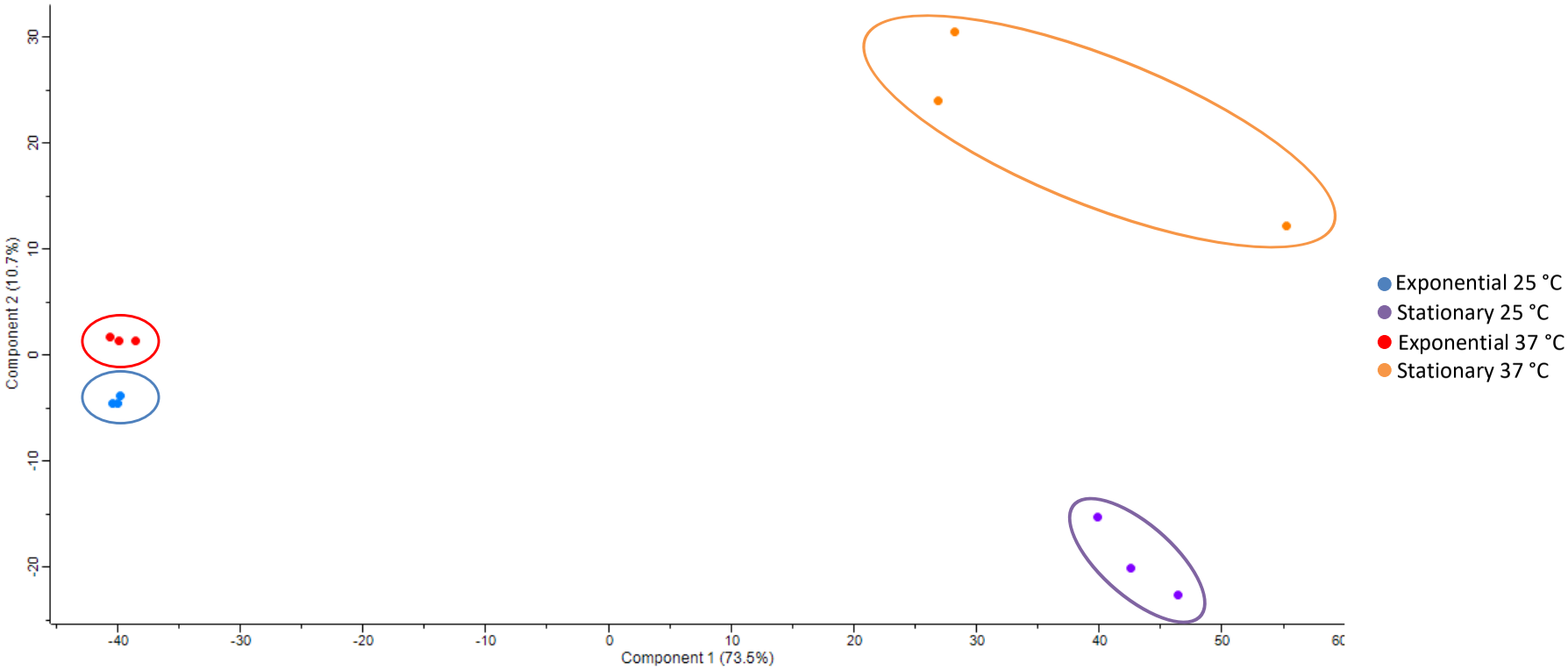

Fig 3.5. Principal component analysis of Secretomes of *B. cereus* G9241. Proteins were extracted from the supernatant of *B. cereus* G9241 growing exponentially and in stationary phase at both 25 °C and 37 °C. The PCA plot was produced using Perseus software (Max Planck Institute). Three points of each colour represent the biological replicates. The biological replicates for all samples clustered together indicating a high replicability between samples. However, the secretome extracted during stationary phase at 37 °C (orange dots) is far more variable than other conditions.

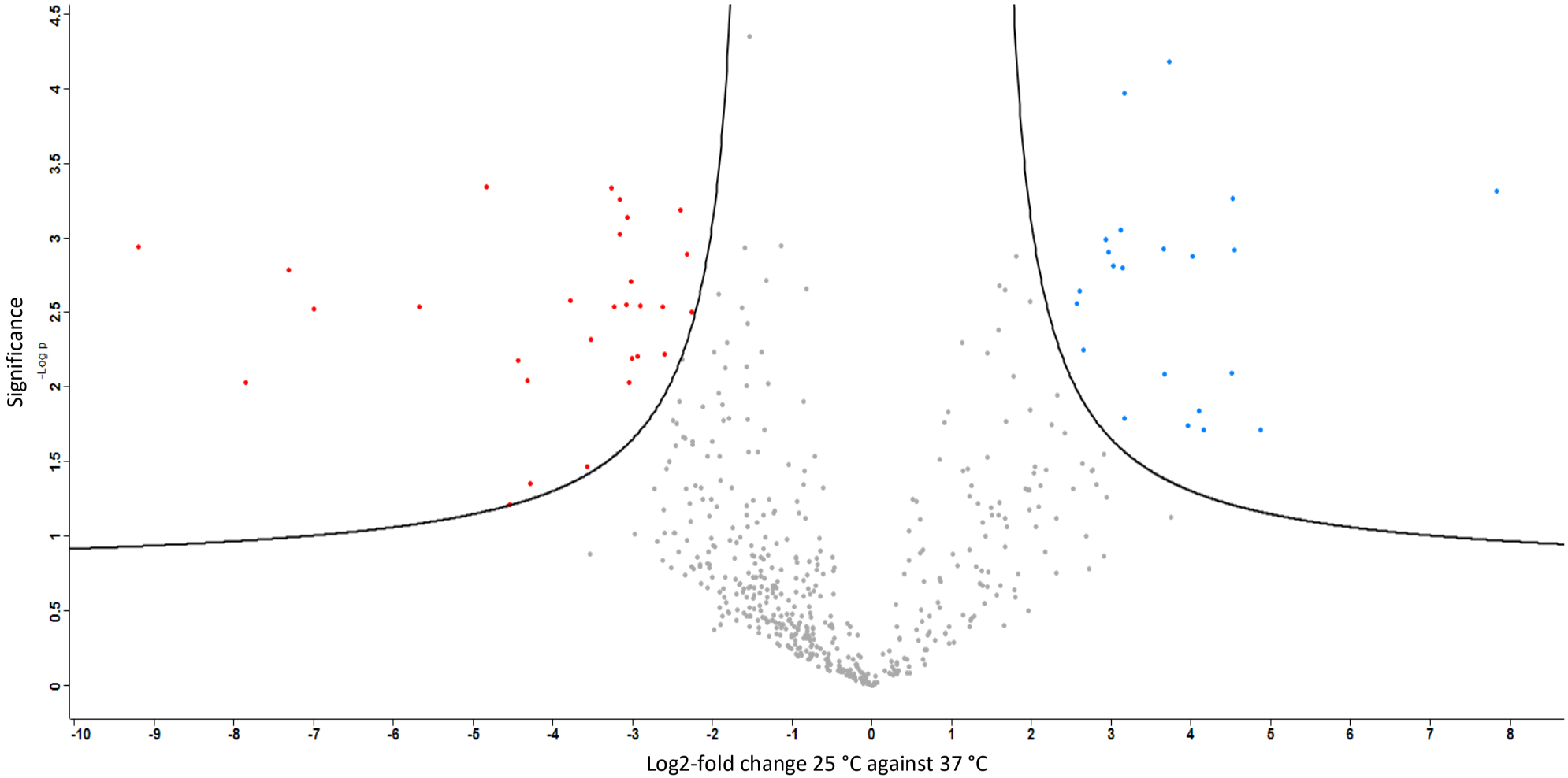

Fig.3.6. Comparison of the secreted proteome of *B. cereus* G9241 during stationary phase growth at 25 °C and 37 °C. Mass spectroscopy was used to analyse the secreted proteins of *B. cereus* G9241 WT, in stationary phase at both 25 °C and 37 °C in LB broth, 200 rpm. Stationary phase growth occurred after 7 and 10 hours growth at 37 °C and 25 °C respectively. Peptide reads were counted using MaxQuant (Max Planck Institute) and comparisons were made with Perseus software and plotted as the difference in proteins expressed at 25 °C against 37 °C. Blue circles denote proteins significantly higher at 25 °C compared to 37 °C. Red circles denote proteins significantly higher at 37 °C compared to 25 °C. Points above solid black lines are both statistically significant and have a significant fold change.

3.2.6.2. Proteins more abundant at 25 °C compared to 37 °C during stationary phase

There was no observable pattern of regulation at 25 °C compared to 37 °C during stationary phase. A thermolysin metallopeptidase was identified as highest at 25 °C compared to 37 °C, being over 200-fold higher (table 3.7). In fact, of the 11 toxins seen to be more abundant at 25 °C during exponential phase growth, only thermolysin, AQ16_5317 was identified as higher at 25 °C during stationary phase. Several proteins (e.g. AQ16_3254, 4226, 374) identified were likely cellular proteins, possibly indicating more cellular lysis at 25 °C compared to 37 °C.

Log2-fold Change	Protein	Gene annotation	Gene Loci (AQ16_)
7.83	Thermolysin metallopeptidase, catalytic domain protein		5317
4.87	Transglutaminase-like superfamily protein		1487
4.54	UDP-N-acetylglucosamine 1-carboxyvinyltransferase	murA	2685
4.52	Ribonuclease J	rnjA	2375
4.51	Ornithine aminotransferase	rocD	1349
4.16	Pyruvate carboxylase	pyc	4104
4.10	Malic enzyme, NAD binding domain protein		3400
4.02	CTP synthase	pyrG	2681
3.96	Glycerophosphoryl diester phosphodiesterase family protein		4572
3.73	Leucine--tRNA ligase	leuS	3254
3.66	Viral enhancin family protein		2918
3.66	Subtilase family protein		4301
3.17	50S ribosomal protein L2	rplB	2391
3.16	Aldo/keto reductase family protein		2308
3.15	Sphingomyelin phosphodiesterase	sph	1822

Table.3.7. Top 15 proteins higher at 25 °C compared to 37 °C in the secretome of *B. cereus* G9241 during stationary phase.

3.2.6.3. Proteins more abundant at 37 °C compared to 25 °C during stationary phase

The top 5 proteins higher at 37 °C compared to 25 °C were all extracellular enzymes including 2 chitinases, a hydrolase, a glucanase and a collagenase (table.3.8). Only the gene encoding the thermolysin protein contains a PlcR

consensus sequence upstream. The production of these enzymes may have indicated the onset of starvation. A matrixin family protein (AQ16_4915), another extracellular enzyme, was identified as 4.3 log2-fold higher at 37 °C. Three ribosomal proteins from the 50S subunit were identified as higher at 37 °C. RecA was also seen to be 2.9 log2-fold higher at 37 °C, which possibly signified cell lysis or cell stress. Only one of the phage capsid proteins identified as higher at 37 °C in the exponential phase secretome, Gp34 (AQ16_5824) was identified as significantly higher at 37 °C.

Log2-fold Change	Protein	Gene Annotation	Gene Loci (AQ16_)
9.20	Chitinase A1	chiA1	2089
7.85	Putative hydrolase		2662
7.32	Glucanase		5335
6.99	Collagenase family protein		4546
5.67	Chitinase A		4342
4.83	Peptide ABC transporter		2309
4.54	Calcineurin-like phosphoesterase family protein		4913
4.44	Urocanate hydratase	hutU	4415
4.31	Single-stranded DNA-binding protein	ssb	2546
4.28	Matrixin family protein		4915
3.77	3-hydroxyacyl-[acyl-carrier-protein] dehydratase FabZ	fabZ	2750
3.57	Formate acetyltransferase	pflB	2025
3.52	Ribose-phosphate pyrophosphokinase	prs	2472
3.27	Putative phage major capsid protein		5824
3.23	50S ribosomal protein L4	rplD	2393

Table.3.8. Top 15 proteins higher at 37 °C compared to 25 °C in the secretome of *B. cereus* G9241 during stationary phase.

3.2.7. Comparing the secretomes of *B. cereus* G9241 grown to exponential and stationary phase at 25 °C and 37 °C

3.2.7.1. Mass spectroscopy of the secreted proteins of *B. cereus* grown to exponential and stationary phase at 25 °C and 37 °C

The comparison of secretomes between temperatures at both growth phases revealed that protein expression in *B. cereus* G9241 changed dramatically dependent on growth phase. This was supported by the PCA plot analysis. Protein expression profiles were compared between growth phases at the same temperature to build a more complete picture of secreted protein regulation across the growth curve.

3.2.7.2. Comparison of secreted proteins of *B. cereus* G9241 grown to exponential and stationary phase at 25 °C

B. cereus G9241 supernatant protein samples extracted from exponential and stationary at 25 °C were quantified and compared. Proteins detected in the supernatant at exponential phase were compared to those at stationary phase. Four hundred and four proteins were identified as significantly more abundant in one growth phase compared to the other. Two hundred and ninety-two proteins were more abundant at exponential phase compared to stationary phase (fig 3.7 pink dots) and 112 proteins were higher during stationary phase growth compared to exponential phase growth (fig 3.7 teal dots).

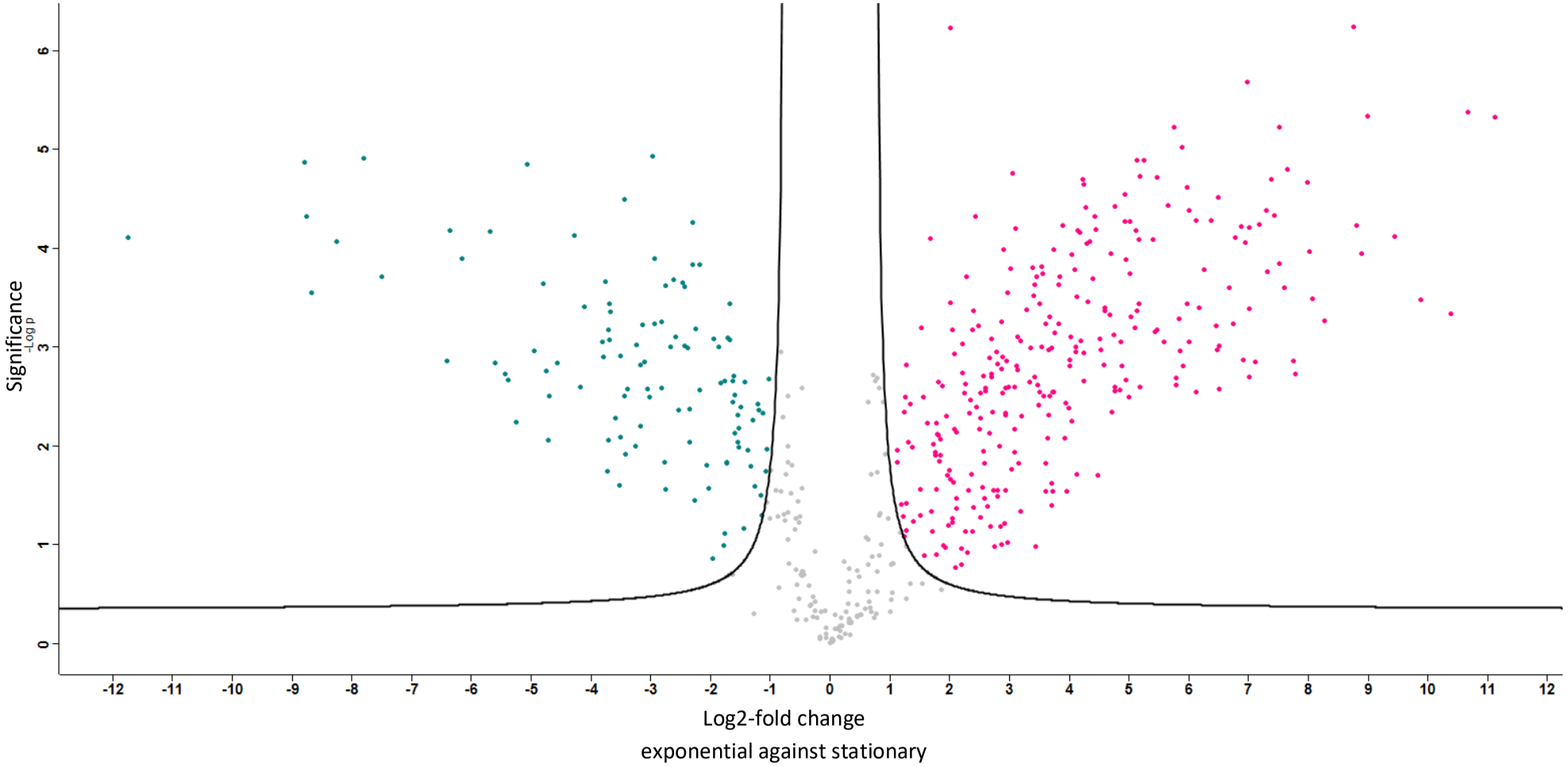

Fig.3.7. Growth phase-dependent protein expression in the secretome of *B. cereus* G9241 growing at 25 °C. Mass spectroscopy was used to analyse the secreted proteins of *B. cereus* G9241 WT at exponentially (OD_{600} = 0.5) and stationary phase, growing at 25 °C in LB broth, 200 rpm. Peptide reads were counted using MaxQuant (Max Planck Institute) and comparisons were made with Perseus software and plotted as the difference in proteins expressed at exponential phase against stationary phase. Proteins significantly higher at exponential phase compared to stationary phase are labelled pink. Proteins significantly more abundant at stationary phase compared to exponential phase are labelled teal. All samples were collected at n=3. Points above solid black lines are both statistically significant and have a significant fold change.

3.2.7.3. Proteins more abundant during exponential phase growth compared to stationary phase growth at 25 °C

Predictably the 5 highest proteins during exponential phase were cell wall modifying enzymes (table 3.9). All were over 9.4 log2-fold higher likely indicating large amounts of cell division. Forty-five ribosomal proteins were identified as higher at exponential phase, including 6 of the top 15 highest proteins. This possibly indicated a higher level of cell lysis during exponential phase. However, it should be noted that these represent comparative levels and do not represent absolute levels so we would not necessarily observe any significant levels of lysis during growth.

Six of the 11 toxins identified as more abundant at 25 °C compared to 37 °C in the secretome during exponential phase were higher at exponential phase compared to stationary phase at 25 °C too. Two Nhe toxin components, three Hbl toxin components and CytK were all more abundant at exponential phase (table 8.5 Appendices). The comparison also revealed the presence of another haemolysin, HlyII (AQ16_4553). HlyII was 1.6 log2-fold more abundant during exponential phase compared to stationary phase. Interestingly two anthrax toxin components, PagA and Lef (AQ16_5705 and 5710 respectively) were also identified as more abundant during exponential at 25 °C.

Log2-Fold Change	Protein	Annotation	Gene Loci (AQ16_)
11.19	Peptidoglycan endopeptidase		576
10.67	Enterotoxin/cell wall binding protein		2777
10.39	Cell wall hydrolase		2783
9.87	N-acetylmuramoyl-L-alanine amidase		2823
9.45	YocH Precursor/ cell wall binding protein		1815
8.99	50S ribosomal protein L1	RplA	2406
8.89	Enterotoxin		1683
8.81	Enoyl-[acyl-carrier-protein] reductase [NADH]	FabI	1275
8.75	30S ribosomal protein S3	RpsC	2388
8.28	30S ribosomal protein S7	RpsG	2398
8.07	50S ribosomal protein L6	RplF	2379
8.02	50S ribosomal protein L19	RplS	4210
7.98	Elongation factor Ts	Tsf	4224
7.78	50S ribosomal protein L22	RplV	2389
7.76	Trigger factor	Tig	3550

Table.3.9. Top 15 proteins higher at exponential phase compared to stationary phase to in the secretome of *B. cereus* G9241 growing at 25 °C.

3.2.7.4. Proteins more abundant during stationary phase growth compared to exponential phase growth at 25 °C

The protein showing the highest level of change at stationary phase was a pheromone binding protein (AQ16_1306), 11.7 log2-fold higher (table 3.10). Another pheromone binding protein was also higher (AQ16_2310) possibly indicating an increase in quorum sensing activity. Three ABC transporters were also seen to be higher during stationary phase growth (AQ16_1312, 1842, 2309) and all within the top 15 highest proteins. The flagellin operon proteins identified as more abundant in the cell proteome (AQ16_827-830) at 25 °C were also increased during stationary phase (table 8.6 Appendices).

Four of the 11 toxins identified as more abundant in the secretome at 25 °C compared to 37 °C during exponential phase, were also identified as higher at

stationary phase compared to exponential phase at 25 °C. Phospholipase C, a collagenase, NheA and a thermolysin protein were all more abundant. Immune inhibitor A (AQ16_1206) was also 2.5 log2-fold higher during stationary phase.

Log2-Fold Change	Protein	Annotation	Gene Loci (AQ16_)
11.74	Pheromone binding protein		1306
8.79	Peptide ABC transporter		1842
8.75	Bacillolysin	npr	1902
8.68	Oligopeptide ABC transporter		1312
8.26	5-methyltetrahydropteroyltriglutamate--homocysteine methyltransferase	metE	4042
7.81	Pheromone binding protein		2310
7.50	S-layer protein (PilC domain)	ctc	1583
6.40	SipW-cognate class signal peptide domain protein		1211
6.36	Chitin binding protein CBP 21	cbp	5228
6.15	Acetyl-CoA acetyltransferase	thlA	4021
5.68	Phosphoenolpyruvate carboxykinase [ATP]	pckA	3226
5.60	Peptide ABC transporter		2309
5.43	Arginase	rocF	2338
5.39	2-methylcitrate dehydratase	prpD	242
5.26	Flagellin		829

Table.3.10. Top 15 proteins higher at stationary phase compared to exponential phase to in the secretome of *B. cereus* G9241 growing at 25 °C.

3.2.7.5. Comparison of secreted proteins of *B. cereus* G9241 grown to exponential and stationary phase at 37 °C

B. cereus G9241 supernatant protein samples extracted from exponential and stationary at 37 °C were quantified and compared. Proteins detected in the supernatant at exponential phase were compared to those at stationary phase. Three hundred and ten proteins were significantly more abundant at one temperature compared to the other. Two hundred and twelve proteins were higher at exponential phase compared to stationary phase (fig 3.8 pink dots). Ninety-eight proteins were more abundant at stationary phase compared to exponential phase at 37 °C (fig 3.8 teal dots).

3.2.7.6. Proteins more abundant during exponential phase growth compared to stationary phase growth at 37 °C

The PCA plot revealed the high similarity between the proteins secreted at 25 °C and 37 °C (fig 3.6). Because of this, the proteins secreted highest at 37 °C during exponential phase compared to stationary phase were similar to those at 25 °C, under the same conditions. The 5 highest cell wall modifying proteins seen higher during exponential phase at 25 °C were also more abudnant during exponential phase at 37 °C (table 3.11).

Forty-one ribosomal proteins were identified as higher during exponential phase growth compared to stationary phase growth at 37 °C. This suggested a higher level of cell lysis during exponential growth than during stationary phase. None of PagA, Cya nor Lef proteins were higher during exponential phase at 37 °C. Six proteins encoded on pBFH_1 were identified as higher at exponential phase at 37 °C. Four phage structural proteins and 1 uncharacterised protein were higher. Interestingly AQ16_5839 on the pBFH_1 phagemid encodes an N-acetylmuramoyl-L-alanine amidase family protein. The protein encoded by this gene was 2.5 log2-fold higher at 37 °C during exponential phase growth compared to stationary phase growth. AQ16_5839 was not significantly

differentially regulated during 25 °C growth which may indicate alteration of the cell wall by pBFH_1 at 37 °C.

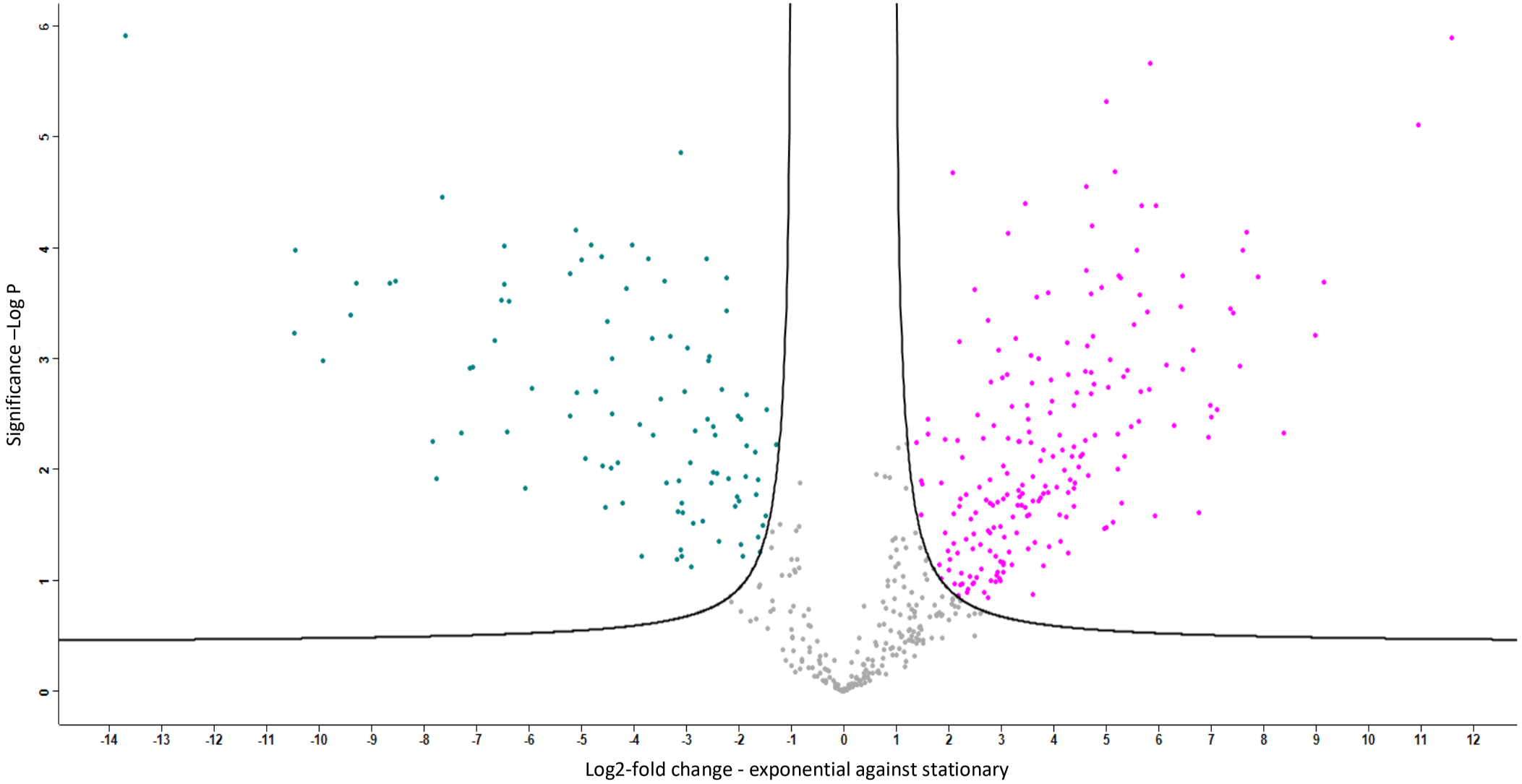

Fig.3.8. Growth phase-dependent protein expression in the secretome of *B. cereus* G9241 growing at 37 °C. Mass spectroscopy was used to analyse the secreted proteins of *B. cereus* G9241 WT at exponentially (OD_{600} = 0.5) and stationary phase, growing at 25 °C in LB broth, 200 rpm. Peptide reads were counted using MaxQuant (Max Planck Institute) and comparisons were made with Perseus software and plotted as the difference in proteins expressed at stationary phase against exponential phase. Proteins significantly higher at exponential phase compared to stationary phase are labelled pink. Proteins significantly more abundant at stationary phase compared to exponential phase are labelled teal. All samples were collected at n=3. All samples were collected at n=3. Points above solid black lines are both statistically significant and have a significant fold change.

Log2-Fold Change	Protein	Gene Annotation	Gene Loci (AQ16_)
11.58	Peptidoglycan endopeptidase		576
10.96	Uncharacterised Enterotoxin		1683
9.15	N-acetylmuramoyl-L-alanine amidase		2823
9.00	Cell wall hydrolase		2783
8.39	Enterotoxin/cell wallbinding protein		2777
7.90	Elongation factor Ts	tsf	4224
7.68	Trigger factor	tig	3550
7.60	50S ribosomal protein L11	rplK	2407
7.56	Enoyl-[acyl-carrier-protein] reductase [NADH]	fabI	1275
7.43	50S ribosomal protein L6	rplF	2379
7.37	50S ribosomal protein L10	rplJ	2405
7.11	50S ribosomal protein L1	rplA	2406
7.01	WxL domain surface cell wall-binding family protein		3215
7.00	50S ribosomal protein L17	rplQ	2366
6.96	30S ribosomal protein S7	rpsG	2398

Table.3.11. Top 15 proteins higher at exponential phase compared to stationary phase to in the secretome of *B. cereus* G9241 growing at 37 °C.

3.2.7.7. Proteins more abundant during stationary phase growth compared to exponential phase growth at 37 °C

A pheromone binding protein (AQ16_1306) had the highest fold change during stationary phase compared to exponential phase at 37 °C (table 3.12). This was the same as at 25 °C, likely indicating the protein's role in quorum sensing at a higher cell density. Thirteen of the top 15 proteins seen to be more abundant at stationary phase at 37 °C were also more abundant at 25 °C during stationary phase compared to exponential phase. Chitinase A1 (AQ16_2089) and an aminopeptidase (AQ16_2662) were the only proteins more abundant at stationary phase at 37 °C that weren't more abundant at 25 °C.

Four of the 11 toxins seen to be more abundant at 25 °C compared to 37 °C during exponential phase were higher at 37 °C during exponential phase compared to stationary phase. Phospholipase C, a collagenase, a thermolysin and NheA were all higher during stationary phase compared to exponential suggesting some cytolytic activity may be gained during stationary phase growth at 37 °C. The flagellin operon was also higher at stationary phase compared to exponential phase suggesting motility might be restored.

Log2-fold Change	Protein	Gene Annotation	Gene Loci (AQ16_)
13.67	Pheromone binding protein		1306
10.47	Collagenase family protein		4546
10.45	Peptide ABC transporter, peptide-binding protein		2309
9.92	Chitinase A1	chiA1	2089
9.39	Oligopeptide ABC transporter		1312
9.29	Glucanase		5335
8.65	Camelysin, metallo peptidase M73	FtsN	1209
8.54	Peptide ABC transporter		1842
7.82	Neutral protease B	nprB	2938
7.75	Aminopeptidase		2662
7.64	Uncharacterized protein		5768
7.28	Chitin binding protein CBP21	cbp	5228
7.11	Chitinase A		4342
7.06	Bacterial extracellular solute-binding s, 5 Middle family protein		2310
6.65	2-methylcitrate dehydratase	prpD	242

Table.3.12. Top 15 proteins higher at stationary phase compared to exponential phase to in the secretome of *B. cereus* G9241 growing at 37 °C.

3.2.8. Haemolytic activity of *B. cereus* G9241 supernatant during stationary phase growth

Certain cytotoxins were higher during stationary phase growth compared to exponential phase at 37 °C. A haemolysis assay was conducted (as in section 3.2.1) using supernatants extracted from stationary phase (fig 3.9). The same temperature-dependent haemolytic phenotype seen during exponential phase was seen between stationary phase samples. On average, supernatant taken from stationary phase at 25 °C lysed 77.5% of RBCs whereas supernatant taken from cells grown to stationary phase at 37 °C lysed an average of 31.4% of RBCs. This difference was determined to be statistically significant by an unpaired t test (P value = 0.0232).

There was a reduction in average haemolytic activity between supernatant extracted during exponential growth at 25 °C and stationary phase growth at 25 °C. This difference was deemed significant by a Welch's t test (P value = 0.0466). There was increase in haemolytic activity between supernatant extracted from cells growing exponentially at 37 °C and cells in stationary phase growth at 37 °C. The difference was statistically insignificant, determined by a Welch's t test (P value = 0.1719).

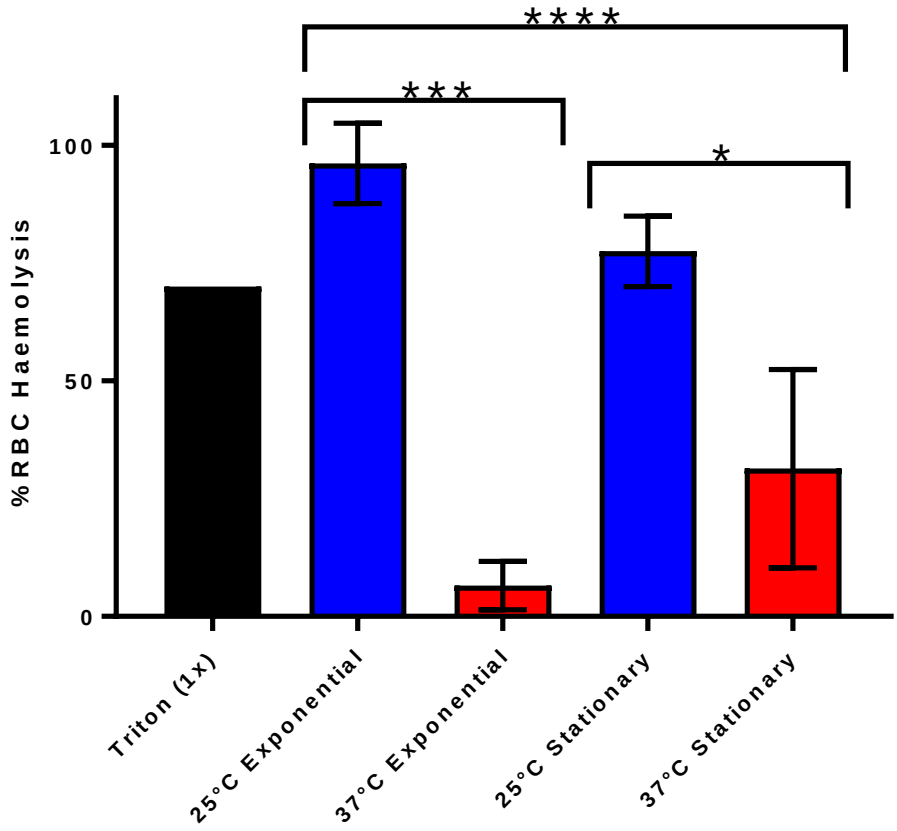

Fig.3.9. *B. cereus* G9241 supernatant is significantly more toxic to sheep red blood cells, when extracted from 25 °C growing culture compared to 37 °C growing culture. The haemolysis assay was conducted by incubating *B. cereus* G9241 supernatant with 4% RBCs for 1 hour at 37 °C. OD_{540} was measured and RBC lysis was calculated as a % of expected RBC lysis by Triton (1x). Stars above columns represent significance levels. * denotes an unpaired t test with a p-value of 0.0232; *** denotes a Welch's t test with a p-value of 0.0003; **** denotes an ordinary one-way ANOVA with a p-value of <0.0001. Error bars

3.2.9. Creating knock-out mutants in candidate toxin genes responsible for haemolytic activity of *B. cereus* G9241 supernatant

Several toxins were identified through nanoLC-ESI-MS that may be responsible for, or contribute to the temperature-dependent haemolytic and cytolytic phenotypes observed. The haemolysis assay revealed that haemolytic activity of the supernatant decreased significantly at 25 °C when extracted during stationary phase growth compared to exponential phase growth. Toxins that were significantly more abundant in the supernatant extracted from exponential phase compared to stationary were Hbl toxin components, Nhe toxin components and CytK.

We opted to quantify the haemolytic activity of Hbl and Nhe toxins as well as cereolysin O toxin (Clo) to act as a negative control. Clo was more abundant in the supernatant during exponential phase at 25 °C compared to 37 °C, but was not significantly less abundant in the stationary phase supernatant compared to exponential phase supernatant at 25 °C. (Fig 3.10) We attempted to create knock-outs of these toxin genes using homologous recombination, a kanamycin selection marker and the *B. cereus* family suicide vector pRN5101.

Construct assembly was attempted using both a classical cloning approach and Gibson Assembly®. Unfortunately, both approaches were unsuccessful. Classical cloning failed because fragments could not be amplified consistently to a high enough concentration, or could not be purified efficiently. Gibson Assembly® produced fragments efficiently but failed to assemble. The reasons for this are not known.

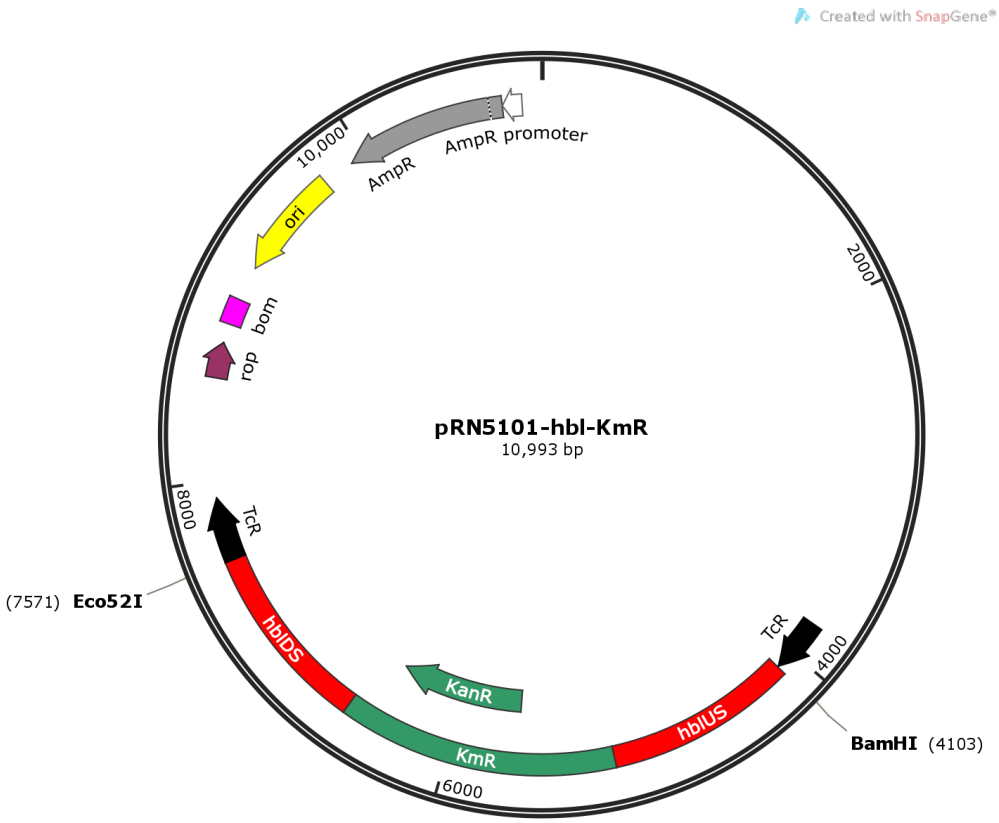

Fig.3.10. Example plasmid map for creating knock-out mutations in *B. cereus* G9241 toxins. The pRN5101 plasmid was digested with Eco52I and BamH1 restriction endonucleases. Upstream and downstream toxin fragments (red) and kanamycin resistance fragment (green) were amplified using primers with artificial restriction sites or with Gibson Assembly® overhangs and ligated using DNA ligase or Gibson Assembly® kits respectively. This same construct design was used for Nhe and Clo toxins where hblUS and hblDS were replaced with US and DS regions from the appropriate gene. The ampicillin resistance cassette (grey) allowed selection in *E. coli*. Tetracycline resistance cassette (black) was disrupted to confirm a positive insertion. An origin of replication (yellow), a Rop protein gene (purple) and basis of mobility region (pink) allowed propagation of the plasmid in *E. coli*.

3.2.10. Expression of PlcR is growth phase dependent and highly heterogeneous.

Whole cell proteomics revealed there was no significant difference in the level of PlcR between 25 °C and 37 °C during exponential growth. To confirm this, a translational fusion was created using the *Bacillus* species shuttle vector pHT315, *plcR* and *gfp*. A *gfp* cassette was ligated to the *plcR* promoter region and the first 15 bp of the *plcR* gene before being ligated to the pHT315 shuttle vector. pHT315-*plcRgfp* was transformed into *B. cereus* G9241. Cells were cultured to mid exponential or stationary phase and images of cells were captured on a fluorescent microscope.

Gfp expression was under the control of the native *plcR* promoter region. Gfp expression was detected at very low levels during exponential phase at 25 °C and 37 °C (fig 3.11 A and B). PlcR expression was therefore low during exponential phase. Gfp and therefore PlcR levels from individual cells greatly increased after 24 hours, as expected during stationary phase growth at both temperatures (fig 3.11 C and D). Gfp expression during stationary phase was very heterogeneous. Only a small percentage of cells expressed PlcR. Cells that did express PlcR, did so to a high level.

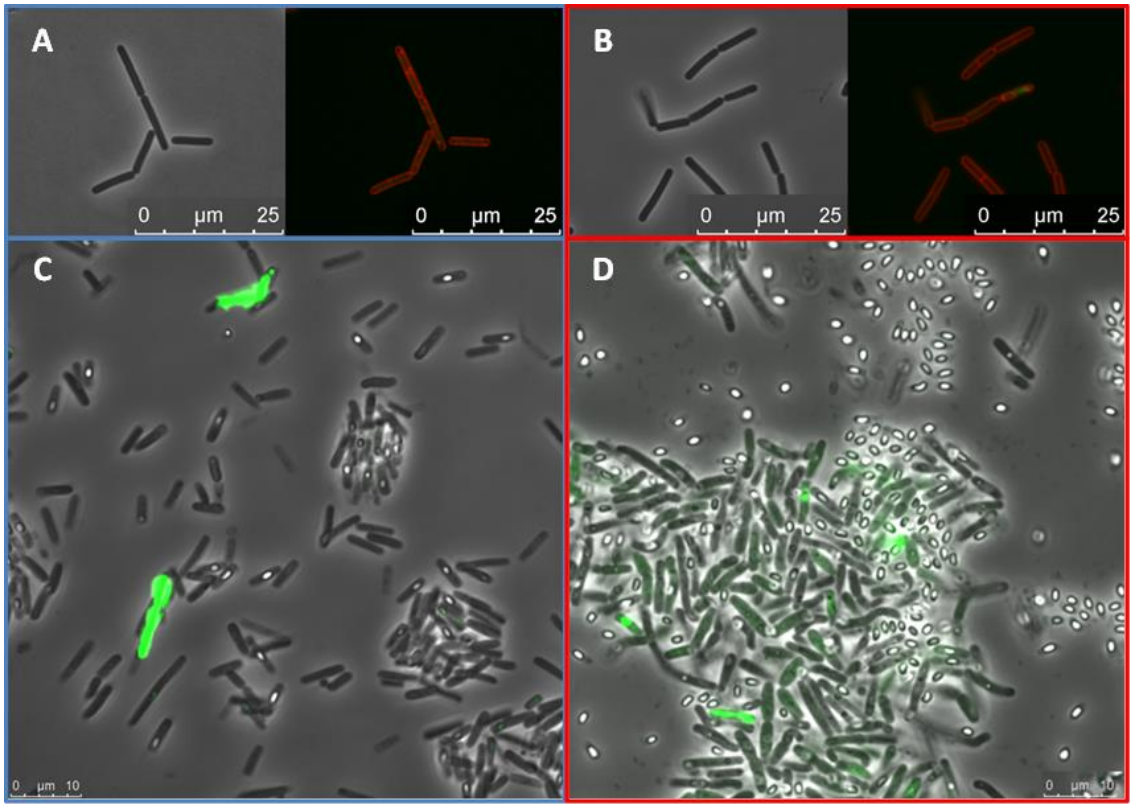

Fig.3.11. pHT315-*plcRgfp* reveals PlcR expression is heterogeneous and higher during stationary phase. *B. cereus* G9241 WT was transformed with pHT315-*plcRgfp* and incubated at 25 °C (A and C) or 37 °C (B and D) in LB at 200 rpm, to mid-exponential phase (A and B) or for 24 hours (C+D). Gfp expression (green) was very low during exponential phase (A and B). However, during stationary phase high Gfp levels were expressed but only from a small percentage of cells. Images were captured in phase contrast mode and overlayed with fluorescent images. (A and B) Phase contrast images were not overlayed to allow visualisation of Gfp. FM4-64x (red) was used to visualise cells without phase contrast microscopy.

3.2.11. BSAC antibiotic disc assay reveals temperature-dependent antibiotic resistance in *B. cereus* G9241

In the interest of biological safety BSAC antibiotic discs were used to assay the antibiotic resistances of *B. cereus* G9241 at both 28 °C and 37 °C. Lawns of *B. cereus* G9241 were plated and BSAC antibiotic discs were overlayed onto them. Plates were incubated at either 28 °C or 37 °C for 18 hours.

B. cereus G9241 WT was sensitive to gentamycin, erythromycin, tetracycline, ciprofloxacin and ampicillin at both temperatures (fig 3.12). The relation of halo size to antibiotic sensitivity was determined by BSAC guidelines. No haloes were observed when *B. cereus* G9241 was exposed to trimethoprim at either temperature. This indicated *B. cereus* G9241 was resistant to trimethoprim at either growth temperature. Interestingly a halo of 11 mm was produced when *B. cereus* G9241 growing at 28 °C was exposed to ceftazidime. However, when grown at 37 °C and exposed to ceftazidime no halo was observed. This indicated *B. cereus* G9241 was sensitive to ceftazidime at 28 °C but is resistant to the antibiotic at 37 °C.

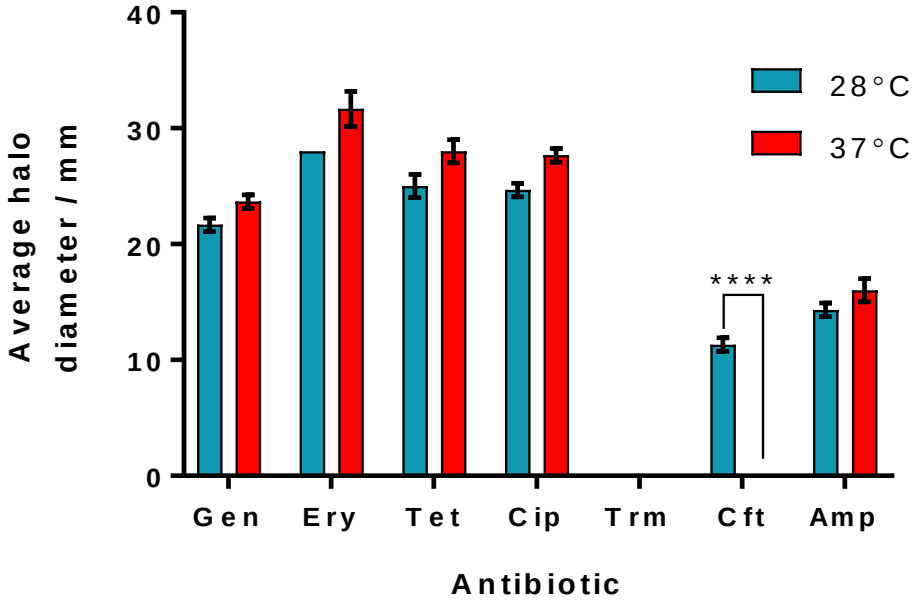

Fig.3.12. *B. cereus* G9241 WT displays a temperature-dependent ceftazidime resistance. Lawns of *B. cereus* G9241 were evenly spread onto Iso-sensitest agar and discs containing antibiotics were applied. After incubation at either 28 °C or 37 °C, halos were measured. Antibiotics tested include gentamycin (Gen), erythromycin (Ery), tetracycline (Tet), ciprofloxacin (Cip), trimethoprim (Trm), ceftazidime (Cft) and ampicillin (Amp). *B. cereus* displays sensitivity to Gen, Ery, Tet, Cip and Amp at both temperatures, but is resistant to Trm. Interestingly, *B. cereus* G9241 gains resistance to Cft when grown at 37 °C. Error bars represent one standard deviation and all samples are n=3. **** represents a significant difference between halo diameters with a p-value < 0.0001.

3.3. Discussion: Using mass spectroscopy to determine the temperature-dependent toxin profile of *B. cereus* G9241.

3.3.1. Is the temperature-dependent haemolytic phenotype regulated by PlcR?

Unpublished haemolysis and cytolysis assays showed that supernatant taken from *B. cereus* G9241 growing exponentially at 25 °C was highly cytotoxic and haemolytic. However, supernatant extracted from *B. cereus* G9241 growing at 37 °C showed a drastically reduced cytotoxicity. Furthermore, motility data showed *B. cereus* G9241 was motile at 25 °C but not at 37 °C. Together these findings led us to the hypothesis that *B. cereus* G9241 'switches' its phenotype from a motile, haemolytic *B. cereus*-like phenotype at 25 °C to a non-motile, non-haemolytic *B. anthracis*-like phenotype at 37 °C. PlcR and AtxA are pleiotropic regulators that define the characteristic phenotypes of *B. cereus* and *B. anthracis* respectively. Both PlcR and AtxA regulate the expression of secreted proteins, therefore the secreted proteome was analysed to determine the role of these pleiotropic regulators in temperature-dependent phenotypes (Dai et al., 1995; Gohar et al., 2008).

The first aim of this chapter was to confirm the temperature-dependent haemolytic activity of the *B. cereus* G9241 supernatant (Hernández-Rodriguez et al., 2013). This study confirmed that supernatant from *B. cereus* G9241 grown at 25 °C lysed RBCs, whereas supernatant taken from *B. cereus* G9241 grown at 37 °C did not, thus substantiating previous findings.

Analysis of the secretome of *B. cereus* G9241 growing exponentially at 25 °C compared to 37 °C revealed the presence of multiple cytolytic and haemolytic toxins. All component sub-units of the Hbl and the Nhe toxins were secreted at far higher levels at 25 °C. PlcB and CytK toxins and a range of proteases were also found to be significantly more abundant at 25 °C compared to 37 °C. This toxin profile is consistent with the published secretome of *B. cereus* ATCC14579 growing exponentially (Clair et al., 2010; Gilois et al., 2007). It should be noted

that the published toxin profiles are from *B. cereus* cultured at either 30 °C or 37 °C.

Attempts to determine which toxins were responsible for the temperature-dependent haemolytic and cytolytic phenotype proved unsuccessful. Gene-knockouts have been successfully made in *B. cereus* sensu lato species in various studies using the temperature sensitive suicide vector pRN5101 (Salamitou et al., 2000; Steggles et al., 2006). However, in this study, attempts to construct in frame deletions in the *hbl* operon, *nhe* operon and *cytK* gene were unsuccessful. Both Gibson Assembly® and classical sub-cloning failed to assemble knock-out cassettes in pRN5101 after multiple attempts. It is not clear why this was the case.

It is tempting to speculate from the secretome data that the temperature-dependent haemolysis is caused by the activity of the Hbl toxin. However Nhe toxin has also been shown to have haemolytic activity against various RBCs despite its name (Fagerlund et al., 2008), as has CytK (Granum and Lund, 1997). This redundancy suggests that all these toxins likely contribute to the haemolytic phenotype and that all must be repressed at 37 °C in order to to see the observed loss of the haemolytic phenotype. This study is interested in determining if the toxin profile is directly regulated by PlcR and therefore if *B. cereus* G9241 has evolved a mechanism to differentially control the PlcR regulon at different growth temperatures. It was decided that creating a *B. cereus* G9241 Δ*plcR* deletion strain was not a wise option due to the possibility that this would create what is functionally a *B. anthracis* strain. Instead the study aimed to determine the activity of PlcR using proteomics and bioinformatics.

Of the *B. cereus* G9241 toxins more abundant at 25 °C compared to 37 °C, all the corresponding genes encode an upstream PlcR box sequence and are known to be transcriptionally regulated by PlcR in *B. cereus* ATCC14579 (Agaisse et al., 1999; Lereclus et al., 2000). Interestingly the PlcR box upstream of the *hblCDAB* operon is encoded further upstream than has previously been observed in other *B. cereus* strains (Gohar et al., 2008). However, Gohar does not comment in their

study if there is a relationship between the level of transcriptional activation and the distance of the PlcR box from the gene. All of the PlcR boxes identified in this study fit the published consensus sequence. However according to Gohar's study, the T and C bases seen at position 7 in the PlcR boxes upstream of *nheABC* and *plc* respectively should result in significant loss of transcriptional activity by PlcR; 90% and 98% loss respectively. Upstream regions were also analysed for the presence of other *Bacillus* transcriptions factors, but none other than those already specified were found (Sierro et al., 2008)

B. cereus secretes a highly haemolytic toxin profile at 25 °C compared to 37 °C. All of the toxins higher at 25 °C contain PlcR box consensus sequences upstream. Together these findings act as preliminary evidence that *B. cereus* G9241 is able to differentially regulate the secretion of PlcR-regulated toxins. However, at this point it is unknown whether this regulation is at a transcriptional level, a translational level or due to differential regulation of toxin secretion. To determine if temperature-dependent toxin expression is due to differential secretion of toxins, the cell proteome was analysed at both 25 °C and 37 °C.

3.3.2. Is the temperature-dependent haemolytic phenotype due to differential regulation of secretion?

Of the eleven toxin proteins identified as higher at 25 °C in the secretome (table 3.1), only four were present in the cell proteome. Of the four proteins, only NheA and NheB were significantly higher in the cell proteome at 25 °C compared to 37 °C (table 3.6). Initial analysis of toxins in the cell proteome may lead one to conclude that temperature dependent cytotoxicity is due to temperature-dependent secretion. However we suggest that the absence of detectable levels of toxin proteins in the cell proteome is likely due to co-translational export of toxins proteins by the Sec secretion system (Fagerlund et al., 2010). Hbl, Nhe and CytK have all contain Sec leader sequences (Vörös et al., 2014) and this mechanism would prevent the accumulation of toxins in the supernatant. If the difference in secretome toxin profiles were due to temperature-dependent secretion, there would be an accumulation of toxins observed in the cell

proteome at 37 °C, but this is not the case. These findings suggest that temperature-dependent toxin expression is not regulated at the level of secretion.

Interestingly, PlcR was detected in the cell proteome at both temperatures with no significant difference between expression levels. Consequently, it can be concluded that the temperature-dependent toxin profile is not due to differential secretion of the toxins, nor due to levels of PlcR in the cell. This suggests that the control point for temperature-dependent toxin secretion may be due to differential activity of the PlcR regulator as opposed to expression levels. To further investigate the level at which temperature dependent regulation of the PlcR-regulon may be operating we performed RNAseq transcriptomic studies. The results of RNAseq analysis are documented in Chapter 4.

3.3.3. PlcR expression is heterogeneous and growth phase dependent

It is known from other members of the *B. cereus sensu lato* that PlcR levels build steadily throughout exponential growth and peak during transition into stationary phase (Lereclus et al., 2000). If the temperature-dependent haemolytic phenotype observed during exponential phase was PlcR-mediated, then after the onset of stationary phase when PlcR levels are higher, toxicity of the supernatants would also be expected to be higher respectively. Growth curves of *B. cereus* G9241 were conducted and the onset of stationary phase was determined as t_3 and t_6 hours after seeding at 37 °C and 25 °C respectively. *plcRgfp* translational reporter fusions were created to visualise and confirm the expression of PlcR during exponential growth at 25 °C and 37 °C.

plcR translational fusions were created in the pHT315 plasmid. pHT315 is a high-copy shuttle vector used in various studies of the *B. cereus* sensu lato (Arantes and Lereclus, 1991). No Gfp expression was observed from exponentially growing *B. cereus* G9241 transformed with the pHT315-*plcRgfp* translational fusion (fig

3.12). This lack of fluorescence is presumably due to low levels of PlcR expression during exponential growth (Lereclus et al., 2000). Expression of Gfp was highly heterogeneous during stationary phase growth, 24 hours after seeding. Importantly spore formation can be seen after 24 hours at 37 °C and early endospore formation can be seen after 24 hours growth at 25 °C. *plcR* transcription is governed by the PlcR box upstream of the gene (Økstad et al., 1999) in an autoregulatory manner. Upstream and downstream of the PlcR-box consensus sequence are found Spo0A transcription factor binding consensus sequences. Spo0A initiates the first stage of the sporulation cascade. It is reasonable to speculate therefore that sporulation initiation at these time points means that Spo0A is repressing the transcription of *plcR*. It should be noted that sporulation initiation typically occurs only in subpopulations of *Bacilli* (Bischofs et al., 2009) in a culture. It is therefore possible that the heterogeneity of Gfp expression observed in *B. cereus* G9241 is the result of a subpopulation of the culture initiating sporulation and thus repressing PlcR expression.

3.3.4. Phage structural proteins detected in the supernatant at 37 °C

Of the 25 proteins identified as significantly more abundant in the secretome of *B. cereus* G9241, 10 of them are encoded on the pBFH_1 phagemid and 6 are known phage structural proteins. Temperature-dependent phage and prophage replication has been widely reported for many years, including for *Bacillus* phages (Egilmez et al., 2018; Jian et al., 2016; Schuster et al., 1973; Tokman et al., 2016). However, to date the only known phage infecting the *B. cereus* sensu lato that has been shown to be produced more highly at 37 °C compared to 27 °C is phage J7W-1 (Gillis and Mahillon, 2014; Kanda et al., 2000). J7W-1 is a temperate phage of the Siphoviridae family originally identified from a strain of *B. thuringiensis*.

In *B. cereus* ATCC14579, PlcR-mediated toxin secretion occurs throughout exponential phase even at 37 °C (Clair et al., 2010). It is therefore formally possible that the expression of phage proteins might be interfering with normal PlcR-regulon toxin production. However, at this stage it cannot be confirmed

whether phage protein expression is the cause or the effect of a loss of PlcR-mediated toxin expression, or indeed entirely independent. It is also worth noting that phage-plaques were not observed when growing *B. cereus* G9241 on agar plates at 37 °C. Furthermore the abundance of phage protein in the supernatant at 37 °C does not necessarily mean that functional phage particles are being produced. Work conducted to elucidate the role of phage protein expression in the ecological niche of *B. cereus* G9241 is discussed in chapter 5.

3.3.5. The secretome of *B. cereus* G9241 during stationary phase growth

In *B. cereus* ATCC14579 toxin levels in the supernatant vary throughout the growth course (Gilois et al., 2007). Gilois showed that levels of Hbl L_2, NheA and PlcB all peak in abundance in the supernatant 2-5 hours after the transition into stationary phase growth. These findings informed the decision to conduct haemolysis assays with supernatant extracted from stationary phase cultures, as well as analysis of the secretome of *B. cereus* G9241 at 25 °C and 37 °C during stationary phase growth.

During stationary phase growth, the supernatant of *B. cereus* G9241 still displays a temperature-dependent haemolytic phenotype. HblA, HblC, NheA and PlcB were all higher in the supernatant at 25 °C compared to 37 °C during stationary phase growth. This pattern of toxin secretion is highly similar to *B. cereus* ATCC14579 growing at 30 °C (Gilois et al., 2007). NprB a neutral protease was one of the most abundant proteins at 25 °C compared to 37 °C. NprB is necessary for cleavage of PapR into its active form and is itself a member of the PlcR regulon (Pomerantsev et al., 2009). Higher expression of NprB may be an indicator of PlcR activity being higher at 25 °C compared to 37 °C during stationary phase growth.

At 37 °C, the secretome of *B. cereus* G9241 mostly contains peptidoglycan processing enzymes and intracellular proteins, including 42 ribosomal proteins. This suggests there is a large amount of cell lysis at 37 °C compared to 25 °C. If

the phage proteins observed in the exponential phase secretome at 37 °C are indicative of lysogenic phage production, then cell lysis would be expected (Howard-Varona et al., 2017). However, cell lysis may also be indicative of sporulation. Interestingly, only 6 of the phage proteins detected in the exponential phase secretome at 37 °C were identified as higher in the secretome during stationary phase growth suggesting phage production has fallen upon transition into stationary phase growth. The lower abundance of phage proteins during stationary phase growth compared to exponential phase growth may suggest that the phage particles produced are unstable, or degraded by host enzymes.

3.3.6. Temperature-dependent flagellin secretion/release and ceftazidime resistance

Unpublished motility assays show that *B. cereus* G9241 is motile at 25 °C but immotile at 37 °C (Hernández-Rodriguez et al., 2013). Proteins encoded by a flagellin operon were seen to be significantly more abundant at 25 °C compared to 37 °C in the secretome during stationary phase growth. Flagellin proteins assemble together to form the filament of the flagellum (Mukherjee and Kearns, 2014). No other components of the flagellum filament or hook were identified, presumably because flagellin is the major component of flagellum filaments. This data suggests that the temperature-dependent motility difference is due to the decreased production of flagella filaments at 37 °C. It may also suggest that flagella filaments are becoming dettached from the cell.

Originally conducted in the interests of biological safety, the antibiotic resistance assay revealed an interesting temperature-dependent ceftazidime resistance. Ceftazidime is a third-generation cephalosporin, a sub-class of β-lactam antibiotics. Two resistance mechanisms to ceftazidime have been identified. The first is the production of extended spectrum β-lactamases that enzymatically degrade ceftazidime (Burwen et al., 1994; Rice et al., 1990), the second is a deletion of the penicillin binding protein 3 observed in a *Burkholderia* strain (Chantratita et al., 2011). Although β-lactamase enzymes have been identified in

B. cereus (Kotiranta et al., 2000; Madgwick and Waley, 1987) no β-lactamase enzymes were detected at at higher level in the secretome at 25 °C compared to 37 °C. Therefore we cannot propose a mechanism of ceftazidime resistance based on the findings of this study.

3.3.7. Growth phase dependent regulation of proteins in *B. cereus* G9241

In the secretome at either temperature ribosomal proteins were at higher levels during exponential phase compared to stationary phase growth. More specifically, 45 and 41 ribosomal proteins were higher during exponential growth compared to stationary phase growth at 25 °C and 37 °C respectively. Ribosomal proteins are native to the cytoplasm and their presence in the secretome suggests cells are lysing during exponential growth at both temperatures. At either temperature extracellular enzymes such as glucanases and chitinases are higher during stationary phase growth compared to exponential growth and this is likely a result of the onset of starvation.

It is widely reported that PlcR reaches its highest level of expression during transition phase and early stationary phase growth (Lereclus et al., 1996). This may account for the higher level of the PlcR-regulated proteins HblA, HblC, collagenase, PlcB and NheC in the supernatant during stationary phase growth compared to exponential phase growth at 37 °C. This is interesting, as whatever is preventing the expression of toxins in the supernatant during exponential growth is reduced during stationary phase growth. These toxins are likely candidates that account for the increase in haemolytic activity of the supernatant during stationary phase at 37 °C compared to supernatant taken from exponential phase at 37 °C (fig 3.10).

3.3.8. Proteins encoded on extrachromosomal elements

No proteins encoded on pBC210 nor pBCX01 were differentially regulated between the two temperatures during exponential growth. Only 4 proteins from these plasmids were differentially regulated during stationary phase, two of

which are uncharacterised. Only 12 proteins encoded on extrachromosomal elements are differentially regulated by growth phase at either temperature. Four of these proteins are phage structural proteins encoded on the pBFH_1 phagemid and were higher during exponential phase growth at 37 °C compared to stationary phase growth. It should be noted that secretion of proteins encoded on pX01 in *B. anthracis* relies on an increase in CO_2/bicarbonate levels which may account for the lack of differential secretion seen in this study. Despite this, it is important to be aware that a lack of differential secretion does not mean that plasmid-encoded proteins are not in fact being secreted, but at equivalent levels. Exceptions are the anthrax toxin components, lethal factor and protective antigen, both of which are encoded on pBCX01, which were both higher in the supernatant during exponential growth at 25 °C compared to during stationary phase growth. As presumably mammalian active toxin components it was unexpected to see them secreted at 25 °C even in the absence of CO_2/bicarbonate.

4. The Effect of Temperature on the Global Transcriptional Profile of *B. cereus* G9241

4.1. Introduction

Analysis of the secretome of *B. cereus* G9241 during exponential growth revealed several candidate toxins responsible for the temperature-dependent haemolytic activity of the supernatant. Hbl, Nhe and CytK have all been shown to have a strong haemolytic activity (Senesi and Ghelardi, 2010) and thus are all candidate toxins responsible for the temperature-dependent haemolytic phenotype observed in *B. cereus* G9241. All of the toxins identified as higher at 25 °C contain PlcR box consensus sequences upstream of their encoding genes suggesting these toxins and the temperature-dependent toxicity could be regulated at a transcriptional level by PlcR. A PlcR protein with temperature-dependent activity has only been observed once previously, in *B. weihenstephanensis* KBAB4 strain (Rejasse et al., 2012). In this case, the PlcR activity increases at low temperatures, although how this is regulated by temperature is not known.

To elucidate the role of PlcR in temperature-dependent toxicity, an informative experiment might be to create a *B. cereus* G9241 *ΔplcR* strain and test if haemolytic activity is lost at 25 °C. Indeed previously a *B. cereus* ATCC14579 *ΔplcR* strain was previously created by Gohar et al. by insertion of a kanamycin resistance cassette (Gohar et al., 2008). However, creating a *B. cereus* G9241 *ΔplcR* strain was ruled out over significant biosafety concerns, as it might result in a strain that is genetically, and therefore phenotypically, very similar to a bona fide *B. anthracis* strain. Nevertheless, as PlcR is a global transcriptional regulator, as an alternative approach we elected to use RNAseq to analyse the transcriptome of *B. cereus* G9241 growing at 25 °C and 37 °C. If genes known to be regulated by PlcR in *B. cereus* type strains are more highly expressed at 25 °C compared to 37 °C in *B. cereus* G9241, it will support the hypothesis that temperature-dependent toxicity is a result of differential regulation by PlcR.

Furthermore, comparison of the transcriptome, proteome and secretome datasets could inform on the level at which the toxic phenotype is regulated.

Transcriptomic analysis is also a widely accepted method to corroborate findings from proteomics experiments. In particular, label-free proteomics and RNAseq have been shown to correlate significantly (Fu et al., 2009; Ning et al., 2012). This study will seek to use both proteomics and transcriptomics to elucidate the global regulation of *B. cereus* G9241 growing exponentially and into stationary phase at 25 °C and 37 °C.

Aims for this chapter were:

1. To determine if the temperature-dependent cytotoxic phenotype is regulated at a transcriptional level.
2. To determine the role, if any, PlcR plays in regulating temperature-dependent phenotypes in *B. cereus* G9241.
3. To analyse the transcriptional landscape of *B. cereus* G9241 to reveal the roles of plasmids in global gene regulation.

During this chapter we will discuss comparative RNAseq data. When comparing transcript levels between different conditions we will say genes are more or less highly “expressed”. This terminology is used widely in the literature to compare transcript levels between RNAseq conditions as differential levels of mRNA may be a result of differential transcription, or differential mRNA degradation.

4.2. Results

4.2.1 Analysing the transcriptome of *B. cereus* G9241 during exponential growth

4.2.1.1 RNAseq analysis of mRNA from *B. cereus* G9241 growing exponentially at 25 °C and 37 °C

As discussed, several candidate toxins were identified using mass spectroscopy that may contribute to the temperature-dependent haemolytic phenotype

observed in the supernatant of *B. cereus* G9241. To determine if the toxins were regulated at a transcriptional level, mRNA was extracted from cultures of *B. cereus* G9241 WT growing exponentially (OD_{600}=0.5) at both 25 °C and 37 °C. mRNA was converted into cDNA libraries using TruSeq library prep and analysed on the Illumina MiSeq. Reads were normalised and reads obtained at 25 °C were compared to those obtained at 37 °C (fig 4.1).

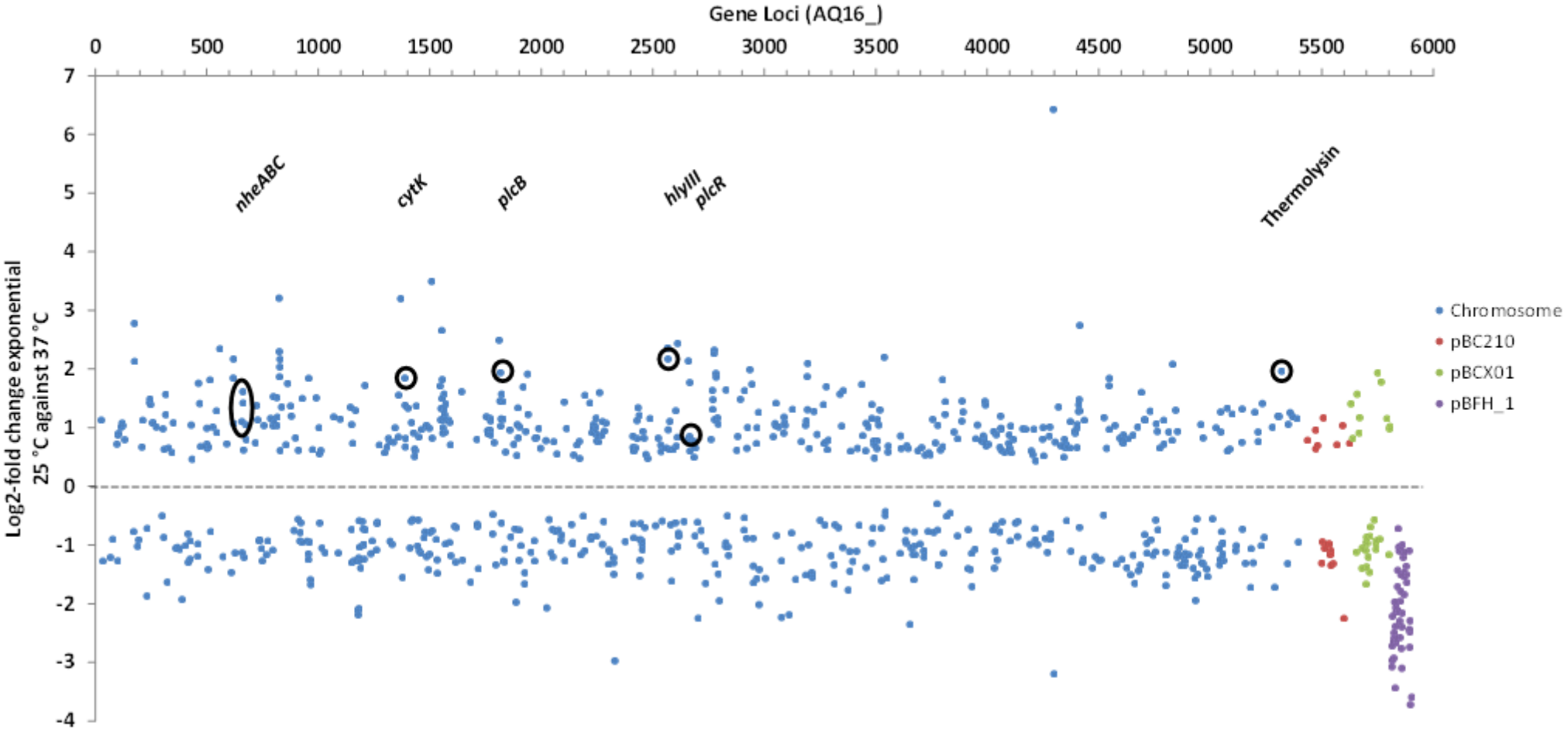

Fig.4.1 *B. cereus* G9241 transcribes a temperature-dependent toxin profile during exponential growth. RNAseq was conducted using RNA extracted from *B. cereus* G9241 WT growing exponentially (OD_{600} = 0.5) in LB broth, 200 rpm. RNAseq reads were processed, normalised and plotted as the log2-fold change in the transcriptional level of each gene at 25 °C compared to at 37 °C. Various haemolytic and cytolytic toxins are more highly transcribed at 25 °C compared to 37 °C (circled and labelled above in black). Interestingly almost all genes on pBFH_1 are more highly transcribed at 37 °C compared to 25 °C. All points plotted are statistically significant (p-value < 0.05; n=3).

4.2.1.2 Toxins secreted at 25 °C by *B. cereus* G9241 are partially regulated at a transcriptional level.

The high throughput nature of RNAseq meant that almost every gene identified was significant beyond threshold of $p < 0.01$. Using a cut-off of 1 log2-fold change 245 genes were identified as up at 25 °C compared to 37 °C during exponential growth in *B. cereus* G9241. The gene highest at 25 °C compared to 37 °C was *sleB* (AQ16_4300), a cell wall hydrolase at 6.4 log2-fold higher (table 4.1). Cold shock genes such as *cspA* and *ydjO* were expectedly up at 25 °C. The flagellin operon (AQ16_827-831) and other chemotaxis and motility genes were also up at 25 °C, coinciding with the temperature-dependent motility phenotype seen.

While no toxin gene mRNAs appeared in the top 15 genes higher at 25 °C, 6 were identified as significantly higher at 25 °C (table 4.2). The mRNAs of all three genes encoding the tripartite Nhe toxin, *cytK*, *plc*, a thermolysin and a haemolysin III toxin were all significantly up at 25 °C. Interestingly the *hblABCD* operon mRNA was slightly higher at 25 °C, but not over 1 log2-fold threshold. This was also true of a collagenase and *clo*. Importantly, *plcR* mRNA did not increase over the log2-fold threshold at 25 °C compared to 37 °C.

Log2-fold Change	Encoded Protein	Gene Annotation	Gene Loci (AQ16_)
6.43	Cell Wall Hydrolase family protein	*sleB*	4300
3.49	YjcZ family sporulation protein		1507
3.21	Flagellin	*flgL*	831
3.20	Cold shock protein	*cspA*	1368
2.77	Cold-inducible YdjO family protein		175
2.74	carD-like/TRCF domain protein		4418
2.65	Membrane protein PgaA superfamily		1559
2.49	Methyl-accepting chemotaxis (MCP) signaling domain protein		1816
2.43	FMN-dependent NADH-azoreductase	*azoR4*	2611
2.36	UDP-glucose 4-epimerase	*galE*	2573
2.34	Hypothetical protein		555
2.32	Glycosyl transferase 21 family protein		2780
2.29	Flagellin		830
2.26	dGTP triphosphohydrolase		2781
2.20	Putative cytoplasmic protein		3545

Table.4.1. Top 15 genes expressed higher at 25 °C compared to 37 °C in *B. cereus* G9241 growing exponentially.

Log2-fold change	Encoded protein	Gene Annotation	Gene Loci (AQ16_)
1.10	Non-haemolytic enterotoxin binding component	*nheC*	658
1.42	Non-hemolytic enterotoxin lytic component L1	*nheB*	659
1.61	Non-hemolytic enterotoxin lytic component L2	*nheA*	660
1.85	Leukotoxin	*cytK*	1392
1.94	Phospholipase C	*plcB*	1823
0.84	Collagenase family protein		1941
2.17	Haemolysin III	*hlyIII*	2572
0.85	Helix-turn-helix family protein	*plcR*	2669
0.18	Cereolysin	*clo*	4769
0.25	Haemolysin BL lytic component L1	*hblD*	4930
0.20	Haemolysin BL lytic component L2	*hblC*	4931
0.22	Hemolysin BL-binding component	*hblB*	4932
0.15	Hemolysin BL-binding component	*hblA*	4933
1.96	Thermolysin metallopeptidase		5317

Table.4.2. Transcription of toxin genes at 25 °C compared to 37 °C in *B. cereus* G9241 growing exponentially. Grey boxes indicate an insignificant fold change.

4.2.1.3 Transcription from pBFH_1 increases at 37 °C compared to 25 °C in *B. cereus* G9241 when growing exponentially.

Using the same significance criteria as for 25 °C, 317 genes were more highly expressed in *B. cereus* G9241 at 37 °C compared to 25 °C during exponential growth. A terminase gene (AQ16_5898) located on the pBFH_1 phagemid was identified as the gene highest at 37 °C (table 4.3). In fact, 13 of the top 15 genes and 54 out of 81 of the total genes present on pBFH_1 were significantly up at 37 °C. These genes included minor capsid, major capsid and phage tail family protein-encoding genes. In addition to structural proteins, an N-acetylemuramoyl-L-alanine amidase encoding gene (AQ16_5839) and two Xre superfamily, transcriptional activator encoding genes (AQ16_5854, 5850) were also higher at 37 °C. The proteins encoded by these genes may play a role in altering the structure of the cell wall and gene regulation respectively. Interestingly levels of a haemolysin toxin gene (AQ16_5837) mRNA were also higher at 37 °C. Ignoring the 1 log2-fold change significance threshold, all but one gene (AQ16_5878) present on pBFH_1 appear more highly expressed at 37 °C.

Nine genes encoded on the pBC210 plasmid had higher levels of mRNA at 37 °C compared to 25 °C including *atxA2* (AQ16_5600) up 2.3 log2-fold and a haemolysin secretion gene *hlyD* (AQ16_5558). Eleven genes encoded on pBCX01 were up at 37 °C including the protective antigen, *pagA* (AQ16_5705) and the RNA chaperone *hfq* (AQ16_5741). Seven genes, known to encode germination-associated proteins were also up at 37 °C. Three were located on the chromosome (AQ16_1713; 3358; 3677), 2 were encoded on the pBC210 plasmid (AQ16_5540; 5541) and 2 on the pBCX01 plasmid (AQ16_5702; 5703).

Log2-fold change	Encoded Protein	Gene Annotation	Gene Loci (AQ16_)
3.72	ATPase subunit of terminase family protein		5898
3.60	Phage terminase- large subunit- PBSX family		5899
3.44	Phage tail family protein		5835
3.20	Septin family protein		4297
3.11	Transposase- IS605 OrfB family		5861
3.08	Phage family protein	*gp49*	5822
2.98	TQO small subunit DoxD family protein		2331
2.97	Hypothetical protein		5820
2.93	Minor capsid family protein		5827
2.77	Hypothetical protein		5863
2.75	Putative membrane protein		5895
2.73	Hypothetical protein		5821
2.68	Putative gp14-like protein	*gp14*	5832
2.66	Minor capsid family protein		5828
2.64	Bacteriophage Gp15 family protein		5833

Table.4.3. Top 15 genes expressed higher at 37 °C compared to 25 °C in *B. cereus* G9241 growing exponentially.

4.2.2 Analysing the transcriptome of *B. cereus* G9241 during stationary phase growth

4.2.2.1 RNAseq analysis of mRNA from *B. cereus* G9241 during stationary phase at 25 °C and 37 °C

Total RNA was extracted from *B. cereus* G9241 grown to stationary phase at both 25 °C and 37 °C. The total RNA was converted into cDNA libraries and analysed using the Illumina MiSeq. Reads were normalised and compared as transcripts obtained at 25 °C against transcripts at 37 °C (fig.4.2). Approximately 39% of the known protein-encoding genome, 2,293 genes were expressed 1 log2-fold higher at either 25 °C or 37 °C. It was decided to concentrate on the top 50 genes differentially expressed at 25 °C or 37 °C as it was deemed unfeasible to analyse all of the genes significantly differentially expressed at both temperatures.

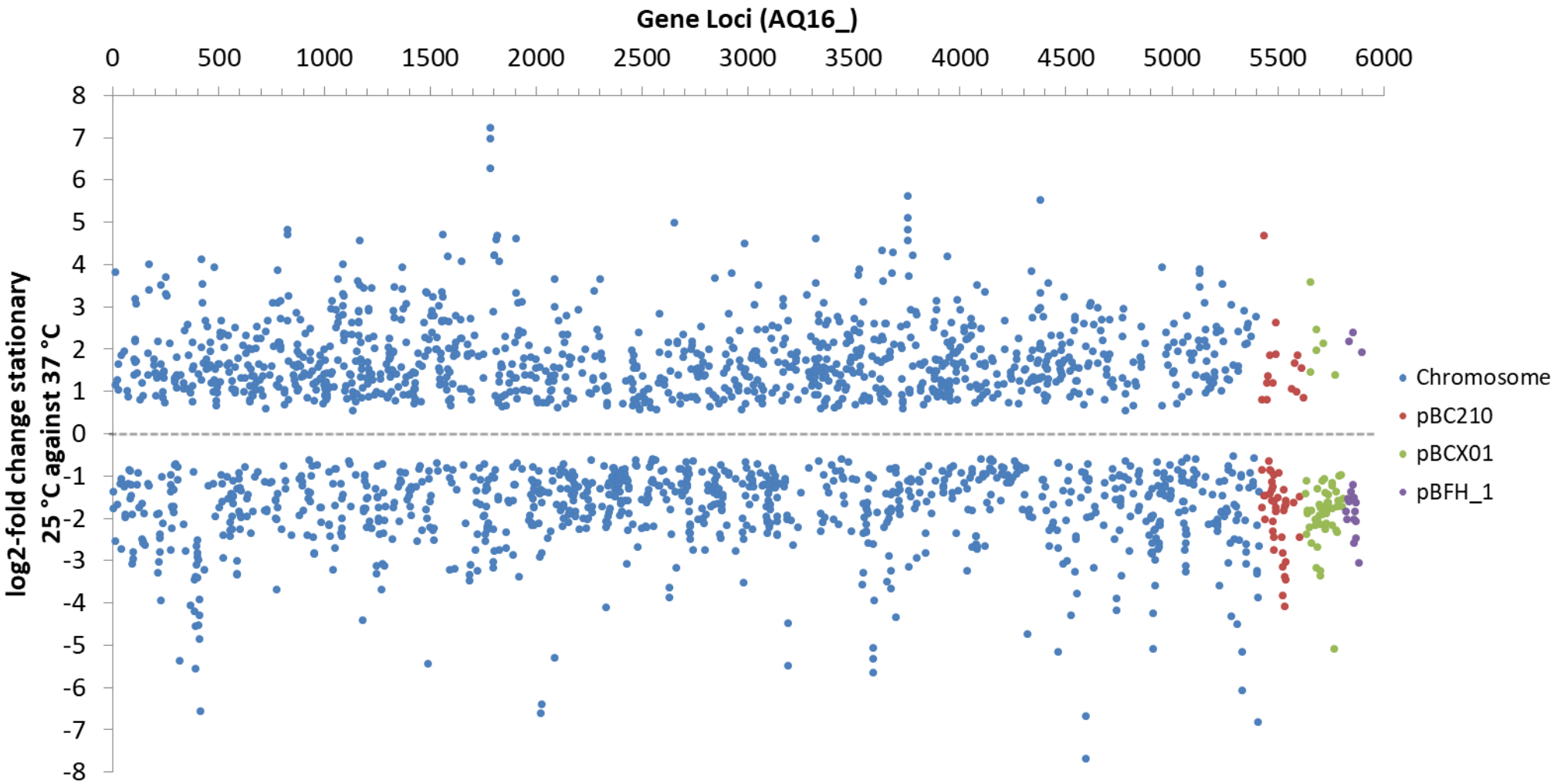

Fig.4.2 Comparison of the transcriptome of *B. cereus* G9241 WT during stationary phase growth at 25 °C and 37 °C. RNAseq was conducted using RNA extracted from *B. cereus* G9241 WT grown to stationary phase at 37 °C and 25 °C in LB broth, 200 rpm. Stationary phase occurred after 7 hours and 10 hours at 37 °C and 25 °C respectively. RNAseq reads were processed, normalised and plotted as the log2-fold change in the transcriptional level of each gene at 25 °C compared to at 37 °C. All points plotted are statistically significant (p-value < 0.05; n=3).

4.2.2.2 Genes more highly expressed at 25 °C compared to 37 °C during stationary phase

10 of the 50 genes most highly expressed at 25 °C compared to 37 °C were involved in metabolism or the acquisition of inorganic phosphate (Table 4.4; Table 8.3 appendices). Seven of these genes were components of a phosphate ABC transporter, including the gene expressed highest (7.2 log2-fold) at 25 °C compared to 37 °C, *pstS* (AQ16_1786). Two cold shock-induced genes (AQ16_175 and 1368) were more highly expressed at 25 °C. These were the same two cold shock induced genes more highly expressed at 25 °C during exponential phase. Two flagellin encoding genes (AQ16_827 and 828) and a chemotaxis protein encoding gene were more highly expressed at 25 °C. Higher transcription of motility and cold shock genes at 25 °C was similar to the pattern seen at the same temperature during exponential growth.

19 genes from the pBC210 plasmid were significantly more highly expressed at 25 °C compared to 37 °C. Only 13 genes on each of the pBCX01 and pBFH_1 plasmids were higher at 25 °C compared to 37 °C during stationary phase. However, only one of the extrachromosomal genes (AQ16_5436) was in the top 50 most highly expressed genes at 25 °C compared to 37 °C. This gene encoded an axoneme-associated protein and may also play a part in regulation of motility.

Log2-fold Change	Encoded Protein	Gene Annotation	Gene Loci (AQ16)
7.22	Phosphate ABC transporter (binding protein)	*pstS*	1786
6.98	Phosphate ABC transporter (permease)	*pstC*	1785
6.27	Phosphate ABC transporter (permease)	*pstA*	1784
5.61	Phosphate ABC transporter (binding protein)	*pstS*	3754
5.52	Phosphonate ABC transporter	*phnD*	4380
5.10	phosphate ABC transporter (ATP-binding protein)	*pstB*	3757
4.97	Hypothetical protein		2653
4.82	Phosphate ABC transporter (permease)	*pstC*	3755
4.81	Flagellin	*hag*	828
4.70	Hypothetical protein		1558
4.69	Flagellin		827
4.67	Methyl-accepting chemotaxis (MCP) signaling domain protein		1816
4.67	Putative axoneme-associated protein		5436
4.61	Hypothetical protein		3319
4.60	Bacterial regulatory- arsR family protein		1907

Table.4.4. Top 15 genes expressed higher at 25 °C compared to 37 °C in *B. cereus* G9241 grown to stationary phase.

4.2.2.3 Genes more highly expressed at 37 °C compared to 25 °C during stationary phase

7 of the top 50 most highly expressed genes at 37 °C compared to 25 °C during stationary phase growth were involved in nitrite and nitrate reduction (Table 4.5 and table 8.4 appendices). Interestingly, several spore coat genes (AQ16_1270; 2630; 2631 and 3595) were more highly expressed at 37 °C compared to 25 °C during stationary phase.

A total of 135 genes encoded on the three plasmids of *B. cereus* G9241 were more highly expressed at 37 °C compared to 25 °C during stationary phase. There were 45, 62 and 28 genes on pBC210, pBCX01 and pBFH_1 respectively. Of these, only 3 appeared in the top 50 genes most highly expressed at 37 °C compared to 25 °C during stationary phase growth (AQ16_5526; 5535 and 5768).

4.2.2.4 Principle component analysis reveals *B. cereus* G9241 transcriptional profile varies more between temperatures during stationary phase than during exponential phase.

A PCA plot of the transcriptome of *B. cereus* G9241 (fig 4.3) revealed a significant overlap between transcriptomes produced at 25 °C and 37 °C during exponential growth (fig 4.3 blue and red points). During stationary phase however, transcriptomes varied far more between 25 °C and 37 °C and biological replicates formed distinct clusters (fig 4.3 green and purple points). This revealed the transcriptional profile of *B. cereus* G9241 varies more between 25 °C and 37 °C during stationary growth compared to exponential growth.

Log2-fold Change	Encoded Protein	Gene Annotation	Gene Loci (AQ16_)
7.68	DUF2690 -containing gene / AAA family ATPase		4594
6.83	Cysteine dioxygenase		5407
6.69	SigE-regulated protein	*yjfA*	4595
6.62	Pyruvate fomrate-lyase 1-activating enzyme; cellular response to DNA damage in *E. coli*	*pflA*	2024
6.57	Nitrate reductase alpha subunit	*narG*	414
6.41	Formate acetyltransferase	*pflB*	2025
6.08	Inosine-uridine preferring nucleoside hydrolase family protein		5336
5.67	Quinolate synthetase complex, subunit A	*nadA*	3594
5.56	Nitrite reductase large subunit	*nirB*	392
5.50	Bacterial Cytochrome Ubiquinol Oxidase family protein		3189
5.45	Hainantoxin F8-35.23 domain protein		1488
5.37	Zinc-binding dehydrogenase family protein		318
5.33	L-aspartate oxidase	*nadB*	3592
5.31	Chitinase A1	*chiA1*	2089
5.18	Aerobic Ribonucleoside-triphosphate reductase	*nrdD*	4464

Table.4.5. Top 15 genes expressed higher at 37 °C compared to 25 °C in *B. cereus* G9241 grown to stationary phase.

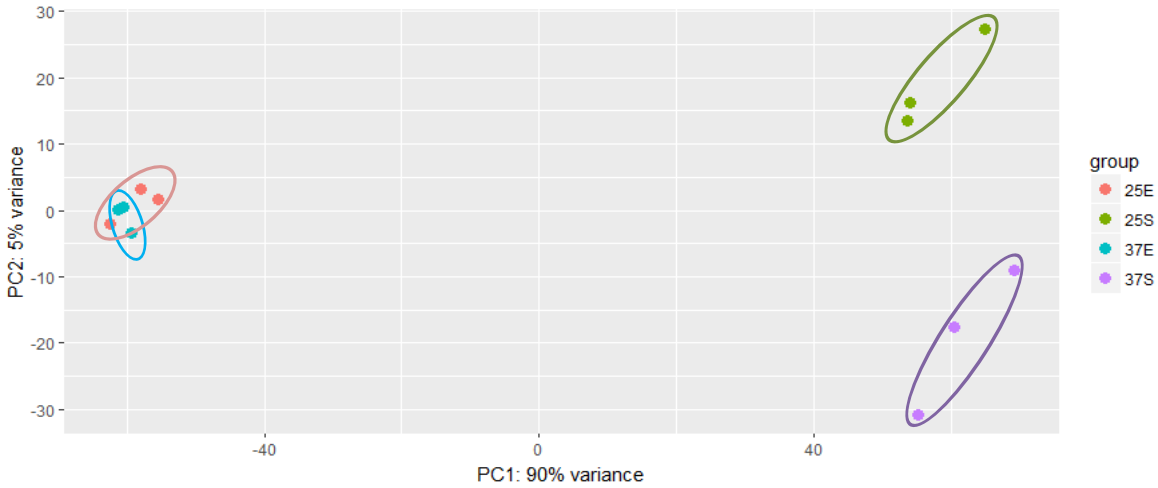

Fig 4.3. Principal component analysis of transcriptome of *B. cereus* G9241. mRNA was extracted from *B. cereus* G9241 growing exponentially and to stationary phase at either 25 °C or 37 °C. Exponential growth was indicated by an OD_{600} of 0.5. Stationary phase occurred after 10 hours growth at 25 °C and after 7 hours growth at 37 °C. The PCA plot was produced in R Studio and the three points of each colour represent three biological replicates. The exponential phase transcriptomes (25E blue, 37E red) clustered together regardless of growth temperature. Stationary phase transcriptomes (25S green, 37S purple) showed a greater

4.2.3 Analysing the transcriptome of *B. cereus* G9241 during growth at 25 °C

4.2.3.1 RNAseq analysis of mRNA from *B. cereus* G9241 during exponential and stationary phase growth at 25 °C

RNAseq reads were previously obtained from *B. cereus* G9241 growing exponentially and to stationary phase at 25 °C (section 4.2.1 and 4.2.2). Reads were normalised and transcript levels obtained during exponential growth at 25 °C were compared to those obtained during stationary phase growth at 25 °C.

3,251 genes were identified as significantly different between the growth phases, i.e. above the 1 log2-fold threshold (fig. 4.4). The high throughput nature of RNAseq meant that all fold changes were statistically significant (p-value < 0.05). Only the top 50 genes up during exponential phase or stationary phase were analysed in detail as it was deemed unfeasible to analyse all significantly changing genes.

4.2.3.2 Genes more highly expressed during exponential growth compared to stationary phase growth at 25 °C

1520 genes were over 1 log2-fold higher during exponential growth compared to stationary phase growth (table 4.6 and table 8.5 appendices). As expected, many genes identified were involved in growth. Six of the 50 genes highest during exponential phase encoded tRNA (AQ16_1772, 1773, 2435, 2436, 3090 and 3092). Two of the 50 highest genes were involved in motility. *fliE* (AQ16_844) and *fliR* (AQ16_819) transcripts were 6.6 and 6.3 log2-fold higher respectively during exponential phase compared to stationary phase growth. In fact a whole motility regulon containing *fliE*, *fliG*, *flgB* and *fliI* was on average 4.5 log2-fold higher during exponential phase.

122 genes encoded across the extrachromosomal elements were over 1 log2-fold higher. Almost all of these plasmid-encoded genes were more highly expressed during exponential approximately 1 - 3 log2-fold. However, an IS1182 family

transposase (AQ16_5693) located downstream of *atxA* (AQ16_5694) was 5.8 log2-fold higher during exponential phase compared to stationary phase growth.

Transcription levels of the *nheABC* operon (AQ16_658-660) did not significantly differ between growth phases at 25 °C. However, *cytK* (AQ16_1392), *plcB* (AQ16_1823), *hlyIII* (AQ16_2572) and the *hblABCD* (AQ16_4930-4933) operon were all expressed more highly during exponential phase. The gene encoding the pleiotrophic regulator *plcR* (AQ16_2669) was also more highly expressed during exponential growth compared to stationary phase growth at 25 °C.

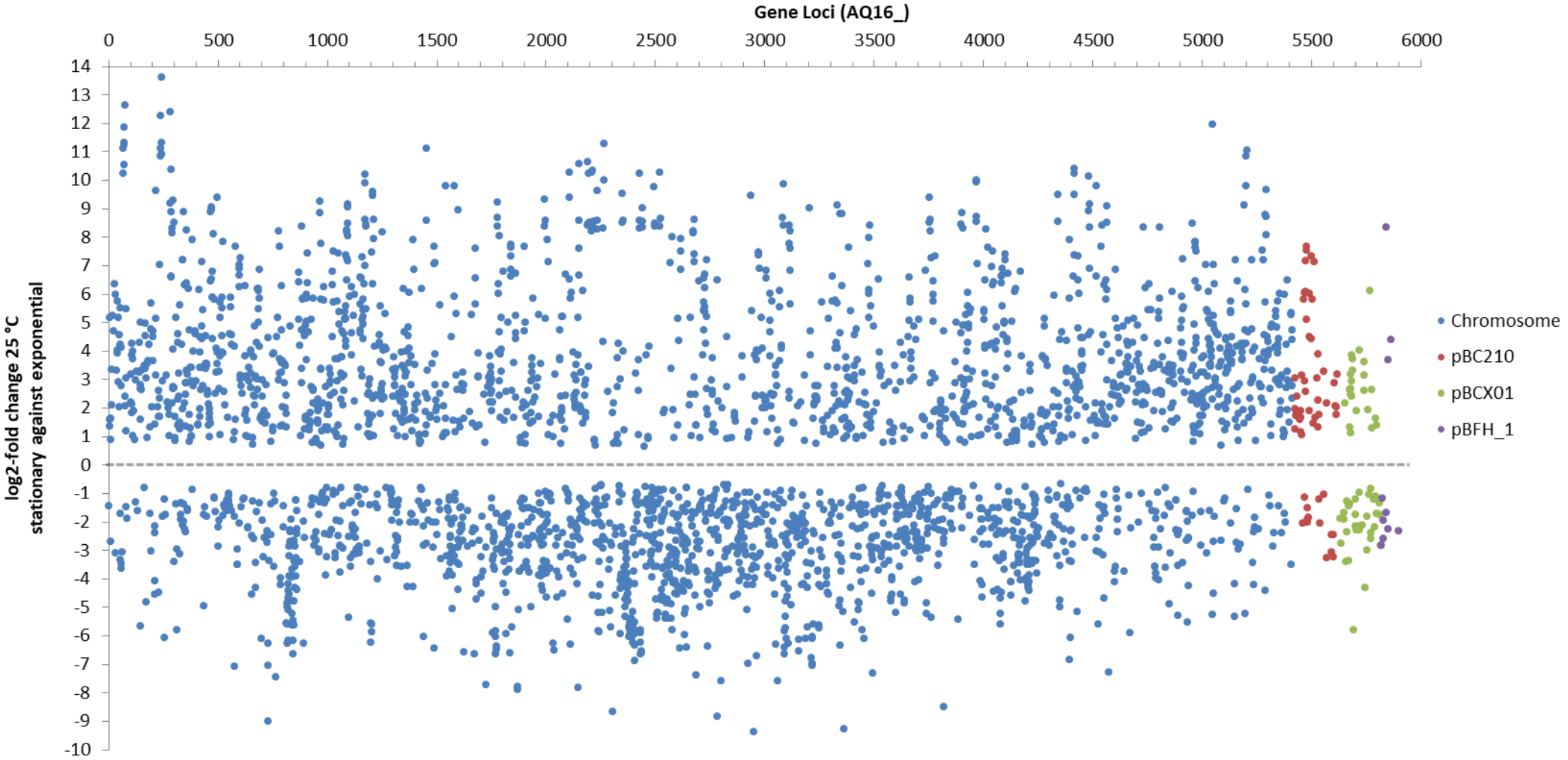

Fig.4.4. Comparison of the transcriptome of *B. cereus* G9241 WT during stationary and exponential phase growth at 25 °C. RNAseq was conducted using RNA extracted from *B. cereus* G9241 WT grown to exponential and stationary phase at 25 °C in LB broth, 200 rpm. Exponential phase samples were taken when *B. cereus* G9241 grew to OD_{600}=0.5. Stationary phase occurred after 10 hours at 25 °C. RNAseq reads were processed, normalised and plotted as the log2-fold change in the transcriptional level of each gene at stationary phase compared to exponential phase. All points plotted are statistically significant (p-value < 0.05; n=3). Hashed line represents a log2-fold change of 0.

Log2-foldChange	Encoded Protein	Gene Annotation	Gene Loci (AQ16_)
10.02	Protein erfK/srfK precursor		2947
9.37	Hypothetical protein		2948
9.27	Acetate kinase	*ackA*	3361
9.01	Major high-affinity Na^+-coupled glutamate/ aspartate symport protein	*gltT*	730
8.83	Nucleoside transporter	*nupC*	2782
8.66	Glucose uptake protein	*glcU*	2305
8.51	Hypothetical protein		3821
7.90	Trehalose phospho-alpha-glucosidase	*treC*	1870
7.84	Pyrimidine nucleoside transporter	*nupC*	2145
7.80	Trehalose permease - phosphotransferase system	*treP*	1871
7.73	Guanine/hypoxanthine permease	*pbuO*	1724
7.58	Proton/sodium-glutamate symport protein		2800
7.58	Hypothetical protein		3059
7.44	Antiport NhaC: Na+/H+ antiporter	*nhaC*	764
7.38	Thymidine kinase	*tdk*	2689

Table.4.6. Top 15 genes expressed higher at during exponential growth compared to stationary phase growth at 25 °C in *B. cereus* G9241.

4.2.3.3 Genes more highly expressed during stationary phase growth compared to exponential growth at 25 °C

1731 genes were expressed over 1 log2-fold higher during stationary phase growth compared to exponential growth (table 4.7 and appendices). The 50 genes more highly expressed during stationary phase mostly encode proteins involved in utilisation of secondary metabolites. The fatty acid utilisation, acyl-CoA operon (AQ16_68 – 74) was more highly expressed during stationary phase

growth compared to exponential phase growth. The histidine utilisation, *hut* operon (AQ16_4414 – 4416) was also expressed higher during stationary phase growth.

The forespore-specific transcriptional regulator *sigF* (AQ16_3969) was 9.9 log2-fold more highly expressed during stationary phase compared to exponential phase. Additionally SigF co-regulators *spoIIAA* (AQ16_3967) and *spoIIAB* (AQ16_3968) were 8.5 and 9.9 log2-fold more highly expressed during stationary phase growth.

log2-Fold Change	Encoded Protein	Gene Annotation	Gene Loci (AQ16_)
13.63	2-methylcitrate synthase	*mmgD*	243
12.64	Acyl-CoA dehydrogenase, short-chain specific		74
12.38	Lysine-2,3-aminomutase	*ablA*	284
12.27	Methylmalonate-semialdehyde dehydrogenase (acylating)	*mmsA*	238
11.95	M6 family metalloprotease domain protein		5047
11.85	3-hydroxybutyryl-CoA dehydratase		70
11.33	2-methylcitrate dehydratase	*prpD*	242
11.32	Hydroxymethylglutaryl-CoA lyase		71
11.28	4-hydroxyphenylpyruvate dioxygenase	*hppD*	2265
11.24	Propionyl-CoA carboxylase, alpha subunit		73
11.13	Acyl-CoA dehydrogenase, short-chain specific		240
11.11	Propionyl-CoA carboxylase, beta chain		69
11.10	Hypothetical protein		1455
11.05	Oligopeptide ABC transporter, oligopeptide-binding protein		5204
10.92	Methylisocitrate lyase	*prpB*	241

Table.4.7. Top 15 genes expressed higher at during stationary growth compared to exponential phase growth at 25 °C in *B. cereus* G9241.

4.2.4 Analysing the transcriptome of *B. cereus* G9241 during growth at 37 °C

4.2.4.1 RNAseq analysis of mRNA from *B. cereus* G9241 during exponential and stationary phase growth at 37 °C

RNAseq reads were previously obtained from *B. cereus* G9241 growing exponentially and to stationary phase at 37 °C (section 4.2.1 and 4.2.2). Reads were normalised and transcript levels obtained during exponential growth at 37 °C were compared to those obtained during stationary phase growth at 37 °C.

3,366 genes were differentially expressed above the 1 log2-fold threshold. The high throughput nature of RNAseq meant that all fold changes were statistically significant (p-value < 0.05). As before, only the top 50 genes up during exponential phase or stationary phase were analysed in detail as it was deemed unfeasible to analyse all significantly changing genes.

4.2.4.2 Genes more highly expressed during exponential growth compared to stationary phase growth at 37 °C

1771 genes were expressed significantly more highly during exponential growth compared to stationary phase growth at 37 °C. As expected *B. cereus* G9241 expressed nutrient acquisition proteins more highly during exponential growth compared to stationary phase growth at 37 °C (table 4.8 and table 8.7 appendices). An aquaporin protein (AQ16_3495), a ferrichrome-binding protein (AQ16_3601) and a glucose uptake protein (AQ16_2305) were 6.8, 6.8 and 8.1 log2-fold more highly expressed during exponential phase growth compared to stationary phase. Four genes encoding nucleoside transporter proteins were also more highly expressed during exponential phase (AQ16_2145, 2782, 2922 and 2923).

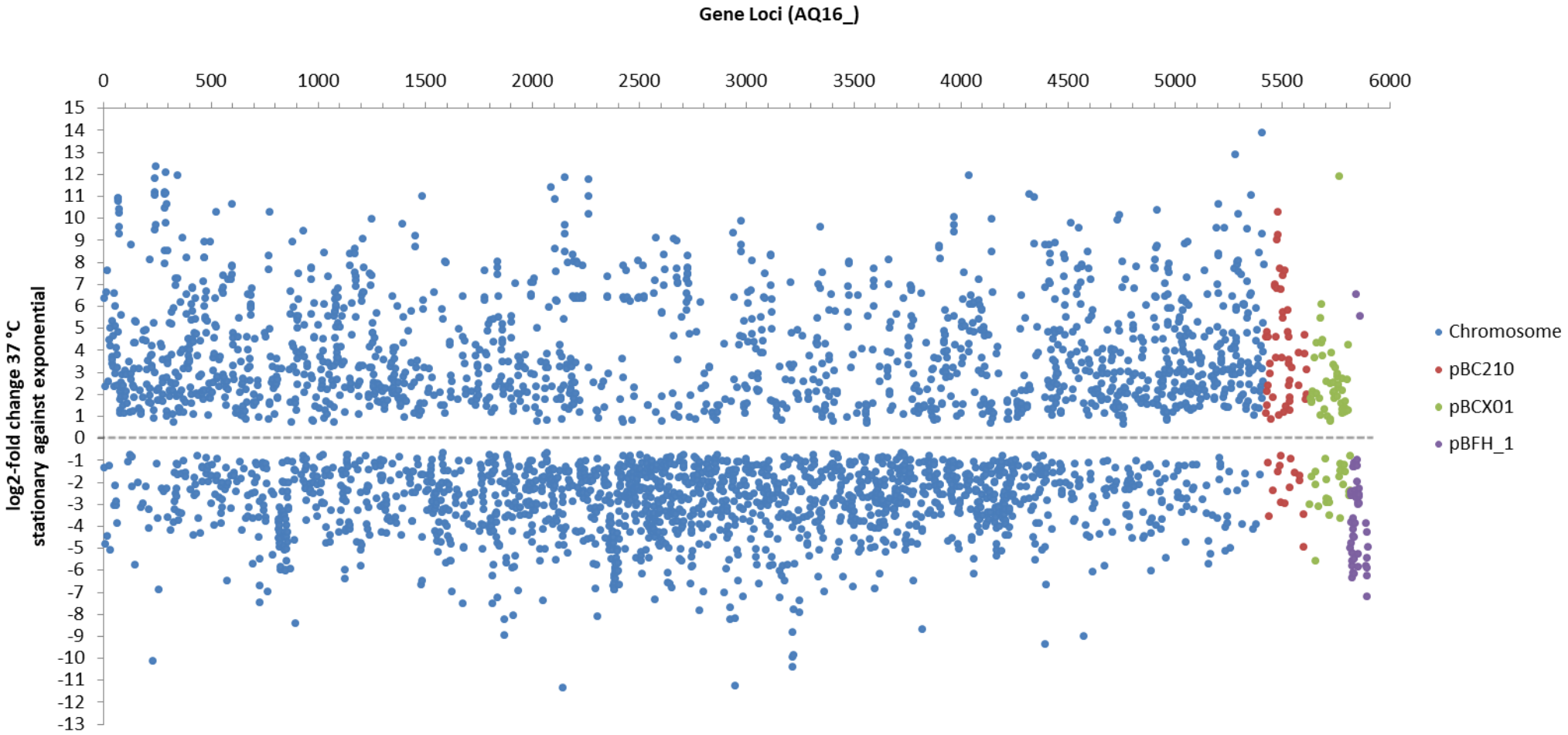

Fig.4.5. Comparison of the transcriptome of *B. cereus* G9241 WT during stationary and exponential phase growth at 37 °C. RNAseq was conducted using RNA extracted from *B. cereus* G9241 WT grown to exponential and stationary phase at 37 °C in LB broth, 200 rpm. Exponential phase samples were taken when *B. cereus* G9241 grew to OD_{600}=0.5. Stationary phase occurred after 7 hours at 37 °C. RNAseq reads were processed, normalised and plotted as the log2-fold change in the transcriptional level of each gene during stationary phase growth compared to during exponential growth. All points plotted are statistically significant (p-value < 0.05; n=3). Hashed line represents a log2-fold change of 0.

Log2-fold change	Encoded Protein	Gene Annotation	Gene Loci (AQ16_)
11.36	Pyrimidine nucleoside transporter	*nupC*	2145
11.25	Protein erfK/srfK precursor		2947
10.42	LPXTG cell wall anchor domain protein		3216
10.12	ArsR family transcriptional repressor		230
9.96	WxL domain surface cell wall-binding family protein		3217
9.85	WxL domain surface cell wall-binding family protein		3218
9.37	Murein hydrolase export regulator		4396
8.99	Glycerophosphoryl diester phosphodiesterase		4572
8.94	Trehalose phospho-alpha-glucosidase	*treC*	1870
8.82	WxL domain surface cell wall-binding family protein		3215
8.71	Hypothetical protein		3821
8.42	QueT family transporter protein		893
8.24	Na+ dependent nucleoside transporter family protein		2922
8.24	Trehalose permease - phosphotransferase system	*treP*	1871
8.19	Hypothetical protein		2948

Table.4.8. Top 15 genes expressed higher at during exponential growth compared to stationary phase growth at 37 °C in *B. cereus* G9241.

44 genes encoded on the pBFH_1 phagemid were more highly expressed during exponential phase compared to only 2 genes at stationary phase. Several genes encoding minor capsid proteins, a phage tail protein and multiple phage terminase proteins are all expressed more highly during exponential growth than during stationary phase growth.

4.2.4.3 Genes more highly expressed during stationary phase growth compared to exponential growth at 37 °C

1595 genes were significantly more highly expressed during stationary phase growth compared to exponential growth at 37 °C (table 4.8 and table 8.8 appendices). Eleven genes across 2 operons encoding genes involved in fatty acid metabolism (AQ16_68 – 74; AQ16_238 – 243) were up at stationary phase compared to exponential phase. *spoIIAB* (AQ16_3968), *spoIIGA* (AQ16_4145) and *spoIIAA* (AQ16_3967) were expressed 10.0, 9.9 and 9.7 log2-fold higher during stationary phase growth compared to during exponential growth. This suggested that *B. cereus* G9241 committed to sporulation as early as after 7 hours growth at 37 °C.

Forty-seven genes encoded on pBC210, 45 genes encoded on pBCX01 and 2 genes encoded on pBFH_1 were expressed more highly during stationary phase. An operon on pBC210 encoding conjugal transfer proteins, tcpE (AQ16_5477) and tcpC (AQ16_5479) was expressed on average 9.5 log2-fold more highly during stationary phase growth. *atxA* (AQ16_5694) was not significantly higher during either growth phase. Encoded on pBCX01, 2 of the highest expressed genes during stationary phase compared to exponential phase were AQ16_5680 and 5682. The genes encoded 2 transposase proteins.

Log2-fold change	Encoded Protein	Gene Annotation	Gene Loci (AQ16_)
13.88	Cysteine dioxygenase		5407
12.88	Hypothetical protein		5281
12.37	2-methylcitrate synthase	mmgD	243
12.09	3-oxacid CoA-transferase, B subunit		288
11.94	Beta-lactamase family protein		345
11.93	Hypothetical protein		4039
11.89	Hypothetical protein		5768
11.88	Gamma-aminobutyrate transaminase, general stress protein	gabT	2152
11.81	Acyl-CoA dehydrogenase, short-chain specific		240
11.76	4-hydroxyphenylpyruvate dioxygenase	hppD	2265
11.43	Chitinase A1	chiA1	2089
11.18	Methylmalonate-semialdehyde dehydrogenase (acylating)	mmsA	238
11.16	unknown function	yokU	283
11.13	3-oxacid CoA-transferase, A subunit		289
11.10	Lysine-2,3-aminomutase	ablA	284

Table.4.9. Top 15 genes expressed higher at during stationary phase growth compared to exponential growth at 37 °C in *B. cereus* G9241.

4.3. Discussion

4.3.1. Transcriptional regulation of the PlcR regulon

The temperature-dependent haemolytic phenotype of the supernatant is not due to a temperature-dependent block on secretion (section 3.3.2) of proteins accumulating in the cytoplasm. In order to determine if the temperature-dependent haemolysis is regulated at a transcriptional level, RNAseq was conducted on *B. cereus* G9241. The transcriptome of *B. cereus* G9241 growing exponentially was analysed and compared at 25 °C and 37 °C. Of the 11 toxin proteins identified as highest at 25 °C compared to 37 °C in the secretome, only 6 were expressed more highly at 25 °C compared to 37 °C in the RNAseq. All 3 genes encoding the components of the Nhe toxin, *plcB*, *cytK* and a thermometalloprotease gene were all more highly expressed at 25 °C compared to 37 °C. Interestingly, all genes encoding the components of the Hbl toxin fell below the threshold to be considered as significantly changing in transcription under the same conditions (fig 4.10).

The *plcR* gene was nearly twice as highly expressed at 25 °C compared to 37 °C during exponential growth and *plcB* nearly 4-fold more highly expressed under the same conditions. The *plcR* operon is a well conserved genetic element in the *B. cereus* sensu lato (Gohar et al., 2008). PlcR positively auto-regulates its own transcription and that of *plcB* within the operon (Agaisse et al., 1999; Økstad et al., 1999). Increased transcription of both *plcR* and *plcB* confirms that PlcR in *B. cereus* G9241 has a higher transcriptional activity at 25 °C compared to 37 °C. However, this finding conflicts with the cell proteome analysis where levels of PlcR protein did not change between the two growth temperatures. The *nheABC* operon and *cytK* both contain upstream PlcR boxes and increase in transcription at 25 °C compared to 37 °C. Thus, it is highly likely that NheABC and CytK toxin production is controlled at a transcriptional level by PlcR in *B. cereus* G9241. This mirrors PlcR-mediated regulation in *B. cereus* ATCC14579 and *B. thuringiensis* (Agaisse et al., 1999; Økstad et al., 1999). These findings suggest that despite the substitutions identified in the PlcR boxes of *nheABC* and the *plc* operon, PlcR still

efficiently initiates transcription. Loss of transcription initiation observed in previous studies may be strain specific (Gohar et al., 2008).

Unlike other genes encoding toxins theoretically regulated by PlcR, transcription of the *hbl* operon does not significantly change between 25 °C and 37 °C during exponential growth. The *hblCDAB* operon has been shown to be transcriptionally regulated by PlcR in *B. cereus* ATCC14579. Unpublished data from Agaisse suggests that deletion of the PlcR box upstream of the hbl greatly reduces β-galactosidase production in a *hbl'-lacZ* fusion (Agaisse et al., 1999). Comparison of the supernatant proteins of *B. cereus* ATCC14579 and *B. cereus* ATCC14579 *ΔplcR* showed that secretion of Hbl toxin components was lost in the *ΔplcR* strain (Gohar et al., 2002). The PlcR box of *hblCDAB* is 896 bp upstream of the operon in *B. cereus* G9241. Though this is much farther upstream than other PlcR boxes, it is similar to the organisation of the *hblCDAB* operon and PlcR box in *B. cereus* ATCC14579 (Agaisse et al., 1999; Økstad et al., 1999). The sequence of the PlcR box is identical in the two strains. The transcriptional profile of *hblCDAB* in *B. cereus* G9241 suggests that regulation of the operon is not the same as in *B. cereus* ATCC14579. Either *hblCDAB* is not under the transcriptional control of PlcR in *B. cereus* G9241, or unknown factors interfere with PlcR regulation of the operon. Interestingly, the *hbl* operon is seen to be absent in strains of *B. anthracis* (Mignot et al., 2001).

Secretome Log2-fold change	Cell Proteome Log2-fold change	RNAseq Log2-fold change	Encoded protein	Gene Annotation	Gene Loci (AQ16_)
5.889979298	-	1.10249278	Non-haemolytic enterotoxin binding component	*nheC*	658
3.776604672	2.474713196	1.41876373	Non-hemolytic enterotoxin lytic component L1	*nheB*	659
3.937641362	2.095966309	1.61091609	Non-hemolytic enterotoxin lytic component L2	*nheA*	660
2.696128577	-	1.84536641	Leukotoxin	*cytK*	1392
3.204744637	-	1.93513541	Phospholipase C	*PlcB*	1823
4.416119745	-	0.84169863	Collagenase family protein		1941
-	-0.072704444	0.84739611	Helix-turn-helix family protein	*plcR*	2669
3.570677872	0.080785773	0.2505876	Haemolysin BL lytic component L1	*hblD*	4930
6.461304188	-	0.20058746	Haemolysin BL lytic component L2	*hblC*	4931
5.67163978	-	0.22214644	Haemolysin BL-binding component	*hblB*	4932
3.985087047	-	0.14565096	Haemolysin BL-binding component	*hblA*	4933
3.840358242	0.439801534	1.95993464	Thermolysin metallopeptidase		5317

Table.4.10. Differential expression of toxins in *B. cereus* G9241 growing exponentially at 25 °C compared to growth at 37 °C. Dark grey cells with "–" indicate the protein was not detected in the analysis. Light grey cells represent an insignificant fold change, less than $\log_2$-fold change of 0.585 or 1.5-fold.

4.3.2. *B. cereus* G9241 temperature-dependent gene regulation

The published annotation of the *B. cereus* G9241 genome is relatively poor, making the analysis of global transcriptional data difficult. In *B. cereus* G9241 growing exponentially 446 genes were expressed significantly higher at 25 °C compared to 37 °C, whereas 437 genes were higher at 37 °C compared to 25 °C. An operon of five flagellin genes was more highly expressed at 25 °C. Flagellin proteins were more abundant at 25 °C in the cell proteome (compared to 37 °C) but not in the secreted proteome suggesting that flagellin proteins are not secreted and flagella are not assembled until later growth phases. In *B. cereus* flagella are used for cell adhesion and virulence against epithelial cells (Ramarao and Lereclus, 2006). It is likely that *B. cereus* G9241 starts transcribing flagellin proteins concurrently with toxins for a fully virulent phenotype. Motility is reduced in *B. thuringiensis ΔplcR* strains, but flagellin encoding genes have not been shown to be directly regulated by PlcR. The loss of motility in *ΔplcR* strains is thought to be due to a loss of PlcR-PapR quorum sensing (Ramarao and Lereclus, 2006). A gene encoding a methyl-accepting chemotaxis protein (MCP) was within the top ten genes more highly expressed at 25 °C compared to 37 °C (table 4.1). MCP proteins are lipoproteins that convert environmental signals into chemotactic cell responses (Hanlon and Ordal, 1994). *mcpA* has previously been identified as a member of the PlcR regulon in *B. cereus* ATCC14579 (Gohar et al., 2008).

Several cold shock genes are more highly expressed at 25 °C compared to 37 °C. *cspA* and *ydjO* are both more highly expressed at 25 °C compared to 37 °C, but in *E. coli* and *B. subtilis* the transcription of these genes occurs at 15 °C and below (Jiang et al., 1997; Kaan et al., 2002). CspA has been shown to prevent mRNA degradation, by preventing secondary structure formation in mRNA at low growth temperatures in *E.coli* (Jiang et al., 1997). The function of YdJO is unknown (Kaan et al., 2002). The transcription of these of these genes in *B. cereus* G9241 at 25 °C suggests that the temperature causes significant stress to the bacterium despite the wide growth range of strains of the *B. cereus* sensu stricto, from 5 °C to over 40 °C (Broussolle et al., 2010; Choma et al., 2000).

The gene expressed most highly at 25 °C compared to 37 °C was identified as a cell wall hydrolase with high similarity to a gene encoding SleB. SleB is a germination-specific spore cortex lytic enzyme in the *B. cereus* sensu lato, *B. subtilis* and other *Bacilli* (Moriyama et al., 1999). The cell wall hydrolase identified in this study (AQ16_4300) is highly unlikely to be a germination-specific spore cortex lytic enzyme. RNAseq samples were taken from exponentially growing cultures and were seeded from exponentially growing starter cultures. Both culture types were visualised by microscope and no spores were observed (images not shown). A cell wall hydrolase with sequence similarity to SleB was previously identified as being regulated by PlcR in *B. cereus* ATCC14579 (Økstad et al., 1999). BLASTp analysis shows this protein named Cwh in *B. cereus* ATCC14579 is 93.96% identical to AQ16_4300 in *B. cereus* G9241. Analysis of the *cwh* gene in *B. cereus* G9241 reveals a PlcR box is present 166 bp upstream suggesting it is regulated by PlcR in this strain too as well as *B. cereus* ATCC14579. AQ16_1488 encodes a hainantoxin domain containing protein more highly expressed during at 37 °C compared to 25 °C during stationary phase. Hainantoxin is a neurotoxin from bird eating spiders that inhibits the insect sodium channel (Li et al., 2003).

A large profile of genes theoretically under the control of PlcR is more highly expressed at 25 °C compared to at 37 °C, including the *plcR* gene. Despite this, there was no detectable difference in PlcR protein levels in the cell proteome. Together these findings suggest that temperature-dependent regulation of PlcR controlled genes is due to temperature-dependent activity of PlcR at 25 °C and 37 °C, not a difference in protein level. This theory relies on previous studies' findings into the PlcR regulon and our analysis of PlcR boxes accurately defining which genes are controlled by PlcR in *B. cereus* G9241.

4.3.3. Temperature-dependent transcriptional regulation of extrachromosomal genes

The transcriptional profile of genes higher at 37 °C compared to 25 °C is dominated by genes on the pBFH_1 phagemid. In fact, all genes encoded on

pBFH_1 that changed significantly by growth temperature were expressed more highly at 37 °C. Thirty four of the top 50 genes more highly expressed at 37 °C compared to 25 °C are located on the pBFH_1 phagemid. Phage gene transcription from pBFH_1 will be discussed more in chapter 5.

On the pBCX01 plasmid, 18 genes were significantly more highly expressed at 37 °C, whereas only 10 genes were more highly expressed at 25 °C. At 25 °C no pattern of ontological regulation could be deduced. However, at 37 °C the *gerX* operon encoded on pBCX01 is more highly expressed. The *gerX* operon encodes proteins needed for *B. anthracis* to germinate inside macrophages (Guidi-Rontani et al., 1999). Reporter fusions have shown that the *gerX* operon is expressed 3 hours after the initiation of sporulation. *pagA* was 1.2-$\log_2$ fold more highly expressed at 37 °C compared to at 25 °C. *hfq3* gene encoded on pBCX01 was seen to be higher at 37 °C. Hfq proteins act as chaperones to mediate the interactions between small RNAs (sRNAs) and mRNA (Valentin-Hansen et al., 2004), but regulation by sRNAs in *B. anthracis* is largely unstudied. Hfq3 encoded by pX01 in *B. anthracis* is known to regulate sRNAs and is shown to be expressed during exponential growth consistent with the data in this study (Panda et al., 2015). This study has identified various putative non-coding RNAs (data not shown) using an sRNA identification tool (Sazinas, 2016). Further analysis has not been conducted on these sRNAs, but identification of sRNAs together with differential regulation of Hfq3 suggests a role for sRNAs in temperature-dependent regulation in *B. cereus* G9241.

The *pagA* along with *cya* and *lef* gene hav been shown to be regulated at a transcriptional level by AtxA using a transposon mutant library and complementation experiments (Uchida et al., 1993). However this study did not detect differential levels of AtxA in the cell proteome. Further to this the *lef* and *cya* genes which are part of the AtxA regulon do not change in transcription between the two growth temperatures. These results would suggest that AtxA activity is not temperature-dependent during exponential growth in *B. cereus* G9241. However, regulation of the anthrax toxin genes is not as simple a model as once thought. AtxA activity has been shown to be regulated post-

translationally by phosphorylation of histidine residues within two phosphophenolpyruvate:sugar phospholtransferase system regulatory domains (PRD) of AtxA (Tsvetanova et al., 2007). This may allow for temperature-dependent activity of AtxA without differential transcription or protein levels. Further to this *pagA*, *lef* and *cya* are transcriptionally activated by AtxA at different levels (Fouet, 2010; Sirard et al., 2000). The *pagA* gene is induced approximately 5-fold more strongly than *lef* and *cya*. Given that *pagA* is expressed approximately twice as highly at 37 °C compared to 25 °C, levels of *lef* and *cya* would not be significantly differentially regulated between the two levels. Transcription of *pagA* is also under autogenous control by the transcriptional repressor PagR (Hoffmaster and Koehler, 1999). This study observed no temperature-dependent transcription of *pagR*, thus its role in *pagR* regulation is inconclusive. The transcriptional profile of *pagR* is preliminary evidence for increased activity of AtxA during growth at higher temperatures in *B. cereus* G9241.

Eleven genes encoded on pBC210 were more highly expressed at 37 °C compared to 25 °C, whereas 8 genes were higher at 25 °C compare to 37 °C. Similar to the transcriptome of pBCX01, at 25 °C there was no obvious pattern of genes more highly expressed. However, at 37 °C another *gerX* operon was transcribed from pBC210. At the time of this study, no previous studies describe the function of this operon in pBC210 and this operon does not exist in the analogous capsule plasmid pX02 in *B. anthracis*. *B. cereus* G9241 has been shown to germinate within the lungs of mice early in the infection process (Wilson et al., 2011) thus multiple *gerX* operons may aid this. The *atxA* homologue *atxA2* encoded on pBC210 was the gene expressed highest at 37 °C compared to 25 °C. In fact, it was the gene most differentially expressed at either temperature from either the pBCX01 or pBC210 plasmids. Whilst AtxA has been shown to be the predominant regulator of anthrax toxin genes, AtxA2 has only been shown to significantly regulate toxin component expression in a *B. cereus* G9241 *ΔatxA* strain. However complementation of a *B. cereus* G9241 *ΔatxAΔatxA2* strain with *atxA2* does restore *pagA* transcription to near WT levels (Scarff et al., 2016). The

data here supports the latter finding and presents AtxA2 as a potential temperature-sensitive activator of *pagA* transcription. AtxA2 is sufficient to regulate the *bpsXABCDEFGH* capsule operon, even in the presence of AtxA (Scarff et al., 2016). The RNAseq showed no differential regulation of the bps capsule operon, in fact *bpsX* (AQ16_5622) was more highly expressed at 25 °C compared to 37 °C suggesting that AtxA2 activity is not higher at 37 °C. It is likely AtxA2 activity is controlled post-translationally, like AtxA1, due to the conserved histidine residues and PRD domains (Scarff et al., 2016; Tsvetanova et al., 2007).

4.3.4. Growth phase dependent regulation of transcription in *B. cereus* G9241

Transcriptional analysis of *B. cereus* G9241 grown to stationary phase revealed a very large number of differentially expressed genes, such that is not possible to be analysed in full within this study. However, it is sensible to discuss general data trends and highlight the differential mRNA abundances of certain genes of interest.

There is no significant difference in the apparent transcriptional levels of *plcR* during stationary growth compared to exponential phase growth at 37 °C. This confirms that the increase in toxin secretion and haemolytic activity of the supernatant seen during stationary phase growth at 37 °C is not due to an increase in transcription of *plcR*. This adds further support to the hypothesis that loss of PlcR-mediated toxicity during exponential growth at 37 °C is due to post-transcriptional regulation of PlcR. Interestingly however, out of all the toxin proteins identified in the secretomics data, only the gene encoding NheB is more highly expressed during stationary phase growth compared to exponential phase growth at 37 °C.

The only condition that saw increased transcription of all three genes encoding the anthrax tripartite toxin was at 37 °C during stationary phase growth. In *B. anthracis*, CodY binds the *atxA* promoter region and transcription of *atxA* is repressed until early stationary phase growth (Sonenshein, 2005). It has also

been shown that CodY is required for accumulation of AtxA in *B. anthracis*, which may also account for the transcription of AtxA-regulated genes during stationary phase in *B. cereus* G9241 (Chateau et al., 2011; van Schaik et al., 2009).

During growth at 37 °C, transcription of ORFs located on the plasmids is highly growth phase-dependent (table 4.11). Whilst more ORFs from pBFH_1 are expressed higher during exponential growth, transcription from pBC210 and pBCX01 increases during stationary phase growth at 37 °C. In general transcription from pBC210 ORFs increases during stationary phase growth and several genes encoding capsule biosynthesis proteins are more highly expressed during stationary phase growth compared to exponential growth at both temperatures. This is in agreement with previous research that shows capsule production at approximately 6 hours growth at 37 °C (Oh et al., 2011)

There is clearly a lot more information available from the comparison of these transcriptomes, but the poor genome annotation means there is a lack of available software to analyse the global data at the time of this study.

				Number of ORFs more highly expressed at			
				25 °C		37 °C	
				Expo	Stat	Expo	Stat
Compared to	pBC210	25 °C	Expo	-	42	11	-
			Stat	14	-	-	45
		37 °C	Expo	8	-	-	47
			Stat	-	19	13	-
	pBCX01	25 °C	Expo	-	23	19	-
			Stat	33	-	-	63
		37 °C	Expo	10	-	-	45
			Stat	-	13	23	-
	pBFH_1	25 °C	Expo	-	3	50	-
			Stat	7	-	-	28
		37 °C	Expo	0	-	-	2
			Stat	-	13	44	-

Table.4.11. Relative transcription of ORFs encoded on the extrachromosomal elements in *B. cereus* G9241. Table reads from the top and compares how many ORFs from each plasmid were more highly expressed under different conditions from MiSeq RNAseq data. Expo – exponential phase, Stat – stationary phase. Colours represent comparative conditions. Blue – 25 °C expo compared to 25 °C stat; pink – 37 °C expo compared to 37 °C stat; green – 25 °C expo compared to 37 °C expo; purple – 25 °C stat compared to 37 °C stat.

5. Temperature-dependent sporulation in *B. cereus* G9241 and the role of pBFH_1 phagemid

5.1. Introduction

Analysis of the secretome, the cell proteome and RNAseq have revealed expression from pBFH_1 phagemid increases during exponential growth at 37 °C compared to 25 °C. The role of the pBFH_1 phagemid in the lifestyle and virulence of *B. cereus* G9241 is unknown. Phage have previously been isolated from the *B. cereus* sensu lato (Schuch and Fischetti, 2009) and are thought to be essential for the lifestyle of some *B. anthracis* strains. This chapter will aim to elucidate whether phage particles are produced by *B. cereus* G9241 at 37 °C and what role they may play in the ecological niche inhabited by *B. cereus* G9241.

Spore formation is characteristic of *Bacillus* species and plays a key role in the lifestyle of *B. anthracis*. Sporulation is thought to be essential for the survival of *B. anthracis* outside of a host organism (Bowen and Turnbull, 1992; Minett and Dhanda, 1941; Saile and Koehler, 2006). Furthermore, spores are the infective form of both inhalational anthrax and the anthrax-like infection caused by *B. cereus* G9241 (Hoffmaster et al., 2004; Koch, 1876). To conclude the hypothesis that *B. cereus* G9241 behaves like a *B. anthracis* strain at 37 °C, the sporulation phenotype needs to be studied. This chapter aims to elucidate the sporulation phenotype of *B. cereus* G9241 at 25 °C and 37 °C to investigate if sporulation is also regulated by growth temperature.

Aims for this chapter were:

1. To characterize and quantify sporulation in *B. cereus* G9241 at both 25 °C and 37 °C.
2. To determine if intact phage pBFH_1 particles are being produced by *B. cereus* G9241 at 37 °C.
3. To determine if phage production by *B. cereus* G9241 is a cause or an effect of rapid sporulation at 37 °C.

5.2. Results

5.2.1. Temperature-dependent sporulation in *B. cereus* G9241

5.2.1.1. Sporulation of *B. cereus* G9241 and *B. cereus* ATCC14579 on LB agar

B. anthracis sporulates rapidly under laboratory conditions (Koch, 1876), a phenotype necessary for its infective lifestyle (Ross, 1957). To determine if *B. cereus* G9241 shares this sporulation phenotype, it was visualised under the microscope after 24 and 48 hrs growth on LB agar. For comparison, *B. cereus* ATCC14579 was imaged under the same conditions.

After 24 hrs growth at 25 °C *B. cereus* G9241 cells appeared vegetative. No endospore formation could be seen and small populations of cells were still athromitic (Fig 5.1). However, after 48 hrs growth, endospores could be observed. In contrast, after 24 hrs growth at 37 °C, *B. cereus* G9241 appeared to be almost 100% mature spores. No cells could be visualised and almost all mother cells had degraded. After 24 or 48 hrs growth on LB agar, *B. cereus* ATCC1479 displayed no endospore formation at either 25 °C or 37 °C. *B. cereus* G9241 was actively sporulating compared to *B. cereus* ATCC14579 and did so more rapidly at 37 °C compared to 25 °C.

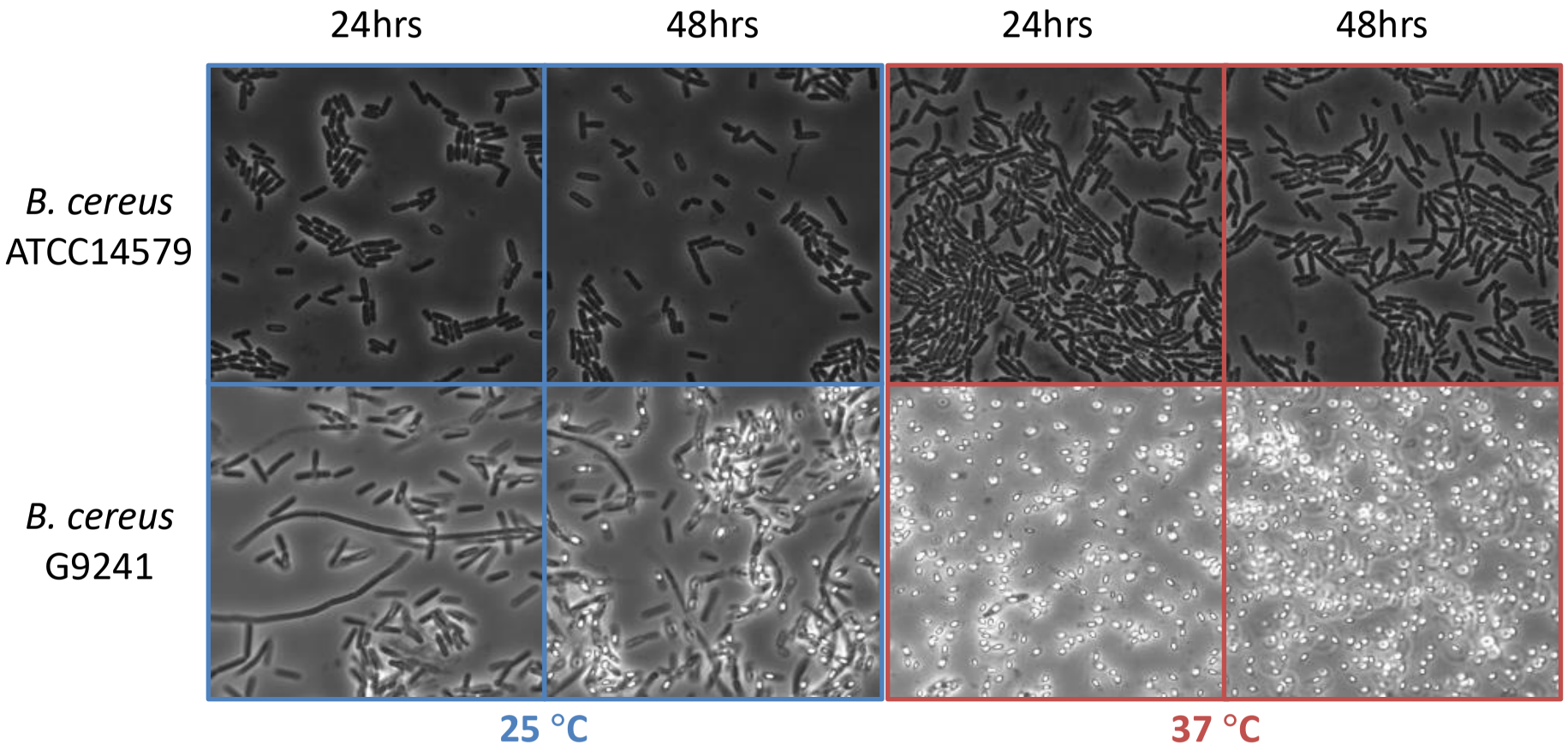

Fig.5.1. Visualisation of *B. cereus* G9241 and *B. cereus* ATCC14579 reveals a temperature induced sporulation phenotype. Both strains of *B. cereus* were grown for 24 or 48 hrs on LB agar at either 25 °C or 37 °C. A loop of bacterial lawn was taken and used to inoculate 25 µl of PBS. 5 µl of this suspension was mounted and images were taken at 100x magnification. No spore formation is seen under any condition in *B. cereus* ATCC14579. *B. cereus* G9241 hasn't formed any spores within 24 hrs at 25 °C. After 48 hrs growth at 25 °C, endospores have begun to form. In contrast, after only 24 hrs growth at 37 °C, fully mature spores had formed.

5.2.1.2. Sporulation of *B. cereus* in LB broth

B. cereus G9241 sporulated rapidly on solid media at 37 °C. To determine if *B. cereus* G9241 displays this same phenotype in liquid media, the WT strain was grown for 48 hrs in LB broth, 200 rpm at 25 °C and 37 °C. Images were taken at 24 and 48 hrs.

In liquid media, *B. cereus* G9241 displayed the same temperature-dependent sporulation phenotype as on solid media. (Fig 5.2) At 25 °C, *B. cereus* G9241 took 48 hrs to form a heterogeneous population of endospores, similar to growth on solid media. At 37 °C *B. cereus* G9241 formed endospores after 24 hrs and a homogeneous culture of spores after 48 hrs. *B. cereus* G9241 sporulated at least 24 hrs earlier on solid LB than in LB broth.

5.2.1.3. Quantifying sporulation of *B. cereus* G9241 in LB broth

Microscopy of *B. cereus* G9241 indicated a temperature-dependent sporulation phenotype. To confirm there was a significant difference in sporulation caused by different growth temperatures, sporulation needed to be quantified. *B. cereus* G9241 was grown at 25 °C and 37 °C for 24 and 48 hrs in LB broth, 200 rpm; these culture conditions were identical to those used to capture microscope images in the previous section. The population of cells having formed spores was measured using a temperature stress of 65 °C for 30 minutes. Whole cell counts were conducted pre-temperature stress for comparison.

(Fig 5.3) After 24 hours growth at both temperatures, the spore counts wholly correlated with microscopy images. There was a significant difference between cells grown at 37 °C and those grown at 25 °C. After 24 hrs growth, at 37 °C 114% of cells had formed spores, whereas at 25 °C only a negligible percentage of the cell population had formed spores (level too low to plot on graph). After 24 hrs growth at 37 °C, a spore count of >100% was recorded. This phenomenon was likely due to heat activation of spores. Heat activation of spores means they have germinated after temperature stress and divided before being plated.

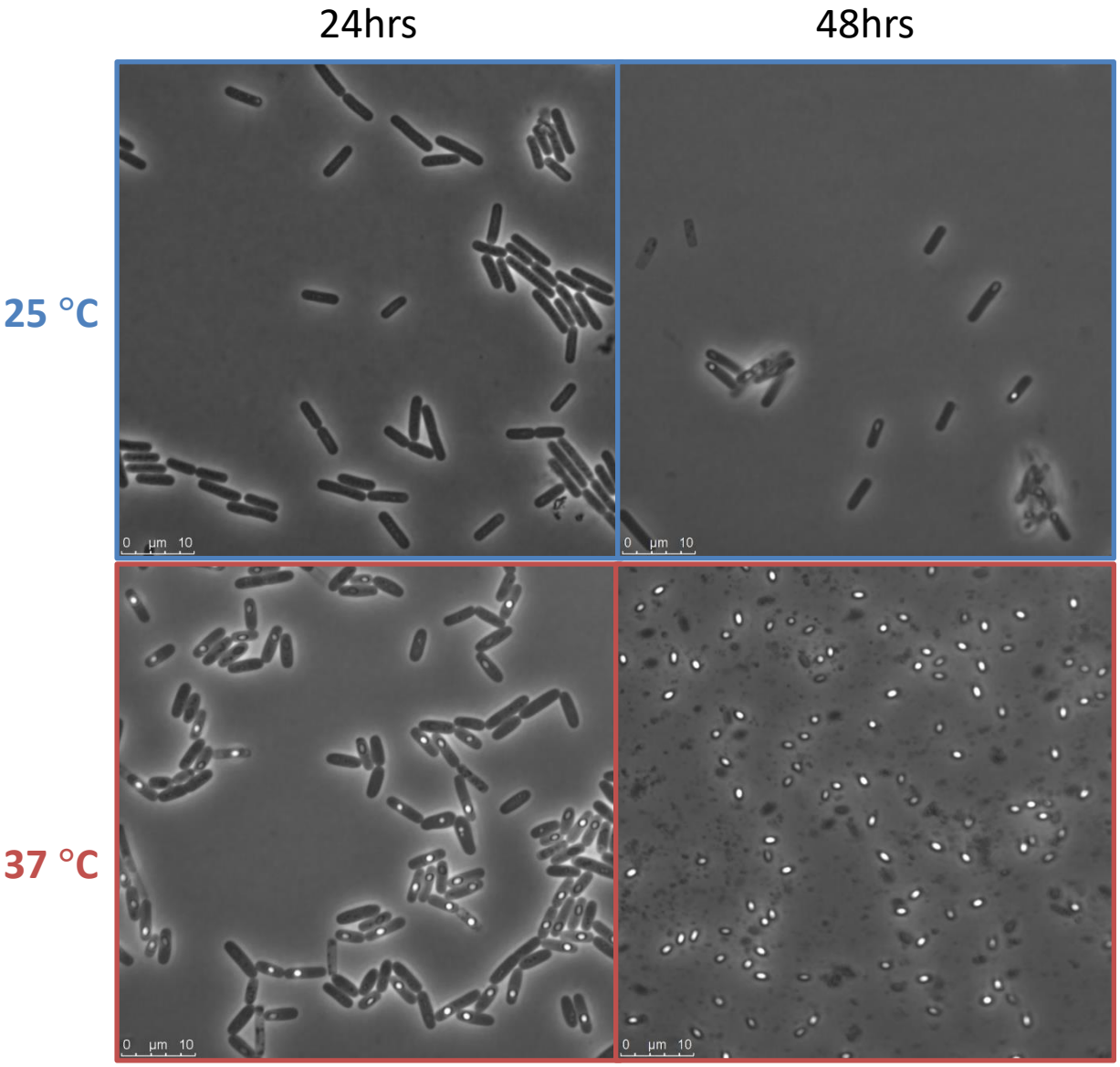

Fig.5.2. *B. cereus* G9241 sporulates rapidly when grown at 37 °C in LB broth. *B. cereus* G9241 was grown at 25 °C and 37 °C in LB broth, 200 rpm for up to 48 hrs. 2 µl of bacterial culture was imaged on agarose pads at 100x magnification after 24 and 48 hrs. After 48 hrs growth at 25 °C, *B. cereus* G9241 cell populations were observed to be heterogeneous. Some cells had formed endospores, whilst some appeared vegetative. However when grown at 37 °C, *B. cereus* G9241 sporulated more rapidly. After 24 hrs, clear endospore formation can be seen in the majority of the cells. Whereas at 37 °C the cell population displays a clear homogeneity, with all cells being fully formed spores. Spores can be seen as phase bright and vegetative cells as phase dark. Dark specs in the bottom right panel are likely pieces of lysed mother cell debris.

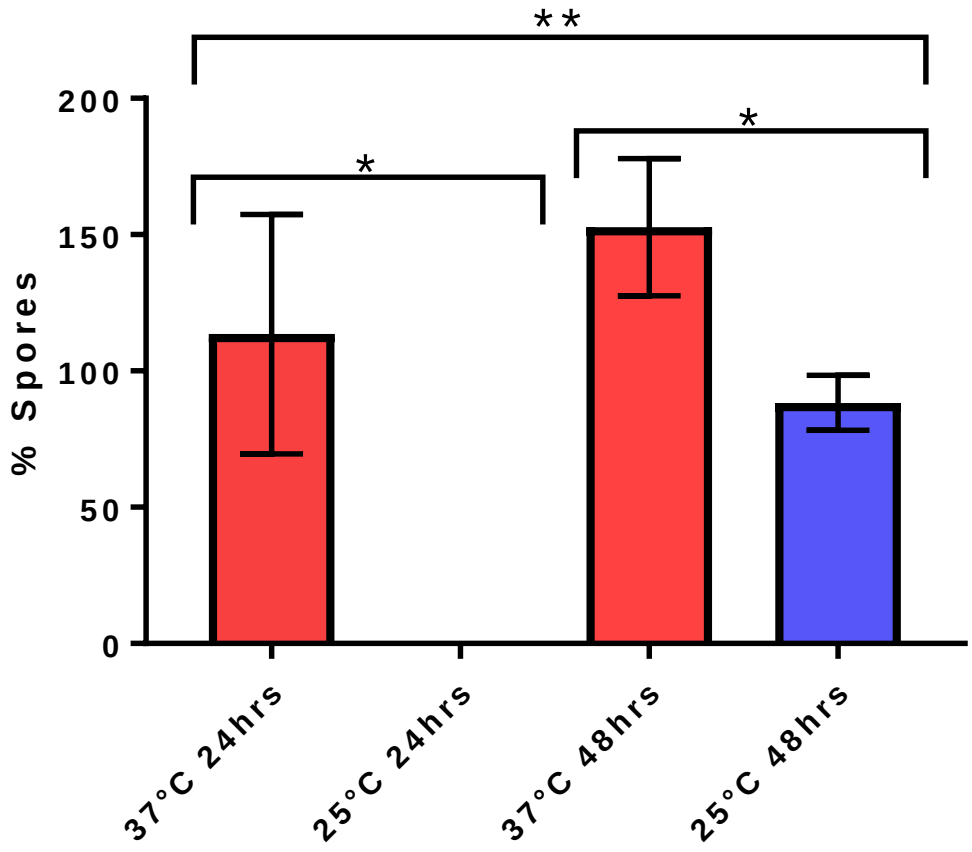

Fig.5.3. *B. cereus* G9241 WT rapidly sporulates at 37 °C in LB broth. *B. cereus* G9241 was cultured in LB broth for 48 hours at 25 °C and 37 °C. At 24 and 48 hours samples were collected and diluted to $1x10^{-6}$. Dilutions were plated onto BHI agar before and after temperature stress at 65 °C for 1 hour. Data was plotted as a % of the culture that were spores, i.e. cfu ml^{-1} post-stress over cfu ml^{-1} pre stress. After 24 hours at 37 °C, 100% of the cell population had formed spores. However at 25 °C, 0.06% of cells have formed spores (not visible on graph). * indicates significance to a p-value < 0.05 using Welch's t test. **indicates significance to a p-value of 0.0014 using an ordinary one-way ANOVA. Error bars are one standard deviation and all bars are n=3, except 25 °C 48 hours where n=2. Spore % >100 is due to heat activation of spores meaning they have germinated post stress and divided before being plated.

After 48 hours growth at 37 °C, the % spore count increased from 114% seen at 24 hrs to 153%. This difference was not deemed statistically significant by an unpaired t-test with Welch's correction. After 48 hrs growth at 25 °C, the spore count increased from 0.06% to 88%, again in agreement with the microscopy images. The sporulation assay revealed that endospores seen in cultures grown for 24 hrs at 37 °C and for 48 hrs at 25 °C, both in LB broth, must be fully formed but not yet released from the mother cell.

5.2.2. Production of pBFH_1 phage at 37 °C

5.2.2.1 pBFH_1 Transcriptomics

RNAseq analysis of *B. cereus* G9241 grown at 25 °C and 37 °C during exponential growth phase revealed that the pBFH_1 phagemid genes were more highly expressed during growth at 37 °C compared to growth at 25 °C. Deeper analysis of the data revealed a more complete picture of the role of this phagemid during growth at 37 °C.

The only gene seen to be higher during 25 °C growth was one encoding Fur-regulated basic protein A (blue circle fig 5.4). The genes highest at 37 °C included 2 genes encoding subunits of a phage terminase protein. The large subunit gene was approximately 12x higher at 37 °C (AQ16_5899) and the ATPase subunit 13x higher (AQ16_5898). Twelve genes encoding capsid or tail proteins were identified as over 4x higher at 37 °C (red squares fig 5.4). Expectedly a phage anti-repressor encoding gene (AQ16_5855) was also seen to be higher at 37 °C. Many transcriptional activators were higher at 37 °C. Two genes encoding Xre superfamily transcriptional regulators (AQ16_ 5850 and 5853) and interestingly an autolysin regulatory protein were all higher at 37 °C.

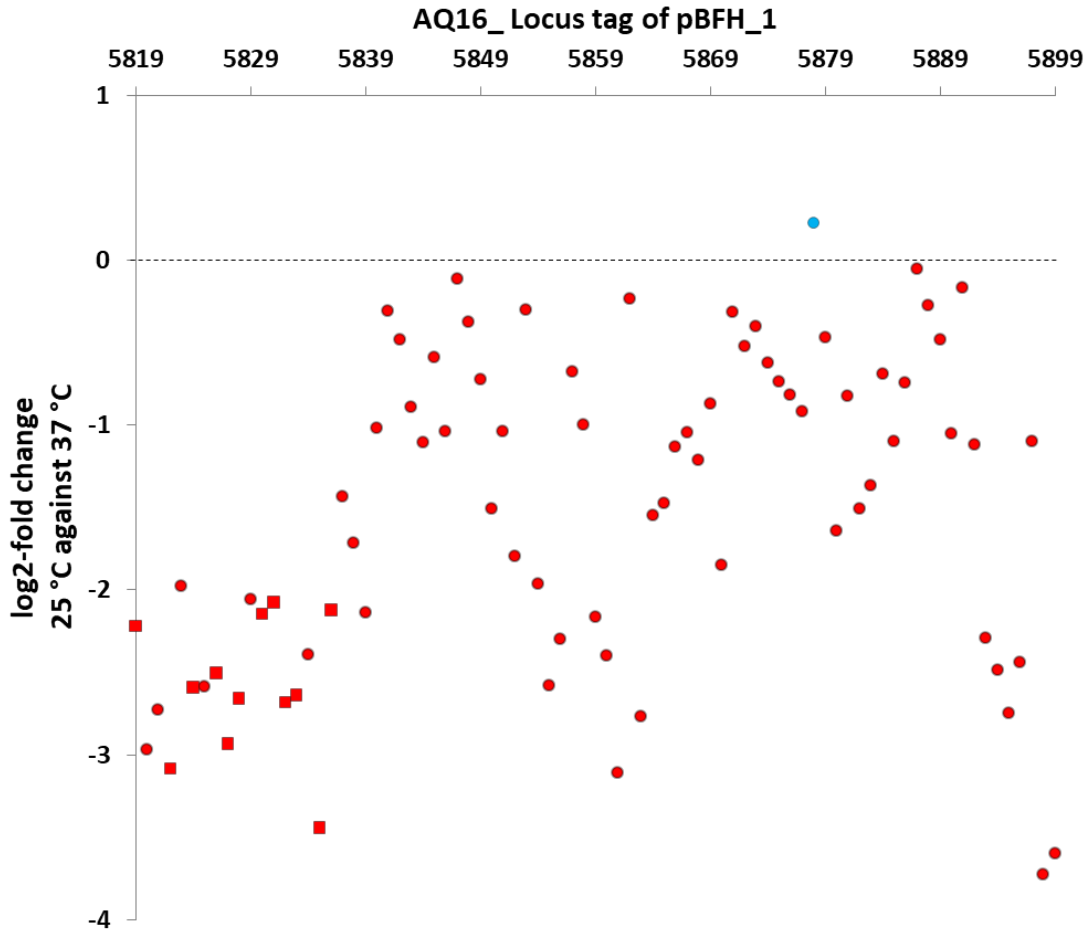

Fig.5.4. Genes on the pBFH_1 phagemid are more highly transcribed when host *B. cereus* G9241 is grown at 37 °C, compared to at 25 °C. *B. cereus* G9241 was grown at 25 °C and 37 °C to exponential phase. RNA was extracted and RNAseq performed. RNAseq reads were processed, normalised and plotted as the log2-fold change in the transcriptional level of each gene at 25 °C compared to at 37 °C. Almost all genes were higher during 37 °C growth (red circles/squares), with the exception of a gene encoding a Fur-regulated protein (blue circle). All known genes encoding capsid and tail proteins (red squares) were higher at 37 °C. All points plotted are significant (p value < 0.05; n=3).

5.2.2.2. Extraction and electron microscopy of pBFH_1 phage from *B. cereus* G9241 growing at 37 °C

RNAseq strongly indicated that phage particles were being produced at 37 °C during exponential growth. To determine if phage particles were produced supernatants were extracted under conditions identical to RNA extractions at exponential phase. Cells were removed by pelleting and filtration (0.02 µm) and phage particles precipitated using PEG6000. Proteins extracted from exponential phase were imaged using electron microscopy at 40,000x (fig 5.5 Panel B). Over 12 images at this magnification, 4 consistent hollow hexagonal shapes were identified (fig 5.5 panel B red arrow). These candidate phage particles were consistently approximately 35 – 40 nm in length. The candidate phage particles were too few and samples too impure to certify the hexagonal particles as phage.

To increase the amount of phage obtained, *B. cereus* G9241 was grown for 48 hours at both 25 °C and 37 °C. Proteins were extracted, precipitated and centrifuged through a CsCl gradient. Proteins extracted at 25 °C produced no bands on either the SDS-PAGE gel nor when centrifuged through the CsCl gradient. Proteins extracted at 37 °C displayed two clear bands when applied to the CsCl gradient. The bands were imaged under the electron microscope (fig 5.5 panel A) at 15,000x magnification. After 48 hours growth at 37 °C, multiple candidate phage particles were observed (fig 5.5 panel A black arrows). The candidate phage particles were consistently approximately 40 nm in width and hexagonal in shape with a recess in the middle.

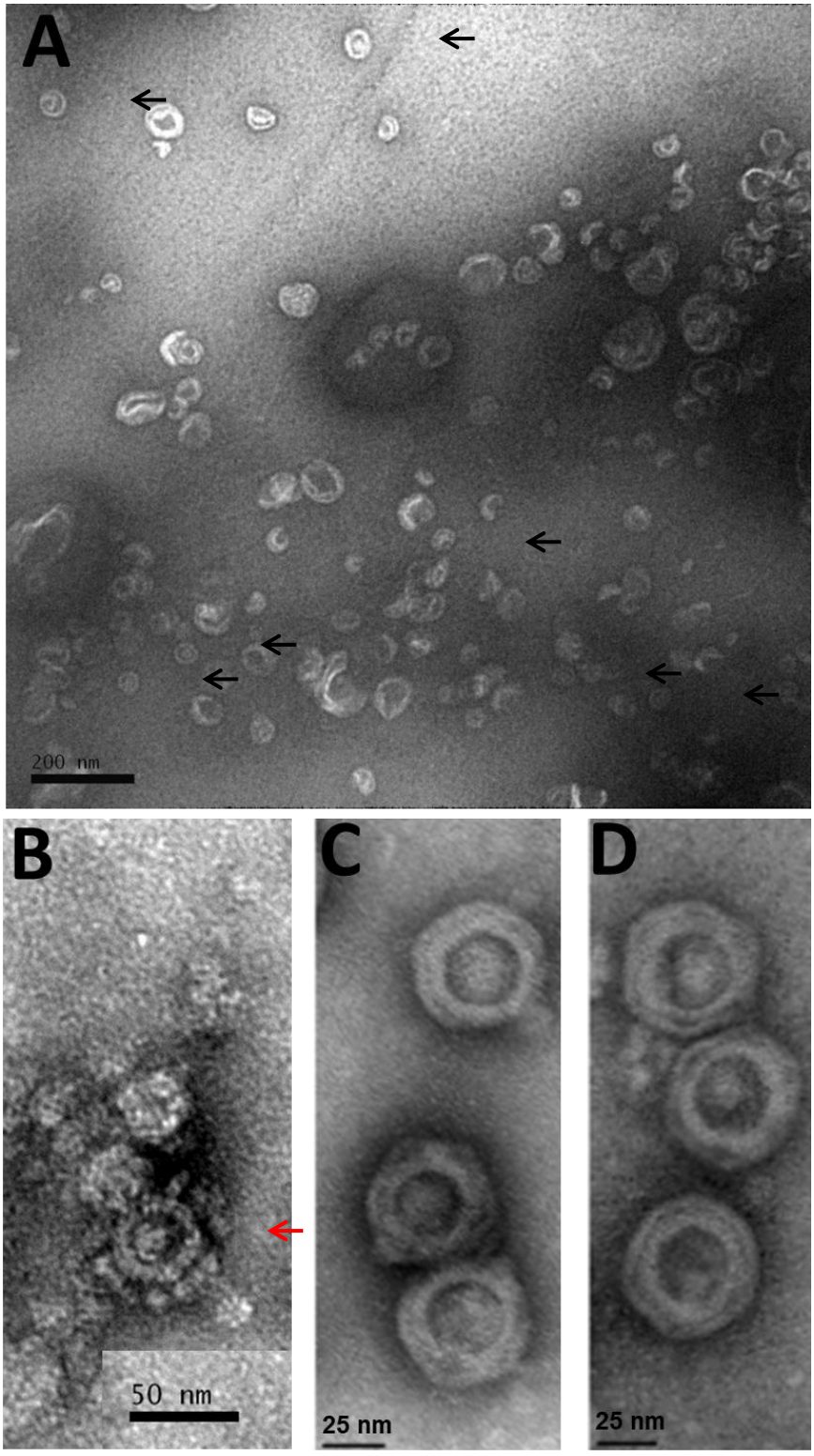

Fig.5.5. Electron microscopy of pBFH_1 phage extracted from *B. cereus* G9241 (A and B) and Wip1 and Htp1 phages (Schuch and Fiscetti. 2009) for comparison (C and D). *B. cereus* G9241 was grown at 37 °C to mid exponential phase (B) or for 48 hours (A). Supernatant was extracted and proteins were PEG-precipitated. Proteins were imaged at 40,000x magnification after resuspension in TM buffer (B) or were filtered through a CsCl gradient and imaged at 15,000x magnification (A). Recurrent hollow hexagonal shapes, approximately 40 nm in length can be seen in A and B (arrows). These bear a resemblance to bacteriophage identified as infecting *B. anthracis* strains (C and D).

5.2.2.3 Transposon mutagenesis for the isolation of pBFH_1

To determine if pBFH_1 plays a role in sporulation, the phagemid needed to be cured from *B. cereus* G9241 and the sporulation phenotype measured. Alternatively, pBFH_1 could be transformed into *B. cereus* ATCC14579 and any associated temperature-dependent sporulation phenotype determined. However, integral to either approach is the requirement to place a selectable marker onto the phagemid.

pBFH_1 was isolated using a plasmid midi-prep. Successful extraction was confirmed by restriction digest and gel electrophoresis. Attempts were made to randomly insert a kanamycin resistance cassette into the phagemid via in vitro transposition with the EZ-Tn5™ <KAN-2> transposon. This approach would have also provided a random knock-out library. The pBFH_1-EZ-Tn5<KAN-2> transposon library was transformed into *E. coli* EC100D pir^+ cells and candidate transformants selected for with kanamycin. Candidate transformants were screened using a combination of plasmid midi-prep with gel electrophoresis and DNA sequencing primed against the transposon. Over 400 candidate transformant colonies grew on selective media. Despite this, no candidates were successfully transformed with pBFH_1-EZ-Tn5<KAN-2>.

5.3. Discussion

5.3.1. Temperature-dependent sporulation in *B. cereus* G9241

This PhD project had not originally been planned to study sporulation in *B. cereus* G9241 due to the potential increased risk of working with the infective form of the bacteria (Oh et al., 2011). However, after transforming a culture of *B. cereus* with the pHT315-*gfp* and growing the transformants for 18 hrs at 30 °C, the bacteria visualised under the microscope clearly showed significant levels of sporulation. This was surprising given that previous studies suggest that the type strain *B. cereus* ATCC14579 does not sporulate in LB broth even after 72 hrs (Vilain et al., 2006). Further to this, the type strain takes approximately 28 hours to sporulate at 30 °C in a chemically defined medium designed to force synchronous sporulation (de Vries et al., 2004). Comparatively *B. anthracis* sporulates within 4-13 hrs at 37 °C and 8-22 hrs at 25 °C (Davies, 1960; Koch, 1876; Minett, 1950). It should be noted that *B. anthracis* sporulation times are determined using blood as a growth substrate.

This study found that when *B. cereus* G9241 is grown on either solid or liquid media, the sporulation phenotype is largely comparable to *B. anthracis*. At 37 °C, *B. cereus* G9241 sporulates on solid LB agar within 24 hrs. At 25 °C on solid LB agar there is no observable spore formation by *B. cereus* G9241 after 24 hrs, but endospores can be visualised after 48 hrs. Although endospore formation is observed after 48 hrs at 25 °C, after 72 hrs mature spores are still not released (data not shown). A similar pattern of sporulation was observed for *B. cereus* G9241 growing in LB broth. After 24 hrs and 48 hrs growth at 37 °C, endospore formation and mature spore formation were observed respectively. At 25 °C endospore formation wasn't seen until after 48 hrs growth. Quantification of this sporulation in LB broth provided interesting results.

When *B. cereus* G9241 was grown at 37 °C for both 24 and 48 hrs over 100% sporulation was observed. Over 100% sporulation has been suggested to be due to either germination/replication of heat-shocked spores before plating or by

clumping in live cell counts. Tween surfactant was added to prevent clumping (Furukawa et al., 2005) but this did not change results of the assay suggesting it was rapid germination of the spores before plating that resulted in cell counts over 100%. After 24 hrs growth at 37 °C, microscopy reveals the majority of cells in the population have formed endospores. The quantitative assay suggests these endospores are fully formed but have yet to be released from the mother cell. Similarly, endospores seen after 48 hrs growth at 25 °C were quantified in the assay showing that approximately 90% of cells formed a endospore but that the mother cell was not yet degraded. As this study did not quantify sporulation past 48 hrs, it is not possible to determine if mother cell lysis is stunted in 25 °C cultures. Quantitative assays of spore formation in *B. cereus* G9241 still needs some refinement in order to be conclusive. It is well reported in *Bacilli* that the temperature at which spores are formed impacts their stability (Baweja et al., 2008; Melly et al., 2002). Thus, the data presented here is preliminary but does show temperature-dependent sporulation in *B. cereus* G9241.

Growth curves revealed that *B. cereus* G9241 reaches equal levels of cell density at both 25 °C and 37 °C over 10 hrs of growth, but that growth is slower at 25 °C. However, the sporulation assay revealed after 24 hrs growth that there were 4 times as many cells in cultures at 25 °C compared to at 37 °C. By 48 hrs there are 3 times as many cells at 25 °C compared to at 37 °C. This suggests that growth at 37 °C is extremely stressful to *B. cereus* G9241. This is an unusual finding, as many studies use 37 °C as a growth temperature with no significant impact on the growth kinetics of *B. cereus* sensu lato strains (Benedict et al., 1993). This suggests that another factor during growth at 37 °C is forcing sporulation of *B. cereus* G9241.

Sporulation is a tightly controlled process in *Bacilli*, mainly induced by a declining nutrient availability (Piggot and Hilbert, 2004). This study has shown that cultures of *B. cereus* G9241 reach the same OD_{600} over a growth course and that after 24 hrs growth there are 4 times fewer cells at 37 °C compared to 25 °C. By this time point fully formed endospores have formed at 37 °C but not at 25 °C despite more cells being present in the 25 °C bacterial population. Together these

findings suggest that at 37 °C, *B. cereus* G9241 is forced into a sporulative phenotype regardless of nutrient availability. This is similar to *B. anthracis* which is "locked" into a sporulation dependent lifecycle (Carlson et al., 2018a). However it should be noted that it is unclear what causes *B. anthracis* to rapidly sporulate or if this is in fact the true lifecycle of the *B. anthracis* species (Van Ness, 1971).

5.3.2. Production of phage in *B. cereus* G9241

5.3.2.1. Regulation of phage genes and proteins

Genes on the pBFH_1 dominated the transcriptional profile of *B. cereus* G9241 when growing exponentially at 37 °C compared to 25 °C. Many structural genes are more highly expressed in the RNAseq and many capsid proteins are found in the secretome under these conditions. Importantly, the most highly expressed genes at 37 °C compared to 25 °C during exponential growth are two terminase family protein encoding genes. Terminases are packaging enzymes responsible for packaging DNA into the phage capsids at the end of phage assembly (Black, 1989). This suggests that at mid-exponential phase at 37 °C in this study phage have finished being assembled. This is supported by comparison of the gene transcription during exponential and stationary phase growth at 37 °C. Forty-four genes from pBFH_1 were expressed 27-fold higher on average during exponential growth compared to stationary phase growth. Despite pBFH_1 gene transcription being comparatively lower during growth at 25 °C compared to 37 °C, growth phase-dependent transcription of pBFH_1 genes is observed at 25 °C too, but to a lesser extent. Despite differences at a transcriptional level no pBFH_1-encoded proteins are detected as significantly higher in the secretome at 25 °C compared to 37 °C during either growth phase, and only 1 uncharacterised pBFH_1-encoded protein is higher in the secretome during exponential growth at 25 °C compared to stationary phase growth. Together these findings provide evidence that *B. cereus* G9241 is expressing a large number of proteins encoded on pBFH_1 during exponential growth at 37 °C and

that this expression is growth phase- and temperature-dependent. However at this stage, it was still unclear if a phage particle was actually produced.

5.3.2.2. Does pBFH_1 encode a phage?

Blast analysis of the pBFH_1 sequence against the Prokaryotic Virus Orthologous Groups (PVOGs) database (Grazziotin et al., 2017) revealed homology to several genes from different *Bacillus* phages (data not shown). The analysis did not confer homology to one clear phage but the majority of genes showed homology to the Siphoviridae family. Phage particles could not be visualised from supernatant extracts prepped from exponential phase cultures at 37 °C. However, phage particles could be identified from supernatant extracts after 48 hrs growth at 37 °C. These phage particles display a large resemblance to Wip1 and Htp1 (Schuch and Fischetti, 2009). Wip1 and Htp1 are Tectiviridae bacteriophage shown to be capable of infecting *B. anthracis* and were isolated from earthworm gut and human tonsil bacteria samples respectively. This observation conflicted with the PVOGs BLAST search and with the annotation of pBFH_1 which contains 2 genes encoding phage tail proteins (AQ16_5835 and 5836) both expressed more highly at 37 °C compared to 25 °C during exponential growth. Since this study, unpublished work from the Waterfield lab has shown that *B. cereus* G9241 does release a phage upon growth at 37 °C morphologicaly similar to a Siphoviridae, possessing a capsid head and tail at 37 °C during exponential growth. Phage particles were produced under experimental conditions matching those of the RNAseq, secretome and cell proteome data at 37 °C during exponential growth. It is possible the Tectiviridae-like particles seen in this study are from a cryptic phage integrated in the chromosome.

5.3.3. Does production of phage influence sporulation in *B. cereus* G9241?

Phage have been isolated from *B. cereus* sensu lato species prior to this study and have been implicated in the survival of anthrax outside of mammalian hosts (Schuch and Fischetti, 2009). There are also several examples of what are known

as “spore-converting phages” which are able to activate sporulation in sporulation-defective strains or enhance sporulation in WT strains of *Bacilli* (Fortier and Sekulovic, 2013). Spore-converting bacteriophages have been identified in *B. cereus*, *B. thuringiensis* and other *Bacilli* species (Boudreaux and Srinivasan, 1981; Bramucci et al., 1977; Perlak et al., 1979). Interestingly a common feature of all the spore-converting phage identified in *Bacilli* is that they are all pseudo-temperate, being able to exist as extrachromosomal elements inside the host bacterium (Fortier and Sekulovic, 2013). Extrachromosomal phage DNA is prone to loss during cell division (Weinbauer, 2004) and it has been hypothesised that phage may increase the frequency of sporulation to increase the likelihood of integration into the spore and subsequent survival.

This study has shown pBFH_1 is a temperature-dependent, pseudo-temperate phage. At the time of this study there has been no research to elucidate the nature of the pBFH_1 phagemid in the ecological niche of the *B. cereus-anthracis* crossover strains, *B. cereus* G9241, 03BB87, LA2007 or FL2013. However, the conservation of pBFH_1 amongst *B. cereus-anthracis* crossover strains may indicate that the phagemid confers an evolutionary advantage to the survival, growth or infectivity of these strains. This study hypothesises that the upregulation of transcription and the production of phage from pBFH_1 in *B. cereus* G9241 at 37 °C results in the rapid onset of sporulation. However, it should be noted that it is extremely difficult at this stage to conclusively determine whether rapid sporulation is caused by pBFH_1 phage production or if phage production is a result of the onset of the sporulation cascade.

The mechanism of sporulation initiation by *Bacillus* spore-converting phage is largely unknown (Boudreaux and Srinivasan, 1981). The evidence presented in this study could be interpreted to suggest that the production of phage at 37 °C leads to a large amount of cell lysis, as seen in the sporulation assay live cell counts. The most effective mechanism of virion escape is to lyse the host cell (Fernandes and São-José, 2018) but it is unknown if pBFH_1 phage are lysogenic. pBFH_1 encodes at least 3 peptidases, an N-acetylmuramoyl-L-alanine amidase, a haemolysin and an autolysin, any of which may contribute to virion escape.

Contrary to this theory, no plaques have been observed on bacterial lawns throughout this study and supernatant extracted from *B. cereus* G9241 grown at 37 °C until exponential phase did not cause plaque formation on a lawn of *B. cereus ATCC14579* (data not shown). Together these finding represent preliminary evidence that *B. cereus* G9241 produces phage when grown at 37 °C but whether this phage production forces the rapid sporulation of *B. cereus* G9241 or vice-versa is unknown at this stage.

6. Final discussion and future work

B. cereus G9241 is the most well studied of a unique group of *B. cereus* sensu lato strains defined by the presence of full length *plcR* and *atxA* genes. The roles of PlcR and AtxA are relatively well defined in *B. cereus* and *B. anthracis* respectively. However due to the rare nature of strains containing both *plcR* and *atxA*, how a bacterium has incorporated two conflicting virulence regulators has not been studied. Discovery of the temperature-dependent haemolytic and motility phenotypes gave an interesting insight into how *B. cereus* G9241 may incorporate the two regulators and provided an opportunity to study the compatibility of AtxA and PlcR. This study provides a preliminary model for how *B. cereus* G9241 has evolved to incorporate the AtxA regulator. This model provides an insight into the ecological niche of *B. cereus* G9241 including virulence and sporulation phenotypes.

6.1. Compatibility of AtxA and PlcR in *B. cereus* G9241

The dogma has long stood that the anthrax toxin regulator - AtxA from *B. anthracis* and the pleiotropic regulator of virulence - PlcR from the *B. cereus* sensu lato are incompatible within a single organism (Mignot et al., 2001). This dogma is largely theoretical due to no strains of *B. anthracis* having been discovered with an intact copy of the *plcR* gene, but instead harbouring a *plcR* gene with a nonsense mutation (Mignot et al., 2001). A study by Mignot suggests that this mutation has arisen to aid sporulation in *B. anthracis* allowing it to lead a mammalian-virulent lifestyle. However, it should be noted a 2010 study has contradicted this finding (Sastalla et al., 2010). Over the last 20 years, several strains of *B. cereus* have been identified with a full length *plcR* and *atxA* gene further contradicting this dogma (Hoffmaster et al., 2006; Hoffmaster et al., 2004; Marston et al., 2006; Pena-Gonzalez et al., 2017; Wright et al., 2011).

I hypothesise that acquisition of the AtxA regulator by *B. cereus* G9241 allows the bacterium to switch from a PlcR-mediated, non-specific virulent phenotype to an AtxA-mediated mammalian virulent phenotype. Suppressing the PlcR regulon at

37 °C would prevent *B. cereus* G9241 from releasing lytic enzymes when infecting a mammalian host. This would mimic the *B. anthracis* infection strategy of remaining immunologically inert. The switch to a mammalian-virulent phenotype is mediated by environmental signals indicative of a mammalian host environment – i.e. 37 °C and CO_2-bicarbonate conditions (Passalacqua et al., 2009). Despite *B. cereus* G9241 possessing full length *plcR* and *atxA* genes, it doesn't necessarily defy the dogma that AtxA and PlcR are incompatible. *B. cereus* G9241 is seemingly able to express both regulators, but in order to do so it expresses them under different environmental conditions. Only two studies focus on the transcription of *atxA* and *plcR*, this study and a 2009 study by Passalacqua (Passalacqua et al., 2009). Both studies show *plcR* and *atxA* are inversely transcribed: *plcR* is transcribed at 25 °C or in aerobic conditions, whereas *atxA* is transcribed at 37 °C or in CO_2-bicarbonate conditions. In this manner I theorize that *B. cereus* G9241 is able express a non-specific virulent phenotype or a mammalian-specific phenotype, governed by the PlcR and AtxA regulators respectively, depending on the environmental cues its receives.

6.2. How does growth temperature determine PlcR and AtxA regulation?

A preliminary model of how temperature regulates the activity of PlcR and AtxA is presented here taking into account previous research and data collected in this study. In brief, at 25 °C global regulation and expression is determined by chromosomally encoded factors included the pleiotropic regulator of virulence PlcR. However, at 37 °C expression of genes on the extrachromosomal DNA has a far greater influence on the phenotypic traits of *B. cereus* G9241.

6.2.1. Global regulation in *B. cereus* G9241 at 25 °C

During exponential growth at 25 °C, *B. cereus* G9241 cells are vegetative, motile and secrete a large profile of non-specific toxins regulated by PlcR (Hernández-Rodriguez et al., 2013). This is identical to the phenotypes of the majority of known *B. cereus* sensu stricto strains but without the restriction of the growth

temperature (Borge et al., 2001; Gohar et al., 2008). PlcR is a global regulator of secreted proteins and the majority of toxins secreted by *B. cereus* sensu lato strains are regulated at a transcriptional level by PlcR (Agaisse et al., 1999; Gohar et al., 2008; Gohar et al., 2002). PlcR is likely to control regulation of secreted toxins in *B. cereus* G9241 as well. Toxin genes in *B. cereus* G9241 were determined to be regulated by PlcR due to the presence of a PlcR box consensus sequences upstream of the genes as well as transcriptome data in the literature (Gohar et al., 2008; Økstad et al., 1999). Interestingly the *hbl* toxin operon normally regulated by PlcR in *B. cereus* sensu lato strains (Økstad et al., 1999) seems to no longer be under the transcriptional control of PlcR in *B. cereus* G9241. This study reveals the PlcR box is further upstream than previously reported and the transcription of the *hbl* operon does not change between temperatures. However, the secretion of Hbl toxins is significantly different between the two temperatures suggesting the Hbl toxin components are post-translationally regulated. Transcription of the PlcR-regulated toxins in *B. cereus* G9241 falls dramatically during 37 °C growth as determined by the RNAseq, secretomics and the haemolysis assays in this study and the cytotoxic assays conducted prior to this study (Hernández-Rodriguez et al., 2013). The PlcR protein levels do not change between the two growth temperatures, nor do the transcription levels of *plcR*. Together this suggests the temperature-dependent regulation of PlcR is at a post-translational level.

As the activity of PlcR relies on activation by the co-regulator quorum sensing peptide signal PapR (Grenha et al., 2013), PapR represents a potential point of regulation for PlcR. PapR must be transcribed, translated, exported, processed and reimported before it can activate PlcR. This means the PlcR-PapR network presents many points at which the activity if PlcR can be regulated. PapR was not differentially expressed between the two growth temperatures nor was it detected in the cell proteome or secretome. However this may be a result of limitations of the MALDI-ToF approach used. The findings of this study suggest that PlcR activity is largely lost at 37 °C and this may be down to temperature-dependent regulation of the PlcR-PapR regulatory network. Further work is

needed to determine how activity of PlcR is downregulated at 37 °C. Unpublished work from the Waterfield group has shown that processed PapR peptide added exogeneously doesn't activate transcription of the *plcR* regulon when *B. cereus* G9241 is growing at 37 °C. This suggests that loss of PlcR activity at 37 °C may be due to a lack of co-regulator activation due to failure to reimport the PapR peptide (Manoharan, 2019).

6.2.2. Global regulation in *B. cereus* G9241 at 37 °C

Downregulation of PlcR activity at 37 °C and a loss of non-specific virulence is necessary but not sufficient enough a change in global regulation to lead to a mammalian virulent phenotype. *B. anthracis* mammalian virulence does rely on a loss of haemolytic phenotype, but also requires the production of the anthrax toxins, a capsule and sporulation (Moayeri et al., 2015). This study did not observe a significant change in the transcription of the *atxA* gene, but as discussed previously (section 4.3.3) there is still evidence that AtxA activity does increase at 37 °C in *B. cereus* G9241 such as the transcription of the *pagA* gene. A growth temperature of 37 °C may not be sufficient to elicit full activity of AtxA in *B. cereus* G9241. Instead the regulator likely relies on another environmental stimulus, the level of CO_2/bicarbonate (Passalacqua et al., 2009). Passalacqua showed that transcription of *atxA* increases 5.6-fold during exponential growth at 37 °C, 14-15% CO_2 + 0.8% bicarbonate compared to growth at 37 °C with normal aeration. *atxA* transcription is regulated the same way in *B. anthracis* (Sirard et al., 1994).

Mignot showed that expression of PlcR in *B. anthracis* led to a huge reduction in sporulation needed for mammalian virulence (Mignot et al., 2001), though evidence does exist in the contrary to this (Sastalla et al., 2010). If we assume Mignot's findings are correct, *B. cereus* G9241 has evolved a mechanism to overcome this reduction in sporulation phenotype. I propose that acquisition of the pBFH_1 phagemid and production of phage at 37 °C forces *B. cereus* G9241 to sporulate in a temperature-dependent phenotype.

If these hypotheses are correct, then this study presents a novel regulatory mechanism that has resulted in the conversion of a diarrhoeal strain of *B. cereus* into a lethal human pathogen capable of causing an inhalational anthrax like disease.

6.3. The virulent lifestyle and ecological niche of *B. cereus* G9241

The model proposed by this study provides a biochemical basis for the regulation of virulence in *B. cereus* G9241, but the question still remains on how this affects the ecological niche occupied by the bacterium. Whilst all species of the *B. cereus* sensu lato are soil-dwelling organisms, their means of survival are very different. *B. cereus* can survive in a vegetative state in the soil niche, colonising the insect gut or plant rhizospheres (Pandey and Palni, 1997; Salamitou et al., 2000). In contrast *B. anthracis* is believed to have to survive as a spore in the soil. *B. anthracis* vegetative cells have been shown to die in soil environments as they are unable to compete with other members of the microflora (Bowen and Turnbull, 1992; Titball et al., 1991; Vasil'eva, 1958). However they can form vegetative colonies in rhizospheres (Saile and Koehler, 2006). The low prevalence of *B. cereus* G9241 and other *B. cereus*-*B. anthracis* (*Bc*-*Ba*) crossover strains makes it hard to determine the ecological niche that the species inhabits. However, there are identifiable patterns in the epidemiology of the *Bc*-*Ba* crossover strains.

All *Bc*-*Ba* crossover strains isolated from patients or the environment have been isolated from the southern states of the USA suggesting a relatively low geographical spread of these strains. All strains causing fulminant infections have been isolated from, "otherwise healthy" metalworkers. However it is should be noted that there is extensive research to suggest that the incidence of pneumonia and other lung diseases occurs at a much higher rate in metalworkers than other individuals (Bennett and Bennett, 1985; Hunting and Welch, 1993). This suggests reduced lung function, perhaps due to exposure to toxic chemicals/material or life-style choices such as smoking. The *B. cereus* FL2013 strain was isolated from an anthrax eschar of a 70 year old man

described as otherwise healthy (Marston et al., 2016). Due to the low occurrence of mammalian infections caused by these pathogenic strains they have been described as opportunistic, but infections in non-immunocompromised mouse models suggest this may not necessarily be true (Oh et al., 2011). Oh's study states that both the *has* and *bps* operon-encoded capsules are necessary for full infectivity in mice. This may indicate that *B. cereus* 03BB102, FL2013 and Elc2 are opportunistic pathogens of human due to not having the bps operon-encoded capsule. There is currently no research into how *B. cereus* G9241 and other *Bc-Ba* crossover strains persist in the environment. However, if we assume that soil temperatures are lower than mammalian host temperatures, then this study suggests that *B. cereus* G9241 would exist in a vegetative state in the soil. This could account for the low occurrence of mammalian infections as like *B. anthracis*, spores are the infectious particles of *B. cereus* G9241. It is unknown whether *B. cereus* G9241 sporulates in the environment before infection because of various environmental triggers, or if *B. cereus* rapidly sporulates upon entry to a host organism.

6.4. Impact on the field of *B. anthracis* biology

6.4.1. Classification of species

B. cereus G9241 and other *Bc-Ba* crossover strains represent a unique group within the *B.* cereus sensu lato, characterised by the presence of WT *plcR* and *atxA* genes. These strains do not fit into the species classification already defined within the sensu lato. The presence of the anthrax toxin genes, the ability to cause a pulmonary anthrax-like pneumonia as well as anthrax eschars means on a phenotypic level that *Bc-Ba* strains are not *B. cereus* sensu stricto. Furthermore, the presence of a WT *plcR* gene means they are not defined as *B. anthracis* species. Debate about the species classification of the *B. cereus* sensu lato is not novel. Conflicting studies define the species in a myriad of ways including virulence phenotypes, presence of extrachromosomal DNA as well as classical genotyping methods (Ash et al., 1991; Helgason et al., 2000; Marston et al., 2006; Okinaka et al., 2006). No one single method has been agreed upon to

differentiate or unify the species and the identification of a group of *Bc-Ba* crossover strains only increases the difficulty of that task.

6.4.2. Biosafety

Bc-Ba crossover strains present a new difficulty in the field of biosafety. Various methods exist for detecting *B. anthracis* in the environment, but do not account for the emergence of *Bc-Ba* crossover strains. Methods include PCR against genes characteristic of *B. anthracis* (Cheun et al., 2003), detection of the spore coat (Arora et al., 2012) and antibodies against the spores (Zhou et al., 2002). pBCX01 is nearly identical to pX01 so PCR against anthrax toxin genes would still be appropriate, but attempts to amplify the *cap* operon of pX02 will fail. If *B. cereus* G9241 exists as a population of vegetative cells in the environment, attempts to detect spores will lead to false negatives. The temperature-dependent lifestyle of *B. cereus* G9241 proposed in this study may necessitate the development of new methods of detection. New methods will need to consider the temperature dependent variable phenotypes displayed by *B. cereus* G9241 and potentially other *Bc-Ba* strains.

6.5. Future work

This study has led to the hypothesis that *B. cereus* G9241 is able to switch from a PlcR-mediated, non-specific virulence phenotype at 25 °C, to an AtxA-mediated mammalian-virulent phenotype at 37 °C. The data provided in this study is valid, but there are experiments needed to validate the hypothesis.

A very informative experiment to perform would be to delete *plcR*, grow *B. cereus* G9241 at 25 °C and determine the haemolytic and cytolytic phenotypes. This would act as confirmation that the non-specific virulence phenotype seen at 25 °C was determined by the PlcR regulator. This experiment would also determine whether the *hblCDAB* operon is still transcriptionally activated by PlcR in *B. cereus* G9241. This experiment would need to be conducted in a category 3 laboratory, as deleting *plcR* may well create what is essentially a *B. anthracis*

strain. Complementation experiments to confirm the role of *plcR* would also need to be conducted.

Secondly it would be beneficial to determine if the loss of activity of PlcR at 37 °C is due the regulator not being activated by PapR. The mature, processed PapR peptide could be expressed in *B. cereus* G9241 when growing at 37 °C to negate the need for its export and processing. This has been conducted previously to show mature PapR peptide is sufficient to activate PlcR (Slamti and Lereclus, 2002). However, it is likely that experiments analysing the transcriptional regulation in *B. cereus* G9241 at 37 °C will be difficult due to the high level of transcription from pBFH_1 and the rapid initiation of sporulation.

Curing the pBFH_1 phagemid and conducting sporulation assays at 37 °C to elucidate the role of the phagemid in sporulation would be a key experiment. If temperature-dependent sporulation is lost when pBFH_1 is cured, it can be determined that the phagemid must be causative of the phenotype. Work leading up to this study involved curing the pBC210 plasmid through repeated high temperature passaging. This method is non-specific and the fact that neither pBCX01 nor pBFH_1 were lost during this passaging suggests they are difficult to cure.

The nature of global transcriptomics and proteomics means that a huge amount of data has been produced from this study. At present the poor annotation of the *B. cereus* G9241 genome is preventing automated processing and analysis of this data. If the reference genome can be re-annotated to provide more information on the genes present in *B. cereus* G9241, it would allow the elucidation of global regulatory pathways and ontological groups transcribed higher or lower under different conditions.

As noted previously, Passalacqua showed *atxA* is more highly transcribed during growth at 37 °C in CO_2-bicarbonate conditions compared to at 25 °C in CO_2-bicarbonate conditions (Passalacqua et al., 2009). Studying the effects of CO_2-bicarbonate on the temperature-dependent regulation already seen in *B. cereus* G9241 may provide a more thorough insight into regulation under mammalian

host conditions. Finally, from an ecological and biosafety perspective it would be useful to know if *B. cereus* G9241 is able to colonise the guts of soil invertebrates, as has been shown for many other members of the sensu lato group. This may be even more pertinent given the current push to farm insects on a factory scale for future “food or feed” animal protein production.

6.6 Concluding remarks

The dogma has long stood that the PlcR and AtxA regulators identified in the *B. cereus* sensu lato are incompatible within a single organism. This is despite the identification of strains such as *B. cereus* G9241 possessing WT copies of genes encoding both regulators. This study suggests that temperature-dependent regulation of the global virulence regulators allows *B. cereus* G9241 to accommodate both to switch between non-specific and mammalian virulent phenotypes.

7. References

Ackermann, H.W. (2006). Classification of bacteriophages. The bacteriophages *2*, 8-16.

Agaisse, H., Gominet, M., Okstad, O.A., Kolsto, A.B., and Lereclus, D. (1999). PlcR is a pleiotropic regulator of extracellular virulence factor gene expression in *Bacillus thuringiensis*. Molecular Microbiology *32*, 1043-1053.

Agata, N., Mori, M., Ohta, M., Suwan, S., Ohtani, I., and Isobe, M. (1994). A novel dodecadepsipeptide, cereulide, isolated from *Bacillus cereus* causes vacuole formation in HEp-2 cells. FEMS microbiology letters *121*, 31-34.

Andersson, A., Granum, P.E., and Rönner, U. (1998). The adhesion of *Bacillus cereus* spores to epithelial cells might be an additional virulence mechanism. International journal of food microbiology *39*, 93-99.

Andrews, J.M. (2009). BSAC standardized disc susceptibility testing method (version 8). Journal of Antimicrobial Chemotherapy *64*, 454-489.

Antonation, K.S., Grutzmacher, K., Dupke, S., Mabon, P., Zimmermann, F., Lankester, F., Peller, T., Feistner, A., Todd, A., Herbinger, I.*, et al.* (2016). *Bacillus cereus* biovar *anthracis* causing anthrax in sub-saharan Africa-chromosomal monophyly and broad geographic distribution. PLoS Negl Trop Dis *10*, e0004923.

Arantes, O., and Lereclus, D. (1991). Construction of cloning vectors for *Bacillus-thuringiensis*. Gene *108*, 115-119.

Arora, R., Petrov, G.I., Yakovlev, V.V., and Scully, M.O. (2012). Detecting anthrax in the mail by coherent Raman microspectroscopy. Proceedings of the National Academy of Sciences *109*, 1151-1153.

Ash, C., Farrow, J.A.E., Dorsch, M., Stackebrandt, E., and Collins, M.D. (1991). Comparative-analysis of *Bacillus-anthracis*, *Bacillus-cereus*, and related species on the basis of reverse-transcriptase sequencing of 16s ribosomal-RNA. International Journal of Systematic Bacteriology *41*, 343-346.

Avashia, S.B., Riggins, W.S., Lindley, C., Hoffmaster, A., Drumgoole, R., Nekomoto, T., Jackson, P.J., Hill, K.K., Williams, K., Lehman, L.*, et al.* (2007). Fatal pneumonia among metalworkers due to inhalation exposure to *Bacillus cereus* containing *Bacillus anthracis* toxin genes. Clinical Infectious Diseases *44*, 414-416.

Baldus, J.M., Green, B.D., Youngman, P., and Moran, C. (1994). Phosphorylation of *Bacillus subtilis* transcription factor Spo0A stimulates transcription from the spoIIG promoter by enhancing binding to weak 0A boxes. Journal of bacteriology *176*, 296-306.

Basi-Chipalu, S., Dischinger, J., Josten, M., Szekat, C., Zweynert, A., Sahl, H.G., and Bierbaum, G. (2015). Pseudomycoicidin, a Class II Lantibiotic from *Bacillus pseudomycoides*. Appl Environ Microbiol *81*, 3419-3429.

Basu, S., Kang, T.J., Chen, W.H., Fenton, M.J., Baillie, L., Hibbs, S., and Cross, A.S. (2007). Role of *Bacillus anthracis* spore structures in macrophage cytokine responses. Infection and immunity *75*, 2351-2358.

Baweja, R.B., Zaman, M.S., Mattoo, A.R., Sharma, K., Tripathi, V., Aggarwal, A., Dubey, G.P., Kurupati, R.K., Ganguli, M., and Chaudhury, N. (2008). Properties of *Bacillus anthracis* spores prepared under various environmental conditions. Archives of microbiology *189*, 71-79.

Beauregard, K.E., Collier, R.J., and Swanson, J.A. (2000). Proteolytic activation of receptor-bound anthrax protective antigen on macrophages promotes its internalization. Cellular microbiology *2*, 251-258.

Belitsky, B.R. (2015). Role of branched-chain amino acid transport in *Bacillus subtilis* CodY activity. J Bacteriol *197*, 1330-1338.

Benedict, R.C., Partridge, T., Wells, D., and Buchanan, R.L. (1993). *Bacillus cereus*: aerobic growth kinetics. Journal of food protection *56*, 211-214.

Bennett, E., and Bennett, D. (1985). Occupational airway diseases in the metalworking industry Part 1: Respiratory infections, pneumonia, chronic bronchitis and emphysema. Tribology International *18*, 169-176.

Berliner, E. (1915). Über die Schlaffsucht der Mehlmottenraupe (Ephestia kühniella Zell.) und ihren Erreger *Bacillus thuringiensis* n. sp. Zeitschrift für angewandte Entomologie *2*, 29-56.

Berry, C., O'Neil, S., Ben-Dov, E., Jones, A.F., Murphy, L., Quail, M.A., Holden, M.T., Harris, D., Zaritsky, A., and Parkhill, J. (2002). Complete sequence and organization of pBtoxis, the toxin-coding plasmid of *Bacillus thuringiensis* subsp. *israelensis*. Appl Environ Microbiol *68*, 5082-5095.

Bischofs, I.B., Hug, J.A., Liu, A.W., Wolf, D.M., and Arkin, A.P. (2009). Complexity in bacterial cell-cell communication: quorum signal integration and subpopulation signaling in the *Bacillus subtilis* phosphorelay. Proc Natl Acad Sci U S A *106*, 6459-6464.

Bishop, A. (2002). *Bacillus thuringiensis* insecticides. Applications and Systematics of Bacillus and Relatives, 160-175.

Black, L.W. (1989). DNA packaging in dsDNA bacteriophages. Annual review of microbiology *43*, 267-292.

Böhm, M.-E., Huptas, C., Krey, V.M., and Scherer, S. (2015). Massive horizontal gene transfer, strictly vertical inheritance and ancient duplications differentially shape the evolution of *Bacillus cereus* enterotoxin operons *hbl, cytK and nhe*. BMC evolutionary biology *15*, 246.

Borge, G.I.A., Skeie, M., Sørhaug, T., Langsrud, T., and Granum, P.E. (2001). Growth and toxin profiles of *Bacillus cereus* isolated from different food sources. International journal of food microbiology *69*, 237-246.

Boudreaux, D.P., and Srinivasan, V. (1981). Bacteriophage-induced sporulation in *Bacillus cereus* T. Microbiology *126*, 459-462.

Bourgogne, A., Drysdale, M., Hilsenbeck, S.G., Peterson, S.N., and Koehler, T.M. (2003). Global effects of virulence gene regulators in a *Bacillus anthracis* strain with both virulence plasmids. Infection and Immunity *71*, 2736-2743.

Bowen, J., and Turnbull, P. (1992). The fate of *Bacillus anthracis* in unpasteurized and pasteurized milk. Letters in applied microbiology *15*, 224-227.

Bradley, K.A., Mogridge, J., Mourez, M., Collier, R.J., and Young, J.A. (2001). Identification of the cellular receptor for anthrax toxin. Nature *414*, 225.

Bramucci, M., Keggins, K., and Lovett, P. (1977). Bacteriophage PMB12 conversion of the sporulation defect in RNA polymerase mutants of *Bacillus subtilis*. Journal of virology *24*, 194-200.

Bravo, A., Gill, S.S., and Soberon, M. (2007). Mode of action of *Bacillus thuringiensis* Cry and Cyt toxins and their potential for insect control. Toxicon *49*, 423-435.

Brittingham, K.C., Ruthel, G., Panchal, R.G., Fuller, C.L., Ribot, W.J., Hoover, T.A., Young, H.A., Anderson, A.O., and Bavari, S. (2005). Dendritic cells endocytose *Bacillus anthracis* spores: implications for anthrax pathogenesis. The Journal of Immunology *174*, 5545-5552.

Broussolle, V., Pandiani, F., Haddad, N., Michaud, C., Carlin, F., Nguyen-the, C., and Brillard, J. (2010). Insertional mutagenesis reveals genes involved in *Bacillus cereus* ATCC 14579 growth at low temperature. FEMS Microbiology Letters *306*, 177-183.

Brunsing, R.L., La Clair, C., Tang, S., Chiang, C., Hancock, L.E., Perego, M., and Hoch, J.A. (2005). Characterization of sporulation histidine kinases of *Bacillus anthracis*. Journal of bacteriology *187*, 6972-6981.

Burkholder, W.F., Kurtser, I., and Grossman, A.D. (2001). Replication initiation proteins regulate a developmental checkpoint in *Bacillus subtilis*. Cell *104*, 269-279.

Burwen, D.R., Banerjee, S.N., Gaynes, R.P., and System, N.N.I.S. (1994). Ceftazidime resistance among selected nosocomial gram-negative bacilli in the United States. Journal of Infectious Diseases *170*, 1622-1625.

Carlson, C.J., Getz, W.M., Kausrud, K.L., Cizauskas, C.A., Blackburn, J.K., Bustos Carrillo, F.A., Colwell, R., Easterday, W.R., Ganz, H.H., Kamath, P.L.*, et al.* (2018a). Spores and soil

from six sides: interdisciplinarity and the environmental biology of anthrax (*Bacillus anthracis*). Biological reviews of the Cambridge Philosophical Society *93*, 1813-1831.

Carlson, C.J., Kracalik, I., Ross, N., Alexander, K., Hugh-Jones, M.E., Fegan, M., Elkin, B., Epp, T., Shury, T., Bagirova, M*., et al.* (2018b). The global distribution of *Bacillus anthracis* and associated anthrax risk to humans, livestock, and wildlife. Nature Microbiology *4*, 1337-1343.

Carrillo, C., Teruel, J.A., Aranda, F.J., and Ortiz, A. (2003). Molecular mechanism of membrane permeabilization by the peptide antibiotic surfactin. Biochimica et Biophysica Acta (BBA)-Biomembranes *1611*, 91-97.

Carter, K.C. (1985). Koch's postulates in relation to the work of Jacob Henle and Edwin Klebs. Medical History *29*, 353-374.

CDC (2014a). Cutaneous Anthrax | Anthrax | CDC. [online] Cdcgov Available at: https://wwwcdcgov/anthrax/basics/types/cutaneoushtml Accessed 12 Aug *2019*.

CDC (2014b). Gastrointestinal Anthrax | Anthrax | CDC. [online] Cdcgov Available at: https://wwwcdcgov/anthrax/basics/types/gastrointestinalhtml Accessed 12 Aug *2019*.

CDC (2014c). Inhalation Anthrax | Anthrax | CDC. [online] Cdcgov Available at: https://wwwcdcgov/anthrax/basics/types/inhalationhtml Accessed 12 Aug *2019*.

CDC (2016). A History of Anthrax | Anthrax | CDC. [online] Cdcgov Available at: https://wwwcdcgov/anthrax/resources/history/indexhtml Accessed 12 Aug *2019*.

Chantratita, N., Rholl, D.A., Sim, B., Wuthiekanun, V., Limmathurotsakul, D., Amornchai, P., Thanwisai, A., Chua, H.H., Ooi, W.F., and Holden, M.T. (2011). Antimicrobial resistance to ceftazidime involving loss of penicillin-binding protein 3 in *Burkholderia pseudomallei*. Proceedings of the National Academy of Sciences *108*, 17165-17170.

Chateau, A., van Schaik, W., Six, A., Aucher, W., and Fouet, A. (2011). CodY regulation is required for full virulence and heme iron acquisition in *Bacillus anthracis*. FASEB J *25*, 4445-4456.

Cheun, H., Makino, S.I., Watarai, M., Erdenebaatar, J., Kawamoto, K., and Uchida, I. (2003). Rapid and effective detection of anthrax spores in soil by PCR. Journal of applied microbiology *95*, 728-733.

Chitlaru, T., Gat, O., Grosfeld, H., Inbar, I., Gozlan, Y., and Shafferman, A. (2007). Identification of in vivo-expressed immunogenic proteins by serological proteome analysis of the *Bacillus anthracis* secretome. Infection and immunity *75*, 2841-2852.

Choma, C., Clavel, T., Dominguez, H., Razafindramboa, N., Soumille, H., Nguyen-the, C., and Schmitt, P. (2000). Effect of temperature on growth characteristics of *Bacillus cereus* TZ415. International Journal of Food Microbiology *55*, 73-77.

Clair, G., Roussi, S., Armengaud, J., and Duport, C. (2010). Expanding the known repertoire of virulence factors produced by *Bacillus cereus* through early secretome profiling in three redox conditions. Molecular & Cellular Proteomics *9*, 1486-1498.

Dai, Z., Sirard, J.C., Mock, M., and Koehler, T.M. (1995). *Bacillus anthracis* gene *atxA* activates toxin expression in vitro and in vivo. Abstracts of the General Meeting of the American Society for Microbiology *95*, 223-223.

Dai, Z.H., and Koehler, T.M. (1997). Regulation of anthrax toxin activator gene (*atxA*) expression in *Bacillus anthracis*: Temperature, not CO_2/bicarbonate, affects AtxA synthesis. Infection and Immunity *65*, 2576-2582.

Dale, J.L., Raynor, M.J., Ty, M.C., Hadjifrangiskou, M., and Koehler, T.M. (2018). A dual role for the *Bacillus anthracis* master virulence regulator Atxa: Control of sporulation and anthrax toxin production. Frontiers in Microbiology *9*.

Davies, D. (1960). The influence of temperature and humidity on spore formation and germination in *Bacillus anthracis*. Epidemiology & Infection *58*, 177-186.

de Vries, Y.P., Hornstra, L.M., de Vos, W.M., and Abee, T. (2004). Growth and sporulation of *Bacillus cereus* ATCC 14579 under defined conditions: temporal expression of genes for key sigma factors. Appl Environ Microbiol *70*, 2514-2519.

Declerck, N., Bouillaut, L., Chaix, D., Rugani, N., Slamti, L., Hoh, F., Lereclus, D., and Arold, S.T. (2007). Structure of PlcR: Insights into virulence regulation and evolution of quorum sensing in Gram-positive bacteria. Proceedings of the National Academy of Sciences *104*, 18490-18495.

Devi, S.N., Vishnoi, M., Kiehler, B., Haggett, L., and Fujita, M. (2015). In vivo functional characterization of the transmembrane histidine kinase KinC in *Bacillus subtilis*. Microbiology *161*, 1092-1104.

Diaz, A.R., Core, L.J., Jiang, M., Morelli, M., Chiang, C.H., Szurmant, H., and Perego, M. (2012). *Bacillus subtilis* RapA phosphatase domain interaction with its substrate, phosphorylated Spo0F, and its inhibitor, the PhrA peptide. J Bacteriol *194*, 1378-1388.

Dierick, K., Van Coillie, E., Swiecicka, I., Meyfroidt, G., Devlieger, H., Meulemans, A., Hoedemaekers, G., Fourie, L., Heyndrickx, M., and Mahillon, J. (2005). Fatal family outbreak of *Bacillus cereus*-associated food poisoning. J Clin Microbiol *43*, 4277-4279.

Dixon, T.C., Fadl, A.A., Koehler, T.M., Swanson, J.A., and Hanna, P.C. (2000). Early *Bacillus anthracis*–macrophage interactions: intracellular survival and escape. Cellular microbiology *2*, 453-463.

Dulmage, H.T. (1981). Insecticidal activity of isolated of *Bacillus thuringiensis* and their potential for pest control. Microbial control of pests and plant diseases *1970-1980*, 193-222.

Egilmez, H.I., Morozov, A.Y., Clokie, M.R., Shan, J., Letarov, A., and Galyov, E.E. (2018). Temperature-dependent virus lifecycle choices may reveal and predict facets of the biology of opportunistic pathogenic bacteria. Scientific reports *8*, 9642.

Elliott, J.L., Mogridge, J., and Collier, R.J. (2000). A quantitative study of the interactions of *Bacillus anthracis* edema factor and lethal factor with activated protective antigen. Biochemistry *39*, 6706-6713.

Escuyer, V., and Collier, R.J. (1991). Anthrax protective antigen interacts with a specific receptor on the surface of CHO-K1 cells. Infection and Immunity *59*, 3381-3386.

Fagerlund, A., Lindbäck, T., and Granum, P.E. (2010). *Bacillus cereus* cytotoxins Hbl, Nhe and CytK are secreted via the Sec translocation pathway. BMC microbiology *10*, 304.

Fagerlund, A., Lindbäck, T., Storset, A.K., Granum, P.E., and Hardy, S.P. (2008). *Bacillus cereus* Nhe is a pore-forming toxin with structural and functional properties similar to the ClyA (HlyE, SheA) family of haemolysins, able to induce osmotic lysis in epithelia. Microbiology *154*, 693-704.

Fedhila, S., Buisson, C., Dussurget, O., Serror, P., Glomski, I., Liehl, P., Lereclus, D., and Nielsen-LeRoux, C. (2010). Comparative analysis of the virulence of invertebrate and mammalian pathogenic bacteria in the oral insect infection model *Galleria mellonella*. Journal of invertebrate pathology *103*, 24-29.

Fernandes, S., and São-José, C. (2018). Enzymes and mechanisms employed by tailed bacteriophages to breach the bacterial cell barriers. Viruses *10*, 396.

Fieldhouse, R.J., Turgeon, Z., White, D., and Merrill, A.R. (2010). Cholera-and anthrax-like toxins are among several new ADP-ribosyltransferases. PLoS computational biology *6*, e1001029.

Firoved, A.M., Miller, G.F., Moayeri, M., Kakkar, R., Shen, Y.Q., Wiggins, J.F., McNally, E.M., Tang, W.J., and Leppla, S.H. (2005). *Bacillus anthracis* edema toxin causes extensive tissue lesions and rapid lethality in mice. American Journal of Pathology *167*, 1309-1320.

Flugge, C. (1886). Microorganisms - Etiology of the infectious diseases. Microbial control of pests and plant diseases *1981*, 193-222.

Fortier, L.-C., and Sekulovic, O. (2013). Importance of prophages to evolution and virulence of bacterial pathogens. Virulence *4*, 354-365.

Fouet, A. (2010). AtxA, a *Bacillus anthracis* global virulence regulator. Research in microbiology *161*, 735-742.

Frankland, G.C., and Frankland, P.F. (1887). Studies on some new microorganisms obtained from air. Royal Soc London Phil Trans, Ser B, Biol Sci

Frenzel, E., Doll, V., Pauthner, M., Lucking, G., Scherer, S., and Ehling-Schulz, M. (2012). CodY orchestrates the expression of virulence determinants in emetic *Bacillus cereus* by impacting key regulatory circuits. Mol Microbiol *85*, 67-88.

Fu, X., Fu, N., Guo, S., Yan, Z., Xu, Y., Hu, H., Menzel, C., Chen, W., Li, Y., Zeng, R.*, et al.* (2009). Estimating accuracy of RNA-Seq and microarrays with proteomics. BMC Genomics *10*, 161.

Fujita, M., González-Pastor, J.E., and Losick, R. (2005). High-and low-threshold genes in the Spo0A regulon of Bacillus subtilis. Journal of bacteriology *187*, 1357-1368.

Fujita, M., and Losick, R. (2005). Evidence that entry into sporulation in *Bacillus subtilis* is governed by a gradual increase in the level and activity of the master regulator Spo0A. Genes & Development *19*, 2236-2244.

Furukawa, S., Narisawa, N., Watanabe, T., Kawarai, T., Myozen, K., Okazaki, S., Ogihara, H., and Yamasaki, M. (2005). Formation of the spore clumps during heat treatment increases the heat resistance of bacterial spores. International Journal of Food Microbiology *102*, 107-111.

Gallego del Sol, F., and Marina, A. (2013). Structural basis of Rap phosphatase inhibition by Phr peptides. PLoS Biol *11*, e1001511.

Garbeva, P., van Veen, J. & van Elsas, J. (2003). Predominant *Bacillus spp*. in Agricultural Soil under Different Management Regimes Detected via PCR-DGGE. J Microb Ecol *45*, 302-316.

Gillis, A., and Mahillon, J. (2014). Phages preying on *Bacillus anthracis, Bacillus cereus,* and *Bacillus thuringiensis*: past, present and future. Viruses *6*, 2623-2672.

Gilois, N., Ramarao, N., Bouillaut, L., Perchat, S., Aymerich, S., Nielsen-LeRoux, C., Lereclus, D., and Gohar, M. (2007). Growth-related variations in the *Bacillus cereus* secretome. Proteomics *7*, 1719-1728.

Glasset, B., Herbin, S., Granier, S.A., Cavalié, L., Lafeuille, E., Guérin, C., Ruimy, R., Casagrande-Magne, F., Levast, M., and Chautemps, N. (2018). *Bacillus cereus*, a serious cause of nosocomial infections: epidemiologic and genetic survey. PloS one *13*, e0194346.

Gohar, M., Faegri, K., Perchat, S., Ravnum, S., Okstad, O.A., Gominet, M., Kolsto, A.-B., and Lereclus, D. (2008). The PlcR virulence regulon of *Bacillus cereus*. Plos One *3*.

Gohar, M., Gilois, N., Graveline, R., Garreau, C., Sanchis, V., and Lereclus, D. (2005). A comparative study of *Bacillus cereus, Bacillus thuringiensis* and *Bacillus anthracis* extracellular proteomes. Proteomics *5*, 3696-3711.

Gohar, M., Okstad, O.A., Gilois, N., Sanchis, V., Kolsto, A.B., and Lereclus, D. (2002). Two-dimensional electrophoresis analysis of the extracellular proteome of *Bacillus cereus* reveals the importance of the PlcR regulon. Proteomics *2*, 784-791.

Gominet, M., Slamti, L., Gilois, N., Rose, M., and Lereclus, D. (2001). Oligopeptide permease is required for expression of the *Bacillus thuringiensis* PlcR regulon and for virulence. Molecular Microbiology *40*, 963-975.

González-Pastor, J.E., Hobbs, E.C., and Losick, R. (2003). Cannibalism by sporulating bacteria. Science *301*, 510-513.

Granum, P.E. (2005). Bacillus cereus. Foodborne pathogens: microbiology and molecular biology, 409-419.

Granum, P.E., and Lund, T. (1997). Bacillus cereus and its food poisoning toxins. FEMS microbiology letters *157*, 223-228.

Grazziotin, A.L., Koonin, E.V., and Kristensen, D.M. (2017). Prokaryotic Virus Orthologous Groups (pVOGs): a resource for comparative genomics and protein family annotation. Nucleic Acids Res *45*, D491-d498.

Green, B.D., Battisti, L., Koehler, T.M., Thorne, C.B., and Ivins, B.E. (1985). Demonstration of a capsule plasmid in *Bacillus anthracis*. Infection and immunity *49*, 291-297.

Grenha, R., Slamti, L., Nicaise, M., Refes, Y., Lereclus, D., and Nessler, S. (2013). Structural basis for the activation mechanism of the PlcR virulence regulator by the quorum-sensing signal peptide PapR. Proc Natl Acad Sci U S A *110*, 1047-1052.

Grossman, A.D., and LoSICK, R. (1988). Extracellular control of spore formation in *Bacillus subtilis*. Proceedings of the National Academy of Sciences *85*, 4369-4373.

Guidi-Rontani, C., Weber-Levy, M., Labruyere, E., and Mock, M. (1999). Germination of *Bacillus anthracis* spores within alveolar macrophages. Molecular Microbiology *31*, 9-17.

Guidi-Rontani, C., Weber-Levy, M., Labruyère, E., and Mock, M. (1999). Germination of *Bacillus anthracis* spores within alveolar macrophages. Molecular microbiology *31*, 9-17.

Guignot, J., Mock, M., and Fouet, A. (1997). AtxA activates the transcription of genes harbored by both *Bacillus anthracis* virulence plasmids. Fems Microbiology Letters *147*, 203-207.

Guinebretiere, M.H., Auger, S., Galleron, N., Contzen, M., De Sarrau, B., De Buyser, M.L., Lamberet, G., Fagerlund, A., Granum, P.E., Lereclus, D.*, et al.* (2013). *Bacillus cytotoxicus sp. nov*. is a novel thermotolerant species of the *Bacillus cereus* Group occasionally associated with food poisoning. Int J Syst Evol Microbiol *63*, 31-40.

Guinebretiere, M.H., Broussolle, V., and Nguyen-The, C. (2002). Enterotoxigenic Profiles of Food-Poisoning and Food-Borne *Bacillus cereus* Strains. Journal of Clinical Microbiology *40*, 3053-3056.

Hammerstrom, T.G., Roh, J.H., Nikonowicz, E.P., and Koehler, T.M. (2011). *Bacillus anthracis* virulence regulator AtxA: oligomeric state, function and CO_2-signalling. Molecular microbiology *82*, 634-647.

Hanlon, D.W., and Ordal, G.W. (1994). Cloning and characterization of genes encoding methyl-accepting chemotaxis proteins in *Bacillus subtilis*. J Biol Chem *269*, 14038-14046.

Hardy, S.P., Lund, T., and Granum, P.E. (2001). CytK toxin of *Bacillus cereus* forms pores in planar lipid bilayers and is cytotoxic to intestinal epithelia. Fems Microbiology Letters *197*, 47-51.

Heinrichs, J.H., Beecher, D., Macmillan, J., and Zilinskas, B. (1993). Molecular cloning and characterization of the *hblA* gene encoding the B component of hemolysin BL from *Bacillus cereus*. Journal of Bacteriology *175*, 6760-6766.

Helgason, E., Okstad, O.A., Caugant, D.A., Johansen, H.A., Fouet, A., Mock, M., Hegna, I., and Kolsto, A.B. (2000). *Bacillus anthracis*, *Bacillus cereus*, and *Bacillus thuringiensis* - One species on the basis of genetic evidence. Applied and Environmental Microbiology *66*, 2627-2630.

Hernández-Rodriguez, C.S., Baillie, L., and Waterfield, N.R. (2013). From *Bacillus cereus* to *Bacillus anthracis* [Unpublished].

Hoffmaster, A.R., Hill, K.K., Gee, J.E., Marston, C.K., De, B.K., Popovic, T., Sue, D., Wilkins, P.P., Avashia, S.B., Drumgoole, R.*, et al.* (2006). Characterization of *Bacillus cereus* isolates associated with fatal pneumonias: Strains are closely related to *Bacillus anthracis* and Harbor *B-anthracis* virulence genes. Journal of Clinical Microbiology *44*, 3352-3360.

Hoffmaster, A.R., and Koehler, T.M. (1999). Autogenous regulation of the *Bacillus anthracis pag* operon. Journal of bacteriology *181*, 4485-4492.

Hoffmaster, A.R., Ravel, J., Rasko, D.A., Chapman, G.D., Chute, M.D., Marston, C.K., De, B.K., Sacchi, C.T., Fitzgerald, C., Mayer, L.W.*, et al.* (2004). Identification of anthrax toxin

genes in a *Bacillus cereus* associated with an illness resembling inhalation anthrax. Proc Natl Acad Sci U S A *101*, 8449-8454.

Höfler, C., Heckmann, J., Fritsch, A., Popp, P., Gebhard, S., Fritz, G., and Mascher, T. (2016). Cannibalism stress response in *Bacillus subtilis*. Microbiology *162*, 164-176.

Höfte, H., and Whiteley, H. (1989). Insecticidal crystal proteins of *Bacillus thuringiensis*. Microbiology and Molecular Biology Reviews *53*, 242-255.

Hoton, F.M., Fornelos, N., N'Guessan, E., Hu, X., Swiecicka, I., Dierick, K., Jääskeläinen, E., Salkinoja-Salonen, M., and Mahillon, J. (2009). Family portrait of *Bacillus cereus* and *Bacillus weihenstephanensis* cereulide-producing strains. Environmental Microbiology Reports *1*, 177-183.

Howard-Varona, C., Hargreaves, K.R., Abedon, S.T., and Sullivan, M.B. (2017). Lysogeny in nature: mechanisms, impact and ecology of temperate phages. The ISME journal *11*, 1511.

Hu, X., Van der Auwera, G., Timmery, S., Zhu, L., and Mahillon, J. (2009). Distribution, diversity, and potential mobility of extrachromosomal elements related to the *Bacillus anthracis* pXO1 and pXO2 virulence plasmids. Appl Environ Microbiol *75*, 3016-3028.

Hunting, K.L., and Welch, L.S. (1993). Occupational exposure to dust and lung disease among sheet metal workers. Occupational and Environmental Medicine *50*, 432-442.

illumina (2013). TruSeq Stranded mRNA Sample Preparation Guide, illumina, ed.

Ivanova, E., Mikhailov, V., and Andreev, L. (1992). Marine *Bacilli* and some approaches to their identification. Microbiol Zhurnal *54*, 27-33.

Ivanova, N., Sorokin, A., Anderson, I., Galleron, N., Candelon, B., Kapatral, V., Bhattacharyya, A., Reznik, G., Mikhailova, N., Lapidus, A.*, et al.* (2003). Genome sequence of *Bacillus cereus* and comparative analysis with *Bacillus anthracis*. Nature *423*, 87-91.

Jian, H., Xiong, L., Xu, G., and Xiao, X. (2016). Filamentous phage SW1 is active and influences the transcriptome of the host at high-pressure and low-temperature. Environmental microbiology reports *8*, 358-362.

Jiang, M., Shao, W., Perego, M., and Hoch, J.A. (2000). Multiple histidine kinases regulate entry into stationary phase and sporulation in *Bacillus subtilis*. Molecular microbiology *38*, 535-542.

Jiang, W., Hou, Y., and Inouye, M. (1997). CspA, the major cold-shock protein of *Escherichia coli,* is an RNA chaperone. Journal of Biological Chemistry *272*, 196-202.

Jiménez, G., Urdiain, M., Cifuentes, A., López-López, A., Blanch, A.R., Tamames, J., Kämpfer, P., Kolstø, A.-B., Ramón, D., and Martínez, J.F. (2013). Description of *Bacillus toyonensis sp. nov*., a novel species of the *Bacillus cereus* group, and pairwise genome comparisons of the species of the group by means of ANI calculations. Systematic and applied microbiology *36*, 383-391.

Johnson, S.L., Daligault, H.E., Davenport, K.W., Jaissle, J., Frey, K.G., Ladner, J.T., Broomall, S.M., Bishop-Lilly, K.A., Bruce, D.C., Gibbons, H.S*., et al.* (2015a). Complete genome sequences for 35 biothreat assay-relevant *Bacillus* species. Genome announcements *3*, e00151-00115.

Johnson, S.L., Minogue, T.D., Teshima, H., Davenport, K.W., Shea, A.A., Miner, H.L., Wolcott, M.J., and Chain, P.S.G. (2015b). Finished genome sequence of *Bacillus cereus* strain 03BB87, a clinical isolate with *B. anthracis* virulence genes. Genome announcements *3*, e01446-01414.

Kaan, T., Homuth, G., Mäder, U., Bandow, J., and Schweder, T. (2002). Genome-wide transcriptional profiling of the *Bacillus subtilis* cold-shock response. Microbiology *148*, 3441-3455.

Kanda, K., Kayashima, T., Kato, F., and Murata, A. (2000). Temperature influences induction of a J7W-1-related phage in *Bacillus thuringiensis* serovar indiana. Acta virologica *44*, 183-187.

Keim, P., Gruendike, J.M., Klevytska, A.M., Schupp, J.M., Challacombe, J., and Okinaka, R. (2009). The genome and variation of *Bacillus anthracis*. Molecular aspects of medicine *30*, 397-405.

Kim, H., and Goepfert, J. (1971). Enumeration and identification of *Bacillus cereus* in foods: I. 24-hour presumptive test medium. Appl Environ Microbiol *22*, 581-587.

Klee, S.R., Ozel, M., Appel, B., Boesch, C., Ellerbrok, H., Jacob, D., Holland, G., Leendertz, F.H., Pauli, G., Grunow, R*., et al.* (2006). Characterization of *Bacillus anthracis*-like bacteria isolated from wild great apes from Cote d'Ivoire and Cameroon. J Bacteriol *188*, 5333-5344.

Klimpel, K.R., Arora, N., and Leppla, S.H. (1994). Anthrax toxin lethal factor contains a zinc metalloprotease consensus sequence which is required for lethal toxin activity. Molecular microbiology *13*, 1093-1100.

Kobir, A., Poncet, S., Bidnenko, V., Delumeau, O., Jers, C., Zouhir, S., Grenha, R., Nessler, S., Noirot, P., and Mijakovic, I. (2014). Phosphorylation of *Bacillus subtilis* gene regulator AbrB modulates its DNA-binding properties. Molecular microbiology *92*, 1129-1141.

Koch, R. (1876). The etiology of anthrax, based on the life history of *Bacillus anthracis*. Beitr Biol Pflanz *2*, 277-310.

Kotiranta, A., Lounatmaa, K., and Haapasalo, M. (2000). Epidemiology and pathogenesis of *Bacillus cereus* infections. Microbes and Infection *2*, 189-198.

Lechner, S., Mayr, R., Francis, K.P., Pruss, B.M., Kaplan, T., Wiessner-Gunkel, E., Stewartz, G., and Scherer, S. (1998). *Bacillus weihenstephanensis sp. nov.* is a new psychrotolerant species of the *Bacillus cereus* group. International Journal of Systematic Bacteriology *48*, 1373-1382.

Leendertz, F.H., Ellerbrok, H., Boesch, C., Couacy-Hymann, E., Mätz-Rensing, K., Hakenbeck, R., Bergmann, C., Abaza, P., Junglen, S., and Moebius, Y. (2004). Anthrax kills wild chimpanzees in a tropical rainforest. Nature *430*, 451-452.

Lehmann, M., Noack, D., Wood, M., Perego, M., and Knaus, U.G. (2009). Lung epithelial injury by *B. anthracis* lethal toxin is caused by MKK-dependent loss of cytoskeletal integrity. PLoS One *4*, e4755.

Leise, J.M., Carter, C.H., Friedlander, H., and Freed, S.W. (1959). Criteria for the identification of *Bacillus anthracis*. Journal of bacteriology *77*, 655.

Leppla, S.H. (1982). Anthrax toxin edema factor: a bacterial adenylate cyclase that increases cyclic AMP concentrations of eukaryotic cells. Proceedings of the National Academy of Sciences *79*, 3162-3166.

Lereclus, D., Agaisse, H., Gominet, M., Salamitou, S., and Sanchis, V. (1996). Identification of a *Bacillus thuringiensis* gene that positively regulates transcription of the phosphatidylinositol-specific phospholipase C gene at the onset of the stationary phase. Journal of Bacteriology *178*, 2749-2756.

Lereclus, D., Agaisse, H., Grandvalet, C., Salamitou, S., and Gominet, M. (2000). Regulation of toxin and virulence gene transcription in *Bacillus thuringiensis*. International Journal of Medical Microbiology *290*, 295-299.

Levine, J.H., Fontes, M.E., Dworkin, J., and Elowitz, M.B. (2012). Pulsed feedback defers cellular differentiation. PLoS biology *10*, e1001252.

Li, D., Xiao, Y., Hu, W., Xie, J., Bosmans, F., Tytgat, J., and Liang, S. (2003). Function and solution structure of hainantoxin-I, a novel insect sodium channel inhibitor from the Chinese bird spider Selenocosmia hainana1. FEBS letters *555*, 616-622.

Lindback, T., Fagerlund, A., Rodland, M.S., and Granum, P.E. (2004). Characterization of the *Bacillus cereus* Nhe enterotoxin. Microbiology *150*, 3959-3967.

López, D., Fischbach, M.A., Chu, F., Losick, R., and Kolter, R. (2009). Structurally diverse natural products that cause potassium leakage trigger multicellularity in *Bacillus subtilis*. Proceedings of the National Academy of Sciences *106*, 280-285.

Luecking, G., Dommel, M.K., Scherer, S., Fouet, A., and Ehling-Schulz, M. (2009). Cereulide synthesis in emetic *Bacillus cereus* is controlled by the transition state regulator AbrB, but not by the virulence regulator PlcR. Microbiology *155*, 922-931.

Lund, T., De Buyser, M.L., and Granum, P.E. (2000). A new cytotoxin from *Bacillus cereus* that may cause necrotic enteritis. Molecular microbiology *38*, 254-261.

Lund, T., and Granum, P.E. (1996). Characterisation of a non-haemolytic enterotoxin complex from *Bacillus cereus* isolated after a foodborne outbreak. FEMS Microbiology Letters *141*, 151-156.

Madgwick, P.J., and Waley, S.G. (1987). β-Lactamase I from *Bacillus cereus*. Structure and site-directed mutagenesis. Biochemical Journal *248*, 657-662.

Magnusson, M., Christiansson, A., and Svensson, B. (2007). *Bacillus cereus* spores during housing of dairy cows: Factors affecting contamination of raw milk. Journal of Dairy Science *90*, 2745-2754.

Mahler, H., Pasi, A., Kramer, J.M., Schulte, P., Scoging, A.C., Bar, W., and Krahenbuhl, S. (1997). Fulminant liver failure in association with the emetic toxin of *Bacillus cereus*. New England Journal of Medicine *336*, 1142-1148.

Manoharan, S. (2019). Addition of exogeneous PapR fails to activate the *plcR* regulon of *B. cereus* G9241 during growth at 37 °C [Unpublished].

Margulis, L., Jorgensen, J.Z., Dolan, S., Kolchinsky, R., Rainey, F.A., and Lo, S.C. (1998). The Arthromitus stage of *Bacillus cereus:* Intestinal symbionts of animals. Proceedings of the National Academy of Sciences of the United States of America *95*, 1236-1241.

Marston, C.K., Gee, J.E., Popovic, T., and Hoffmaster, A.R. (2006). Molecular approaches to identify and differentiate *Bacillus anthracis* from phenotypically similar *Bacillus* species isolates. BMC microbiology *6*, 22.

Marston, C.K., Ibrahim, H., Lee, P., Churchwell, G., Gumke, M., Stanek, D., Gee, J.E., Boyer, A.E., Gallegos-Candela, M., Barr, J.R., *et al.* (2016). Anthrax Toxin-Expressing *Bacillus cereus* Isolated from an Anthrax-Like Eschar. PLoS One *11*, e0156987.

Marxen, S., Stark, T.D., Rutschle, A., Lucking, G., Frenzel, E., Scherer, S., Ehling-Schulz, M., and Hofmann, T. (2015). Depsipeptide intermediates interrogate proposed biosynthesis of cereulide, the emetic toxin of *Bacillus cereus*. Sci Rep *5*, 10637.

McGregor, J.A., Lawellin, D., Franco-Buff, A., and Todd, J.K. (1991). Phospholipase C activity in microorganisms associated with reproductive tract infection. American Journal of Obstetrics and Gynecology *164*, 682-686.

Melly, E., Genest, P., Gilmore, M., Little, S., Popham, D., Driks, A., and Setlow, P. (2002). Analysis of the properties of spores of *Bacillus subtilis* prepared at different temperatures. Journal of applied microbiology *92*, 1105-1115.

Mignot, T., Mock, M., Robichon, D., Landier, A., Lereclus, D., and Fouet, A. (2001). The incompatibility between the PlcR- and AtxA-controlled regulons may have selected a nonsense mutation in *Bacillus anthracis*. Molecular Microbiology *42*, 1189-1198.

Miller, C.J., Elliott, J.L., and Collier, R.J. (1999). Anthrax Protective Antigen: Prepore-to-Pore Conversion. Biochemistry *38*, 10432-10441.

Minakhin, L., Semenova, E., Liu, J., Vasilov, A., Severinova, E., Gabisonia, T., Inman, R., Mushegian, A., and Severinov, K. (2005). Genome sequence and gene expression of *Bacillus anthracis* bacteriophage Fah. Journal of molecular biology *354*, 1-15.

Minett, F. (1950). Sporulation and viability of *B. anthracis* in relation to environmental temperature and humidity. Journal of comparative pathology *60*, 161-176.

Minett, F., and Dhanda, M. (1941). Multiplication of *B. anthracis* and Cl. chauvei in soil and water. Indian journal of veterinary science and animal husbandry *11*, 308-328.

Moayeri, M., Leppla, S.H., Vrentas, C., Pomerantsev, A.P., and Liu, S. (2015). Anthrax pathogenesis. Annual review of microbiology *69*, 185-208.

Molle, V., Fujita, M., Jensen, S.T., Eichenberger, P., González-Pastor, J.E., Liu, J.S., and Losick, R. (2003a). The Spo0A regulon of *Bacillus subtilis*. Molecular microbiology *50*, 1683-1701.

Molle, V., Nakaura, Y., Shivers, R.P., Yamaguchi, H., Losick, R., Fujita, Y., and Sonenshein, A.L. (2003b). Additional targets of the *Bacillus subtilis* global regulator CodY identified by chromatin immunoprecipitation and genome-wide transcript analysis. Journal of bacteriology *185*, 1911-1922.

Moriyama, R., Fukuoka, H., Miyata, S., Kudoh, S., Hattori, A., Kozuka, S., Yasuda, Y., Tochikubo, K., and Makino, S. (1999). Expression of a germination-specific amidase, SleB, of *Bacilli* in the forespore compartment of sporulating cells and its localization on the exterior side of the cortex in dormant spores. Journal of bacteriology *181*, 2373-2378.

Msadek, T., Dartois, V., Kunst, F., Herbaud, M.L., Denizot, F., and Rapoport, G. (1998). ClpP of *Bacillus subtilis* is required for competence development, motility, degradative enzyme synthesis, growth at high temperature and sporulation. Molecular microbiology *27*, 899-914.

Mukherjee, S., and Kearns, D.B. (2014). The structure and regulation of flagella in *Bacillus subtilis*. Annu Rev Genet *48*, 319-340.

Nakamura, L.K. (1998). *Bacillus pseudomycoides sp. nov*. International Journal of Systematic Bacteriology *48*, 1031-1035.

Ning, K., Fermin, D., and Nesvizhskii, A.I. (2012). Comparative Analysis of Different Label-Free Mass Spectrometry Based Protein Abundance Estimates and Their Correlation with RNA-Seq Gene Expression Data. Journal of Proteome Research *11*, 2261-2271.

Ochi, K., Kandala, J., and Freese, E. (1981). Initiation of *Bacillus subtilis* sporulation by the stringent response to partial amino acid deprivation. Journal of Biological Chemistry *256*, 6866-6875.

Oh, S.Y., Budzik, J.M., Garufi, G., and Schneewind, O. (2011). Two capsular polysaccharides enable *Bacillus cereus* G9241 to cause anthrax-like disease. Mol Microbiol *80*, 455-470.

Okegbe, C., Price-Whelan, A., and Dietrich, L.E. (2014). Redox-driven regulation of microbial community morphogenesis. Current opinion in microbiology *18*, 39-45.

Okinaka, R., Cloud, K., Hampton, O., Hoffmaster, A., Hill, K., Keim, P., Koehler, T., Lamke, G., Kumano, S., and Manter, D. (1999a). Sequence, assembly and analysis of pX01 and pX02. Journal of Applied Microbiology *87*, 261-262.

Okinaka, R., and Keim, P. (2016). The Bacterial Spore: from Molecules to Systems (ASM Press, Washington, DC.).

Okinaka, R., Pearson, T., and Keim, P. (2006). Anthrax, but not *Bacillus anthracis*? PLoS Pathog *2*, e122.

Okinaka, R.T., Cloud, K., Hampton, O., Hoffmaster, A.R., Hill, K.K., Keim, P., Koehler, T.M., Lamke, G., Kumano, S., Mahillon, J.*, et al.* (1999b). Sequence and organization of pXO1, the large *Bacillus anthracis* plasmid harboring the anthrax toxin genes. Journal of Bacteriology *181*, 6509-6515.

Økstad, O.A., Gominet, M., Purnelle, B., Rose, M., Lereclus, D., and Kolstø, A.-B. (1999). Sequence analysis of three *Bacillus cereus* loci carrying PlcR-regulated genes encoding degradative enzymes and enterotoxin. Microbiology *145*, 3129-3138.

Oliva, C., Turnbough, C.L., and Kearney, J.F. (2009). CD14-Mac-1 interactions in *Bacillus anthracis* spore internalization by macrophages. Proceedings of the National Academy of Sciences *106*, 13957-13962.

Oncu, S., Oncu, S., and Sakarya, S. (2003). Anthrax–an overview. Medical science monitor *9*, RA276-RA283.

Oppenheimer-Shaanan, Y., Wexselblatt, E., Katzhendler, J., Yavin, E., and Ben-Yehuda, S. (2011). c-di-AMP reports DNA integrity during sporulation in *Bacillus subtilis*. EMBO reports *12*, 594-601.

Panda, G., Tanwer, P., Ansari, S., Khare, D., and Bhatnagar, R. (2015). Regulation and RNA-binding properties of Hfq-like RNA chaperones in *Bacillus anthracis*. Biochimica et Biophysica Acta (BBA)-General Subjects *1850*, 1661-1668.

Pandey, A., and Palni, L.M.S. (1997). *Bacillus* species: The dominant bacteria of the rhizosphere of established tea bushes. Microbiological Research *152*, 359-365.

Park, J.M., Greten, F.R., Li, Z.-W., and Karin, M. (2002). Macrophage apoptosis by anthrax lethal factor through p38 MAP kinase inhibition. Science *297*, 2048-2051.

Passalacqua, K.D., Varadarajan, A., Byrd, B., and Bergman, N.H. (2009). Comparative transcriptional profiling of *Bacillus cereus* sensu lato strains during growth in CO_2-bicarbonate and aerobic atmospheres. PLoS One *4*, e4904.

Pena-Gonzalez, A., Marston, C.K., Rodriguez-R, L.M., Kolton, C.B., Garcia-Diaz, J., Theppote, A., Frace, M., Konstantinidis, K.T., and Hoffmaster, A.R. (2017). Draft genome sequence of *Bacillus cereus* LA2007, a human-pathogenic isolate harboring anthrax-like plasmids. Genome Announc *5*, e00181-00117.

Peng, J.-S., Tsai, W.-C., and Chou, C.-C. (2001). Surface characteristics of *Bacillus cereus* and its adhesion to stainless steel. International Journal of Food Microbiology *65*, 105-111.

Perego, M., Spiegelman, G., and Hoch, J. (1988). Structure of the gene for the transition state regulator, *abrB*: regulator synthesis is controlled by the *spo0A* sporulation gene in *Bacillus subtilis*. Molecular microbiology *2*, 689-699.

Perlak, F.J., Mendelsohn, C., and Thorne, C. (1979). Converting bacteriophage for sporulation and crystal formation in *Bacillus thuringiensis*. Journal of bacteriology *140*, 699-706.

Peterson, S.B., Dunn, A.K., Klimowicz, A.K., and Handelsman, J. (2006). Peptidoglycan from *Bacillus cereus* mediates commensalism with rhizosphere bacteria from the *Cytophaga-Flavobacterium* group. Applied and Environmental Microbiology *72*, 5421-5427.

Piggot, P.J., and Hilbert, D.W. (2004). Sporulation of *Bacillus subtilis*. Current Opinion in Microbiology *7*, 579-586.

Pomerantsev, A.P., Pomerantseva, O.M., Camp, A.S., Mukkamala, R., Goldman, S., and Leppla, S.H. (2009). PapR peptide maturation: role of the NprB protease in *Bacillus cereus* 569 PlcR/PapR global gene regulation. FEMS Immunol Med Microbiol *55*, 361-377.

Price, E., P. , Seymour, M., L. , Sarovich, D., S. , Latham, J., Wolken, S., R., Mason, J., Vincent, G., Drees, K., P. , Beckstrom-Sternberg, S., M. , Phillippy, A., M. *, et al.* (2012). Molecular Epidemiologic Investigation of an Anthrax Outbreak among Heroin Users, Europe. Emerging Infectious Disease journal *18*, 1307.

Ramarao, N., and Lereclus, D. (2005). The InhA1 metalloprotease allows spores of the *B. cereus* group to escape macrophages. Cellular microbiology *7*, 1357-1364.

Ramarao, N., and Lereclus, D. (2006). Adhesion and cytotoxicity of *Bacillus cereus* and *Bacillus thuringiensis* to epithelial cells are FlhA and PlcR dependent, respectively. Microbes and Infection *8*, 1483-1491.

Raymond, B., and Federici, B.A. (2017). In defence of *Bacillus thuringiensis*, the safest and most successful microbial insecticide available to humanity—a response to EFSA. FEMS microbiology ecology *93*, 84.

Read, T.D., Peterson, S.N., Tourasse, N., Baillie, L.W., Paulsen, I.T., Nelson, K.E., Tettelin, H., Fouts, D.E., Eisen, J.A., and Gill, S.R. (2003). The genome sequence of *Bacillus anthracis* Ames and comparison to closely related bacteria. Nature *423*, 81.

Rejasse, A., Gilois, N., Barbosa, I., Huillet, E., Bevilacqua, C., Tran, S., Ramarao, N., Stenfors Arnesen, L.P., and Sanchis, V. (2012). Temperature-dependent production of

various PlcR-controlled virulence factors in *Bacillus weihenstephanensis* strain KBAB4. Appl Environ Microbiol *78*, 2553-2561.

Remy, K.E., Qiu, P., Li, Y., Cui, X., and Eichacker, P.Q. (2013). *B. anthracis* associated cardiovascular dysfunction and shock: the potential contribution of both non-toxin and toxin components. BMC medicine *11*, 217.

Rice, L.B., Willey, S.H., Papanicolaou, G.A., Medeiros, A.A., Eliopoulos, G.M., Moellering, R.C., and Jacoby, G.A. (1990). Outbreak of ceftazidime resistance caused by extended-spectrum beta-lactamases at a Massachusetts chronic-care facility. Antimicrobial agents and chemotherapy *34*, 2193-2199.

Roh, J.Y., Choi, J.Y., Li, M.S., Jin, B.R., and Je, Y.H. (2007). *Bacillus thuringiensis* as a specific, safe, and effective tool for insect pest control. Journal of microbiology and biotechnology *17*, 547.

Ross, J.M. (1957). The pathogenesis of anthrax following the administration of spores by the respiratory route. The Journal of pathology and bacteriology *73*, 485-494.

Rowland, S.L., Burkholder, W.F., Cunningham, K.A., Maciejewski, M.W., Grossman, A.D., and King, G.F. (2004). Structure and mechanism of action of Sda, an inhibitor of the histidine kinases that regulate initiation of sporulation in *Bacillus subtilis*. Molecular cell *13*, 689-701.

Ruhfel, R.E., Robillard, N.J., and Thorne, C.B. (1984). Interspecies transduction of plasmids among *Bacillus anthracis, B. cereus*, and *B. thuringiensis*. Journal of bacteriology *157*, 708-711.

Ryter, A. (1965). Morphologic study of the sporulation of *Bacillus subtilis*. Paper presented at: Annales de l'Institut Pasteur.

Sacchi, C.T., Whitney, A.M., Mayer, L.W., Morey, R., Steigerwalt, A., Boras, A., Weyant, R.S., and Popovic, T. (2002). Sequencing of 16S rRNA gene: a rapid tool for identification of *Bacillus anthracis*. Emerging infectious diseases *8*, 1117.

Saile, E., and Koehler, T.M. (2006). *Bacillus anthracis* multiplication, persistence, and genetic exchange in the rhizosphere of grass plants. Appl Environ Microbiol *72*, 3168-3174.

Salamitou, S., Ramisse, F., Brehelin, M., Bourguet, D., Gilois, N., Gominet, M., Hernandez, E., and Lereclus, D. (2000). The *plcR* regulon is involved in the opportunistic properties of *Bacillus thuringiensis* and *Bacillus cereus* in mice and insects. Microbiology *146*, 2825-2832.

Sandle, T. (2014). The risk of *Bacillus cereus* to pharmaceutical manufacturing. American Pharmaceutical Review *17*, 56.

Sastalla, I., Fattah, R., Coppage, N., Nandy, P., Crown, D., Pomerantsev, A.P., and Leppla, S.H. (2013). The *Bacillus cereus* Hbl and Nhe tripartite enterotoxin components assemble sequentially on the surface of target cells and are not interchangeable. PLoS One *8*, e76955.

Sastalla, I., Maltese, L.M., Pomerantseva, O.M., Pomerantsev, A.P., Keane-Myers, A., and Leppla, S.H. (2010). Activation of the latent PlcR regulon in *Bacillus anthracis*. Microbiology *156*, 2982-2993.

Sazinas, P. (2016). The application of high-throughput sequencing to study the genome composition and transcriptional response of Haemophilus influenzae. Ph.D Thesis. (University of Warwick).

Scarff, J.M., Raynor, M.J., Seldina, Y.I., Ventura, C.L., Koehler, T.M., and O'Brien, A.D. (2016). The roles of AtxA orthologs in virulence of anthrax-like *Bacillus cereus* G9241. Mol Microbiol *102*, 545-561.

Scheldeman, P., Pil, A., Herman, L., De Vos, P., and Heyndrickx, M. (2005). Incidence and diversity of potentially highly heat-resistant spores isolated at dairy farms. Appl Environ Microbiol *71*, 1480-1494.

Schuch, R., and Fischetti, V.A. (2009). The secret life of the anthrax agent *Bacillus anthracis:* bacteriophage-mediated ecological adaptations. PloS one *4*, e6532.

Schultz, D., Wolynes, P.G., Jacob, E.B., and Onuchic, J.N. (2009). Deciding fate in adverse times: sporulation and competence in *Bacillus subtilis*. Proceedings of the National Academy of Sciences *106*, 21027-21034.

Schuster, H., Beyersmann, D., Mikolajczyk, M., and Schlicht, M. (1973). Prophage induction by high temperature in thermosensitive DNA mutants lysogenic for bacteriophage lambda. Journal of Virology *11*, 879-885.

Seldina, Y.I., Petro, C.D., Servetas, S.L., Vergis, J.M., Ventura, C.L., Merrell, D.S., and O'Brien, A.D. (2018). Certhrax is an antivirulence factor for the anthrax-like organism *Bacillus cereus* strain G9241. Infection and immunity *86*, e00207-00218.

Senesi, S., and Ghelardi, E. (2010). Production, secretion and biological activity of *Bacillus cereus* enterotoxins. Toxins (Basel) *2*, 1690-1703.

Shafikhani, S.H., and Leighton, T. (2004). AbrB and Spo0E control the proper timing of sporulation in *Bacillus subtilis*. Curr Microbiol *48*, 262-269.

Sierro, N., Makita, Y., de Hoon, M.J.L., and Nakai, K. (2008). DBTBS: a database of transcriptional regulation in Bacillus subtilis containing upstream intergenic conservation information. Nucleic Acids Res *36*, D93-96.

Simon, N.C., and Barbieri, J.T. (2014). *Bacillus cereus* Certhrax ADP-ribosylates vinculin to disrupt focal adhesion complexes and cell adhesion. Journal of Biological Chemistry *289*, 10650-10659.

Sirard, J.-C., Guidi-Rontani, C., Fouet, A., and Mock, M. (2000). Characterization of a plasmid region involved in *Bacillus anthracis* toxin production and pathogenesis. International journal of medical microbiology *290*, 313-316.

Sirard, J.-C., Mock, M., and Fouet, A. (1994). The three *Bacillus anthracis* toxin genes are coordinately regulated by bicarbonate and temperature. Journal of Bacteriology *176*, 5188-5192.

Slamti, L., Lemy, C., Henry, C., Guillot, A., Huillet, E., and Lereclus, D. (2015). CodY regulates the activity of the virulence quorum sensor PlcR by controlling the import of the signaling peptide PapR in *Bacillus thuringiensis*. Front Microbiol *6*, 1501.

Slamti, L., and Lereclus, D. (2002). A cell-cell signaling peptide activates the PlcR virulence regulon in bacteria of the *Bacillus cereus* group. Embo Journal *21*, 4550-4559.

Slamti, L., and Lereclus, D. (2005). Specificity and polymorphism of the PlcR-PapR quorum-sensing system in the *Bacillus cereus* group. J Bacteriol *187*, 1182-1187.

Slamti, L., Perchat, S., Gominet, M., Vilas-Bôas, G., Fouet, A., Mock, M., Sanchis, V., Chaufaux, J., Gohar, M., and Lereclus, D. (2004). Distinct mutations in PlcR explain why some strains of the *Bacillus cereus* group are nonhemolytic. Journal of bacteriology *186*, 3531-3538.

Sonenshein, A.L. (2005). CodY, a global regulator of stationary phase and virulence in Gram-positive bacteria. Current opinion in microbiology *8*, 203-207.

Sonenshein, A.L. (2007). Control of key metabolic intersections in *Bacillus subtilis*. Nature Reviews Microbiology *5*, 917.

Sozhamannan, S., Chute, M.D., McAfee, F.D., Fouts, D.E., Akmal, A., Galloway, D.R., Mateczun, A., Baillie, L.W., and Read, T.D. (2006). The *Bacillus anthracis* chromosome contains four conserved, excision-proficient, putative prophages. BMC microbiology *6*, 34.

Steggles, J.R., Wang, J., and Ellar, D.J. (2006). Discovery of *Bacillus thuringiensis* virulence genes using signature-tagged mutagenesis in an insect model of septicaemia. Current microbiology *53*, 303-310.

Stenfors Arnesen, L.P., Fagerlund, A., and Granum, P.E. (2008). From soil to gut: *Bacillus cereus* and its food poisoning toxins. FEMS microbiology reviews *32*, 579-606.

Stenfors Arnesen, L.P., O'Sullivan, K., and Granum, P.E. (2007). Food poisoning potential of *Bacillus cereus* strains from Norwegian dairies. International Journal of Food Microbiology *116*, 292-296.

Stenfors, L.P., and Granum, P.E. (2001). Psychrotolerant species from the *Bacillus cereus* group are not necessarily *Bacillus weihenstephanensis*. FEMS Microbiology Letters *197*, 223-228.

Stephenson, K., and Hoch, J.A. (2001). PAS-A domain of phosphorelay sensor kinase A: a catalytic ATP-binding domain involved in the initiation of development in *Bacillus subtilis*. Proceedings of the National Academy of Sciences *98*, 15251-15256.

Stephenson, S., Mueller, C., Jiang, M., and Perego, M. (2003). Molecular analysis of Phr peptide processing in *Bacillus subtilis*. Journal of bacteriology *185*, 4861-4871.

Stiube, P., and Dimitriu, C. (1969). Electron microscopic studies of mesophilic and psychrophilic *cereus-anthracis-mycoides* (CAM) bacteriophages. Archives roumaines de pathologie experimentales et de microbiologie *28*, 809-821.

Stranzl, G.R., Santelli, E., Bankston, L.A., La Clair, C., Bobkov, A., Schwarzenbacher, R., Godzik, A., Perego, M., Grynberg, M., and Liddington, R.C. (2011). Structural insights into inhibition of *Bacillus anthracis* sporulation by a novel class of non-heme globin sensor domains. J Biol Chem *286*, 8448-8458.

Stratford, J.P., Woodley, M.A., and Park, S. (2013). Variation in the morphology of *Bacillus mycoides* due to applied force and substrate structure. PLoS One *8*, e81549.

Swiecicka, I., and Mahillon, J. (2006). Diversity of commensal *Bacillus cereus* sensu lato isolated from the common sow bug (*Porcellio scaber, Isopoda*). FEMS microbiology ecology *56*, 132-140.

Swiecicka, I., Van der Auwera, G.A., and Mahillon, J. (2006). Hemolytic and nonhemolytic enterotoxin genes are broadly distributed among *Bacillus thuringiensis* isolated from wild mammals. Microbial ecology *52*, 544-551.

Tan, I.S., and Ramamurthi, K.S. (2014). Spore formation in *Bacillus subtilis*. Environmental microbiology reports *6*, 212-225.

Thorne, C.B. (1968). Transducing bacteriophage for *Bacillus cereus*. Journal of virology *2*, 657-662.

Thorsen, L., Hansen, B.M., Nielsen, K.F., Hendriksen, N.B., Phipps, R.K., and Budde, B.B. (2006). Characterization of emetic *Bacillus weihenstephanensis,* a new cereulide-producing bacterium. Appl Environ Microbiol *72*, 5118-5121.

Titball, R., Turnbull, P., and Hutson, R. (1991). The monitoring and detection of *Bacillus anthracis* in the environment. Journal of applied bacteriology *70*, 9S-18S.

Tojo, S., Hirooka, K., and Fujita, Y. (2013). Expression of *kinA* and *kinB* of *Bacillus subtilis*, necessary for sporulation initiation, is under positive stringent transcription control. Journal of bacteriology *195*, 1656-1665.

Tokman, J.I., Kent, D.J., Wiedmann, M., and Denes, T. (2016). Temperature significantly affects the plaquing and adsorption efficiencies of *Listeria* phages. Frontiers in microbiology *7*, 631.

Tonello, F., and Zornetta, I. (2012). *Bacillus anthracis* factors for phagosomal escape. Toxins *4*, 536-553.

Tsvetanova, B., Wilson, A.C., Bongiorni, C., Chiang, C., Hoch, J.A., and Perego, M. (2007). Opposing effects of histidine phosphorylation regulate the AtxA virulence transcription factor in *Bacillus anthracis*. Molecular microbiology *63*, 644-655.

Uchida, I., Hornung, J.M., Thorne, C.B., Klimpel, K.R., and Leppla, S.H. (1993). Cloning and characterization of a gene whose product is a transactivator of anthrax toxin synthesis. Journal of Bacteriology *175*, 5329-5338.

Uchida, I., Makino, S., Sekizaki, T., and Terakado, N. (1997). Cross-talk to the genes for *Bacillus anthracis* capsule synthesis by *atxA*, the gene encoding the trans-activator of anthrax toxin synthesis. Molecular Microbiology *23*, 1229-1240.

Valentin-Hansen, P., Eriksen, M., and Udesen, C. (2004). MicroReview: The bacterial Sm-like protein Hfq: a key player in RNA transactions. Molecular microbiology *51*, 1525-1533.

Van Ness, G.B. (1971). Ecology of anthrax. Science *172*, 1303-1307.

van Schaik, W., Chateau, A., Dillies, M.A., Coppee, J.Y., Sonenshein, A.L., and Fouet, A. (2009). The global regulator CodY regulates toxin gene expression in *Bacillus anthracis* and is required for full virulence. Infect Immun *77*, 4437-4445.

van Sorge, N.M., Ebrahimi, C.M., McGillivray, S.M., Quach, D., Sabet, M., Guiney, D.G., and Doran, K.S. (2008). Anthrax toxins inhibit neutrophil signaling pathways in brain endothelium and contribute to the pathogenesis of meningitis. PloS one *3*, e2964.

Vasil'eva, V. (1958). Soil bacteria as antagonists of anthrax *Bacilli*. Sborn Nauch Tr L'vov Zootekh Vet Inst *9*, 149-153.

Vera, T., Grumbles, L., Franklin, T., and Jungerman, P. (1968). Effect of lysogenicity on the virulence of *Bacillus anthracis*. American journal of veterinary research *29*, 1059-1066.

Vilain, S., Luo, Y., Hildreth, M.B., and Brozel, V.S. (2006). Analysis of the life cycle of the soil saprophyte *Bacillus cereus* in liquid soil extract and in soil. Appl Environ Microbiol *72*, 4970-4977.

Villafane, R., Bechhofer, D., Narayanan, C., and Dubnau, D. (1987). Replication control genes of plasmid pE194. Journal of bacteriology *169*, 4822-4829.

Visschedyk, D., Rochon, A., Tempel, W., Dimov, S., Park, H.W., and Merrill, A.R. (2012). Certhrax toxin, an anthrax-related ADP-ribosyltransferase from *Bacillus cereus*. J Biol Chem *287*, 41089-41102.

Von Stetten, F., Mayr, R., and Scherer, S. (1999). Climatic influence on mesophilic *Bacillus cereus* and psychrotolerant *Bacillus weihenstephanensis* populations in tropical, temperate and alpine soil. Environmental Microbiology *1*, 503-515.

Vörös, A., Simm, R., Slamti, L., McKay, M.J., Hegna, I.K., Nielsen-LeRoux, C., Hassan, K.A., Paulsen, I.T., Lereclus, D., and Økstad, O.A. (2014). SecDF as part of the Sec-translocase facilitates efficient secretion of *Bacillus cereus* toxins and cell wall-associated proteins. PLoS One *9*, e103326.

Weinbauer, M.G. (2004). Ecology of prokaryotic viruses. FEMS microbiology reviews *28*, 127-181.

Wheelis, M. (1998). First shots fired in biological warfare. Nature *395*, 213.

White, A.K., Hoch, J.A., Grynberg, M., Godzik, A., and Perego, M. (2006). Sensor domains encoded in *Bacillus anthracis* virulence plasmids prevent sporulation by hijacking a sporulation sensor histidine kinase. J Bacteriol *188*, 6354-6360.

Wilson, M.K., Vergis, J.M., Alem, F., Palmer, J.R., Keane-Myers, A.M., Brahmbhatt, T.N., Ventura, C.L., and O'Brien, A.D. (2011). *Bacillus cereus* G9241 makes anthrax toxin and capsule like highly virulent *B. anthracis* Ames but behaves like attenuated toxigenic nonencapsulated *B. anthracis* Sterne in rabbits and mice. Infect Immun *79*, 3012-3019.

Wintzingerode, F.V., Goebel, U.B., and Stackebrandt, E. (1997). Determination of microbial diversity in environmental samples: Pitfalls of PCR-based rRNA analysis. FEMS Microbiology Reviews *21*, 213-229.

Wootton, M. (2015). BSAC Methods for Antimicrobial Susceptibility Testing, T.B.S.f.A. Chemotherapy, ed.

Wright, A.M., Beres, S.B., Consamus, E.N., Long, S.W., Flores, A.R., Barrios, R., Richter, G.S., Oh, S.Y., Garufi, G., Maier, H.*, et al.* (2011). Rapidly Progressive, Fatal, Inhalation Anthrax-like Infection in a Human: Case Report, Pathogen Genome Sequencing, Pathology, and Coordinated Response. Archives of Pathology & Laboratory Medicine *135*, 1447-1459.

Wu, L.J., and Errington, J. (2003). RacA and the Soj-Spo0J system combine to effect polar chromosome segregation in sporulating *Bacillus subtilis*. Molecular microbiology *49*, 1463-1475.

Wu, R., Gu, M., Wilton, R., Babnigg, G., Kim, Y., Pokkuluri, P.R., Szurmant, H., Joachimiak, A., and Schiffer, M. (2013). Insight into the sporulation phosphorelay: crystal structure of the sensor domain of *Bacillus subtilis* histidine kinase, KinD. Protein science : a publication of the Protein Society *22*, 564-576.

Yepes, A., Schneider, J., Mielich, B., Koch, G., García-Betancur, J.C., Ramamurthi, K.S., Vlamakis, H., and López, D. (2012). The biofilm formation defect of a *Bacillus subtilis* flotillin-defective mutant involves the protease FtsH. Molecular microbiology *86*, 457-471.

Yuan, Y., Gao, M., Peng, Q., Wu, D., Liu, P., and Wu, Y. (2014). Genomic analysis of a phage and prophage from a *Bacillus thuringiensis* strain. Journal of General Virology *95*, 751-761.

Zhou, B., Wirsching, P., and Janda, K.D. (2002). Human antibodies against spores of the genus *Bacillus*: a model study for detection of and protection against anthrax and the bioterrorist threat. Proceedings of the National Academy of Sciences *99*, 5241-5246.

Zimmermann, F., Köhler, S.M., Nowak, K., Dupke, S., Barduhn, A., Düx, A., Lang, A., De Nys, H.M., Gogarten, J.F., and Grunow, R. (2017). Low antibody prevalence against *Bacillus cereus* biovar anthracis in Taï National Park, Côte d'Ivoire, indicates high rate of lethal infections in wildlife. PLoS neglected tropical diseases *11*, e0005960.

8. Appendices

8.1. Comparative proteomics

8.1.1. Secretome – Exponential Phase Growth

Table.8.1. Proteins higher at 25 °C compared to 37 °C in the secretome of *B. cereus* G9241 during exponential growth.

Log2-Fold Change	Protein	Gene Loci (AQ16_)
6.461304188	Haemolytic enterotoxin family protein	4931

5.889979298	Haemolytic enterotoxin family protein	658
5.67163978	Haemolysin BL-binding component (HblA)	4932
4.416119745	Collagenase family protein	1941
4.311992764	Extracellular ribonuclease (Bsn)	4754
3.985087047	Haemolysin BL-binding component (HblA)	4933
3.937641362	Haemolytic enterotoxin family protein	660
3.840358242	Thermolysin metallopeptidase, catalytic domain protein	5317
3.776604672	Haemolytic enterotoxin family protein	659
3.570677872	Haemolytic enterotoxin family protein	4930
3.204744637	Phospholipase C (Plc)	1823
2.696128577	Leukotoxin (CytK)	1392
2.498550137	THUMP domain protein	931
2.435173353	Probable butyrate kinase (Buk)	3880
2.421052823	DEAD-box ATP-dependent RNA helicase (CshA)	2258
2.315771441	N-acetylmuramoyl-L-alanine amidase family protein	1574
2.249887238	M6 family metalloprotease domain protein	1827
2.213554929	Transglutaminase-like superfamily protein	1487
2.188925048	30S ribosomal protein S4 (RpsD)	3343
2.176348209	Subtilase family protein	4301
2.119378805	Aspartate ammonia-lyase (AspA)	729
2.1121632	Thiol-activated cytolysin family protein	4769
2.084093571	Ribonuclease R (Rnr)	2887
1.996190468	Ornithine aminotransferase (RocD)	1349
1.93416218	GTPase Obg (CgtA)	3582
1.932947109	Transglutaminase-like superfamily protein	531
1.788129052	UDP-N-acetylmuramoyl-tripeptide--D-alanyl-D-alanine ligase (MurF)	2259
1.732289871	Uncharacterized protein	4251
1.556266546	LPXTG cell wall anchor domain protein	1597
1.541603724	Ribosome-binding ATPase (YchF)	2544
1.540734351	Acetate kinase (AckA)	3361
1.476639728	Formate acetyltransferase (PflB)	2025
1.436757177	30S ribosomal protein S8 (RpsH)	2380

Table.8.2. Proteins higher at 37 °C compared to 25 °C in the secretome of *B. cereus* G9241 during exponential growth.

Log2-Fold Change	Protein	Gene Loci (AQ16_)
5.270403147	Phage family protein (Gp49)	5822
4.965080182	Putative phage major capsid protein (Gp34)	5824
4.531369964	Prophage minor structural protein	5836
4.322101479	Putative gp14-like protein (Gp14)	5832
4.31904606	N-acetylmuramoyl-L-alanine amidase family protein	5839
3.658805609	Phage tail family protein	5835
3.409561182	Putative major capsid protein (GpP)	5831
2.898699363	Uncharacterized protein	5823
2.357575151	WxL domain surface cell wall-binding family protein	3215
2.339542329	WxL domain surface cell wall-binding family protein	3217
2.334489187	Phage antirepressor KilAC domain protein	5855
2.302981059	Dihydropteroate synthase (FolP)	2448
2.193649848	Zinc-binding dehydrogenase family protein	318
2.067646305	WxL domain surface cell wall-binding family protein	3218
1.947421789	Toxic anion resistance family protein	2068
1.891851823	60 kDa chaperonin (GroL)	2222
1.850107829	Putative lipid kinase (BmrU)	3165
1.765464465	Chitin binding protein CBP21 (Cbp)	5228
1.761660407	10 kDa chaperonin (GroS)	2223
1.683429543	Protein (GrpE)	3713
1.628313551	3D domain protein	4315
1.534492905	Uncharacterized protein	5849
1.482365449	Stress response protein SCP2 (YceC)	2073
1.448414008	Transcription elongation factor (GreA)	3644
1.437396049	L-asparaginase, type I family protein	4939

8.1.2. Secretome – Stationary Phase Growth

Table.8.3. Proteins higher at 25 °C compared to 37 °C in the secretome of *B. cereus* G9241 during stationary phase growth.

Log2-Fold Change	Protein	Gene Loci (AQ16_)
13.67425426	Pheromone binding protein	1306
10.46753685	Collagenase family protein	4546
10.44560647	Peptide ABC transporter substrate-binding protein	2309
9.92237854	Chitinase A1	2089
9.390093327	Peptide ABC transporter substrate-binding protein	1312
9.288374821	Glucanase	5335
8.651034037	FtsN Cell division protein	1209
8.540471156	Oligopeptide ABC transporter, oligopeptide-binding protein	1842
7.821544468	Neutral protease B	2938
7.753190637	Aminopeptidase	2662
7.638925453	Uncharacterized protein	5768
7.283205122	Chitin binding protein CBP21	5228
7.112490555	Chitinase A	4342
7.057614883	DppE Dipeptide-binding protein	2310
6.654506539	2-methylcitrate dehydratase	242
6.515860995	M6 family metalloprotease domain protein	1827
6.470729311	Fungalysin metallopeptidase family protein	369
6.46897471	Zinc-binding dehydrogenase family protein	1825
6.417500367	Bacillolysin	1902
6.37035202	Bacterial extracellular solute-binding s, 5 Middle family protein	4481
6.056341012	Matrixin family protein	4915
5.944121813	5-methyltetrahydropteroyltriglutamate--homocysteine methyltransferase	4042
5.20986263	Phosphoenolpyruvate carboxykinase [ATP]	3226
5.207335768	S-layer protein	1583
5.102285929	Oligopeptidase	1152
5.075511793	Uncharacterized protein	1559
4.984163438	Arginase	2338
4.911012088	DNA protection during starvation protein 1	512

4.814951768	Bacterial extracellular solute-binding s, 5 Middle family protein	496
4.725935181	M6 family metalloprotease domain protein	5047
4.605835279	Nucleoside diphosphate kinase	976
4.588642781	Uncharacterized protein	74
4.530639898	Collagenase family protein	1941
4.49458229	Haemolysin BL lytic component L1	4930
4.432966659	Urocanate hydratase	4415
4.418860336	(NheA) Non-hemolytic enterotoxin lytic component L2	660
4.410473978	5-nucleotidase, lipoprotein e(P4) family	3491
4.304110895	NLP/P60 family protein	5203
4.207248489	Flagellin	828
4.137116631	Probable glycine dehydrogenase (decarboxylating) subunit 1	3802
4.036815643	Probable glycine dehydrogenase (decarboxylating) subunit 2	3803
3.891310891	2-(Hydroxymethyl)glutarate dehydrogenase	239
3.840016539	4-hydroxyphenylpyruvate dioxygenase	2265
3.713575919	Alanine dehydrogenase	1909
3.649474204	Peptidase M20/M25/M40 family protein	3296
3.627889673	ATP synthase gamma chain	2713
3.490279496	Phospholipase C	1823
3.405557175	Alanine dehydrogenase	3375
3.371960024	Acetyl-CoA acetyltransferase	4021
3.295967023	Dihydrolipoyl dehydrogenase	3881
3.175309201	Flagellin	829
3.146744569	Acetyl-CoA C-acyltransferase family protein	2675
3.145316919	SipW-cognate class signal peptide domain protein	1211
3.104189495	Flagellin	830
3.095020771	Sulfatase family protein	5100
3.086110651	Putative aminopeptidase ysdC	3433
3.079984502	Deblocking aminopeptidase	1575
3.069181586	Oligoendopeptidase F	2567
3.028406858	Phosphate butyryltransferase	3878
2.964806805	Formate--tetrahydrofolate ligase	
2.9229514	LPXTG cell wall anchor domain protein	1597
2.896616191	Flagellin	827
2.858923674	Peptidase T	4324
2.827479648	2-oxoisovalerate dehydrogenase subunit alpha	3882

2.685727278	2-methylisocitrate lyase	241
2.609927466	TerD domain protein	2071
2.596480221	Thermophilic metalloprotease family protein	2148
2.571034729	ATP synthase subunit beta	2714
2.563262284	Purine nucleoside phosphorylase	3955
2.516609679	Immune inhibitor A	1206
2.482111399	Probable cytosol aminopeptidase	3055
2.477294008	LPXTG cell wall anchor domain protein	3919
2.445685287	Uncharacterized protein	3833
2.412743618	(HblA) Hemolysin BL-binding component	4932
2.378135443	NADH dehydrogenase-like protein yjlD	2911
2.315944477	2-oxoisovalerate dehydrogenase subunit beta	3883
2.233669482	ATP synthase subunit alpha	2712
2.226159811	Pyridoxal phosphate-dependent acyltransferase family protein	1883
2.200028658	Electron transfer flavodomain protein	3478
2.072163453	Uncharacterized protein	1557
2.030131539	Chitin binding domain protein	5259
2.001212915	S-layer protein sap	1584
1.992105166	Uncharacterized protein	4789
1.960299373	Thermophilic metalloprotease family protein	3314
1.951483329	Glyoxalase/Bleomycin resistance /Dioxygenase superfamily protein	3354
1.918800155	Uncharacterized protein	642
1.858562443	Thiol-activated cytolysin family protein	4769
1.845422111	Adenylosuccinate synthetase	2552
1.844588617	Putative heme-dependent peroxidase AQ16_2633	2633
1.674663266	Putative nucleic acid binding OB-fold tRNA/helicase-type	1808
1.672127247	Electron transfer flavodomain protein	3479
1.624946979	Purine nucleoside phosphorylase DeoD-type	1029
1.62197455	1-pyrroline-5-carboxylate dehydrogenase	2169
1.597129663	Thioredoxin	3480
1.535931786	Pyridoxal 5-phosphate synthase subunit PdxS	2514
1.475134869	Glutamine--fructose-6-phosphate aminotransferase [isomerizing]	2334
1.468244871	Methylmalonate semialdehyde dehydrogenase [acylating]	238
1.285952687	Leucine dehydrogenase	3879

Table.8.4. Proteins higher at 37 °C compared to 25 °C in the secretome of *B. cereus* G9241 during stationary phase growth.

Log2-Fold Change	Protein	Gene Loci (AQ16_)
11.58175596	Peptidoglycan endopeptidase	576
10.9609429	Enterotoxin	1683
9.151043256	N-acetylmuramoyl-L-alanine amidase	2823
8.995394309	Cell wall hydrolase	2783
8.390513738	Enterotoxin	2777
7.902417183	Elongation factor Ts	4224
7.676326195	Trigger factor	3550
7.60319225	50S ribosomal protein L11	2407
7.556121747	Enoyl-[acyl-carrier-protein] reductase [NADH]	1275
7.428866227	50S ribosomal protein L6	2379
7.369898319	50S ribosomal protein L10	2405
7.114146312	50S ribosomal protein L1	2406
7.005558451	WxL domain surface cell wall-binding family protein	3215
6.995487173	50S ribosomal protein L17	2366
6.958193103	30S ribosomal protein S7	2398
6.767446876	3D domain protein	1815
6.66465958	50S ribosomal protein L14	2384
6.471577565	Glyceraldehyde-3-phosphate dehydrogenase	2877
6.460992217	30S ribosomal protein S3	2388
6.434344331	50S ribosomal protein L7/L12	2404
6.306999902	30S ribosomal protein S13	2369
6.155244629	50S ribosomal protein L3	2394
5.957626184	L,D-transpeptidase catalytic domain protein	2947
5.940161516	Pyrimidine-nucleoside phosphorylase	650
5.853178819	Ribosome-recycling factor	4226
5.833424608	Peptidase M23 family protein	1060
5.798904578	Fructose-1,6-bisphosphate aldolase, class II	2684
5.673025409	3-oxoacyl-[acyl-carrier-protein]	4515
5.657619782	Penicillin binding transpeptidase domain protein	3753
5.646173875	30S ribosomal protein S2	4223
5.633604552	Polysaccharide deacetylase family protein	5106
5.597603599	Phosphoenolpyruvate-protein phosphotransferase	3995

5.534719785	Dihydrolipoamide acetyltransferase component of pyruvate dehydrogenase complex	4080
5.482430935	FeS assembly protein SufB	2999
5.403589716	Phosphoglucosamine mutase	2335
5.353002985	50S ribosomal protein L24	2383
5.340333263	Pyruvate dehydrogenase (Acetyl-transferring) E1 component, alpha subunit	4078
5.292134479	DNA polymerase III subunit beta	5347
5.276771396	Transcription termination/antitermination protein NusA	4234
5.243302623	30S ribosomal protein S10	2395
5.226336529	Transglutaminase-like superfamily protein	531
5.223149717	Chaperone protein DnaK	3714
5.173308134	FeS assembly protein SufD	2996
5.131014473	FeS assembly ATPase SufC	2995
5.084453384	Inosine-5-monophosphate dehydrogenase	2516
5.036522349	Hypoxanthine phosphoribosyltransferase	2456
5.009496311	30S ribosomal protein S15	4242
5.000770807	GTP-sensing transcriptional pleiotropic repressor CodY	4222
4.968295897	Type I phosphodiesterase / nucleotide pyrophosphatase family protein	1073
4.908828715	50S ribosomal protein L19	4210
4.785270546	Lysine--tRNA ligase	2443
4.766001991	30S ribosomal protein S9	2360
4.756134431	50S ribosomal protein L22	2389
4.74253577	30S ribosomal protein S5	2377
4.724000255	CTP synthase	2681
4.713088989	50S ribosomal protein L21	3578
4.709088812	3-oxoacyl-[acyl-carrier-protein] synthase 2	1317
4.664169773	Glucokinase	3763
4.639016054	UDP-N-acetylglucosamine 1-carboxyvinyltransferase	2732
4.631363273	50S ribosomal protein L2	4211
4.620172183	Glucose-specific phosphotransferase enzyme IIA component	2700
4.605668336	30S ribosomal protein S8	2380
4.604813416	Fructose-1,6-bisphosphatase	3017
4.54952544	Translation initiation factor IF-3	3429
4.525606645	Glutamate dehydrogenase	1001
4.487101555	50S ribosomal protein L27	3580

4.447480748	Adenylate kinase	2373
4.414413979	3D domain protein	4351
4.388995723	Translation initiation factor IF-2	4236
4.385148138	Probable thiol peroxidase	
4.385136783	30S ribosomal protein S11	2368
4.383201579	50S ribosomal protein L18	2378
4.349538942	4-hydroxy-3-methylbut-2-en-1-yl diphosphate synthase (flavodoxin)	3747
4.31619823	Glycerophosphoryl diester phosphodiesterase family protein	4572
4.287320822	Elongation factor G	2397
4.284348528	Glutamyl-tRNA(Gln) amidotransferase subunit A	2157
4.273912847	30S ribosomal protein S16	4223
4.254251029	1,4-dihydroxy-2-naphthoyl-CoA synthase	3129
4.250771403	GTP-binding protein TypA/BipA	4095
4.211242189	50S ribosomal protein L20	3431
4.18037955	30S ribosomal protein S6	2545
4.137722373	Cell envelope-related function transcriptional attenuator common domain protein	553
4.12587593	30S ribosomal protein S17	2385
4.122030874	Serine--tRNA ligase	2512
4.06681474	Peptide chain release factor 1	2690
3.990569105	50S ribosomal protein L29	2386
3.963001321	50S ribosomal protein L15	2375
3.945359528	Ribonuclease J	4073
3.934632401	30S ribosomal protein S18	2547
3.924547985	Beta-channel forming cytolysin family protein	4553
3.908191284	30S ribosomal protein S4	3343
3.901696702	UDP-N-acetylglucosamine 2-epimerase	2749/2818
3.851283848	Cell division protein FtsZ	4144
3.811615467	Phage family protein	5822
3.806519995	Aspartate ammonia-lyase	1893
3.801692804	Short chain dehydrogenase family protein	565
3.761061703	Thioredoxin reductase	2858
3.745505383	50S ribosomal protein L23	2392
3.714892725	50S ribosomal protein L4	2393
3.711977303	Pyruvate kinase	4735
3.68884221	50S ribosomal protein L13	2361

3.645166198	UDP-N-acetylmuramoylalanine--D-glutamate ligase	4138
3.606019775	Uncharacterized protein	5836
3.6054643	Malic enzyme, NAD binding domain protein	3400
3.604360501	DNA-directed RNA polymerase subunit beta	2402
3.589906931	Glutamate-1-semialdehyde 2,1-aminomutase	3562
3.579686808	Uncharacterized protein	993
3.572119425	Leucine--tRNA ligase	3254
3.534355323	Transcription elongation factor GreA	3644
3.529591759	4-hydroxy-tetrahydrodipicolinate synthase	5222
3.516013841	Arginine--tRNA ligase	2656
3.508872916	Transglutaminase-like superfamily protein	1487
3.505426278	DEAD-box ATP-dependent RNA helicase CshA	2259
3.504386206	Asparagine--tRNA ligase	723
3.470430404	ATP-dependent Clp protease ATP-binding subunit ClpX	3551
3.454301894	LPXTG cell wall anchor domain protein	4818
3.401266992	Acetate kinase	3361
3.400178313	Phenylalanine--tRNA ligase beta subunit	3442
3.389187694	Acetyl-CoA carboxylase, biotin carboxylase subunit	3848
3.36103948	Transketolase	4678
3.353117307	S-adenosylmethionine synthase	3227
3.332959374	Putative tRNA binding domain protein	3300
3.328464662	D-alanine--D-alanine ligase	
3.311315477	5-methylthioadenosine/S-adenosylhomocysteine nucleosidase	5184
3.307510356	3-oxoacyl-[acyl-carrier-protein] synthase 3	1318
3.288503091	N-acetylmuramoyl-L-alanine amidase family protein	4391
3.220897834	Tyrosine--tRNA ligase	3339
3.210694949	Ribonucleoside-diphosphate reductase	1137
3.209984104	FMN-dependent NADH-azoreductase	2611
3.157040715	33 kDa chaperonin	2453
3.133148114	30S ribosomal protein S12	2399
3.128855973	Pyruvate dehydrogenase 1 component subunit beta	4079
3.118302088	ABC transporter family protein	5099
3.113709986	Uracil phosphoribosyltransferase	2705
3.112314979	UPF0234 protein AQ16_1339	1339
3.056874474	Cell envelope-related function transcriptional attenuator common domain protein	1694
3.050618609	L-lactate dehydrogenase	3879

3.046781659	Isoleucine--tRNA ligase	370
3.040917436	Alanine--tRNA ligase	3635
3.04014121	Putative major capsid protein gpP	5831
3.037267327	Acetyl-CoA carboxylase, biotin carboxyl carrier protein	3847
3.018522906	DNA-directed RNA polymerase subunit beta	2401
2.998457968	Glutamate-1-semialdehyde 2,1-aminomutase	2004
2.987741033	Cysteine synthase	5597
2.9812422	Methionine--tRNA ligase	2943
2.970919132	50S ribosomal protein L9	2550
2.947868625	N-acetylmuramoyl-L-alanine amidase family protein	1574
2.943714182	Cell division ATP-binding protein Fts	2831
2.937586705	3D domain protein	5075
2.912907759	30S ribosomal protein S19	2390
2.902529955	VanW like family protein	4535
2.896939715	Uncharacterized protein	2912
2.861613492	GMP synthase [glutamine-hydrolyzing]	2221
2.854743242	DNA-binding protein HU	981
2.837993344	Aldo/keto reductase family protein	2308
2.815370043	Serine hydroxymethyltransferase	
2.815276667	Putative gp14-like protein	5832
2.788201511	50S ribosomal protein L16	2387
2.784653982	Adenine phosphoribosyltransferase	3615
2.783261051	Ribonuclease J	4260
2.781079451	Aspartate--tRNA(Asn) ligase	3620
2.759492834	Plasmid replication protein repX	5817
2.75190258	Type III pantothenate kinase	2454
2.746869261	Type I phosphodiesterase / nucleotide pyrophosphatase family protein	2785
2.71263663	Aldose 1-epimerase family protein	894
2.685643037	Phage tail family protein	5835
2.661474148	Efflux transporter, RND family, MFP subunit	1680
2.631472588	Pyruvate carboxylase	4104
2.599970897	Aspartyl/glutamyl-tRNA(Asn/Gln) amidotransferase subunit B	2156
2.598440925	UTP--glucose-1-phosphate uridylyltransferase	2617
2.562345147	Lipoyl synthase	3007
2.537789504	DNA-binding protein HU	4339
2.519305905	N-acetylmuramoyl-L-alanine amidase family protein	5839

2.494948227	Triosephosphate isomerase	2879
2.476218525	Protein Grp	3713
2.473844051	Polysaccharide deacetylase family protein	549
2.465330203	Cysteine--tRNA ligase	2414
2.462865392	Adenylosuccinate lyase	2187
2.427301129	Peptidyl-prolyl cis-trans isomerase	3981
2.400987426	Probable transcriptional regulatory protein AQ16_1976	1976
2.37643671	FAD dependent oxidoreductase family protein	3051
2.345564842	Acetyltransferase domain protein	1918
2.338821938	Aspartate-semialdehyde dehydrogenase	167
2.32703503	YmdB-like family protein	4279
2.264272928	Proline--tRNA ligase	4231
2.254182537	Uncharacterized protein	4954
2.251788855	Probable tRNA sulfurtransferase	3351
2.23072206	Superoxide dismutase	3751
2.229095856	Isocitrate dehydrogenase [NADP]	3410
2.216359536	Methylenetetrahydrofolate--tRNA-(uracil-5-)-methyltransferase TrmF	4218
2.209207555	Alkyl hydroperoxide reductase subunit F	2133
2.19245704	Flagellar hook-associated protein 2	849
2.172038237	GTPase Der	987
2.170985778	UDP-N-acetylmuramate--L-alanine ligase	3305
2.115354419	30S ribosomal protein S20	3706
2.102603316	Elongation factor Tu	2396
2.098730604	Ribosomal protein L11 methyltransferase	3716
2.083415747	Ribonuclease PH	3540
2.031767766	Uncharacterized protein	5591
2.003609141	DAK2 domain fusion YloV family protein	4194
1.99813048	RNA polymerase sigma factor SigA	3734
1.938310941	Flagellar hook-associated protein 3	850
1.926499645	Glycine--tRNA ligase	3063
1.865431507	Threonine--tRNA ligase	209
1.856237094	Beta-channel forming cytolysin family protein	1392
1.821284056	Histidine--tRNA ligase	4741
1.605300824	Uncharacterized protein	5234
1.602983236	Quinol oxidase subunit 2	1798
1.500477155	Cof-like hydrolase family protein	2625

1.489486376	Dihydrolipoamide acetyltransferase component of pyruvate dehydrogenase complex	3884
1.487024153	DNA-directed RNA polymerase subunit alpha	2367
1.383960803	Ribose-phosphate pyrophosphokinase	2472

8.1.3. Secretome – 25 °C

Table.8.5. Proteins higher during exponential phase growth compared to stationary phase growth in the secretome of *B. cereus* G9241 at 25 °C.

Log2-Fold Change	Protein	Gene Annotation	Gene Loci (AQ16_)
11.1183904	Peptidoglycan endopeptidase		576
10.67259781	Enterotoxin/cell wallbinding protein		2777
10.38823374	Cell wall hydrolase		2783
9.871902863	N-acetylmuramoyl-L-alanine amidase		2823
9.445892811	YocH Precursor/ cell wall binding protein		1815
8.98772049	50S ribosomal protein L1	*rplA*	2406
8.894918521	Enterotoxin		1683
8.805155436	Enoyl-[acyl-carrier-protein] reductase [NADH]	*fabI*	1275
8.752532085	30S ribosomal protein S3	*rpsC*	2388
8.277270079	30S ribosomal protein S7	*rpsG*	2398
8.066717982	50S ribosomal protein L6	*rplF*	2379
8.018956065	50S ribosomal protein L19	*rplS*	4210
7.982931534	Elongation factor Ts	*tsf*	4224
7.778544466	50S ribosomal protein L22	*rplV*	2389
7.755741119	Trigger factor	*tig*	3550
7.646921555	50S ribosomal protein L11	*rplK*	2407
7.601343413	FeS assembly protein SufD	*sufD*	2996
7.515867949	Acetate kinase	*ackA*	3361
7.508313258	Glyceraldehyde-3-phosphate dehydrogenase	*gap*	2877
7.431816975	30S ribosomal protein S2	*rpsB*	4223
7.377725999	30S ribosomal protein S5	*rpsE*	2377
7.312197844	Calcineurin-like phosphoesterase family protein		4913
7.290194035	50S ribosomal protein L4	*rplD*	2393
7.180574993	50S ribosomal protein L24	*rplX*	2383
7.104884028	30S ribosomal protein S11	*rpsK*	2368
7.018236438	50S ribosomal protein L3	*rplC*	2394
7.009564335	Haemolytic enterotoxin family protein	*NheC*	658
7.005555511	50S ribosomal protein L13	*rplM*	2361
6.985169093	50S ribosomal protein L21	*rplU*	3578
6.943115711	30S ribosomal protein S13	*rpsM*	2369

6.912085553	30S ribosomal protein S4	*rpsD*	3343
6.880876939	DEAD-box ATP-dependent RNA helicase CshA	*cshA*	2259
6.779571613	30S ribosomal protein S15	*rpsO*	4242
6.740806381	FeS assembly protein SufB	*sufB*	2999
6.672404801	Translation initiation factor IF-2	*infB*	4237
6.513750255	Phosphoenolpyruvate-protein phosphotransferase	*ptsI*	3995
6.511848677	30S ribosomal protein S18	*rpsR*	2547
6.492755552	GTP-sensing transcriptional pleiotropic repressor CodY	*codY*	4222
6.47696209	Haemolytic enterotoxin family protein	*HblC*	4931
6.465537796	30S ribosomal protein S9	*rpsI*	2360
6.366192182	Transglutaminase-like superfamily protein		531
6.258554022	50S ribosomal protein L14	*rplN*	2384
6.176235497	Cell envelope-related function transcriptional attenuator common domain protein		1694
6.120433887	Inosine-5-monophosphate dehydrogenase	*guaB*	2516
6.120044045	Pyrimidine-nucleoside phosphorylase	*pdp*	3956
6.001831055	Penicillin binding transpeptidase domain protein		3753
5.998441398	Hemolysin BL-binding component	*HblA*	4933
5.97324193	Phosphoglucosamine mutase	*glmM*	2335
5.969932636	Chaperone protein DnaK	*dnaK*	3714
5.902466019	50S ribosomal protein L10	*rplJ*	2405
5.882163405	DNA polymerase III subunit beta	*dnaN*	2529
5.85169665	L,D-transpeptidase catalytic domain protein		2947
5.843504608	Ribose-phosphate pyrophosphokinase	*prs*	2472
5.792537048	FeS assembly ATPase SufC	*sufC*	2993
5.785070231	Beta-channel forming cytolysin family protein	*CytK*	1392
5.753962989	3-oxoacyl-[acyl-carrier-protein] reductase	*fabG*	4199
5.647486986	S-adenosylmethionine synthase	*metK*	3227
5.591728399	ABC transporter family protein		5099
5.465464473	Translation initiation factor IF-3	*infC*	3429
5.461262266	30S ribosomal protein S8	*rpsH*	2380
5.425914228	LPXTG cell wall anchor domain protein		4818
5.394454082	50S ribosomal protein L23	*rplW*	2392
5.254892647	Adenylate kinase	*adk*	2373
5.183754891	Asparagine--tRNA ligase	*asnS*	3443
5.183731139	Cell division protein FtsZ	*ftsZ*	4144
5.170863067	Transcription termination/antitermination protein	*nusA*	4234

	NusA		
5.158093482	ATP-dependent Clp protease ATP-binding subunit ClpX	*clpX*	3551
5.134565224	50S ribosomal protein L16	*rplP*	2387
5.132436434	Glutamyl-tRNA(Gln) amidotransferase subunit A	*gatA*	2157
5.113533763	50S ribosomal protein L15	*rnjA*	2375
5.090741754	THUMP domain protein		931
5.024375935	Uridylate kinase	*pyrH*	4225
5.021502544	Peptide chain release factor 1	*prfA*	2690
5.008158882	Fructose-1,6-bisphosphate aldolase, class II	*fba*	2684
5.006101529	Peptidase M23 family protein		1060
4.952538619	FMN-dependent NADH-azoreductase	*azoR4*	2611
4.943569283	30S ribosomal protein S17	*rpsQ*	2385
4.933147907	DAK2 domain fusion YloV family protein		4194
4.931220621	Elongation factor Tu	*tuf*	2396
4.876603723	Serine--tRNA ligase	*serS*	2512
4.870446245	Phenylalanine--tRNA ligase beta subunit	*pheT*	3442
4.839088639	50S ribosomal protein L20	*rplT*	3431
4.768136909	UDP-N-acetylglucosamine 2-epimerase		2749 or 2818
4.766686161	50S ribosomal protein L7/L12	*rplL*	2404
4.756076376	UDP-N-acetylmuramoylalanine--D-glutamate ligase	*murD*	4138
4.741758506	50S ribosomal protein L17	*rplQ*	2366
4.716569086	30S ribosomal protein S12	*rpsL*	2399
4.691031456	30S ribosomal protein S16	*rpsP*	4223
4.675294705	WxL domain surface cell wall-binding family protein		3215
4.597455263	Uracil phosphoribosyltransferase	*upp*	2705
4.591838519	Probable thiol peroxidase	*tpx*	n/a
4.575548669	Hypoxanthine phosphoribosyltransferase	*hpt*	2456
4.52049005	3D domain protein		5075
4.503517628	5-methylthioadenosine/S-adenosylhomocysteine nucleosidase	*mtnN*	3649
4.482152065	FAD dependent oxidoreductase family protein		3051
4.439363162	Flagellar hook-associated protein 3	*flgL*	850
4.42251569	Protein RecA	*recA*	4277
4.389782588	UTP--glucose-1-phosphate uridylyltransferase	*galU*	3058
4.343656063	Dihydrolipoamide acetyltransferase component of pyruvate dehydrogenase complex	*pdhC*	4080

4.303348144	Aspartate--tRNA(Asn) ligase	*aspS*	3620
4.297238191	GTPase Der	*engA*	987
4.277523677	Uncharacterized protein		1407
4.249729037	Proline--tRNA ligase	*proS*	4231
4.23922046	Short chain dehydrogenase family protein		565
4.238344749	Glycerol-3-phosphate dehydrogenase		1439
4.221736034	30S ribosomal protein S10	*rpsJ*	2395
4.187804302	Peptidyl-prolyl cis-trans isomerase	*ppiB*	3981
4.172469775	30S ribosomal protein S19	*rpsS*	2390
4.140687048	Glycerol kinase	*glpK*	1440
4.131132603	Queuine tRNA-ribosyltransferase	*tgt*	3606
4.118468781	Fructose-1,6-bisphosphatase	*glpX*	2686
4.109982411	GTP-binding protein TypA/BipA	*typA*	4095
4.109815558	Cell division ATP-binding protein FtsE	*ftsE*	2831
4.086595933	Ribosome-binding ATPase YchF	*ychF*	2544
4.048898419	UPF0234 protein		1339
4.044809302	UDP-N-acetylmuramate--L-alanine ligase	*murC*	3305
4.021023552	4-hydroxy-tetrahydrodipicolinate synthase	*dapA*	4259
4.006192327	Glucokinase	*glcK*	3763
4.006127357	Peptide chain release factor 2	*prfB*	2829
3.987300421	Polysaccharide deacetylase family protein		5106
3.958989124	50S ribosomal protein L27	*rpmA*	3580
3.932847341	DNA-binding protein HU	*hup*	981
3.919135531	Cell shape determining, MreB/Mrl family protein		3570
3.896694422	Aspartyl/glutamyl-tRNA(Asn/Gln) amidotransferase subunit B	*gatB*	2156
3.845800922	Haemolytic enterotoxin family protein	*NheB*	659
3.830914219	Uncharacterized protein		993
3.819522217	Glutamate dehydrogenase	*gudB*	1001
3.762368123	Catabolite control protein A	*ccpA*	3318
3.742751598	RNA polymerase sigma factor SigA	*sigA*	3734
3.739037246	1,4-dihydroxy-2-naphthoyl-CoA synthase	*menB*	3129
3.728790601	VanW like family protein		4535
3.718813539	3D domain protein		4351
3.709269683	Probable tRNA sulfurtransferase	*thiI*	3351
3.705990314	33 kDa chaperonin	*hslO*	2453
3.698483904	Histidine--tRNA ligase	*hisS*	3619

3.670485179	30S ribosomal protein S6	*rpsF*	2545
3.665276408	N-acetylmuramoyl-L-alanine amidase family protein		4391
3.650084178	Uncharacterized protein		4954
3.648204486	tRNA uridine 5-carboxymethylaminomethyl modification enzyme MnmG	*gidA*	2536
3.637397965	Adenine phosphoribosyltransferase	*apt*	3615
3.611231486	Tyrosine--tRNA ligase	*tyrS*	3339
3.604555468	50S ribosomal protein L29	*rpmC*	2386
3.59859848	L-lactate dehydrogenase	*ldh*	3879
3.565563679	Plasmid replication protein repX	*repX*	5817
3.551839352	Cell envelope-related function transcriptional attenuator common domain protein		553
3.544319789	Glutamate-1-semialdehyde 2,1-aminomutase	*hemL*	3562
3.535814404	Probable transcriptional regulatory protein		1976
3.5075411	Protective antigen	*PagA*	5705
3.497626344	Putative tRNA binding domain protein		3300
3.490366975	GTPase Obg	*cgtA*	3582
3.468399922	UDP-N-acetylglucosamine 1-carboxyvinyltransferase	*murA*	2732
3.446424325	50S ribosomal protein L18	*rplR*	2378
3.429521441	Dihydrolipoamide acetyltransferase component of pyruvate dehydrogenase complex		3884
3.426001986	xtracellular ribonuclease	*bsn*	4754
3.415770531	Cysteine synthase	*cysK*	2452
3.405766805	ATP-dependent Clp protease proteolytic subunit	*clpP*	2865
3.387120465	Formate acetyltransferase	*pflB*	2025
3.350712856	Methionyl-tRNA formyltransferase	*fmt*	4184
3.336325487	50S ribosomal protein L35	*rpmI*	3430
3.334241947	Acetyl-CoA carboxylase, biotin carboxylase subunit	*accC*	3848
3.287790775	3-hydroxyacyl-[acyl-carrier-protein] dehydratase FabZ	*fabZ*	2750
3.197015206	ATP-dependent zinc metalloprotease FtsH	*ftsH*	2455
3.192216953	D-alanine--D-alanine ligase	*ddl*	n/a
3.188217481	L-threonine dehydratase catabolic TdcB	*ilvA*	133
3.153206428	50S ribosomal protein L31 type B	*rpmE*	2688
3.13700064	Aspartate ammonia-lyase	*aspA*	1893
3.13551418	Quinol oxidase subunit 2	*qoxA*	1798
3.117386653	Mannosyl-glycoendo-beta-N-acetylglucosaminidase family protein		714

3.094841003	longation factor G	*fusA*	2397
3.087154309	Uncharacterized protein		5591
3.082213879	NH(3)-dependent NAD(+) synthetase	*nadE*	528
3.07931153	Efflux transporter, RND family, MFP subunit		1680
3.047347069	Glycine--tRNA ligase	*glyS*	3063
3.02868096	Cof-like hydrolase family protein		2625
3.024851322	DNA ligase	*ligA*	2172
2.991670926	50S ribosomal protein L9	*rplI*	2550
2.973874807	DNA-binding protein HU	*hup*	4339
2.969365676	tRNA-specific 2-thiouridylase MnmA	*trmU*	3627
2.95350488	Probable butyrate kinase	*buk*	3880
2.935623884	Elongation factor 4	*lepA*	3709
2.935521841	Ribosomal protein L11 methyltransferase	*prmA*	3716
2.93521759	Glucose-specific phosphotransferase enzyme IIA component	*crr*	2700
2.93448774	Pseudouridine synthase	*rluB*	1019
2.925958892	4-hydroxy-3-methylbut-2-en-1-yl diphosphate synthase (flavodoxin)	*ispG*	3747
2.892903566	DNA gyrase subunit A	*gyrA*	2525
2.883038697	Methionine--tRNA ligase	*metG*	2943
2.875824054	30S ribosomal protein S20	*rpsT*	3706
2.868568182	Ribosomal RNA small subunit methyltransferase H	*rsmH*	4132
2.866203626	Acetyl-CoA carboxylase, biotin carboxyl carrier protein	*accB*	3847
2.863134394	Fumarate hydratase class I		2049
2.844397267	Flagellar hook-associated protein 2		849
2.839814186	Probable DNA-directed RNA polymerase subunit delta	*rpoE*	2680
2.80681328	Lipoyl synthase	*lipA*	3007
2.796132406	Radical SAM methylthiotransferase, MiaB/RimO family protein		3718
2.792979042	YmdB-like family protein		4279
2.777295341	Pyruvate dehydrogenase (Acetyl-transferring) E1 component, alpha subunit	*pdhA*	4078
2.745673577	Elongation factor P	*efp*	3834
2.733221054	Ribosomal RNA small subunit methyltransferase G	*rsmG*	2537
2.717632453	Chaperone protein DnaJ	*dnaJ*	3715
2.697164436	N-acetylmuramoyl-L-alanine amidase family protein		1574
2.695966164	Malonyl CoA-acyl carrier protein transacylase	*fabD*	4198

2.692621549	Lysine--tRNA ligase	*lysS*	2443
2.684690873	tRNA pseudouridine synthase B	*truB*	4240
2.663949887	50S ribosomal protein L30	*rpmD*	2376
2.66276741	Ribonucleoside-diphosphate reductase		1137
2.630686323	UDP-N-acetylmuramoyl-tripeptide--D-alanyl-D-alanine ligase	*murF*	2259
2.600889047	Bacterial extracellular solute-binding s, 3 family protein		1619
2.596972227	Pur operon repressor PurR	*purR*	2476
2.581613938	Transition state regulatory protein AbrB	*abrB*	2485
2.578462044	Fructose-1,6-bisphosphatase	*glpX*	3017
2.561115185	tRNA modification GTPase MnmE	*trm*	2535
2.559323788	Cytidylate kinase	*cmk*	994
2.547944993	Thioredoxin reductase	*trxB*	2858
2.522272587	Transcription elongation factor GreA	*greA*	3644
2.510103305	Cysteine--tRNA ligase	*cysS*	2414
2.509786288	Uncharacterized protein		3186
2.490331888	Acetohydroxy acid isomeroreductase, catalytic domain protein		1075
2.47406594	Beta-lactamase enzyme family protein		4520
2.454941511	DNA gyrase subunit B	*gyrB*	2526
2.436951637	Bifunctional protein FolD	*folD*	3851
2.404072762	CRS1 / YhbY domain protein		3695
2.393445571	Transcription termination/antitermination protein NusG	*nusG*	2408
2.378059228	Bacterial extracellular solute-binding family protein		1200
2.374266307	30S ribosomal protein S14 type Z	*rpsN1*	2381
2.360779285	Type III pantothenate kinase	*coaX*	2454
2.35413003	Ribosome biogenesis GTPase YqeH	*yqeH*	3693
2.325345516	Methyltransferase small domain protein		3360
2.314940929	Probable dual-specificity RNA methyltransferase RlmN	*rlmN*	4186
2.295127153	Ribonuclease R	*rnr*	2887
2.278498535	50S ribosomal protein L2	*rplB*	2391
2.263619105	DEAD-box ATP-dependent RNA helicase CshB	*cshB*	3740
2.257608374	3-oxoacyl-[acyl-carrier-protein] synthase 3	*fabH*	1318
2.239669243	7-cyano-7-deazaguanine synthase	*queC*	1148
2.217332482	Pyruvate dehydrogenase E1 component subunit beta	*pdhB*	4079
2.217200438	Glycosyltransferase like 2 family protein		2589

2.19371446	Uncharacterized protein		2912
2.193383137	Periplasmic binding family protein		2126
2.112287045	Ribonucleotide reductase, barrel domain protein		1136
2.109725433	Methylenetetrahydrofolate--tRNA-(uracil-5-)-methyltransferase TrmF	*trmFO*	4218
2.107561906	Single-stranded DNA-binding protein	*ssb*	2546
2.088040272	Septum site-determining protein divIVA	*divIVA*	4154
2.078684568	Bacillolysin		52
2.078593274	3-oxoacyl-[acyl-carrier-protein] synthase 2	*fabF*	1317
2.054615498	Uncharacterized protein		3980
2.050677617	ATP-dependent protease ATPase subunit HslU	*hslU*	4221
2.045925379	Carboxylesterase	*est*	2886
2.041204691	Guanylate kinase	*gmk*	4179
2.018961986	Type I phosphodiesterase / nucleotide pyrophosphatase family protein		2785
2.018142064	Hypoxanthine phosphoribosyltransferase	*hpt*	3166
2.010787129	DNA-directed RNA polymerase subunit beta	*rpoC*	2401
1.996811469	Tetratricopeptide repeat family protein		972
1.970229467	Signal recognition particle protein	*ffh*	4205
1.954934398	Uncharacterized protein		5849
1.941402435	Ribosomal RNA small subunit methyltransferase A	*rsmA*	2481
1.921236912	Asparagine synthase	*asnB*	331
1.900596937	L-asparaginase, type I family protein		4939
1.881451925	4-hydroxy-tetrahydrodipicolinate reductase	*dapB*	959
1.850859165	Chromosomal replication initiator protein DnaA	*dnaA*	2530
1.839164495	Foldase protein PrsA	*prsA1*	1431
1.831020753	Cell shape determining, MreB/Mrl family protein		2741
1.817793051	Signal recognition particle receptor FtsY	*ftsY*	4203
1.817762454	YwhD family protein		2645
1.788160026	Ribosome-recycling factor	*frr*	4226
1.780011415	Uncharacterized protein		5234
1.778510888	Transcriptional regulator LytR	*lytR*	2751
1.769229492	Hemolysin BL-binding component	*HblA*	4932
1.759576559	Bifunctional protein GlmU	*glmU*	2473
1.754889766	Flagellar hook-associated protein 1	*flgK*	851
1.7214849	Polysaccharide deacetylase family protein		549
1.710999966	Lethal factor	*Lef*	5710

1.689617683	Beta-channel forming cytolysin family protein	*HlyII*	4553
1.669536471	DNA-directed RNA polymerase subunit beta	*rpoB*	2402
1.623327096	tRNA N6-adenosine threonylcarbamoyltransferase	*tsaD*	2228
1.571073691	Pyridoxal phosphate-dependent enzyme, D-cysteine desulfhydrase family protein		4829
1.553956191	DNA helicase	*pcrA*	2173
1.529343163	Transketolase	*tkt*	4384
1.51058046	NADPH-dependent 7-cyano-7-deazaguanine reductase	*queF*	1145
1.501784801	Peptidase U32 family protein		3641
1.394497395	Signal peptidase I	*lepB*	4964
1.376137892	Single-stranded-DNA-specific exonuclease RecJ	*recJ*	3614
1.336419702	Alanine--tRNA ligase	*alaS*	3635
1.299826493	Arginine--tRNA ligase	*argS*	374
1.28117392	Type I phosphodiesterase / nucleotide pyrophosphatase family protein		1073
1.279497464	Protein translocase subunit SecA	*secA*	2828
1.276779056	Chitin binding domain protein		5259
1.25894551	Aspartate ammonia-lyase	*aspA*	729
1.245357434	Calcineurin-like phosphoesterase family protein		3941
1.243505677	Glutamate-1-semialdehyde 2,1-aminomutase	*hemL*	2004
1.219396075	Succinate--CoA ligase [ADP-forming] subunit beta	*sucC*	4214
1.191611446	LPXTG cell wall anchor domain protein		4757
1.126125524	WxL domain surface cell wall-binding family protein		3218
1.121282975	60 kDa chaperonin	*groL*	2222

Table.8.6. Proteins higher during stationary phase growth compared to exponential phase growth in the secretome of *B. cereus* G9241 at 25 °C.

Log2-Fold Change	Protein	Gene Annotation	Gene Loci (AQ16_)
11.74154639	Pheromone binding protein		1306
8.787773212	Peptide ABC transporter		1842
8.749587456	Bacillolysin	*npr*	1902
8.679865201	Oligopeptide ABC transporter		1312
8.255502343	5-methyltetrahydropteroyltriglutamate--homocysteine methyltransferase	*metE*	4042
7.80597496	Pheromone binding protein		2310
7.499271075	S-layer protein (PilC domain)	*ctc*	1583
6.401028211	SipW-cognate class signal peptide domain protein		1211
6.360189478	Chitin binding protein CBP 21	*cbp*	5228
6.154549877	Acetyl-CoA acetyltransferase	*thlA*	4021
5.681411346	Phosphoenolpyruvate carboxykinase [ATP]	*pckA*	3226
5.60268945	Peptide ABC transporter		2309
5.433148809	Arginase	*rocF*	2338
5.388390283	2-methylcitrate dehydratase	*prpD*	242
5.259892814	Flagellin		829
5.073899468	Camelysin, metallo peptidase M73	*FtsN*	1209
4.95111381	Bacterial extracellular solute-binding s, 5 Middle family protein		4481
4.799983988	Acetyl-CoA C-acyltransferase family protein		2675
4.746330996	Uncharacterized protein		74
4.707237065	Collagenase family protein		4546
4.704832971	Fungalysin metallopeptidase family protein		369
4.564574589	Neutral protease B	*nprB*	2938
4.286147118	Ornithine aminotransferase	*rocD*	1349
4.175691326	Isocitrate lyase	*aceA*	1370
4.112858415	Bacterial extracellular solute-binding s, 5 Middle family protein		496
3.802422891	Zinc-binding dehydrogenase family protein		1825
3.798294385	DNA protection during starvation protein 1	*dps1*	512
3.754143794	Probable cytosol aminopeptidase	*pepA*	3055
3.719355424	S-layer protein sap	*sap*	1584

3.714954456	Sphingomyelin phosphodiesterase	*sph*	1822
3.707098126	Glyceraldehyde-3-phosphate dehydrogenase	*gap*	3421
3.694431345	Nucleoside diphosphate kinase	*ndk*	976
3.68593053	4-hydroxyphenylpyruvate dioxygenase	*hppD*	2265
3.672788342	Electron transfer flavodomain protein		3479
3.587779085	Deblocking aminopeptidase		1575
3.521409621	Flagellin		828
3.512846351	Subtilase family protein		1863
3.502851665	Flagellin		830
3.447113951	Probable glycine dehydrogenase (decarboxylating) subunit 1	*gcvPA*	3802
3.432146867	Methylmalonate semialdehyde dehydrogenase [acylating]	*mmsA*	238
3.419712067	Putative aminopeptidase ysdC		3433
3.388283004	Glyoxalase/Bleomycin resistance /Dioxygenase superfamily protein		3354
3.256334782	Flagellin		827
3.230958104	Uncharacterized protein		5768
3.171929399	Bacterial extracellular solute-binding s, 5 Middle family protein		2276
3.165592829	Stress response protein SCP2	*yceC*	2073
3.144699166	Uncharacterized protein		3833
3.105273525	5-nucleotidase, lipoprotein e(P4) family		3491
3.04958721	Electron transfer flavodomain protein		3478
3.024379889	Putative septation protein SpoVG	*spoVG*	2474
2.977498611	Uncharacterized protein		1559
2.933224902	Putative nucleic acid binding OB-fold tRNA/helicase-type		1808
2.930148443	Thermolysin metallopeptidase, catalytic domain protein		5317
2.823909203	TerD domain protein		2071
2.81327951	Dihydrolipoyl dehydrogenase	*lpdA*	3881
2.760959506	Glycine cleavage system H protein	*gcvH*	2987
2.753802776	Collagenase family protein		1941
2.752566894	M6 family metalloprotease domain protein		5047
2.667643497	1-pyrroline-5-carboxylate dehydrogenase	*pruA*	2169
2.610061804	Immune inhibitor A	*ina*	1206

2.589270562	Probable transaldolase	*fsa*	1828
2.53000172	Oligopeptidase	*pz-A*	1152
2.468756557	Sulfatase family protein		5100
2.432843844	Leucine dehydrogenase	*ldh*	3879
2.425853272	Thermophilic metalloprotease family protein		3314
2.390895983	Pyridoxal phosphate-dependent acyltransferase family protein		1883
2.357318203	Iron-containing alcohol dehydrogenase family protein		4347
2.353099426	Uncharacterized protein		642
2.306289117	Alanine dehydrogenase	*ald*	1909
2.298531473	Formate--tetrahydrofolate ligase	*fhs*	431
2.258646806	2-methylisocitrate lyase	*prpB*	241
2.253330906	Uncharacterized protein		1557
2.189481854	Probable glycine dehydrogenase (decarboxylating) subunit 2	*gcvPB*	3803
2.180232286	Peptidase T	*pepT*	4324
2.06476452	Peptidase M20/M25/M40 family protein		3296
2.029461722	Malate dehydrogenase	*mdh*	3411
1.966592153	2-(Hydroxymethyl)glutarate dehydrogenase	*hgd*	239
1.949682315	Uncharacterized protein		3798
1.870050222	M6 family metalloprotease domain protein		1827
1.827155611	Uncharacterized protein		3514
1.786558231	Glucanase		5335
1.764124552	Periplasmic binding family protein		2891
1.759870847	Matrixin family protein		4915
1.727925142	Thioredoxin	*trxA*	3480
1.721856117	Periplasmic binding family protein		2641
1.705184937	Haemolytic enterotoxin family protein		660
1.682577644	Purine nucleoside phosphorylase		3955
1.675341884	Alanine dehydrogenase	*ald*	3375
1.628635714	ATP synthase gamma chain	*atpG*	2713
1.621441245	LPXTG cell wall anchor domain protein		3919
1.617969275	Phospholipase C	*plc*	1823
1.590428089	Purine nucleoside phosphorylase DeoD-type	*deoD*	1029
1.587333143	General stress protein 16U	*yceD*	2072
1.552252054	ATP synthase subunit delta	*atpH*	2711

1.547007481	Pyridoxal 5-phosphate synthase subunit PdxS	*pdxS*	2514
1.52982233	Oligoendopeptidase F	*pepF*	4585
1.527521104	2-oxoisovalerate dehydrogenase subunit alpha	*bfmBAA*	3882
1.491494119	Putative heme-dependent peroxidase 2633		2633
1.443706354	Uncharacterized protein		4789
1.431607803	Subtilase family protein		4301
1.380381624	Aldo/keto reductase family protein		2308
1.324110866	Glutamine--fructose-6-phosphate aminotransferase [isomerizing]	*glmS*	2334
1.287803034	Phosphate butyryltransferase	*ptb*	3878
1.26429598	UDP-N-acetylglucosamine 1-carboxyvinyltransferase	*murA*	2685
1.208660086	ATP synthase subunit alpha	*atpA*	2712
1.19208614	Deoxyribose-phosphate aldolase	*deoC*	652
1.154181172	Pyruvate carboxylase	*pyc*	4104
1.144205332	Chitinase A		4342
1.124693642	LPXTG cell wall anchor domain protein		1597
1.077574839	2-oxoisovalerate dehydrogenase subunit beta	*bfmBAB*	3883
1.060463443	Adenylosuccinate synthetase	*purA*	2552
1.01742057	Alpha,alpha-phosphotrehalase	*treC*	1870

8.1.4. Secretome – 37 °C

Table.8.7. Proteins higher during exponential phase growth compared to stationary phase growth in the secretome of *B. cereus* G9241 at 37 °C.

Log2-Fold Change	Protein	Gene Annotation	Gene Loci (AQ16_)
11.58175596	Peptidoglycan endopeptidase		576
10.9609429	Enterotoxin		1683
9.151043256	N-acetylmuramoyl-L-alanine amidase		2823
8.995394309	Cell wall hydrolase		2783
8.390513738	Enterotoxin/cell wallbinding protein		2777
7.902417183	Elongation factor Ts	*tsf*	4224
7.676326195	Trigger factor	*tig*	3550
7.60319225	50S ribosomal protein L11	*rplK*	2407
7.556121747	Enoyl-[acyl-carrier-protein] reductase [NADH]	*fabI*	1275
7.428866227	50S ribosomal protein L6	*rplF*	2379
7.369898319	50S ribosomal protein L10	*rplJ*	2405
7.114146312	50S ribosomal protein L1	*rplA*	2406
7.005558451	WxL domain surface cell wall-binding family protein		3215
6.995487173	50S ribosomal protein L17	*rplQ*	2366
6.958193103	30S ribosomal protein S7	*rpsG*	2398
6.767446876	YocH Precursor/ cell wall binding protein		1815
6.66465958	50S ribosomal protein L14	*rplN*	2384
6.471577565	Glyceraldehyde-3-phosphate dehydrogenase	*gap*	2877
6.460992217	30S ribosomal protein S3	*rpsC*	2388
6.434344331	50S ribosomal protein L7/L12	*rplL*	2404
6.306999902	30S ribosomal protein S13	*rpsM*	2369
6.155244629	50S ribosomal protein L3	*rplC*	2394
5.957626184	L,D-transpeptidase catalytic domain protein		2947
5.940161516	Pyrimidine-nucleoside phosphorylase	*pdp*	650/3956
5.853178819	Ribosome-recycling factor	*frr*	4226
5.833424608	Peptidase M23 family protein		1060

5.798904578	Fructose-1,6-bisphosphate aldolase, class II	*fba*	2684
5.673025409	3-oxoacyl-[acyl-carrier-protein] reductase	*fabG*	4855/4199
5.657619782	Penicillin binding transpeptidase domain protein		3753;4975
5.646173875	30S ribosomal protein S2	*rpsB*	4223
5.633604552	Polysaccharide deacetylase family protein		5106
5.597603599	Phosphoenolpyruvate-protein phosphotransferase	*ptsI*	3995
5.534719785	Dihydrolipoamide acetyltransferase component of pyruvate dehydrogenase complex	*pdhC*	4080
5.482430935	FeS assembly protein SufB	*sufB*	2999
5.403589716	Phosphoglucosamine mutase	*glmM*	2335
5.353002985	50S ribosomal protein L24	*rplX*	2383
5.340333263	Pyruvate dehydrogenase (Acetyl-transferring) E1 component, alpha subunit	*pdhA*	4078
5.292134479	DNA polymerase III subunit beta	*dnaN*	2529
5.276771396	Transcription termination/antitermination protein NusA	*nusA*	4234
5.243302623	30S ribosomal protein S10	*rpsJ*	2395
5.226336529	Transglutaminase-like superfamily protein		531
5.223149717	Chaperone protein DnaK	*dnaK*	3714
5.173308134	FeS assembly protein SufD	*sufD*	2996
5.131014473	FeS assembly ATPase SufC	*sufC*	2993
5.084453384	Inosine-5-monophosphate dehydrogenase	*guaB*	2516
5.036522349	Hypoxanthine phosphoribosyltransferase	*hpt*	2456
5.009496311	30S ribosomal protein S15	*rpsO*	4242
5.000770807	GTP-sensing transcriptional pleiotropic repressor CodY	*codY*	4222
4.968295897	Type I phosphodiesterase / nucleotide pyrophosphatase family protein		1073
4.908828715	50S ribosomal protein L19	*rplS*	4210
4.785270546	Lysine--tRNA ligase	*lysS*	2443
4.766001991	30S ribosomal protein S9	*rpsI*	2360
4.756134431	50S ribosomal protein L22	*rplV*	2389
4.74253577	30S ribosomal protein S5	*rpsE*	2377
4.724000255	CTP synthase	*pyrG*	2681

4.713088989	50S ribosomal protein L21	*rplU*	3578
4.709088812	3-oxoacyl-[acyl-carrier-protein] synthase 2	*fabF*	1317
4.664169773	Glucokinase	*glcK*	3763
4.639016054	UDP-N-acetylglucosamine 1-carboxyvinyltransferase	*murA*	2685/2732
4.631363273	50S ribosomal protein L2	*rplB*	2391
4.620172183	Glucose-specific phosphotransferase enzyme IIA component	*crr*	2700
4.605668336	30S ribosomal protein S8		2287;2380
4.604813416	Fructose-1,6-bisphosphatase	*glpX*	2686/3017
4.54952544	Translation initiation factor IF-3	*infC*	3429
4.525606645	Glutamate dehydrogenase	*gudB*	1001
4.487101555	50S ribosomal protein L27	*rpmA*	3580
4.447480748	Adenylate kinase	*adk*	2373
4.414413979	3D domain protein		4351
4.388995723	Translation initiation factor IF-2	*infB*	4237
4.385148138	Probable thiol peroxidase	*tpx*	n/a
4.385136783	30S ribosomal protein S11	*rpsK*	2368
4.383201579	50S ribosomal protein L18	*rplR*	2378
4.349538942	4-hydroxy-3-methylbut-2-en-1-yl diphosphate synthase (flavodoxin)	*ispG*	3747
4.31619823	Glycerophosphoryl diester phosphodiesterase family protein		4572
4.287320822	Elongation factor G	*fusA*	2397
4.284348528	Glutamyl-tRNA(Gln) amidotransferase subunit A	*gatA*	2157
4.273912847	30S ribosomal protein S16	*rpsP*	4223
4.254251029	1,4-dihydroxy-2-naphthoyl-CoA synthase	*menB*	3129
4.250771403	GTP-binding protein TypA/BipA	*typA*	4095
4.211242189	50S ribosomal protein L20	*rplT*	3431
4.18037955	30S ribosomal protein S6	*rpsF*	2545
4.137722373	Cell envelope-related function transcriptional attenuator common domain protein		553
4.12587593	30S ribosomal protein S17	*rpsQ*	2385
4.122030874	Serine--tRNA ligase	*serS*	2512
4.06681474	Peptide chain release factor 1	*prfA*	2690

3.990569105	50S ribosomal protein L29	*rpmC*	2386
3.963001321	50S ribosomal protein L15	*rplO*	2375
3.945359528	Ribonuclease J	*rnjA*	4073
3.934632401	30S ribosomal protein S18	*rpsR*	2547
3.924547985	Beta-channel forming cytolysin family protein		4553
3.908191284	30S ribosomal protein S4	*rpsD*	3343
3.901696702	UDP-N-acetylglucosamine 2-epimerase		2749;2818;mnaA
3.851283848	Cell division protein FtsZ	*ftsZ*	4144
3.811615467	gp49 phage family protein		5822
3.806519995	Aspartate ammonia-lyase	*aspA*	729/1893/4940
3.801692804	Short chain dehydrogenase family protein		565
3.761061703	Thioredoxin reductase	*trxB*	2858
3.745505383	50S ribosomal protein L23	*rplW*	2392
3.714892725	50S ribosomal protein L4	*rplD*	2393
3.711977303	Pyruvate kinase	*pyk*	3405
3.68884221	50S ribosomal protein L13	*rplM*	2384
3.645166198	UDP-N-acetylmuramoylalanine--D-glutamate ligase	*murD*	4138
3.606019775	Uncharacterized protein		5836
3.6054643	Malic enzyme, NAD binding domain protein		3400
3.604360501	DNA-directed RNA polymerase subunit beta	*rpoB*	2402
3.589906931	Glutamate-1-semialdehyde 2,1-aminomutase	*hemL*	2004/3562
3.579686808	Uncharacterized protein		993
3.572119425	Leucine--tRNA ligase	*leuS*	3254
3.534355323	Transcription elongation factor GreA	*greA*	3644
3.529591759	4-hydroxy-tetrahydrodipicolinate synthase	*dapA*	4259/5222
3.516013841	Arginine--tRNA ligase	*argS*	374
3.508872916	Transglutaminase-like superfamily protein		1487
3.505426278	DEAD-box ATP-dependent RNA helicase CshA	*cshA*	2259
3.504386206	Asparagine--tRNA ligase	*asnS*	3443
3.470430404	ATP-dependent Clp protease ATP-binding subunit ClpX	*clpX*	3551

3.454301894	LPXTG cell wall anchor domain protein		4818
3.401266992	Acetate kinase	*ackA*	3361
3.400178313	Phenylalanine--tRNA ligase beta subunit	*pheT*	3442
3.389187694	Acetyl-CoA carboxylase, biotin carboxylase subunit	*accC*	3848
3.36103948	Transketolase	*tkt*	4384
3.353117307	S-adenosylmethionine synthase	*metK*	3227
3.332959374	Putative tRNA binding domain protein		3300
3.328464662	D-alanine--D-alanine ligase		2260
3.311315477	5-methylthioadenosine/S-adenosylhomocysteine nucleosidase	*mtnN*	56/3649/4752/5184
3.307510356	3-oxoacyl-[acyl-carrier-protein] synthase 3	*fabH*	707/1318
3.288503091	N-acetylmuramoyl-L-alanine amidase family protein		4391
3.220897834	Tyrosine--tRNA ligase	*tyrS*	2910/3339
3.210694949	Ribonucleoside-diphosphate reductase		1137
3.209984104	FMN-dependent NADH-azoreductase	*azoR4*	2611/623
3.157040715	33 kDa chaperonin	*hslO*	2453
3.133148114	30S ribosomal protein S12	*rpsL*	2399
3.128855973	Pyruvate dehydrogenase E1 component subunit beta	*pdhB*	4079
3.118302088	ABC transporter family protein		5099
3.113709986	Uracil phosphoribosyltransferase	*upp*	2705
3.112314979	UPF0234 protein		1339
3.056874474	Cell envelope-related function transcriptional attenuator common domain protein		1694
3.050618609	L-lactate dehydrogenase		3111
3.046781659	Isoleucine--tRNA ligase	*ileS*	4155
3.040917436	Alanine--tRNA ligase	*alaS*	3635
3.04014121	Putative major capsid protein gpP		5831
3.037267327	Acetyl-CoA carboxylase, biotin carboxyl carrier protein	*accB*	3847
3.018522906	DNA-directed RNA polymerase subunit beta	*rpoC*	2401
2.998457968	Glutamate-1-semialdehyde 2,1-aminomutase	*hemL*	2004/3562

2.987741033	Cysteine synthase	*cysK*	2452
2.9812422	Methionine--tRNA ligase	*metG*	2943
2.970919132	50S ribosomal protein L9	*rplI*	2550
2.947868625	N-acetylmuramoyl-L-alanine amidase family protein		1574
2.943714182	Cell division ATP-binding protein FtsE	*ftsE*	2831
2.937586705	3D domain protein		5075
2.912907759	30S ribosomal protein S19	*rpsS*	2390
2.902529955	VanW like family protein		4535
2.896939715	Uncharacterized protein		2912
2.861613492	GMP synthase [glutamine-hydrolyzing]	*guaA*	2221
2.854743242	DNA-binding protein HUP	*hup;hupA*	4339
2.837993344	Aldo/keto reductase family protein		2308
2.815370043	Serine hydroxymethyltransferase	*glyA*	
2.815276667	Putative gp14-like protein		5832
2.788201511	50S ribosomal protein L16	*rplP*	2387
2.784653982	Adenine phosphoribosyltransferase	*apt*	3615
2.783261051	Ribonuclease J	*rnjB*	4260
2.781079451	Aspartate--tRNA(Asn) ligase	*aspS*	367/3620
2.759492834	Plasmid replication protein repX	*repX*	5817
2.75190258	Type III pantothenate kinase	*coaX*	2454
2.746869261	Type I phosphodiesterase / nucleotide pyrophosphatase family protein		2785;4298
2.71263663	Aldose 1-epimerase family protein		894
2.685643037	Phage tail family protein		5835
2.661474148	Efflux transporter, RND family, MFP subunit		1680
2.631472588	Pyruvate carboxylase	*pyc*	4104
2.599970897	Aspartyl/glutamyl-tRNA(Asn/Gln) amidotransferase subunit B	*gatB*	2156
2.598440925	UTP--glucose-1-phosphate uridylyltransferase	*galU*	3058/5616/5678
2.562345147	Lipoyl synthase	*lipA*	3007
2.537789504	DNA-binding protein HUP	*hup*	981
2.519305905	N-acetylmuramoyl-L-alanine amidase family protein		5839
2.494948227	Triosephosphate isomerase	*tpiA*	2879

2.476218525	Protein GrpE	*grpE*	3713
2.473844051	Polysaccharide deacetylase family protein		549
2.465330203	Cysteine--tRNA ligase	*cysS*	2414
2.462865392	Adenylosuccinate lyase	*purB*	2187
2.427301129	Peptidyl-prolyl cis-trans isomerase	*ppiB*	3981
2.400987426	Probable transcriptional regulatory protein		1976
2.37643671	FAD dependent oxidoreductase family protein		3051
2.345564842	Acetyltransferase domain protein		1918
2.338821938	Aspartate-semialdehyde dehydrogenase	*asd*	4257
2.32703503	YmdB-like family protein		4279
2.264272928	Proline--tRNA ligase	*proS*	4231
2.254182537	Uncharacterized protein		4954
2.251788855	Probable tRNA sulfurtransferase	*thiI*	3351
2.23072206	Superoxide dismutase	*sodA1*	3751
2.229095856	Isocitrate dehydrogenase [NADP]	*icd*	3410
2.216359536	Methylenetetrahydrofolate--tRNA-(uracil-5-)-methyltransferase TrmFO	*trmFO*	4218
2.209207555	Alkyl hydroperoxide reductase subunit F	*ahpF*	2133
2.19245704	Flagellar hook-associated protein 2		849
2.172038237	GTPase Der	*engA*	987
2.170985778	UDP-N-acetylmuramate--L-alanine ligase	*murC*	3305
2.115354419	30S ribosomal protein S20	*rpsT*	3706
2.102603316	Elongation factor Tu	*tuf*	2396
2.098730604	Ribosomal protein L11 methyltransferase	*prmA*	3716
2.083415747	Ribonuclease PH	*rph*	3540
2.031767766	Uncharacterized protein		5591
2.003609141	DAK2 domain fusion YloV family protein		4194
1.99813048	RNA polymerase sigma factor SigA	*sigA*	3734
1.938310941	Flagellar hook-associated protein 3	*flgL*	850
1.926499645	Glycine--tRNA ligase	*glyS*	3063
1.865431507	Threonine--tRNA ligase	*thrS*	3428
1.856237094	Beta-channel forming cytolysin family protein		1392
1.821284056	Histidine--tRNA ligase	*hisS*	3619
1.605300824	Uncharacterized protein		5234
1.602983236	Quinol oxidase subunit 2	*qoxA*	1798

1.500477155	Cof-like hydrolase family protein		2625
1.489486376	Dihydrolipoamide acetyltransferase component of pyruvate dehydrogenase complex		3884
1.487024153	DNA-directed RNA polymerase subunit alpha	*rpoA*	2367
1.383960803	Ribose-phosphate pyrophosphokinase	*prs*	2472

Table.8.8. Proteins higher during stationary phase growth compared to exponential phase growth in the secretome of *B. cereus* G9241 at 37 °C.

Log2-fold Change	Protein	*Gene Annotation*	Gene Loci (AQ16_)
13.67425426	Pheromone binding protein		1306
10.46753685	Collagenase family protein		4546
10.44560647	Peptide ABC transporter, peptide-binding protein		2309
9.92237854	Chitinase A1	*chiA1*	2089
9.390093327	Oligopeptide ABC transporter		1312
9.288374821	Glucanase		5335
8.651034037	Camelysin, metallo peptidase M73	*FtsN*	1209
8.540471156	Peptide ABC transporter		1842
7.821544468	Neutral protease B	*nprB*	2938
7.753190637	Peptidase M20/M25/M40 family protein		2662
7.638925453	Uncharacterized protein		5768
7.283205122	Chitin binding protein CBP21	*cbp*	5228
7.112490555	Chitinase A		4342
7.057614883	Bacterial extracellular solute-binding s, 5 Middle family protein		2310
6.654506539	2-methylcitrate dehydratase	*prpD*	242
6.515860995	M6 family metalloprotease domain protein		1827
6.470729311	Fungalysin metallopeptidase family protein		369
6.46897471	Zinc-binding dehydrogenase family protein		1825
6.417500367	Bacillolysin	*npr*	1902
6.37035202	Bacterial extracellular solute-binding s, 5 Middle family protein		4481
6.056341012	Matrixin family protein		4915
5.944121813	5-methyltetrahydropteroyltriglutamate--homocysteine methyltransferase	*metE*	4042
5.20986263	Phosphoenolpyruvate carboxykinase [ATP]	*pckA*	3226
5.207335768	S-layer protein	*ctc*	1583
5.102285929	Oligopeptidase	*pz-A*	1152
5.075511793	Uncharacterized protein		1559
4.984163438	Arginase	*rocF*	2338
4.911012088	DNA protection during starvation protein 1	*dps1*	512

4.814951768	Bacterial extracellular solute-binding s, 5 Middle family protein		496
4.725935181	M6 family metalloprotease domain protein		5047
4.605835279	Nucleoside diphosphate kinase	*ndk*	976
4.588642781	Uncharacterized protein		74
4.530639898	Collagenase family protein		1941
4.49458229	Haemolytic enterotoxin family protein		4930
4.432966659	Urocanate hydratase	*hutU*	4415
4.418860336	Haemolytic enterotoxin family protein		660
4.410473978	5-nucleotidase, lipoprotein e(P4) family		3491
4.304110895	NLP/P60 family protein		5203
4.207248489	Flagellin		828
4.137116631	Probable glycine dehydrogenase (decarboxylating) subunit 1		3802
4.036815643	Probable glycine dehydrogenase (decarboxylating) subunit 2		3803
3.891310891	2-(Hydroxymethyl)glutarate dehydrogenase	*hgd*	239
3.840016539	4-hydroxyphenylpyruvate dioxygenase	*hppD*	2265
3.713575919	Alanine dehydrogenase	*ald*	1909
3.649474204	Peptidase M20/M25/M40 family protein		3296
3.627889673	ATP synthase gamma chain	*atpG*	2713
3.490279496	Phospholipase C	*plc*	1823
3.405557175	Alanine dehydrogenase	*ald*	3375
3.371960024	Acetyl-CoA acetyltransferase	*thlA*	4021
3.295967023	Dihydrolipoyl dehydrogenase	*lpdA*	3881
3.175309201	Flagellin		829
3.146744569	Acetyl-CoA C-acyltransferase family protein		2675
3.145316919	SipW-cognate class signal peptide domain protein		1211
3.104189495	Flagellin		830
3.095020771	Sulfatase family protein		5100
3.086110651	Putative aminopeptidase ysdC		3433
3.079984502	Deblocking aminopeptidase		1575
3.069181586	Oligoendopeptidase F	*pepF*	1299
3.028406858	Phosphate butyryltransferase	*ptb*	3878
2.964806805	Formate--tetrahydrofolate ligase	*fhs*	431
2.9229514	LPXTG cell wall anchor domain protein		1597

2.896616191	Flagellin		827
2.858923674	Peptidase T	*pepT*	4324
2.827479648	2-oxoisovalerate dehydrogenase subunit alpha	*bfmBAA*	3882
2.685727278	2-methylisocitrate lyase	*prpB*	241
2.609927466	TerD domain protein		2071
2.596480221	Thermophilic metalloprotease family protein		2148
2.571034729	ATP synthase subunit beta	*atpD*	2714
2.563262284	Purine nucleoside phosphorylase		3955
2.516609679	Immune inhibitor A	*ina*	1206
2.482111399	Probable cytosol aminopeptidase		3055
2.477294008	LPXTG cell wall anchor domain protein		3919
2.445685287	Uncharacterized protein		3833
2.412743618	Hemolysin BL-binding component	*hblA*	4932
2.378135443	NADH dehydrogenase-like protein yjlD	*yjlD*	2911
2.315944477	2-oxoisovalerate dehydrogenase subunit beta	*bfmBAB*	3883
2.233669482	ATP synthase subunit alpha	*atpA*	2712
2.226159811	Pyridoxal phosphate-dependent acyltransferase family protein		1883
2.200028658	Electron transfer flavodomain protein		3478
2.072163453	Uncharacterized protein		1557
2.030131539	Chitin binding domain protein		5259
2.001212915	S-layer protein sap	*sap*	1584
1.992105166	Uncharacterized protein		4789
1.960299373	Thermophilic metalloprotease family protein		3314
1.951483329	Glyoxalase/Bleomycin resistance /Dioxygenase superfamily protein		3354
1.918800155	Uncharacterized protein		642
1.858562443	Thiol-activated cytolysin family protein		4769
1.845422111	Adenylosuccinate synthetase	*purA*	2552
1.844588617	Putative heme-dependent peroxidase AQ16		2633
1.674663266	Putative nucleic acid binding OB-fold tRNA/helicase-type		1808
1.672127247	Electron transfer flavodomain protein		3479
1.624946979	Purine nucleoside phosphorylase DeoD-type	*deoD*	1029
1.62197455	1-pyrroline-5-carboxylate dehydrogenase	*pruA*	2169
1.597129663	Thioredoxin	*trxA*	3480
1.535931786	Pyridoxal 5-phosphate synthase subunit PdxS	*pdxS*	2514

1.475134869	Glutamine--fructose-6-phosphate aminotransferase [isomerizing]	*glmS*	2334
1.468244871	Methylmalonate semialdehyde dehydrogenase [acylating]	*mmsA*	238
1.285952687	Leucine dehydrogenase	*ldh*	3879

8.1.5. Cell Proteome – Exponential Phase

Table.8.9. Proteins higher at 25 °C compared to 37 °C in the cell proteome of *B. cereus* G9241 during exponential growth.

Log2-Fold Change	Protein	Gene Loci (AQ16_)
5.098430951	(CspA) Major cold shock protein	1368
4.724312027	Uncharacterized protein	4251
4.488564452	Cold-inducible YdjO family protein	175
4.103798866	Uncharacterized protein	4821
3.182483594	Transglutaminase-like superfamily protein	1487
3.060092693	Flagellar motor switch FliM family protein	858
2.778102239	(AzoR4) FMN-dependent NADH-azoreductase	2611
2.57019454	Uncharacterized protein	1372
2.474713196	Haemolytic enterotoxin family protein	659
2.410309151	Uncharacterized protein	1559
2.215556145	(CspA) Major cold shock protein	174
2.208459169	SET domain protein	2908
2.195774773	Transposase family protein	1725 / 4355
2.151026939	Rhodanese-like domain protein	1704
2.095966309	Haemolytic enterotoxin family protein	660
1.985961859	Uncharacterized protein	3777
1.943176989	Uncharacterized protein	3545
1.872211913	GIY-YIG catalytic domain protein	5364
1.730037481	N-acetylmuramoyl-L-alanine amidase family protein	4552
1.727843235	Uncharacterized protein	3508
1.664332628	Uncharacterized protein	1593
1.619285102	Ribosomal L7Ae/L30e/S12e/Gadd45 family protein	4236
1.605672836	Flagellin	827
1.577232758	Bacterial SH3 domain protein	576
1.563333308	Pseudouridine synthase	210
1.550445219	Flagellin	830
1.520435767	Uncharacterized protein	937
1.504268169	(CspD) Cold shock protein	3123
1.477887876	Uncharacterized protein	1573
1.467638642	(pfkB) 1-phosphofructokinase	4349

1.450817744	3D domain protein	1683
1.447155754	(Cdd) Cytidine deaminase	3727
1.43959107	(NagB) Glucosamine-6-phosphate deaminase	3989
1.41567719	DNA binding, excisionase family domain protein	2123
1.398676395	Cell wall hydrolase OS=Bacillus cereus G9241	2783
1.32305487	(IspF) 2-C-methyl-D-erythritol 2,4-cyclodiphosphate synthase	2417
1.301495301	DinB superfamily protein	4598
1.294121305	ABC transporter family protein	1131
1.289675673	Bacterial extracellular solute-binding s, 5 Middle family protein	671
1.289051294	Glyoxalase/Bleomycin resistance /Dioxygenase superfamily protein	3354
1.274530152	Glyoxalase/Bleomycin resistance /Dioxygenase superfamily protein	621
1.25446558	YppF-like family protein	936
1.232457315	Uncharacterized protein	4409
1.203045011	Iron-sulfur cluster biosynthesis family protein	4462
1.199973087	Uncharacterized protein	2141
1.197727124	Bacterial regulatory, arsR family protein	230
1.177642246	Uncharacterized protein	3902
1.163511445	Putative transcriptional regulator	4035
1.137157132	(RnmV) Ribonuclease M5	2482
1.133542448	Flagellin	828
1.112063527	UPF0223 protein	4090
1.111396551	Rhodanese-like domain protein	1703
1.098789374	(DbpA) ATP-dependent RNA helicase	2570
1.078344623	Mycolic acid cyclopropane synthetase family protein	4703
1.070229029	Uncharacterized protein	4430
1.049846888	CRS1 / YhbY domain protein	3695
1.047287978	Uncharacterized protein	123
1.030222416	(RpsH) 30S ribosomal protein S8	2380
1.019117693	(PhoP) Alkaline phosphatase synthesis transcriptional regulatory protein	3415
1.016571045	(TypA) GTP-binding protein TypA/BipA	4095
0.998080095	Nucleoid-associated protein	2504
0.977222761	Bacterial regulatory, arsR family protein	1891

0.97369051	S1 RNA binding domain protein	1338
0.970126192	(HemC) Porphobilinogen deaminase	3559
0.90664651	(Hfq) RNA-binding protein	4354
0.89607811	Pseudouridine synthase	4158
0.85206	(RpmC) 50S ribosomal protein L29	2386

Table.8.10. Proteins higher at 37 °C compared to 25 °C in the cell proteome of *B. cereus* G9241 during exponential growth.

Log2-Fold Change	Protein	Gene Loci (AQ16_)
4.348679791	WxL domain surface cell wall-binding family protein	3218
3.747184296	Uncharacterized protein	3219
2.872912575	(PflB) Formate acetyltransferase	2025
2.739925782	Uncharacterized protein	1429
2.298796559	(RecN) DNA repair protein	3857
2.277796527	(Dps1) DNA protection during starvation protein 1	512
2.252966583	Uncharacterized protein OS=Bacillus cereus G9241 GN=AQ16_5765 PE=4 SV=1	5765
2.250371739	(PflA) Pyruvate formate-lyase-activating enzyme	2024
2.237389882	(Ldh) L-lactate dehydrogenase	3111
2.169678946	CamS sex pheromone cAM373 family protein	2171
2.09221358	L-asparaginase, type I family protein	4939
1.987717385	(HrcA) Heat-inducible transcription repressor	3712
1.970180909	Uncharacterized protein	5849
1.967143724	Membrane MotB of proton-channel complex MotA/MotB family protein	3490
1.842345675	Periplasmic binding family protein	1888
1.835478504	(CadA) Cadmium-translocating P-type ATPase	1906
1.825552459	Uncharacterized protein	3980
1.819376816	(AspA) Aspartate ammonia-lyase	4940
1.725505749	Winged helix-turn-helix DNA-binding family protein	3075
1.704338928	(CoaBC) Phosphopantothenoylcysteine decarboxylase / phosphopantothenate--cysteine ligase	4181
1.675105135	Uncharacterized protein	4954
1.670505541	Universal stress protein	3373
1.632183691	WxL domain surface cell wall-binding family protein	3217
1.579106389	(Ldh) L-lactate dehydrogenase	2981
1.507349114	Penicillin-binding, 1A family protein	247
1.506611268	Peptidase M16 inactive domain protein	4269
1.500955294	(PyrK) Dihydroorotate dehydrogenase B (NAD(+)), electron transfer subunit	4165
1.493474861	Helix-turn-helix domain protein	3782

1.490899205	Uncharacterized protein	4177
1.490223169	Septin family protein	4297
1.489464124	Uncharacterized protein	4853
1.390934986	(GuaC) GMP reductase	2568
1.310638806	Aminotransferase	3076
1.301021536	Bacterial PH domain protein	3546
1.294339329	Periplasmic binding family protein	2891
1.281742163	Phage integrase family protein	5734
1.267887841	(MiaB) tRNA-2-methylthio-N(6)-dimethylallyladenosine synthase	4284
1.267277062	Pyridoxal-phosphate dependent enzyme family protein	3650
1.23213762	(Ung) Uracil-DNA glycosylase	2623
1.205962354	D-isomer specific 2-hydroxyacid dehydrogenase, NAD binding domain protein	3074
1.167416905	(MreC) Cell shape-determining protein MreC	3571
1.130305042	Periplasmic binding family protein	3601
1.130074739	(ModA) Molybdate ABC transporter, periplasmic molybdate-binding protein	2303
1.129542828	(GroL) 60 kDa chaperonin	2222
1.097011606	TIR domain protein	3531
1.083708713	(ProS) Proline--tRNA ligase	2076
1.082418934	Uncharacterized protein	5858
1.040463368	(RaiA) Ribosomal subunit interface protein	2827
1.04030482	(DnaK) Chaperone protein DnaK	3714
1.000633935	(PyrE) Orotate phosphoribosyltransferase	4168
0.982752616	Uncharacterized methyltransferase	3648

8.2. RNAseq

8.2.1. RNAseq – Exponential Phase

Table.8.11. Genes more highly expressed at 25 °C compared to 37 °C in *B. cereus* G9241 growing exponentially. Cut-off >log2-fold =0.43 / >1.5-fold change.

Gene Loci (AQ16_)	Log2-fold Change
4300	6.426025364
1507	3.4906425
831	3.207420105
1368	3.197240886
175	2.774796071
4418	2.743774661
1559	2.65492016
1816	2.48974871
2611	2.434478763
2573	2.357422554
555	2.341751361
2780	2.319179041
830	2.29315513
2781	2.26192473
3545	2.195750569
619	2.170012049
2572	2.168437817
827	2.164805988
2660	2.132691521
174	2.125948607
3194	2.090416533
4834	2.080167682
828	2.033724962
2940	1.984829694
5317	1.959934642
1823	1.93513541
5746	1.930677331
2787	1.92398155
1938	1.910415253
3196	1.867569498
829	1.864363633
2786	1.859046605
1392	1.845366405
620	1.84146153
962	1.838045569
4548	1.837336825
1557	1.819577459
3797	1.814286461
516	1.807511376
5773	1.773952414
2668	1.768658634
464	1.754662666
862	1.748746131
2944	1.738145877
3437	1.734507656
1209	1.718435671
4550	1.711625885
1553	1.710188863
3277	1.693968498
1915	1.690162782
2825	1.641163706
2775	1.634328804
2908	1.628070194
3354	1.62727669
1650	1.611262761
660	1.610916085
4696	1.600067422
2267	1.594979576
1562	1.570628593
3341	1.569392047
1818	1.568495257
5658	1.568127394
311	1.564002117
1364	1.551083307
2194	1.548890498
801	1.527630694
813	1.511631423
998	1.506073353
1558	1.492641601
935	1.491514402
244	1.482985412
2899	1.482001695
4413	1.475646229
2773	1.474781302
3890	1.45221465
1811	1.452196624
3996	1.446416975
1827	1.441860603
3813	1.439900882
2106	1.433741348
245	1.420409085
659	1.418763731

2213	1.417532104
3059	1.41222979
465	1.410827182
5237	1.408313693
5631	1.403513935
1568	1.399190765
255	1.393877287
3490	1.393022762
3262	1.389552461
4408	1.385861715
3993	1.381809821
1390	1.379957621
723	1.37446754
1437	1.367284114
877	1.364756782
4319	1.350904185
833	1.348470435
1150	1.343956226
2435	1.337411894
1898	1.331253672
5075	1.330696096
1405	1.329341737
1548	1.325431615
5147	1.317546035
1563	1.314201706
2774	1.309660847
3123	1.305489587
3195	1.301295613
3523	1.300609786
4848	1.296334858
1168	1.292273215
2606	1.286187039
4417	1.284083731
542	1.281338475
4726	1.276053555
3222	1.273446352
4409	1.27236039

5049	1.267306276
3892	1.266561187
5201	1.260346322
2970	1.257129355
5362	1.254151402
5093	1.227355703
1942	1.22256502
3814	1.221118624
312	1.220313498
1574	1.217842281
2436	1.206975697
4065	1.195028181
5306	1.194590529
880	1.193761139
5314	1.190859863
1755	1.187209507
5364	1.185058219
1072	1.183034242
811	1.178523473
3092	1.175535769
5675	1.168531198
4531	1.167354794
5504	1.165344056
2794	1.162058438
2241	1.161104963
786	1.157270017
3489	1.155576626
1772	1.155384101
5788	1.152429834
5386	1.152398865
2485	1.151815266
1820	1.148150998
1564	1.142828721
1098	1.141749316
1824	1.141086076
3758	1.138304213
1567	1.13676001

4710	1.136453724
2779	1.134873409
3506	1.134048729
732	1.131052104
1550	1.12994415
1584	1.127217452
32	1.125070373
4707	1.125060157
214	1.123849268
4790	1.122027892
4439	1.120323612
2433	1.11821522
1770	1.114947996
3187	1.112573179
3891	1.109675636
2577	1.104754639
658	1.102492782
800	1.101267763
4376	1.100603063
2269	1.099340562
1593	1.087572728
1417	1.082801359
260	1.081000663
3090	1.080966129
347	1.080516302
257	1.080330229
118	1.076460428
2294	1.076194531
3460	1.070870868
3049	1.069116158
618	1.06880922
4754	1.063993347
2790	1.059734838
2239	1.05379164
5357	1.052410367
1151	1.051555748
1893	1.051458717

4401	1.04955713
4957	1.049477225
675	1.046612795
3514	1.043745093
3960	1.042962397
434	1.041467299
1489	1.039363298
3190	1.038448748
3094	1.037686198
3777	1.036399303
812	1.035452521
5599	1.035260003
3047	1.035260003
130	1.035260003
4578	1.034235903
760	1.032285229
802	1.030637934
1822	1.025770047
3347	1.02471863
4102	1.024179803
5803	1.014704903
4671	1.009556807
271	1.009214575
1904	1.008665034
3463	1.007904479
4281	1.007297897
123	1.007228137
531	1.006911729
3060	1.006399767
5274	1.004840955
2242	1.003734684
1560	1.001147828
2922	0.999975187
4400	0.999447162
4249	0.998395493
2963	0.996312519
999	0.996101889

1345	0.996069464
5028	0.993613304
2240	0.990661873
1504	0.988790202
503	0.9876896
4063	0.984917456
1984	0.983016948
2110	0.98083747
310	0.980515685
4159	0.980451612
5805	0.976556194
4061	0.972504202
4174	0.970680774
4207	0.969437156
1469	0.965933547
4549	0.965143013
2570	0.960016282
1865	0.95637859
5470	0.956265433
1773	0.955911366
1756	0.946627962
4398	0.942230167
2287	0.939125844
4764	0.934181344
1932	0.934032203
4026	0.932556351
4854	0.930818885
2462	0.930135398
4809	0.925395688
3857	0.925038708
5048	0.922912179
5214	0.922903827
1573	0.919673296
540	0.911756604
2232	0.909544943
1428	0.907549305
5663	0.906510863

1554	0.902738116
3093	0.901526043
4396	0.900761992
2245	0.89831445
107	0.897194128
1768	0.893232884
3235	0.880148556
4042	0.878335171
2251	0.873373966
1769	0.87301576
4095	0.872712583
103	0.872639267
4611	0.871957814
4651	0.87060085
2271	0.8672994
3447	0.859388589
3989	0.856457182
3611	0.856292016
4277	0.853747591
2409	0.852529379
2669	0.84739611
2883	0.845860009
3043	0.844696362
1365	0.841235502
1454	0.837242382
2613	0.830750393
1981	0.82492166
897	0.821575349
4975	0.821529935
1897	0.82138856
2532	0.820307372
1511	0.820271543
1973	0.820130947
2463	0.81687557
4598	0.816282002
1312	0.814925258
5636	0.814140526

1388	0.814103675
2432	0.813480905
3953	0.805245072
4632	0.804546848
3868	0.804106469
4251	0.802850283
2662	0.802101605
4118	0.798041874
4348	0.797914974
2767	0.797167784
3985	0.79708022
1707	0.795193032
672	0.793321566
135	0.793136732
3282	0.785707292
4829	0.779169073
5436	0.779112306
2022	0.775441668
2252	0.772309224
3495	0.770634305
3507	0.770214596
3982	0.769149304
2680	0.765558045
2177	0.765443002
3987	0.761786347
3168	0.758076088
2057	0.757886225
5213	0.757231185
2258	0.756330632
1319	0.756139132
4305	0.751063649
1338	0.749393773
3281	0.747085446
5148	0.744724324
4608	0.743831557
1796	0.742922553
4607	0.740735231

3774	0.738350099
714	0.737573268
5622	0.730226465
4098	0.730221454
1153	0.729076032
2966	0.725742471
2687	0.725109785
3273	0.723574623
593	0.72164307
4789	0.71850255
101	0.715945027
502	0.715226436
3494	0.713036042
1874	0.71083065
4008	0.710713742
4353	0.708316075
5569	0.705413253
1589	0.703720237
855	0.702666538
1269	0.70176412
2534	0.701334073
2161	0.698730281
5482	0.690306768
3990	0.689129341
4335	0.687177849
3638	0.686617754
3555	0.684126829
2604	0.683367546
4354	0.674615149
475	0.674347463
3796	0.671413881
1389	0.669380209
1304	0.667227542
210	0.666282409
509	0.665845186
4053	0.661437408
2408	0.660895742

3710	0.659901436
4402	0.657654722
4344	0.656239023
2425	0.65530793
4377	0.650593436
2566	0.650312481
4107	0.65019007
327	0.649887241
2691	0.648913137
4781	0.648672516
3646	0.647350062
3415	0.647273532
2926	0.647234033
1998	0.647025244
500	0.644892125
4533	0.643944198
3201	0.642784527
3615	0.642036333
3508	0.639419213
5469	0.636156815
1430	0.633734311
5091	0.631255854
305	0.628299177
2589	0.622883309
2579	0.622793479
3286	0.621499819
972	0.619506298
671	0.61624417
2418	0.615727053
3792	0.615682307
4060	0.61197281
911	0.610070055
2874	0.609674452
1019	0.608021148
1442	0.606148793
826	0.60592165
3685	0.603442826

3462	0.601684997
4204	0.601452141
5073	0.599797029
2667	0.598648098
3391	0.595606421
2419	0.594192346
2533	0.588471763
1842	0.581562767
3556	0.581236115
4075	0.577619666
339	0.574895227

4113	0.570120561
1302	0.569038855
3734	0.567832746
1011	0.552488552
2070	0.546936636
2476	0.539560957
3740	0.535052611
4211	0.534160308
3723	0.531931816
2147	0.530438139
1889	0.520918479

4260	0.512861397
1431	0.506154599
2690	0.492850866
4350	0.492406649
3492	0.482499584
2482	0.472987692
2176	0.472889632
429	0.461591972
4212	0.430032987

Table.8.12. Genes more highly expressed at 37 °C compared to 25 °C in *B. cereus* G9241 growing exponentially. Cut-off >log2-fold =0.43 / >1.5-fold change.

Gene Loci (AQ16_)	Log2-fold Change
5898	3.724488704
5899	3.597376511
5835	3.4412312
4297	3.203024054
5861	3.10687823
5822	3.081539276
2331	2.979234183
5820	2.971489331
5827	2.931744076
5863	2.766260197
5895	2.745238044
5821	2.72631625
5832	2.680517191
5828	2.657601632
5833	2.63779722
5824	2.591479079
5825	2.588314204
5855	2.579750968
5826	2.501977172
5894	2.48301976
5896	2.441609876
5860	2.40154618
5834	2.39090162
3652	2.359554279
5856	2.296990498
5893	2.293664294
5600	2.256945217
2699	2.254378408
3075	2.236382275
5819	2.219973439
3111	2.192582433
1184	2.191857341
5859	2.162166896
5830	2.143252482
5839	2.135242308
5836	2.120682512
1185	2.112210373
1181	2.089523262
5831	2.074127948
2025	2.073578005
5829	2.060761377
2982	2.020247098
1892	1.979315436
5823	1.97459617
5854	1.962808308
2799	1.953014228
4939	1.948967519
392	1.931414488
229	1.873646579
5870	1.846860346
5852	1.793606683
3373	1.770792455
5178	1.729333768
5292	1.724409082
5838	1.713282672
3929	1.712329204
4802	1.695481291
967	1.67959958
5702	1.669371281
1923	1.668245085
3310	1.661523636
4656	1.659533668
2736	1.658765735
2951	1.649374124
5880	1.640134251
318	1.637255109
1679	1.636843257
2583	1.619109373
3530	1.613404129
968	1.595399794
3676	1.593963255
3137	1.588428854
2965	1.575694884
3009	1.575126442
4927	1.568627757
3546	1.565868871
1374	1.557532623
3215	1.55565597
5864	1.545752901
4989	1.545538343
3217	1.52892423
2448	1.52855474
4808	1.520702871
3189	1.516718311
5850	1.509467974
4647	1.508528388
5882	1.506415289
4944	1.502786957
2328	1.501786703
2789	1.495612534
1537	1.485065687
1922	1.475590102
615	1.47267912
3218	1.472503136
5865	1.471581769
5714	1.469489262
3380	1.44926007

4682	1.444031772
5837	1.435001297
1494	1.426227944
3922	1.423158476
2981	1.420967316
510	1.419908614
4987	1.415173153
1713	1.409947371
3919	1.406560827
5678	1.402632243
4921	1.40009589
4472	1.396462562
4037	1.396222261
1186	1.396211487
4623	1.394060566
3459	1.388900124
5700	1.37665132
5883	1.367796065
2952	1.364544672
5540	1.35073352
4867	1.349997888
4891	1.349993845
3781	1.347728745
4687	1.345793485
5039	1.342164594
1802	1.340816393
3312	1.339810515
3782	1.336108814
2303	1.332247072
2776	1.332132602
4586	1.328676229
5346	1.32252851
4968	1.320783906
5558	1.319927752
5160	1.315976657
5498	1.312751387
2330	1.306817301

5194	1.305973238
4967	1.305681949
4433	1.304749816
1157	1.304482688
419	1.299805531
1621	1.295238756
1833	1.292713706
3394	1.283653605
39	1.279852322
4890	1.278342011
1183	1.276963158
1831	1.276213324
1975	1.276201908
3076	1.275550074
2103	1.275308927
1162	1.272851457
96	1.27272595
753	1.272299075
5063	1.270428112
1907	1.264853155
4499	1.260129884
1647	1.260057792
2447	1.259981104
1538	1.25869137
4051	1.257408351
4516	1.255845706
5050	1.252750989
956	1.250919912
4604	1.249312077
5047	1.247580624
4429	1.246108667
3537	1.244087868
425	1.243695333
1206	1.243089431
1182	1.22240173
2329	1.220036999
669	1.217044213

74	1.216233725
5868	1.214951958
5705	1.210312958
3714	1.209970988
4855	1.208754091
2053	1.205023976
4486	1.204046487
1488	1.202942755
568	1.200281918
460	1.197683685
4881	1.194659195
1601	1.186725753
3297	1.184698983
2841	1.182958479
4954	1.179662074
4741	1.178722982
4650	1.176032291
4906	1.170473754
769	1.169551148
5807	1.169291823
3677	1.168391773
2184	1.168153842
3666	1.164439108
5538	1.164192433
5052	1.159850611
1503	1.158396324
957	1.155209621
5539	1.151463241
1238	1.149966815
3613	1.148767889
3930	1.147438117
4889	1.146550613
1457	1.145040468
4713	1.144441686
3807	1.142680091
4853	1.139757634
1093	1.138679661

626	1.138239819
2040	1.138104301
1028	1.134070273
663	1.133041051
5866	1.130443384
4271	1.129014829
4801	1.127430434
5662	1.125324425
1950	1.124341028
4758	1.123292909
2304	1.121141394
3713	1.11575182
3381	1.114148987
4033	1.113103563
4374	1.110459628
3420	1.108680004
1451	1.107108766
2584	1.103735219
5844	1.103490665
5120	1.103096518
3715	1.100956938
5541	1.100141324
2735	1.100137319
5897	1.099811871
2195	1.099648322
5703	1.096836412
4956	1.092982343
797	1.09106167
2309	1.090372389
1262	1.086363077
2449	1.08552749
374	1.076497248
5741	1.075347045
3943	1.07474109
1832	1.070563453
5190	1.06862331
742	1.068533262

5040	1.068471306
5513	1.060153665
364	1.057876208
1013	1.056730183
1411	1.055656552
3660	1.054745306
5677	1.052849426
3167	1.047676109
3356	1.046417056
370	1.044994562
4859	1.041161614
1192	1.040999884
5851	1.040479992
5846	1.037331573
2844	1.033013232
2612	1.027662857
3675	1.024562157
188	1.024391138
2827	1.023605156
1446	1.020637343
5228	1.017715753
1912	1.015764949
405	1.015304682
5118	1.015128885
2716	1.009401599
5858	1.001719466
3204	0.998409986
1201	0.997888793
1202	0.997340937
4232	0.995133598
1337	0.992677152
2275	0.990485663
4195	0.990348181
2451	0.990076834
1570	0.989085611
3704	0.988212336
5535	0.988148751

5534	0.98795876
459	0.987835077
5055	0.985081615
2139	0.98225604
5739	0.979222498
4714	0.976065407
5711	0.972523429
5054	0.970981488
3641	0.970012441
3483	0.969550089
2826	0.968061771
1594	0.961079487
2138	0.960867175
923	0.958763488
5701	0.957714122
5394	0.953149297
958	0.951635878
5509	0.950484458
2374	0.945568711
955	0.939893403
1318	0.939472078
770	0.937772874
1246	0.93699281
2452	0.936652987
424	0.935946065
4104	0.935037046
918	0.93478941
5740	0.934381104
740	0.934266865
1970	0.933108727
3629	0.926407425
4214	0.919286592
2094	0.918928259
4737	0.916940485
197	0.916407833
738	0.913882468
1528	0.911540469

2446	0.910446669
4285	0.907607554
2223	0.906951098
77	0.905769877
5765	0.903594289
4888	0.903289564
4267	0.892101387
2953	0.88923102
2927	0.888228665
2420	0.883280018
1471	0.882474955
307	0.874129527
5242	0.874004824
5699	0.871159459
2222	0.864335513
1860	0.863481684
4141	0.859020225
5712	0.855949165
2254	0.854523719
2620	0.850694343
3869	0.849575492
2686	0.848047421
3057	0.841961139
2091	0.833106689
4709	0.826361892
1789	0.815940705
420	0.814106672
4284	0.811795301
2621	0.803388368
3128	0.797659486
3767	0.790516847
917	0.790284391
1502	0.787157109
3674	0.780545396
4055	0.779957361
1481	0.779292781
512	0.777548555

178	0.77665601
5051	0.77547766
3737	0.773973858
4929	0.768388134
2063	0.76588157
1518	0.759188144
889	0.756044519
3640	0.755553559
2714	0.755223169
2076	0.751665955
3778	0.75065104
2910	0.75003304
4029	0.749215811
4760	0.745601326
1906	0.745564862
3918	0.743708371
1207	0.742061721
2049	0.739250443
1144	0.737977341
5146	0.733169928
1203	0.730566741
1883	0.728360449
4215	0.724569476
5849	0.724133168
228	0.720233649
3531	0.718494217
3484	0.715398573
3334	0.709448722
4419	0.706609497
1619	0.705508271
2467	0.703057713
5724	0.69571851
1718	0.68794643
1612	0.683881187
2516	0.675701251
4044	0.671866016
3421	0.668576051

3270	0.661101338
2587	0.657130449
3322	0.656214547
2143	0.653231818
1719	0.645547069
2421	0.642183093
1266	0.638463224
2444	0.637926469
4122	0.630665557
1819	0.630108728
1010	0.628685183
2607	0.625960852
928	0.623741018
2702	0.616655035
1265	0.614021076
4071	0.607368249
2276	0.60452664
1200	0.602665162
4140	0.601651488
2638	0.601322783
1418	0.600196259
2542	0.596036358
1180	0.592107423
4351	0.58986405
3250	0.581107653
4757	0.578587357
1449	0.57782193
5734	0.574243286
1426	0.569962541
2035	0.569296041
912	0.564287076
5016	0.556762226
4940	0.556049922
2909	0.538560601
3820	0.514002493
2187	0.510300077
2832	0.504793692

301	0.504478591
3541	0.498616054
4518	0.493923366
1788	0.480523149
3832	0.460282381
3540	0.433762203
3780	0.302503581

8.2.1.1. Exponential Phase – pBFH_1

Table.8.13. pBFH_1 genes up at 37 °C compared to 25 °C in *B. cereus* G9241 during mid exponential growth.

Log2-Fold Change	Gene Details	Gene Loci (AQ16_)
2.219973439	Phage minor capsid 2 family protein	5819
2.971489331	Hypothetical protein*	5820
2.72631625	Hypothetical protein*	5821
3.081539276	Gp49 superfamily	5822
1.97459617	Peptidase M23 superfamily	5823
2.591479079	Putative phage major capsid protein	5824
2.588314204	Molybdopterin -binding superfamily	5825
2.501977172	Putative protein Gp8	5826
2.931744076	Minor capsid family protein	5827
2.657601632	Minor capsid family protein	5828
2.060761377	Hypothetical protein**	5829
2.143252482	Minor capsid from bacteriophage family protein	5830
2.074127948	Putative major capsid protein Gpp	5831
2.680517191	Putative gp14-like protein	5832
2.63779722	Bacteriophage Gp15 family protein	5833
2.39090162	Putative membrane protein	5834
3.4412312	Phage tail family protein	5835
2.120682512	Phage tail protein with endopeptidase activity	5836
1.435001297	Hemolysin XhlA family protein	5837
1.713282672	Hypothetical protein	5838
2.135242308	N-acetylmuramoyl-L-alanine amidase family protein	5839
1.015622275	Phage regulatory, Rha family protein	5840
0.305125109	MerR family transcriptional regulators	5841
0.484308022	YolD superfamily	5842
0.892874869	SoxR (MerR superfamily)	5843
1.103490665	Hypothetical protein	5844
0.589539533	Hypothetical protein	5845
1.037331573	4Fe-4S iron sulfur cluster binding s, nifh/frxc family protein	5846
0.111054388	Hypothetical protein	5847
0.374462756	Hypothetical protein	5848

0.724133168	99% sequence identity to telomeric repeat-binding factor 2 of Streptococcus pneumoniae	5849
1.509467974	Xre superfamily transcriptional regulator	5850
1.040479992	Hypothetical protein	5851
1.793606683	Putative DNA polymerase III, delta prime chain	5852
0.299710729	Xre superfamily transcriptional regulator	5853
1.962808308	Helix-turn-helix family protein	5854
2.579750968	Phage antirepressor KilAC domain protein	5855
2.296990498	Putative membrane protein	5856
0.676634273	Hypothetical protein	5857
1.001719466	Periplasmic binding protein type 2	5858
2.162166896	Hypothetical protein	5859
2.40154618	Hypothetical protein	5860
3.10687823	Transposase, IS605 OrfB family	5861
0.232816658	KTSC superfamily (RNA binding)	5862
2.766260197	Hypothetical protein***	5863
1.545752901	Hypothetical protein	5864
1.471581769	NUMOD4 motif family protein	5865
1.130443384	Hypothetical protein	5866
1.044253462	Hypothetical protein	5867
1.214951958	ERF superfamily protein	5868
0.868734229	Hypothetical protein	5869
1.846860346	DnaD domain protein	5870
0.31652832	IstB-like ATP binding family protein (DnaC superfamily)	5871
0.522558441	Hypothetical protein	5872
0.399079645	Hypothetical protein Contains P loop NTPase domain	5873
0.620822474	Hypothetical protein	5874
0.738096013	Hypothetical protein	5875
0.815881211	Hypothetical protein	5876
0.918677965	Hypothetical protein	5877
-0.226211166	Fur regulated basic protein A	5878
0.466114936	Hypothetical protein	5879
1.640134251	Hypothetical protein	5880
0.825683402	NrdH or GrxC thioredoxin like superfamily	5881
1.506415289	Peptidase, M23/M37 family	5882
1.367796065	Dutpase family protein	5883
0.692395602	Hypothetical protein	5884

1.097361259	Putative membrane protein	5885
0.743679161	Hypothetical protein	5886
0.050992199	Hypothetical protein***	5887
0.276871207	Hypothetical protein	5888
0.480132296	Hypothetical protein	5889
1.051548828	Hypothetical protein	5890
0.169736177	Hypothetical protein	5891
1.120518871	arpU putative autolysin regulatory protein superfamily	5892
2.293664294	Hypothetical protein	5893
2.48301976	Hypothetical protein	5894
2.745238044	Putative membrane protein	5895
2.441609876	Hypothetical protein	5896
1.099811871	Phage integrase family protein	5897
3.724488704	ATPase subunit of terminase family protein	5898
3.597376511	Phage terminase, large subunit, PBSX family	5899

8.2.2. RNAseq – Stationary Phase

Table.8.14. Genes more highly expressed at 25 °C compared to 37 °C in *B. cereus* G9241 during stationary phase growth. Cut-off >log2-fold=2 / >4-fold change.

Gene Loci (AQ16_)	Log2-fold Change
1786	7.223933058
1785	6.976541981
1784	6.272073052
3754	5.613046782
4380	5.518246546
3757	5.097412761
2653	4.967976495
3755	4.816781827
828	4.809999969
1558	4.701152296
827	4.691722844
1816	4.674855155
5436	4.669702625
3319	4.614620022
1907	4.602606607
1811	4.587956474
1167	4.560971775
3756	4.549816367
2985	4.484257417
3634	4.321893764
3683	4.270928017
1804	4.205808893
3780	4.203291633
1805	4.20147975
1583	4.187834409
3942	4.177308357
5133	4.131786715
419	4.103526528
1827	4.077753018
1650	4.061428612
1087	3.990771345
175	3.98717161
481	3.933675822
1368	3.931484841
4956	3.920629333
3526	3.885575519
5132	3.869549966
781	3.845371137
4341	3.84162183
15	3.81698189
2923	3.797224202
3682	3.791040616
5134	3.783423454
3524	3.730465845
3758	3.711028908
253	3.687974799
2846	3.666877673
1065	3.645942584
2301	3.641268323
2088	3.637474775
3638	3.602768366
1160	3.602081625
5656	3.575708641
4418	3.56360039
3320	3.544283956
425	3.538024819
5240	3.527902481
1166	3.514088032
4083	3.504984534
3049	3.504940137
230	3.500698209
5131	3.45865853
1332	3.452525676
1187	3.445745741
1222	3.425420018
1370	3.414328824
171	3.388141432
2276	3.366357376
1481	3.340820778
4118	3.337823007
1557	3.336686803
1486	3.329298756
4382	3.326427317
1906	3.323374703
252	3.305398197
1088	3.291914383
3277	3.277217959
1092	3.260174326
830	3.252365464
255	3.242056431
1515	3.233724404
4494	3.227707069
1559	3.218247149
3169	3.183105774
109	3.170054172
3991	3.149682318
3891	3.13286642
795	3.124394882
1036	3.123400629
1935	3.119796158
3545	3.106955921

782	3.09545824
1915	3.094428753
4618	3.091315648
3359	3.090456549
5158	3.081162488
758	3.077081337
424	3.076029558
1388	3.054792248
111	3.054393698
3030	3.050157524
5282	3.041669771
1089	3.020208127
1543	3.013440472
3166	3.012626981
4614	3.006721642
2087	3.001060088
4381	2.98017578
4654	2.957461933
4772	2.954336202
1211	2.952279462
1371	2.952227811
1032	2.946118809
2050	2.945118432
3768	2.930048395
4370	2.92180298
4003	2.920936889
2202	2.919498472
1056	2.913525541
3892	2.911489986
1326	2.909433423
1210	2.905516221
1507	2.904602205
1164	2.901004767
5345	2.899238833
3793	2.883936888
1797	2.879401134
1161	2.87062371

869	2.844602029
2583	2.836717479
2908	2.819006668
3798	2.801740924
3336	2.796527505
1090	2.793812262
5074	2.792284176
1619	2.78672147
1517	2.786199852
1504	2.779465939
2145	2.775633999
5398	2.76639652
1068	2.75890921
4396	2.750599326
4544	2.749436262
3422	2.747606295
4770	2.741109383
1333	2.737821907
4345	2.727748373
1692	2.72180565
794	2.718963658
3504	2.716473145
4056	2.700688233
4543	2.696483963
1645	2.693831217
1365	2.692745628
889	2.691592001
4710	2.689518646
4670	2.682630737
4214	2.675725172
1554	2.674903893
1568	2.669103952
2106	2.666251733
3377	2.664885773
829	2.659085147
440	2.657267708
515	2.656707247

3192	2.656106892
731	2.65458996
3432	2.653139426
1162	2.652658067
3335	2.639932193
3879	2.639619722
1589	2.638029795
1553	2.631479593
5493	2.62566693
1067	2.623403403
1132	2.617521529
1469	2.609623735
3960	2.608893826
1165	2.608400385
3648	2.605580973
4588	2.60539921
3529	2.601092823
3597	2.598348029
5011	2.595921902
5364	2.591516765
3651	2.588586245
4632	2.573076482
3749	2.572813922
3367	2.571821529
357	2.569658017
4053	2.551085282
3113	2.543357093
4063	2.537426143
4857	2.533547401
2780	2.533099307
5213	2.532176381
3722	2.531773444
449	2.531289277
684	2.530485083
1055	2.511222613
580	2.5108515
3878	2.50054038

4020	2.497873849
5357	2.497245701
3144	2.494802565
4101	2.487771604
4875	2.473699766
936	2.472410551
3503	2.465939258
2287	2.465141129
5684	2.457191129
3044	2.45231952
3081	2.450033647
5163	2.449757341
5230	2.440904712
4668	2.439645259
1918	2.437942855
4541	2.433977023
3502	2.433945392
2960	2.431598961
341	2.425596769
5313	2.415288764
4021	2.408769797
724	2.406412502
1508	2.395061487
4976	2.394441686
3527	2.394081742
5214	2.387252274
509	2.384163833
2485	2.382525041
5260	2.381295484
1938	2.376529964
5855	2.373393075
910	2.369406025
1094	2.366495251
3928	2.360819883
522	2.354025324
1128	2.347974921
3472	2.337011998

1103	2.335831961
2123	2.334794543
2147	2.331415964
2696	2.331205057
1163	2.320410068
4473	2.319132966
1914	2.31630382
4052	2.315437572
4432	2.312449138
1711	2.312194128
1095	2.309477563
630	2.309098948
548	2.30464673
1852	2.302138761
5376	2.296466544
1235	2.295820076
4771	2.295372295
511	2.295325014
2296	2.29494548
3298	2.294782976
3481	2.291026839
5075	2.280853079
3636	2.279530306
3767	2.275741016
1534	2.271024678
1476	2.266834559
3480	2.257050494
1644	2.254599708
1649	2.247652085
4277	2.242161463
3177	2.242048248
1306	2.239978449
1209	2.237811377
4042	2.234543893
700	2.23390522
3111	2.233713742
683	2.232991042

4032	2.228612482
3598	2.223812737
107	2.221903921
1493	2.215009098
3637	2.214820004
1091	2.208970058
3483	2.204474956
5157	2.204301236
5130	2.204241886
2916	2.203569412
4676	2.201974773
3621	2.193450942
3965	2.188636109
3323	2.183435308
1849	2.182969295
2668	2.18197599
216	2.179475138
5244	2.177953901
2737	2.174438755
5838	2.170499233
108	2.169481908
379	2.161852258
4523	2.160938652
463	2.159421987
5052	2.152439206
1902	2.150082584
1389	2.149613676
2624	2.148661016
790	2.148474999
5013	2.148447697
3406	2.147722421
1622	2.147264038
784	2.144518757
783	2.14315607
2134	2.142107596
3944	2.141452997
1173	2.139401825

5358	2.134974629
3354	2.134615736
3464	2.131043527
2669	2.123338222
4379	2.121945647
273	2.121362833
4876	2.121206441
1179	2.119528882
5719	2.117398974
124	2.11666597
873	2.114941311
3691	2.1113632
4383	2.11038211
3168	2.104518008
4485	2.102096769
5346	2.097932737
1678	2.095751402
3723	2.090626832
4712	2.083460458
2736	2.077948635
3794	2.077400972
1967	2.076098471
113	2.071318451
618	2.071228653
5167	2.058611769
3957	2.056870809
32	2.053369999
4598	2.05125365
1029	2.050744288
792	2.049941133
763	2.046489705
5135	2.042765222
4002	2.040436862
4982	2.038787352
3375	2.037252662
3341	2.034258825
2896	2.032822723
3329	2.031204176
2929	2.028901662
1302	2.027404016
418	2.023641389
1617	2.023525513
526	2.022545061
646	2.021038562
3536	2.020251216
1237	2.017553075
2356	2.017067524
3728	2.015247523
4378	2.013943748
1588	2.011727727
1854	2.004162408
2932	2.004008639
677	2.003757972

Table.8.15. Genes more highly expressed at 37 °C compared to 25 °C in *B. cereus* G9241 during stationary phase growth. Cut-off >log2-fold=2 / >4-fold change.

Gene Loci (AQ16_)	Log2-fold Change
4594	7.682071
5407	6.830198
4595	6.691393
2024	6.61633
414	6.569605
2025	6.412805
5336	6.084666
3594	5.667393
392	5.56417
3189	5.502147
1488	5.44881
318	5.3745
3592	5.328758
2089	5.310496
4464	5.1764
5335	5.17441
4915	5.102016
5768	5.088541
3593	5.066897
413	4.868047
4322	4.746501
393	4.5671
404	4.52706
5309	4.500289
3188	4.478973
1181	4.420191
3700	4.35231
5281	4.32731
4524	4.309824
412	4.299244
4914	4.244703
387	4.20947
4741	4.195289
2331	4.124658
5535	4.090542
369	4.058379
3595	3.955413
227	3.954973
411	3.936433
4739	3.899379
2631	3.885395
5408	3.871371
5526	3.843265
4552	3.781698
1270	3.698323
773	3.691841
3677	3.658686
2630	3.636312
4923	3.608338
5228	3.600744
3539	3.566798
2982	3.53241
3657	3.504846
1686	3.493432
5540	3.469383
388	3.457303
403	3.409327
394	3.396918
1921	3.393658
5536	3.385304
5702	3.376762
4762	3.366446
1684	3.348613
589	3.337651
588	3.318169
1249	3.312567
5406	3.307544
3544	3.296342
214	3.291011
5067	3.278535
4546	3.261627
1724	3.255629
5701	3.252687
3676	3.250067
4037	3.247621
5404	3.243013
1040	3.231299
1591	3.229107
434	3.219147
1616	3.204816
5682	3.187516
4633	3.183388
1800	3.176112
2662	3.168181
3759	3.162043
5524	3.148437
5069	3.142608
1248	3.128221
1284	3.120731
1693	3.119117
395	3.10953
4490	3.096973
92	3.096009
1273	3.088784
5352	3.080027
2431	3.079696
5883	3.058016

5268	3.055803
221	3.043961
1799	3.031325
5539	3.030217
4505	3.026559
590	3.016397
405	2.992912
4924	2.985616
98	2.965051
3795	2.945836
525	2.943847
2016	2.924979
400	2.915911
3665	2.904314
1890	2.882401
4908	2.859865
952	2.857516
4905	2.832546
5525	2.828455
3837	2.822773
2028	2.822773
951	2.820265
402	2.817499
5354	2.810342
4910	2.809518
224	2.808858
97	2.794407
1801	2.783663
2943	2.778047
345	2.773374
4802	2.770358
275	2.759925
1826	2.758991
2799	2.75842
2740	2.756748
5065	2.753082
5483	2.751619

1714	2.746557
4935	2.745373
40	2.742821
4080	2.736235
1858	2.715268
1051	2.707472
4465	2.700952
5690	2.695707
4057	2.691789
2478	2.683812
4943	2.679728
5413	2.670917
4121	2.665399
396	2.665282
4421	2.662078
4081	2.657932
155	2.646721
3212	2.642728
3591	2.622653
5353	2.620742
4079	2.617947
3567	2.606133
5278	2.602827
5662	2.599456
147	2.592744
5068	2.590861
4909	2.588601
5864	2.588134
4941	2.584336
146	2.55506
14	2.549905
1439	2.547824
1761	2.538889
1518	2.533817
5321	2.526352
401	2.522542
2981	2.507843

139	2.507536
1320	2.501999
4547	2.501755
4732	2.498806
2727	2.491036
5297	2.490296
2873	2.488122
4927	2.4846
5872	2.482423
2053	2.472458
225	2.471932
950	2.465777
5484	2.454325
5522	2.44382
5606	2.443758
4551	2.437282
4078	2.433249
4077	2.427008
1082	2.423175
1028	2.42271
557	2.422202
524	2.416136
4897	2.41306
845	2.408591
3140	2.406443
920	2.404752
5071	2.394282
1723	2.38938
1759	2.389176
5066	2.386159
223	2.380631
2638	2.377901
1260	2.375568
3139	2.375451
2869	2.374113
5639	2.373604
1282	2.371027

2728	2.369866
3838	2.363591
3543	2.361934
3984	2.358328
655	2.351698
3090	2.350848
1081	2.349151
2723	2.343184
3560	2.340018
5781	2.334073
2974	2.328577
1859	2.327301
5217	2.32478
3491	2.318189
3344	2.316665
2067	2.316207
3558	2.315957
5477	2.310079
2432	2.301487
4460	2.294584
4918	2.294038
1464	2.292833
558	2.291341
4755	2.289636
4422	2.287006
5778	2.284364
1513	2.282746
797	2.273857
1798	2.269695
567	2.267502
4921	2.267008
1769	2.264525
5728	2.262165
3024	2.261709
603	2.259739
2203	2.258107
1772	2.257047

5070	2.255634
2499	2.253346
1223	2.251761
1520	2.251488
280	2.242654
1083	2.235427
2239	2.232659
1499	2.23061
3641	2.227904
5650	2.227879
2523	2.225186
2330	2.223942
3237	2.218206
1202	2.215183
3102	2.2129
2729	2.198034
2553	2.197632
2516	2.197576
5218	2.197223
4439	2.192718
1768	2.191397
2127	2.188142
4438	2.187281
1021	2.180838
5758	2.18019
4944	2.180002
1991	2.174258
4682	2.173629
1980	2.172295
5402	2.168373
2992	2.166047
2901	2.163448
5681	2.162136
334	2.159928
1286	2.157876
3428	2.156547
2726	2.154451

3559	2.148275
5705	2.147098
2458	2.146458
4940	2.144365
1022	2.144003
5176	2.138863
5216	2.138184
2791	2.137495
1981	2.137353
1666	2.135814
2039	2.134212
5730	2.13183
5200	2.126093
1773	2.125624
1982	2.124981
5057	2.121976
3104	2.121883
2015	2.120344
2341	2.117762
237	2.116482
1774	2.115777
4441	2.114153
986	2.10873
3655	2.104264
3352	2.101865
3093	2.101828
2152	2.100249
556	2.092595
5478	2.090964
1216	2.090352
5871	2.089389
4881	2.087883
4946	2.087396
2329	2.084898
1356	2.083326
1255	2.08268
3138	2.075839

3206	2.067028
4504	2.059753
1283	2.057775
5350	2.055175
5307	2.054694
3094	2.051829
1966	2.047609
776	2.042322
3185	2.042156
3404	2.041169

5215	2.040576
5443	2.039124
2766	2.033723
5680	2.032942
2243	2.031909
5829	2.031189
5863	2.027611
5691	2.024787
95	2.021986
1285	2.01877

4904	2.018617
3668	2.018487
2131	2.017493
1084	2.016435
2973	2.016359
2222	2.009819
2789	2.009326
1256	2.009046
1487	2.001156
2245	2.000044

8.2.3. RNAseq – 25 °C

Table.8.16. Genes more highly expressed during exponential growth compared to stationary phase growth at 25 °C in *B. cereus* G9241 Cut-off >log2-fold=4 / >16-fold change.

Gene Loci (AQ16_)	Log2-fold Change
2947	10.01830031
2948	9.371436051
3361	9.266026178
730	9.013952967
2782	8.829112064
2305	8.65739679
3821	8.509753911
1870	7.897813351
2145	7.835257792
1871	7.797975296
1724	7.725259706
2800	7.577200859
3059	7.576243112
764	7.435319714
2689	7.381363593
3495	7.301442544
4572	7.280756912
575	7.094688042
3218	7.036311897
729	7.033026049
3217	6.99005743
2922	6.983588583
2405	6.872324173
4396	6.83261407
3215	6.781532574
2963	6.701764418
2433	6.651189514
3092	6.642995577
1675	6.637068466
844	6.627718872
1770	6.627028356
2435	6.612506005
1837	6.594576484
1625	6.579641981
2436	6.547614506
3155	6.542657933
2036	6.494832162
1772	6.467991535
2611	6.448032884
1487	6.43597742
3090	6.418757486
2641	6.412812323
1773	6.372973429
2739	6.354865944
2404	6.346280629
3343	6.326388366
2110	6.313825126
3051	6.308451548
819	6.283013256
2035	6.280599431
893	6.263609049
3109	6.261236313
728	6.254719684
1201	6.246218519
2399	6.232425999
2431	6.219483105
845	6.170416474
820	6.16655915
3156	6.122758472
3101	6.112576444
3219	6.107242256
3453	6.100439041
3185	6.09925844
698	6.088719863
2395	6.079089031
4397	6.064316306
257	6.057299279
1439	6.049182545
1771	6.035305711
3216	6.034186406
2381	6.019798707
2634	5.964988645
2383	5.958974701
2398	5.942980583
2342	5.942402217
1817	5.940829508
2406	5.938474614
4671	5.90719395
2434	5.902297175
1757	5.894570438
1202	5.870518075
2242	5.851691461
3091	5.831753832
1769	5.830226954
2239	5.816495755
2575	5.809139274
5693	5.806845801
2382	5.798894001
312	5.796632985
2432	5.792029068
3444	5.785057361

2384	5.773746321
2403	5.767888816
3093	5.739569108
3249	5.73622407
2394	5.69955928
3196	5.699215335
1845	5.689914039
2297	5.686683385
2380	5.683275901
2392	5.676862111
145	5.647305894
841	5.643263944
846	5.639514922
2387	5.617022937
3248	5.61606233
818	5.605059241
4078	5.604022804
2386	5.598722408
3224	5.587918666
4527	5.580789834
1203	5.578801642
815	5.566747214
1200	5.556965136
2393	5.533580552
4933	5.530875453
3413	5.529946499
2388	5.529559614
2385	5.523620296
2407	5.522117553
842	5.468449663
2389	5.462517365
3886	5.438744468
2391	5.436475726
2097	5.423738007
2554	5.400039778
2545	5.395294906
2508	5.38775579

2572	5.38049456
2390	5.380046348
1097	5.370394965
3760	5.348229192
5147	5.324558826
2361	5.310803576
3094	5.309624251
4888	5.298822904
2509	5.268011082
2547	5.264958079
2546	5.24574741
5048	5.239648413
3740	5.233175604
2635	5.228112134
4079	5.227985606
840	5.216109546
5196	5.206170818
2258	5.20169673
2240	5.196799571
2511	5.195695895
3601	5.175708441
2510	5.174432998
2397	5.171107965
4427	5.157493491
3360	5.152281289
2294	5.106286896
822	5.088844717
1873	5.077076315
3430	5.0768665
2921	5.070837809
2637	5.069064479
1574	5.057814714
4349	5.001197516
817	4.994620649
2360	4.992350015
2705	4.985292926
1768	4.982235033

1934	4.971389736
434	4.960839082
3339	4.950047705
3123	4.932628555
4851	4.897669122
2571	4.884263703
3431	4.86724172
3741	4.859264386
2553	4.859014961
816	4.844037977
3640	4.84188011
2748	4.834672649
3429	4.833217421
174	4.808426242
850	4.79856844
3097	4.794320642
843	4.788473825
2374	4.782789916
3578	4.780839353
4192	4.77525358
3347	4.763208767
4348	4.752536968
3641	4.747569979
2529	4.742103538
2501	4.730613357
2556	4.729181948
1680	4.722602497
2362	4.704875473
4080	4.693703725
4552	4.682233285
821	4.668296544
2003	4.662697785
3579	4.66031622
2051	4.65554816
3993	4.632411958
2241	4.629527971
2859	4.618404798

2532	4.615771007
2531	4.612278821
3103	4.605637108
2319	4.595342029
4128	4.592888818
2213	4.585233202
2681	4.581902908
2373	4.567356562
825	4.559551831
2747	4.556194769
2598	4.555983516
655	4.548087377
2877	4.54053726
3293	4.537308398
3047	4.533966379
212	4.533966379
3621	4.531995299
3581	4.53179081
5053	4.528996016
2746	4.525840988
1704	4.524991277
2078	4.515197072
3491	4.506193288
2591	4.497913461
2376	4.497480177
1819	4.493082802
4081	4.487247098
2741	4.47757384
230	4.474389613
3286	4.47082825
4048	4.452377669
2631	4.449630384
823	4.419528324
4208	4.412977903
2613	4.410630892
1986	4.402303813
5290	4.400231779

4063	4.394529835
1597	4.387879327
860	4.374554664
2530	4.364542524
3108	4.359680037
2341	4.354722778
2773	4.349660053
851	4.324082095
2372	4.316021548
3392	4.3141412
672	4.306563208
3195	4.303502589
5747	4.297925478
4207	4.296355988
2375	4.286402912
1364	4.28098796
1392	4.277144309
3256	4.271462211
1979	4.242086024
2655	4.239631673
4940	4.23885804
2599	4.234794785
2780	4.232511524
3996	4.225425015
3168	4.223484449
2944	4.216809205
786	4.216114493
3247	4.214615553
2920	4.208340703
5235	4.206598898
4206	4.200993198
2632	4.199444826
2246	4.195315343
2144	4.188210726
2347	4.184968217
824	4.183109026
5148	4.177111923

3089	4.176173285
3177	4.175902903
2788	4.164677767
1806	4.16379321
1681	4.161081141
2408	4.160861968
3285	4.159221587
2592	4.156303137
2544	4.152316354
2650	4.133831465
2580	4.129082844
3686	4.124585805
4127	4.11327886
3443	4.110345371
4126	4.108009222
2379	4.105650474
4601	4.104686877
2378	4.100993548
4209	4.097375523
2377	4.097004933
4196	4.089634283
2589	4.089211355
2781	4.083055973
213	4.077318735
2630	4.07711624
2883	4.066818496
3986	4.061727989
3706	4.050856649
1682	4.050631333
2742	4.04219849
4168	4.039696324
2744	4.038701363
2371	4.036435388
3582	4.034364824
2340	4.033908237
4801	4.032431468
1232	4.017981612

Table.8.17. Genes more highly expressed during stationary phase growth compared to exponential growth at 25 °C in *B. cereus* G9241. Cut-off >log2-fold=6 / >64-fold change.

Gene Loci (AQ16_)	Log2-fold Change
243	13.62844213
74	12.64296858
284	12.38454335
238	12.27460285
5047	11.94672481
70	11.85408647
242	11.332252
71	11.32317186
2265	11.27845748
73	11.24174902
240	11.12520494
69	11.11156167
1455	11.10431849
5204	11.04800056
241	10.92315258
239	10.85960163
5203	10.85902041
2190	10.64722064
2152	10.58996859
72	10.54117045
4415	10.40923944
287	10.38660967
2214	10.33041335
2208	10.26831614
2108	10.26700243
2518	10.25550834
68	10.25025427
2196	10.244918
4414	10.22819913
2426	10.22362075
1172	10.20649606
4483	10.12614018
2264	9.995763873
3969	9.994129886
3968	9.922521768
1173	9.892476957
3086	9.853748897
4516	9.807128901
5202	9.799939647
1583	9.793099549
1543	9.781132756
2495	9.768457866
5292	9.664674842
2234	9.639367035
218	9.623595414
1209	9.583927045
2349	9.536104341
4342	9.50723062
4416	9.481328043
1206	9.451374176
2938	9.445110954
2107	9.387141089
3755	9.378098554
496	9.3776044
1993	9.309036732
296	9.29417561
967	9.242565377
1777	9.225135158
283	9.2064167
1093	9.164486606
4484	9.149469609
3334	9.129101703
5192	9.113289357
4566	9.073185482
1094	9.059091205
469	9.043485009
3205	9.021633401
2439	9.018184111
1598	8.956246418
470	8.955529163
4481	8.926666331
468	8.895449993
286	8.894204185
345	8.875867042
3901	8.862110595
968	8.84832697
3353	8.831260322
3346	8.812986375
5291	8.780985889
3970	8.727464435
5294	8.718946275
3083	8.687498175
1780	8.669258378
2524	8.64607405
3756	8.629438396
1211	8.616778235
2676	8.611666058
1174	8.609445092
2429	8.599167309
2151	8.585840001
2237	8.583599349
1453	8.580557842
1996	8.571708924
2352	8.571199912
4343	8.561594139
2217	8.547436527
2442	8.538223531

3967	8.533262201
4567	8.527527543
2350	8.513232441
3754	8.511807155
300	8.509436817
2199	8.505141614
4955	8.488573155
2500	8.482120955
1096	8.477927763
1176	8.456072027
2193	8.450938725
3900	8.450313807
3113	8.420841439
3479	8.413104814
2211	8.411639908
2191	8.410550323
4541	8.402198857
3085	8.400853871
2197	8.397680602
1778	8.388208964
1994	8.386926125
2520	8.373432932
1177	8.370594035
882	8.370141247
2496	8.369655782
2215	8.368925639
2440	8.356957188
4732	8.347748148
5843	8.342623745
4485	8.342137207
4808	8.336821873
2427	8.329109204
2263	8.32540165
289	8.315681004
3906	8.301685776
4013	8.283685362
2235	8.268045628

358	8.255853912
1091	8.254173028
2209	8.226573036
2674	8.217015818
3757	8.216167214
776	8.212217413
3116	8.211669507
1251	8.186407981
1088	8.16996428
290	8.139082127
2675	8.127667662
481	8.106583363
5293	8.062038666
1786	8.04912888
1095	8.028897202
2577	8.018801603
3478	7.972555853
2616	7.949224313
1212	7.932912543
1394	7.924133234
4394	7.913942408
385	7.897506726
2005	7.895324591
525	7.840544118
4970	7.833480266
4969	7.790795258
3114	7.789296559
969	7.776840673
1839	7.749957208
1902	7.683324225
5478	7.683177241
4540	7.671030371
781	7.665872188
1488	7.662189278
581	7.660711833
3384	7.647960848
4021	7.64586807

4968	7.626027963
1841	7.621358137
1678	7.620279234
3115	7.59555569
2150	7.587442847
5479	7.545530583
5276	7.529232272
1028	7.518544389
4971	7.514593983
4043	7.499645287
2617	7.486487019
2973	7.476940174
1205	7.460708534
1049	7.434467898
908	7.431527838
4100	7.404763543
2677	7.387284935
1087	7.381695247
4417	7.376854593
2974	7.356642929
4432	7.346200666
5501	7.334048435
3781	7.333162728
1838	7.323814066
1158	7.314912527
1089	7.283000967
3764	7.272198396
601	7.254092287
4911	7.245485612
5153	7.211046249
2734	7.207802979
338	7.196085881
5228	7.19318783
5281	7.19274269
4099	7.18575423
337	7.184772026
1092	7.169697538

5474	7.158578732
5511	7.137254711
2678	7.12917714
2009	7.125856327
427	7.125740691
2567	7.095445197
1492	7.080882467
1491	7.07336293
3971	7.067992681
3473	7.067266688
5050	7.04449195
5019	7.021536452
597	7.015687178
236	7.015602426
1175	7.009168702
4039	6.963344312
4486	6.909280708
4085	6.907100047
598	6.905980331
2975	6.888369578
689	6.864894261
4605	6.860197908
1840	6.855881391
2615	6.854775958
1398	6.846983675
3735	6.825849774
3009	6.816585485
3118	6.811146533
1807	6.802543696
4169	6.789660956
476	6.787666375
1024	6.784341199
872	6.755846131
1860	6.741928383
4112	6.733421637
2725	6.690528188
2089	6.677151991

599	6.666890867
4086	6.66584205
2153	6.661121624
288	6.631538496
4084	6.629352524
4413	6.626704708
3310	6.62600789
4515	6.612723472
1842	6.611669859
285	6.60488018
1151	6.59123413
3659	6.590606206
3008	6.567177896
1157	6.560057712
1677	6.558519986
2723	6.543471523
471	6.538694242
2109	6.535344081
3519	6.516760478
5390	6.498995054
1090	6.486562243
4009	6.4828312
4433	6.481773581
2784	6.476824319
4561	6.475150923
467	6.466447476
5160	6.448603599
4967	6.447474579
3770	6.444896202
2698	6.444512961
4049	6.417417069
870	6.407983807
909	6.401564693
4083	6.400474185
357	6.399735466
1210	6.370898616
29	6.362307653

1785	6.359613097
1167	6.353872564
4756	6.351327128
5057	6.349966975
4042	6.335907
346	6.325111618
4551	6.324241518
1025	6.316358445
792	6.291784121
626	6.289286759
3356	6.281361598
1110	6.247472246
983	6.246908277
600	6.243262418
2727	6.227288196
4739	6.212139491
4980	6.208559682
4146	6.201470245
683	6.196266845
687	6.19603328
367	6.177097577
1350	6.174228597
1434	6.170111218
415	6.161138624
4564	6.149227224
5199	6.147000344
3477	6.145477215
686	6.117508171
2167	6.115724376
3070	6.106567163
5768	6.105321974
5473	6.092778866
4865	6.092033201
5031	6.090405652
4145	6.082079185
2115	6.06529054
1373	6.049364721

5467	6.036273558
3929	6.035899504
5491	6.033864125
1784	6.032444351
3024	6.031804968
3475	6.029846105
4438	6.020506888
5353	6.005229306

8.2.3. RNAseq – 37 °C

Table.8.18. Genes more highly expressed during exponential growth compared to stationary phase growth at 37 °C in *B. cereus* G9241. Cut-off >log2-fold=4 / >16-fold change.

Gene Loci (AQ16_)	Log2-fold Change
2145	11.35868016
2947	11.25396206
3216	10.42413966
230	10.11655943
3217	9.957353103
3218	9.848374557
4396	9.372226508
4572	8.989025108
1870	8.939989343
3215	8.815405435
3821	8.709191057
893	8.424398714
2922	8.240567372
1871	8.236090279
2948	8.191550265
2305	8.124880839
1914	8.059785608
3249	7.916533114
2782	7.853138311
3219	7.788678525
2923	7.709201227
1675	7.535403149
1817	7.499771968
730	7.481170195
3248	7.394245105
2050	7.375512538
2571	7.345645209
3155	7.241410319
1837	7.238606894
2985	7.216688423
5894	7.184248542
2895	7.03521927
1625	6.989660174
764	6.976334916
3361	6.966423016
2800	6.958599464
1934	6.913908279
257	6.899091938
2383	6.889521092
2381	6.867684112
2296	6.857051757
3601	6.837344039
2653	6.782702715
3495	6.774180946
728	6.703503979
2380	6.696785503
2405	6.677514204
4397	6.656728373
1481	6.645030207
2739	6.626565549
2641	6.617273818
3059	6.605496495
2634	6.57429367
2382	6.561527402
575	6.498741521
3780	6.498140168
2963	6.49464379
1486	6.46650996
3177	6.459289779
1127	6.388002789
2386	6.371485726
5828	6.333709826
2385	6.328338179
3453	6.322955668
3335	6.308457287
5895	6.265629669
3166	6.262046641
1816	6.237324266
2384	6.200605832
3621	6.188040494
4063	6.166544145
5837	6.166092697
2511	6.164061789
2632	6.141281827
5831	6.124409915
2395	6.091788046
4614	6.074274513
851	6.042746703
2392	6.034487624
2403	6.028243168
4889	6.02315972
2390	6.017063138
3156	6.01417134
850	5.976433657
827	5.974809801
1128	5.968106032
2905	5.954530514
874	5.936410719
5896	5.918062806
2387	5.883603818
2389	5.883021351

1907	5.882129588
1918	5.855754254
828	5.85257434
5855	5.842589888
2746	5.836402154
2748	5.825914872
4671	5.809802773
5825	5.807900822
1201	5.806783214
5893	5.803166694
3168	5.796425508
3110	5.793378524
2301	5.776632617
3192	5.77642039
3123	5.774494455
145	5.760443476
3051	5.755296026
1819	5.748490927
3224	5.736732799
2287	5.732945077
5158	5.730524053
698	5.703860984
2394	5.703433734
1597	5.687143297
2388	5.680607074
2404	5.667951106
1879	5.650722844
2391	5.61355554
5656	5.575707935
1619	5.575448988
2699	5.569261595
5827	5.568168835
1618	5.567829166
2035	5.561837837
2510	5.560952614
854	5.559018616
2921	5.552483266

2110	5.531154022
4348	5.514057059
2689	5.510294423
5838	5.487937573
4062	5.485139069
729	5.479274015
2370	5.474838826
5898	5.466793277
1878	5.451362031
2485	5.438414169
4956	5.433495632
2393	5.430434818
2545	5.429114527
2745	5.419718783
3044	5.395137329
3119	5.389200109
3413	5.384670388
2508	5.364119086
4168	5.362320173
1923	5.349584569
3293	5.336980755
787	5.30194654
2962	5.293037505
5167	5.284925238
5856	5.244932638
5826	5.238067646
2168	5.22734778
1560	5.191272778
3524	5.176473553
2506	5.174319843
3648	5.169781972
2747	5.144869892
4192	5.128525528
3429	5.126832663
2399	5.122705345
5234	5.122122219
3430	5.118835061

2957	5.096445016
4378	5.095384648
1200	5.094742698
2376	5.087368963
3092	5.085572887
2359	5.082810511
4167	5.082333091
32	5.082326971
3339	5.07875228
2532	5.076134135
3741	5.067302556
842	5.06286199
3532	5.052886373
2061	5.045883814
1770	5.045682767
2433	5.042758799
2398	5.039325487
2693	5.033782809
3045	5.030656276
3991	5.029823674
852	5.023072854
2036	5.021460497
1681	5.000931632
3581	4.999974755
5819	4.994661329
2637	4.982203091
5260	4.978067913
5899	4.97099259
1680	4.954832352
841	4.953659111
4395	4.944060041
5600	4.942326141
823	4.941806745
3599	4.928146757
2598	4.895226848
1849	4.892257072
844	4.889401687

2123	4.880854949
3686	4.874039747
2147	4.865263493
1845	4.863694304
1203	4.862749378
2371	4.84859718
2820	4.848177484
3286	4.840530938
2361	4.831748583
1622	4.82913588
4349	4.821531896
3986	4.813268627
8	4.812897595
2590	4.811083894
2297	4.80906028
3798	4.806521424
3749	4.805153917
2624	4.803495536
825	4.800580825
4166	4.799507423
2780	4.799063922
1836	4.786296729
2379	4.785499498
3535	4.78441277
1202	4.783026211
2375	4.77567728
3285	4.767548318
820	4.764712425
5821	4.761485995
1038	4.752553764
3768	4.738560302
1180	4.73460754
3651	4.730763752
859	4.728643022
5048	4.727548928
1574	4.724747305
3431	4.714750049

1058	4.712807424
2000	4.710050351
2611	4.702916714
1558	4.684862165
5157	4.672033296
3942	4.660889277
2242	4.660615255
889	4.647527007
3740	4.632239719
4053	4.623575759
3640	4.618778796
1617	4.612782123
2258	4.606257554
2599	4.600318145
2374	4.597156596
3021	4.591665976
2406	4.589515179
3144	4.581326338
3578	4.580331989
4851	4.561356503
3961	4.561112659
2547	4.558195154
3504	4.551229682
3360	4.541677909
824	4.540322479
818	4.537794869
3247	4.533266674
2912	4.531480724
2369	4.530642145
2342	4.530061375
2275	4.529669812
4801	4.522020972
1487	4.519094595
2377	4.517496321
4339	4.517235814
855	4.516563338
2846	4.508076244

4603	4.506825376
843	4.506599053
2575	4.497909395
1835	4.49769536
4052	4.496596478
724	4.491719604
5835	4.480737649
1607	4.47205089
5830	4.461116817
849	4.455173645
15	4.452029665
2144	4.450690741
2373	4.449497124
840	4.439671856
4857	4.434388452
3283	4.424468274
4588	4.42420001
1059	4.422708414
4210	4.417372254
3748	4.416038636
4224	4.406826384
1554	4.405341706
1244	4.401961378
419	4.39824354
1388	4.397567862
1978	4.393576591
2920	4.383572363
4647	4.377864405
2915	4.377487101
3101	4.362570466
2681	4.362482747
3111	4.349507727
2743	4.315597382
451	4.313557579
2397	4.310768134
4888	4.308806374
1318	4.30392995

2459	4.294265884
4090	4.287757255
1568	4.28588803
860	4.281279404
2591	4.277406029
2613	4.27566213
4710	4.274664442
3706	4.27093444
822	4.270933372
2001	4.270583499
2213	4.270059438
2564	4.269827096
2583	4.269268591
1805	4.266852601
2378	4.266834073
1097	4.257671418
5897	4.257057794
1295	4.255700916
846	4.254720758
3348	4.247451648
2232	4.245085375
2509	4.242219022
1757	4.23872554
1818	4.235534704
1909	4.232409047
2372	4.231051045
1548	4.225194803
2556	4.22310049
2682	4.218913256
1130	4.217146421
2202	4.214844827
3820	4.210527379
2904	4.208668418
647	4.1912445
2668	4.19072257
2146	4.189923552
2319	4.185295574

2876	4.17794609
2744	4.177058464
312	4.17088411
1132	4.154219012
4933	4.153041147
2570	4.151260355
815	4.145014246
5364	4.141444858
3036	4.140697162
2051	4.136923031
1143	4.132230584
3256	4.126519366
3819	4.125482029
1147	4.125433759
5833	4.125394518
4427	4.124989281
1232	4.123125029
2134	4.108329219
4165	4.101782597
1802	4.095636025
3619	4.09134275
2696	4.086160011
213	4.083866775
3343	4.08048527
2794	4.076745071
3597	4.075235145
3579	4.068303219
2546	4.066979846
3213	4.065049518
1039	4.048546332
2158	4.046545866
2563	4.046505964
4227	4.042554932
4788	4.032891566
5236	4.029476141
4118	4.024383341
2434	4.018709899

2362	4.017417171
2436	4.016511753
2700	4.015580573
3582	4.012607649
4180	4.012236961
3793	4.009692265
3109	4.005190702
4078	4.00419026
2916	4.004020844
1145	4.003644702

Table.8.19. Genes more highly expressed during stationary phase growth compared to exponential growth at 37 °C in *B. cereus* G9241. Cut-off >log2-fold=6 / >64-fold change.

Gene Loci (AQ16_)	Log2-fold Change
5407	13.87554633
5281	12.87747353
243	12.36689276
288	12.08838387
345	11.93972731
4039	11.9250867
5768	11.89093341
2152	11.87878566
240	11.8115323
2265	11.76070582
2089	11.42541475
238	11.18154871
283	11.16187574
289	11.12797908
284	11.10368509
4322	11.09066443
5353	11.05539012
239	11.02470415
1488	11.01369109
2264	10.97863117
4342	10.96791959
69	10.89392619
70	10.89236996
2107	10.84371971
68	10.77101101
296	10.65991528
5203	10.65834392
600	10.65486779
287	10.47041587
74	10.42988343
4915	10.39030294
5479	10.30009315
525	10.28784266
776	10.2830536
72	10.22924902
5297	10.19756844
2263	10.18531547
4739	10.13977889
3968	10.03412752
1251	9.969856971
4145	9.948691342
4732	9.905812972
2974	9.865647184
4516	9.784438035
290	9.783068765
1394	9.728836441
242	9.702703334
2153	9.698071647
3967	9.683727559
71	9.612397747
3346	9.582922147
5192	9.564824635
5228	9.561186782
4551	9.549285905
5335	9.494575948
241	9.44956378
934	9.431628597
3969	9.394494842
2938	9.331256149
2151	9.29823014
5408	9.280195702
73	9.275101064
5478	9.262494357
1455	9.216414214
369	9.112830176
2577	9.103977096
2662	9.07544862
1209	9.063929977
5477	9.026946962
2675	8.96148849
468	8.945261513
496	8.935393146
5057	8.934257597
882	8.917165586
4438	8.904200647
5047	8.849515431
4343	8.827987303
2973	8.812891885
130	8.812191265
4414	8.800578823
4394	8.780789032
3901	8.734664686
4914	8.731488557
1453	8.714953237
3900	8.67293397
4910	8.635765933
2108	8.628012183
1172	8.607514581
285	8.518340413
300	8.505471956
4594	8.477477145
2150	8.469076398
4146	8.468013046
2975	8.455628221
5390	8.450027665
1028	8.419563527
1173	8.401609126

5202	8.388892007
1150	8.387561344
4415	8.381773214
2616	8.363718147
3113	8.332425848
2190	8.329850634
4483	8.321344275
771	8.287075544
2725	8.280584135
3114	8.279591227
5204	8.276773575
470	8.220423144
387	8.20867059
469	8.19345842
4484	8.173310676
3906	8.168063923
4909	8.136830315
3665	8.11887919
218	8.094423606
2495	8.09233319
5293	8.077823939
3024	8.075724842
1591	8.044210579
3478	8.039980158
4755	8.038622008
2208	8.025434229
5291	8.011029677
2196	8.00889385
1839	8.004442138
2167	7.989798433
4416	7.979388024
1598	7.963366704
286	7.948907819
3479	7.948647978
2214	7.940571209
4970	7.92256959
5413	7.903833515

5292	7.893498508
4567	7.885580557
599	7.867118868
2234	7.863900221
1151	7.854218138
2426	7.847920666
2518	7.843049019
601	7.820525743
4819	7.79326283
4566	7.784449971
967	7.76788027
1838	7.75747406
1212	7.748628173
4904	7.740165944
2726	7.735940825
2674	7.732090342
2727	7.731430976
5276	7.72809557
968	7.720537711
4969	7.718919203
4908	7.712527208
5491	7.70990695
4595	7.699869544
3595	7.698477156
4546	7.691255494
772	7.680444829
2617	7.654219067
2439	7.639434178
5137	7.624685169
19	7.620858174
1777	7.614240847
5511	7.602252242
5294	7.575524851
2109	7.56758697
1174	7.543989353
3353	7.537516527
4971	7.529164096

4013	7.526876013
3086	7.505702949
2724	7.501006812
909	7.489011273
1243	7.464185423
2723	7.45737235
1840	7.440618791
5309	7.428599852
598	7.420464695
5503	7.411808049
557	7.410440599
1249	7.375820361
1049	7.371653573
4481	7.363488375
1175	7.351939559
2349	7.330454567
2676	7.318578605
5056	7.298824461
2009	7.282611107
346	7.263042793
338	7.257754668
4768	7.232961358
4084	7.228608623
597	7.213507379
969	7.206685564
4605	7.200406089
2722	7.195959143
581	7.194359965
1176	7.187480505
3592	7.186917437
2573	7.177773329
467	7.143218086
4413	7.117798969
5338	7.103263672
1993	7.10090568
2005	7.090864593
2678	7.089906124

3205	7.076294355
4561	7.061575551
4955	7.049673772
1921	7.036667366
2677	7.034670139
4417	7.026888351
2728	7.016799167
5200	7.011951733
3334	7.011925251
3664	6.999852166
5466	6.981836823
1248	6.963531544
3115	6.955614309
337	6.942882625
2615	6.931060065
3764	6.926637041
3594	6.918364441
5467	6.903876801
3473	6.900495715
1177	6.891431279
4756	6.873088532
558	6.868667172
4392	6.867636968
4547	6.857191611
3770	6.838017326
415	6.834197891
1094	6.831811151
5474	6.829285909
3344	6.820511521
690	6.815698306
413	6.81115961
5473	6.801009821
4808	6.799142036
5492	6.752136783
3771	6.710495573
555	6.710196026
3023	6.699691037

481	6.695806211
4489	6.685953755
870	6.668026732
1082	6.645183918
1543	6.643328423
4147	6.639823234
3008	6.638088599
1211	6.632352258
14	6.617043535
1216	6.616428017
5354	6.60629195
2720	6.597672296
556	6.594716527
5201	6.587929384
49	6.582883694
3818	6.580554571
2567	6.572091543
5153	6.559409853
4540	6.556184774
5843	6.551088955
3395	6.543638386
4968	6.536179562
385	6.535399592
1996	6.521598471
673	6.518771671
686	6.514678548
4281	6.507810572
5352	6.5039858
1205	6.495776302
3477	6.487130071
4049	6.486395794
2235	6.478160952
3519	6.476599829
5266	6.4716154
2191	6.467632892
4951	6.45611232
2209	6.450846609

1841	6.44986723
1350	6.447801568
1678	6.446347783
2524	6.444061407
2350	6.442867789
1994	6.439065019
4905	6.43171687
1778	6.422042179
1096	6.415142055
4911	6.414130607
2442	6.411902604
2427	6.404067729
2211	6.402031286
2352	6.397028231
3083	6.396444733
2500	6.394951424
2942	6.39478727
2193	6.383171123
2440	6.379944792
2199	6.379608157
2237	6.377138254
519	6.374987917
2496	6.373995999
2215	6.37189898
427	6.367806716
3085	6.367737729
3735	6.366937716
2217	6.364082754
2197	6.36313026
5034	6.360510402
1084	6.357396146
2729	6.355401448
4	6.353941917
473	6.339321431
2520	6.339304531
2429	6.335839695
3116	6.334278368

908	6.318894178
4009	6.31348392
1081	6.305658107
4439	6.302130168
1780	6.289835244
4086	6.286447907
5031	6.280134907
2112	6.279797437
1491	6.252368624
2458	6.233949478
1206	6.208629355
2115	6.203685505
2721	6.200125244
4061	6.198678136
5050	6.187250992
2784	6.174614424
358	6.166727405
3009	6.140478513
984	6.118740899
1158	6.114903977
4043	6.111232339
4562	6.106047448
4058	6.09090243
1027	6.084737242
412	6.08361466
5322	6.082378607
5682	6.079676124
685	6.077397184
5316	6.074840972
4485	6.065951562
5064	6.054989718
4087	6.04863098
4865	6.047624437
5321	6.044307082
1085	6.035957171
3593	6.006132714
5226	6.005991795

56	6.000179886